# RESEARCH ON DIPLATINUM POLYYNE COMPLEXES:

# ATROPISOMERISM AND BOTTOM-UP SYNTHESES OF GRAPHENE

A Dissertation

by

TIANYI ZHANG

Submitted to the Office of Graduate and Professional Studies of
Texas A&M University
in partial fulfillment of the requirements for the degree of

DOCTOR OF PHILOSOPHY

| | |
|---|---|
| Chair of Committee, | John A. Gladysz |
| Committee Members, | Abraham Clearfield |
| | Timothy R. Hughbanks |
| | Tahir Cagin |
| Head of Department, | Simon North |

May 2017

Major Subject: Chemistry

## ABSTRACT

Major objectives of this dissertation pay attention to synthesis, probe the feasibility of a new type of inorganic atropisomerism of diplatinum ethynediyl and butadiynediyl complexes, and explore the feasibility of Diels-Alder functionalization of polyyne chains to achieve graphene-like structures.

Reaction of *trans*-($C_6F_5$)($Me_2PhP$)(*p*-$tol_3P$)Pt(Cl) and *trans*-($C_6F_5$)($Me_2PhP$)(*p*-$tol_3P$)Pt(C≡$CSiEt_3$) (cat. *n*-$Bu_4NF$/CuCl, $HNEt_2$, –45 °C) gives a series of PtC≡CPt complexes in which the two phosphine ligands have been scrambled. Preparative TLC affords the target complex *trans*,*trans*-($C_6F_5$)(*p*-$tol_3P$)($Me_2PhP$)Pt(C≡C)Pt($PPhMe_2$)(P*p*-$tol_3$)($C_6F_5$) (2.3%). The crystal structure of *trans*,*trans*-($C_6F_5$)(*p*-$tol_3P$)($Me_2PhP$)Pt(C≡C)Pt($PPhMe_2$)(P*p*-$tol_3$)($C_6F_5$) is determined, shows much congestion about the PtC≡CPt linkage. Low temperature $^1$H NMR spectra of *trans*,*trans*-($C_6F_5$)(*p*-$tol_3P$)($Me_2PhP$)Pt(C≡C)Pt($PPhMe_2$)(P*p*-$tol_3$)($C_6F_5$) are recorded. However, no decoalescence is observed ($CD_2Cl_2$/–95 °C; $CDFCl_2$/–100 °C); this suggests that interconversion of the putative atropisomers remains rapid on the NMR time scale at ≤ –95 °C.

Cross couplings of *trans*-($C_6F_5$)($R_2PhP$)(*p*-$tol_3P$)Pt(Cl) (**Pt'Cl-a-c**, R = **a**/Me, **b**/*p*-*t*-$BuC_6H_4$, **c**/*p*-$MeOC_6H_4$, **d**/*n*-Pr) and *trans*-($C_6F_5$)($R_2PhP$)(*p*-$tol_3P$)Pt(C≡$C)_2H$ (**Pt'$C_4$H-a-c**) (cat. CuI, $HNEt_2$) give mixtures of diplatinum butadiynyl complexes in

which the two phosphine ligands scramble over all four positions (**PtC$_4$Pt**, **PtC$_4$Pt'-a-c**, **PtC$_4$Pt"-a-c**, **Pt'C$_4$Pt'-a-c**, **Pt'C$_4$Pt"-a-c**, **Pt"C$_4$Pt"-b**; 27-2% each). A modified coupling recipe is tested with **Pt'Cl-b**,**d** and **Pt'C$_4$H-b**,**d** (*t*-BuOK, $KPF_6$, cat. CuCl), and gives **Pt'C$_4$Pt'-b**,**d** (21-76%) with traces of scrambling. The crystal structures of **Pt'C$_4$Pt'-a-d** are determined, and the endgroup/endgroup interactions analyzed. Low temperature NMR spectra do not reveal any dynamic processes.

Reactions of **PtC$_4$H** or **PtC$_6$TES** and the 1,4-dihydro-2,3-benzoxathiin-3-oxide in refluxing toluene are investigated. Mass spectrometric data give evidence for 1:1 aromatized cycloadducts. A similar reaction of **PtC$_8$Pt** and 1,3-dihydrobenzo[*c*]thiophene-2,2-dioxide in 1,2,4-trichlorobenzene (160 °C) affords 1:1, 1:2, and 1:3 aromatized cycloadducts, as assayed by mass spectrometry. These reactions are viewed as possible initial steps in bottom up syntheses of graphene, but appear to lack generality in diplatinum homologs with longer *sp* carbon chains. Other types of cycloadditions are attempted with $B_{10}H_{12}{\cdot}2[S(CH_3)_2]$ (**TESC$_4$TES**, **TESC$_8$TES**, **PtC$_8$Pt**; refluxing toluene, *o*-carborane targets) and the cyclotrimerization catalyst [CpCo(CO)(dimethyl fumarate)] (**PtC$_4$H**, **TESC$_8$TES**, **PtC$_6$Pt**, **PtC$_8$Pt**; reluxing toluene, dark/ambient lighting, arene targets). However, no tractable products could be isolated, and in most cases the platinum containing reactant was recovered. These data suggest that the polyynes investigated are less reactive in various cycloaddition processes than many simple organic alkynes.

## DEDICATION

This dissertation is dedicated to my parents Yepeng Zhang, Jinhua Geng and my wife Ruixue Wu. Your love and support have been invaluable to me throughout this entire process and I wouldn't have been able to do it without you.

## ACKNOWLEDGEMENTS

First and foremost, I would like to thank my research advisor, Dr. John A. Gladysz. For 5 years, he has put incredible effort towards my research and help me growing fast, especially recently spends much time and effort on this dissertation. I have learned a lot from him. I would also like to thank my committee members, Dr. Abraham Clearfield, Dr. Timothy R. Hughbanks and Dr. Tahir Cagin.

In the past 5 years, many people have come in and out of Gladysz group. I want to thank everyone for your friendships, but there are a few that I would like to acknowledge specifically. First and foremost I would like to thank Dr. Zhengxing Xi who taught me so much and helped me a lot in my first three years. A special thanks to Dr. Tobias Fiedler. You were a great co-worker for me and you helped me get through Mercury, Ortep3 and Adobe Illustrator. Zuzana Baranova, thank you for your help in all the chemical discussions related to polynes. Bryan Stewart, you have helped me throughout the entire dissertation writing process.

To my parents, I have no words to describe what your support has meant to me in my past 30 years. You taught me that there was always a lesson to learn in everything that I did and in everyone that I knew. That drive to learn has brought me to where I am today. Thank you for helping me to be the best myself.

Last, but certainly not least, Ruixue Wu, thank you both for loving and supporting me. I hope that in the future we will be able to spend much more time together, I owe you too much.

## CONTRIBUTORS AND FUNDING SOURCES

### Contributors

This work was supervised by a dissertation committee consisting of Professors John A. Gladysz, Abraham Clearfield and Timothy R. Hughbanks of the Department of Chemistry and Professor Tahir Cagin of the Department of Chemical Engineering.

The work of section 3 of dissertation was completed by the student, in collaboration with Dr. Sandip Dey of the Department of Chemistry.

All crystal structures were determined by a crystallographer, although all crystallographic data were interpreted by the student.

All other work conducted for the dissertation was completed by the student independently.

### Funding Sources

This work was made possible in part by US National Science Foundation under Grant Number CHE-0719267, CHE-1153085, and CHE-1566601.

## TABLE OF CONTENTS

Page

Page

## LIST OF FIGURES

FIGURE Page

FIGURE Page

FIGURE Page

FIGURE Page

## LIST OF SCHEMES

SCHEME Page

## LIST OF TABLES

# 1. INTRODUCTION

## 1.1 Introduction to atropisomerism

Atropisomerism is a type of stereoisomerism arising because rotation about a single covalent bond is impeded sufficiently so as to allow different stereoisomers to be isolated. Energy differences due to steric strain or other contributors create a barrier to rotation that is high enough to allow for isolation of individual conformers.[1] It is manifested typically in *ortho*-substituted biphenyls (or, more generally, biaryls) where steric congestion between the substituents restricts free rotation about the $sp^2$–$sp^2$ carbon–carbon bond.

The definition of atropisomers is further refined taking into account the temperature-dependence associated with the interconversion of conformers, specifying that atropisomers interconvert with a half-life of at least 1000 seconds at a given temperature, corresponding to an energy barrier of 93 kJ $mol^{-1}$ (22 kcal $mol^{-1}$) at 300 K (27 °C).[2]

Atropisomerism is not restricted to biaryls. Within systems having the $sp^2$–$sp^2$ single bond type, it may also be manifested in sterically impeded substituted styrenes and in certain aromatic amides and anilides. Cases of atropisomerism about single $sp^2$–$sp^3$ carbon–carbon bonds are known and, more unusually, some highly sterically hindered $sp^3$–$sp^3$ single bonds also exhibit degrees of restricted rotation that permit stereoisomers to be resolved. Complex molecular architectures such as those of the vancomycin group of antibiotics present nonconventional stereochemical issues that originate in the

restricted rotation of substituted aromatic rings within macrocyclic structures. The practitioners of the first total syntheses of these molecules have considered these stereochemical phenomena to be cases of atropisomerism.

Three basic factors contribute to the stability of individual atropisomers: the repulsive interactions (e.g., steric bulk; atropisomer stability is, however, considerably reduced when two or more of the substituents are small.) of substituents near the axis of rotation, the length and rigidity of the single bond, a largely $sp^2$-$sp^2$ type of bond joining the aryl rings, and whether there are photochemical or other mechanisms to induce rotation in addition to thermal pathways.[1]

The importance of atropisomers arises to a significant degree because with sufficient stability of a conformer, they can display axial chirality (planar chirality). Atropisomers that display axial chirality often have substituents ortho to the bond joining the aryl rings, substituents that cause significant steric repulsion that hinders rotation about the bond. The degree of hindrance correlates with the van der Waals radii of the particular substituents, and other properties that contribute to their repulsive potentials. Atropisomers are involved in a chemical equilibrium that, for a given structure, is thermally controlled; they differ in this way from most other types of chiral structures, where interconversion involves a chemical isomerization (i.e., with breaking and reforming of covalent bonds).

Determining the axial stereochemistry of biaryl atropisomers can be accomplished through the use of a Newman projection along the axis of hindered rotation. The configuration of a molecule having a chirality axis may be specified as *R* or *S* by

application of the Cahn–Ingold–Prelog priority rules. Alternatively such molecules may be treated as helices and assigned *M* or *P* stereochemistry (see Scheme 1.1). The *ortho*, and in some cases *meta* substituents are first assigned priority based on Cahn–Ingold–Prelog priority rules. Starting with the substituent of highest priority in the closest ring and moving along the shortest path to the substituent of highest priority in the other ring, the absolute configuration is assigned *P* for clockwise and *M* for counterclockwise. In the example shown, A has priority over B.[1]

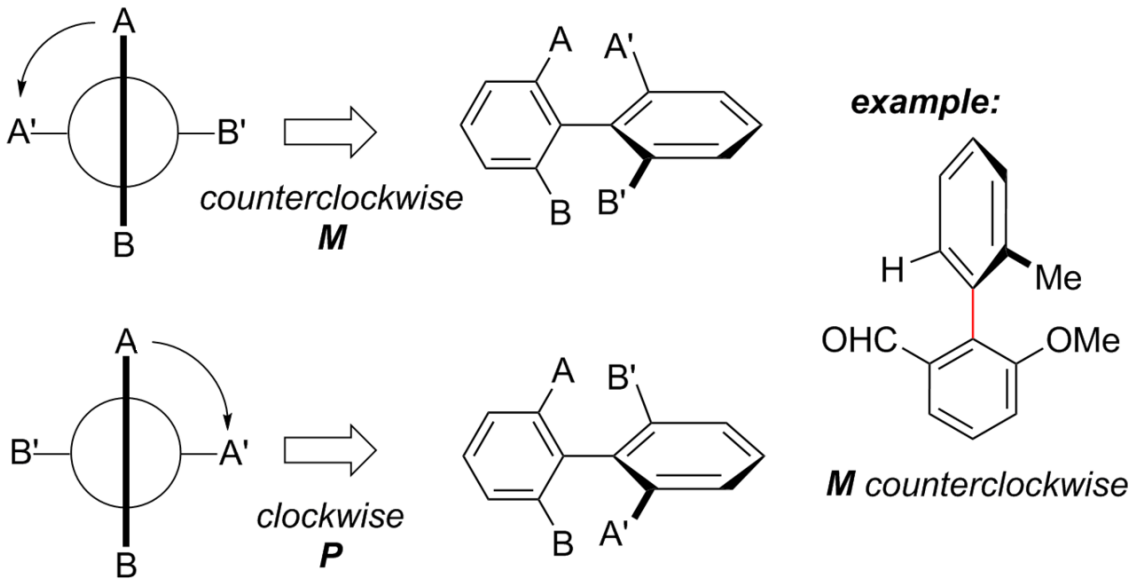


**Scheme 1.1**. How to determine stereochemistry in atropisomers

Many atropisomers occur in nature. Some natural products can be used as drugs and an example of this is mastigophorene A (Scheme 1.2, left).[3] Mastigophorene A has been found to aid in nerve growth. Other examples of naturally occurring atropisomers include vancomycin isolated from an Actinobacterium, and knipholone (Scheme 1.2, middle), which is found in the roots of Kniphofia foliosa of the family Asphodelaceae. The structure complexity in vancomycin is significant because it can bind with peptides

due to the complexity of its stereochemistry, which includes multiple stereocenters, two chiral planes in its stereogenic biaryl axis. Knipholone, with its axial chirality, occurs in nature and has been shown to offer good antimalarial and antitumor activities particularly in the *M* form.

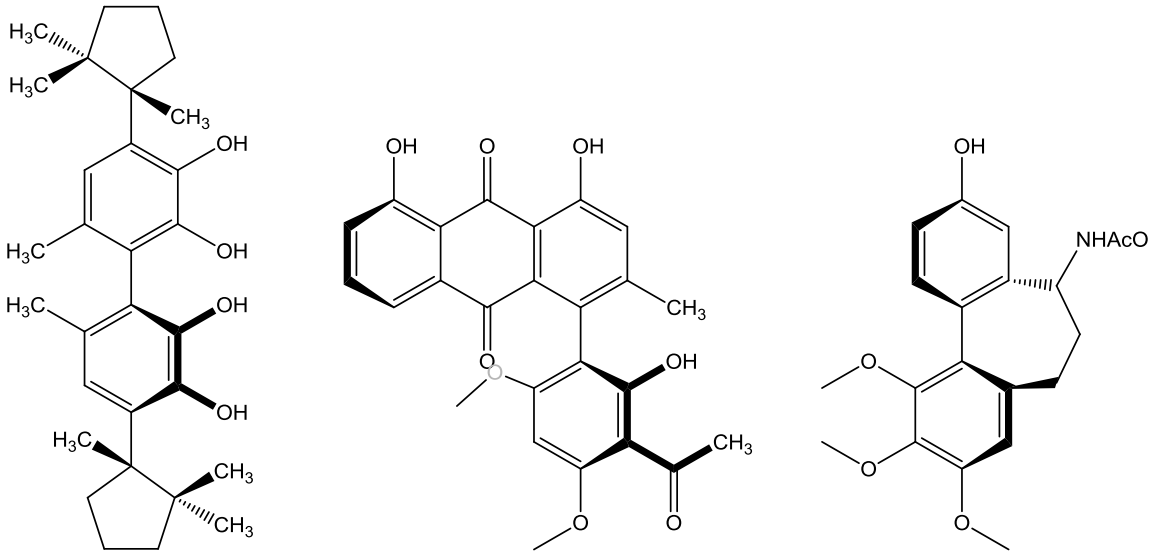


mastigophorene A knipholone (-)-N-acetylallocolchinol

**Scheme 1.2**. Examples of atropisomers in nature or pharmaceutical industry

The pharmaceutical industry focuses its energy on producing enantiomerically pure compounds to be used as drugs. The use of atropisomers in synthesizing drugs allows for more stereochemical control. One example is (−)-N-acetylallocolchinol (Scheme 1.2, right), a drug that was discovered to aid in chemotherapy cancer treatment.[4]

## 1.2 Introduction to diastereotopic groups

Diastereotopic refers to the relationship between two groups in a molecule which, if replaced, would generate compounds that are diastereomers. The concept of diastereotopicity was first introduced during the early days of NMR spectroscopy.

Diastereotopic groups are often, but not always, identical groups attached to the same atom in a molecule containing at least one chiral center.

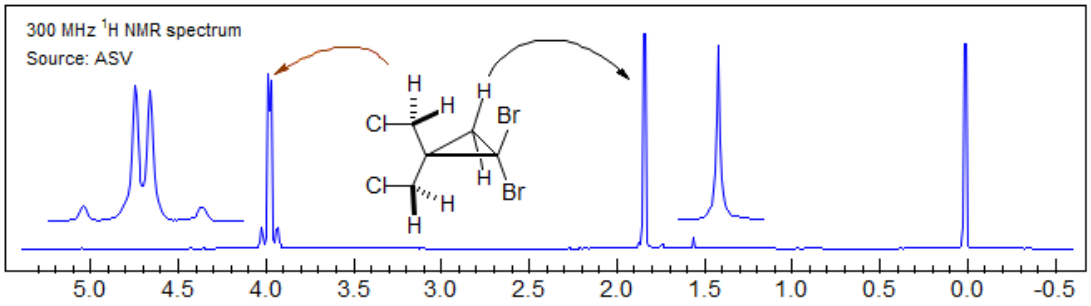


**Figure 1.1**. Example of diastereotopic groups in NMR spectroscopy (ASV: Aldrich Spectral Viewer[5])

In NMR spectroscopy:

1. Homotopic groups have the exact same chemical shift
2. Enantiotopic groups have the same chemical shift in the vast majority of situations. However, if they are placed in a chiral environment (e.g. a chiral solvent) they will have different chemical shifts.
3. Diastereotopic groups have different chemical shifts in all situations. (Figure 1.1)

## 1.3 Introduction to graphene

Graphene is an allotrope of carbon in the form of a two-dimensional, atomic-scale, honey-comb lattice in which one atom forms each vertex (Figure 1.2). It is the basic structural element of other allotropes, including graphite, charcoal, carbon nanotubes and in part fullerenes. It can also be considered as an indefinitely large aromatic molecule, the ultimate case of the family of flat polycyclic aromatic hydrocarbons. The Nobel Prize in Physics in 2010 was granted "for groundbreaking experiments regarding the two-dimensional material graphene."

Graphene has many extraordinary properties. It is about 200 times stronger than the strongest steel. It conducts heat and electricity efficiently and is nearly transparent. Graphene also shows a large and nonlinear diamagnetism, even greater than graphite.[6]

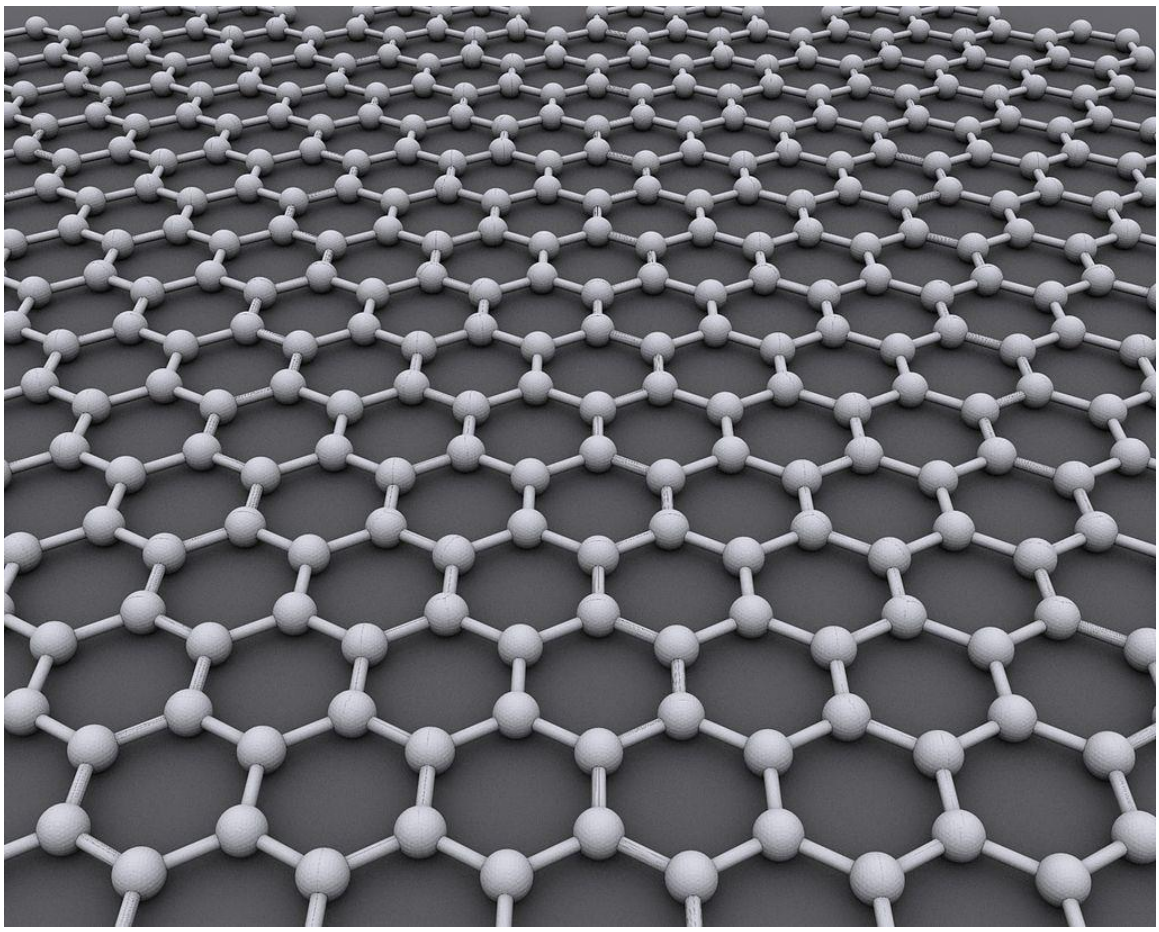

**Figure 1.2**. Graphene is an atomic-scale hexagonal lattice made of carbon atoms

Graphene is the only form of carbon (or solid material) in which every atom is available for chemical reaction from two sides (due to the 2D structure). Atoms at the edges of a graphene sheet have special chemical reactivity. Graphene has the highest ratio of edge atoms of any allotrope. Defects within a sheet increase its chemical reactivity.[7] The onset temperature of reaction between the basal plane of single-layer graphene and

oxygen gas is below 260 °C (530 K).[8] Graphene burns at very low temperature (e.g., 350 °C (620 K)).[9] Graphene is commonly modified with oxygen- and nitrogen-containing functional groups and analyzed by infrared spectroscopy and X-ray photoelectron spectroscopy. However, determination of structures of graphene with oxygen-[10] and nitrogen-[11] functional groups requires the structures to be well controlled.

# 2. A QUEST FOR ATROPISOMERISM IN COJOINED SQUARE PLANAR METAL COMPLEXES: SYNTHESES AND STRUCTURES OF STERICALLY CONGESTED DIPLATINUM ETHYNEDIYL ADDUCTS*

## 2.1 Introduction

Atropisomers are stereoisomers that arise due to restricted rotation about a single sigma bond.[12] With very rare exceptions, they are associated with axial chirality, and have played multifaceted roles in organic chemistry. Organic atropisomers are well known for their fascinating fundamental properties,[1,4a,12,13] use as chiral ligands for enantioselective catalysis,[14] and importance as determinants of biological activity.[15] Most but by no means all[16] examples involve substituted biphenyls, as illustrated in Scheme 2.1 (left). Various types of atropisomerism have also been encountered in inorganic and organometallic molecules.[17]

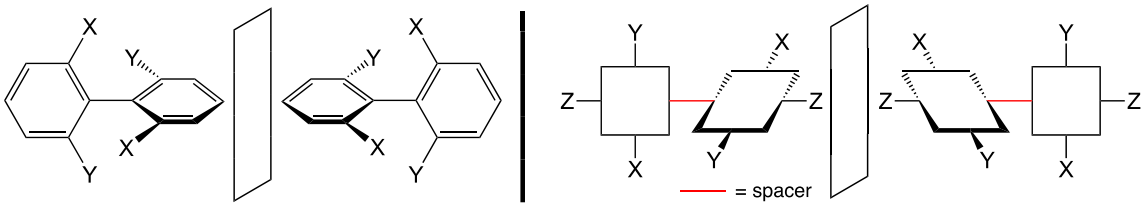


**Scheme 2.1**. Atropisomerism in substituted biphenyls (left) and cojoined square planar metal complexes (right); pairs of enantiomers.

We wondered whether a simple analogy to biaryl atropisomerism might be realized by linking two square planar metal fragments with a suitable spacer, as illustrated in Scheme 2.1 (right). In both cases, the atropisomers are depicted with X/Y

* Reprinted with permission from Zhang, T.; Bhuvanesh, N.; Gladysz, J. A. *Eur. J. Inorg. Chem.* **2017**, *2017*, in press. DOI: 10.1002/ejic.201601307. Copyright 2017, Wiley-VCH Verlag GmbH & Co. KGaA.

substituents on the cojoined moieties, which leads to non-superimposable mirror images. However, a 180° rotation about the spacer bonds would interconvert the enantiomers. Such atropisomers can of course have lower symmetries – for example, an X/Y substitution pattern on one moiety and A/B on the other. In cases where a substituent carries a stereocenter, diastereomeric atropisomers become possible.

For the examples in Scheme 2.1, atropisomerism can be established by separating and characterizing each enantiomer (or diastereomer). However, there is a well established alternative protocol. This entails the introduction of substituents with diastereotopic groups (or that render other groups diastereotopic), such as illustrated in Scheme 2.2.[18] Given the axis of chirality, separate NMR signals would be expected provided that the interconversion of enantiomers (or epimers) is sufficiently slow on the NMR time scale. In compounds with lower barriers, NMR spectra can be recorded below

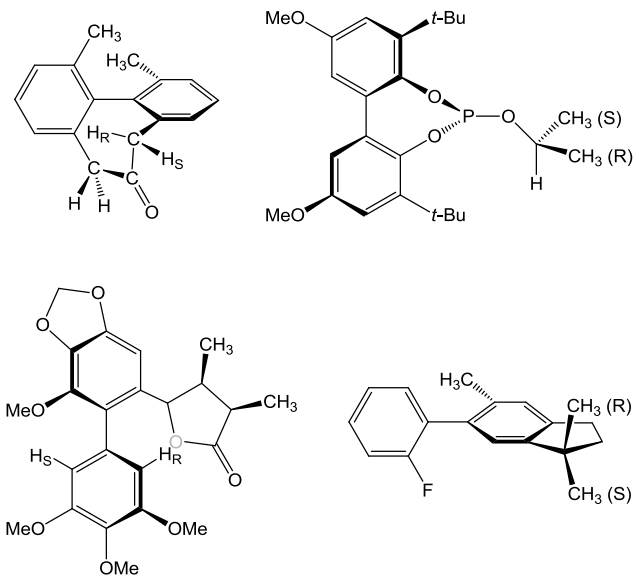


**Scheme 2.2**. Biphenyls for which slowly interconverting atropisomers have been established by the observation of separate NMR signals for diastereotopic groups.

room temperature, in hopes of observing decoalescence to separate signals. In general, activation parameters are easily extracted from the NMR data.

Many square planar metal complexes are potent catalysts or catalyst precursors for organic reactions.[19] Thus, we were curious whether linked square planar complexes capable of atropisomerism might provide new platforms for enantioselective catalysis. Accordingly, in this paper we report the synthesis, structure, and dynamic properties of a diplatinum ethynediyl complex in which two square planar termini are separated by a C≡C unit. Each endgroup features *trans* $Me_2PhP$ and *p*-$tol_3P$ ligands, which serve as the X/Y substituents in Scheme 2.1. Although these types of systems have not yet, to our surprise, definitively fulfilled their promise for atropisomerism, much interesting chemistry has been established. Furthermore, the data suggest ways to achieve more congested environments in which the target phenomenon might be realized.

## 2.2 Results

### 2.2.1 Syntheses of monoplatinum and diplatinum complexes

As shown in Scheme 2.2, the previously reported square planar bis((tri-*p*-tolyl)phosphine) platinum complex *trans*-($C_6F_5$)(*p*-$tol_3P$)$_2$Pt(Cl) (**1**)[20] was treated with commercial $Me_2PhP$ (4 equiv). After 3 days, a chromatographic workup gave the monosubstitution product *trans*-($C_6F_5$)($Me_2PhP$)(*p*-$tol_3P$)Pt(Cl) (**2**) in 68% yield. The air stable compound was characterized by NMR ($^1H/^{13}C\{^1H\}/^{31}P\{^1H\}$; all $CDCl_3$) and microanalysis, as summarized in the experimental section. The $^{31}P\{^1H\}$ NMR spectrum

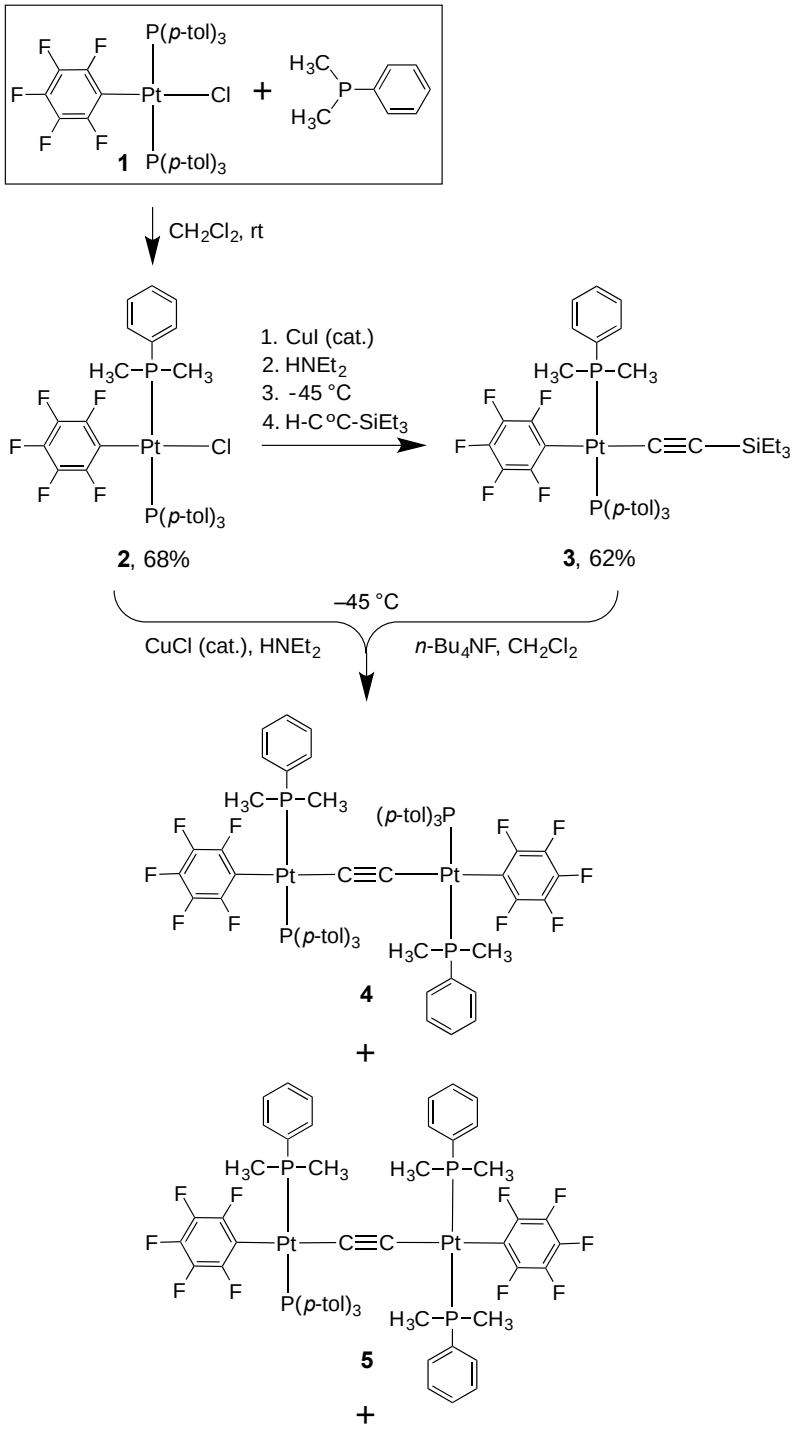


**Scheme 2.3**. Syntheses of the title complexes.

exhibited two strongly coupled doublets ($CDCl_3$: δ 19.49 (*p*-$tol_3P$) and –6.00 ($Me_2PhP$), $^2J_{PP}$ = 450 Hz). The phosphorus-bound methyl groups showed a single $^1H$ NMR signal, and were coupled to both proximal phosphorus atoms (δ 1.78, dd, $^2J_{HP}$ = 10.5 Hz, $^4J_{HP}$ = 2.7 Hz). They also showed a single $^{13}C$ NMR signal (δ 12.3, dd, $^1J_{CP}$ = 36.6 Hz, $^3J_{CP}$ = 1.7 Hz). The identity of **2** was further secured by a crystal structure below.

As shown in Scheme 2.3, a procedure that has been used to cross couple a variety of platinum chloride complexes and terminal alkynes[20,21] was applied to **2** and $HC{\equiv}CSiEt_3$. This entailed the solvent $HNEt_2$ (which also neutralizes the HCl generated) and the catalyst CuI.[22] A chromatographic workup gave the air stable triethylsilylethynyl complex *trans*-($C_6F_5$)($Me_2PhP$)(*p*-$tol_3P$)Pt($C{\equiv}CSiEt_3$) (**3**) as an orange oil in 62% yield. The NMR properties were similar to those of **2** ($^{31}P\{^1H\}$ δ 14.77 (*p*-$tol_3P$), –14.51 ($Me_2PhP$); 2d, $^2J_{PP}$ = 448 Hz).

Interestingly, small amounts of two additional products were evident by TLC, and crude samples were isolated. Each exhibited a single $^{31}P\{^1H\}$ NMR signal. One was assigned as *trans*-($C_6F_5$)(*p*-$tol_3P$)$_2$Pt($C{\equiv}CSiEt_3$), the trimethylsilyl analog of which has been completely characterized (δ 14.55, s).[21] The other was believed to be *trans*-($C_6F_5$)($Me_2PhP$)$_2$Pt($C{\equiv}CSiEt_3$) (δ –14.31, s). Thus, a modest amount of phosphine exchange takes place under the cross coupling conditions. Purified samples of **3** also underwent slow disproportionation to these two species in $CH_2Cl_2$.

It was next sought to cross couple the monoplatinum complexes **2** and **3** to give the target diplatinum ethynediyl complex *trans*,*trans*-($C_6F_5$)(*p*-$tol_3P$)($Me_2PhP$)Pt(C≡C)Pt($PPhMe_2$)(P*p*-$tol_3$)($C_6F_5$) (**4**). Accordingly, a procedure that has been used for a variety of platinum chloride and triethylsilylpolyynyl complexes was applied.[20,23] As shown in Scheme 2.3, a –45 °C $CH_2Cl_2$ solution of **3** was treated with a catalytic amount of *n*-$Bu_4NF$ in wet THF. This was added to a –45 °C $HNEt_2$ solution of **2** that contained a catalytic amount of CuCl.

In previous cases where this type of cross coupling has been employed, all of the phosphine ligands on both monoplatinum reactants have been identical.[20,23] Unfortunately, under the conditions of Scheme 2.3, extensive exchange of the $Me_2PhP$ and *p*-$tol_3P$ ligands occurred. This can lead to as many as six products ($X_2/X_2$, $X_2$/XY, XY/XY, $X_2/Y_2$, $Y_2$/XY, $Y_2/Y_2$), and TLC analyses showed six principal bands. The combined yield of these species was high (>>50%). Preparative TLC afforded a reasonable separation, and efforts were focused on two bands with intermediate $R_f$ values. The less polar species proved to be the desired complex **4**, as verified by spectroscopic and structural data below. However, it could only be isolated in a maximum of 2.3% yield. The more polar species was the tris($Me_2PhP$)/mono(*p*-$tol_3P$) or $X_2$/XY type complex *trans*,*trans*-($C_6F_5$)($Me_2PhP$)$_2$Pt(C≡C)Pt($PPhMe_2$)(P*p*-$tol_3$)($C_6F_5$) (**5**, 5.6%).

Both **4** and **5** were air stable light yellow solids. Complex **4** exhibited NMR properties that were generally comparable to those of the precursors **2** and **3**. For example, the $^1H$ chemical shift of the methyl signal associated with the *p*-$tol_3P$ ligand (δ 2.28, s)

was practically identical to those of **2** (2.34) and **3** (2.33). However, that associated with the $Me_2PhP$ ligand (δ 1.37, dd, $^2J_{HP}$ = 10.5 Hz, $^4J_{HP}$ = 2.3 Hz) was shifted upfield relative to those of **2** (1.78) and **3** (1.85). In contrast, the $^{13}C$ chemical shifts of the methyl signals of the *p*-$tol_3P$ and $Me_2PhP$ ligands of **2** and **4** were similar.

### 2.2.2 Crystallography, NMR studies, and other experiments

Single crystals of **2**, **4** and **5** could be obtained, and the crystal structures were determined as outlined in Table 2.1 and the experimental section. Key metrical parameters are provided in Table 2.2. Most values are comparable, but the P-Pt-P angles in **4** deviate more from the idealized value of 180° than in **2** and **5** (168.61(4)° vs. 175.81(3)-175.88(3)°). The C≡C bond lengths in the diplatinum complexes (1.213(5)-1.215(4) Å) are diagnostic of alkynyl linkages.[20,23]

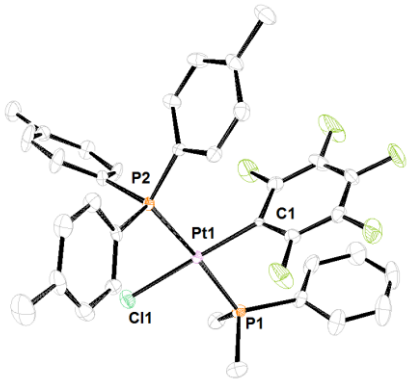


**Figure 2.1**. Molecular structure of the monoplatinum complex **2** with thermal ellipsoids at 50% probability level.

Thermal ellipsoid diagrams and/or space filling representations are provided in Figures 2.1-2.3. The congested nature of the diplatinum complexes is evident and further

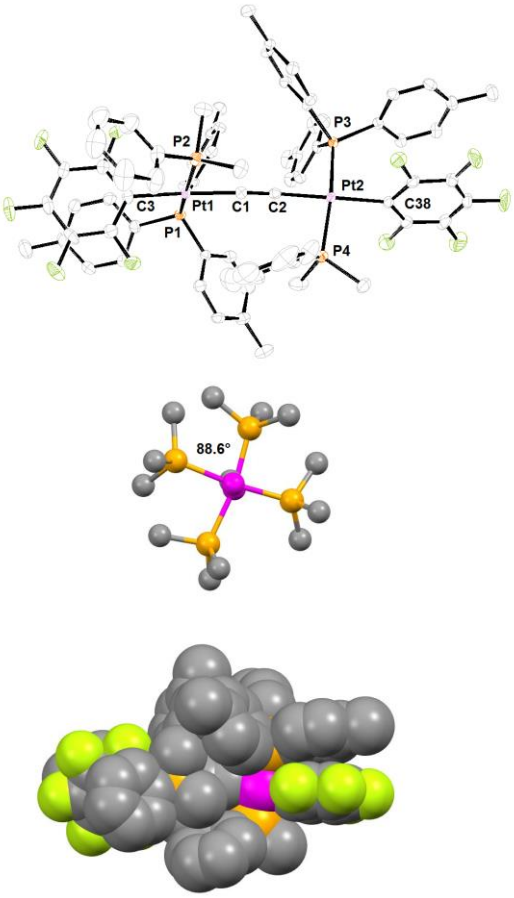


**Figure 2.2**. Thermal ellipsoid (top; 50% probability level), Newman (middle), and space-filling (bottom) representations of diplatinum complex **4**.

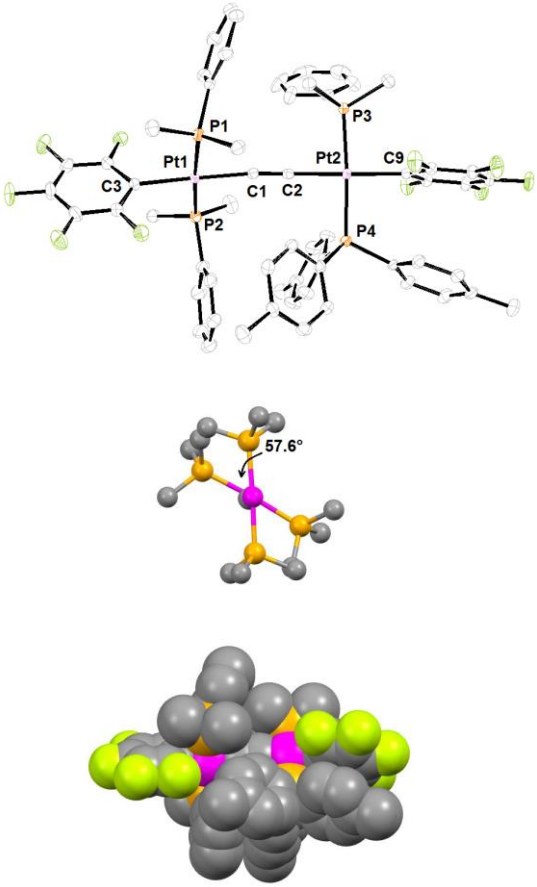


**Figure 2.3**. Thermal ellipsoid (top; 50% probability level), Newman (middle), and space-filling (bottom) representations of diplatinum complex **5**.

analyzed in the discussion section. As expected, **4** crystallized in a chiral PtC≡CPt conformation, but both enantiomers were present in the unit cell.

Next, $^{1}$H NMR spectra of **4** were recorded in $CD_2Cl_2$ as the temperature was lowered from room temperature to near the freezing point (–95 °C). Special attention was given to the **Me**$_2$PhP signal. As shown in Figure 2.4, only a single doublet of doublets was observed. As with the corresponding signal of **2**, it exhibited a larger two-bond

phosphorus coupling ($^2J_{HP}$ = 10.5 Hz) and a smaller four-bond phosphorus coupling ($^4J_{HP}$ = 2.3 Hz). The chemical shift varied

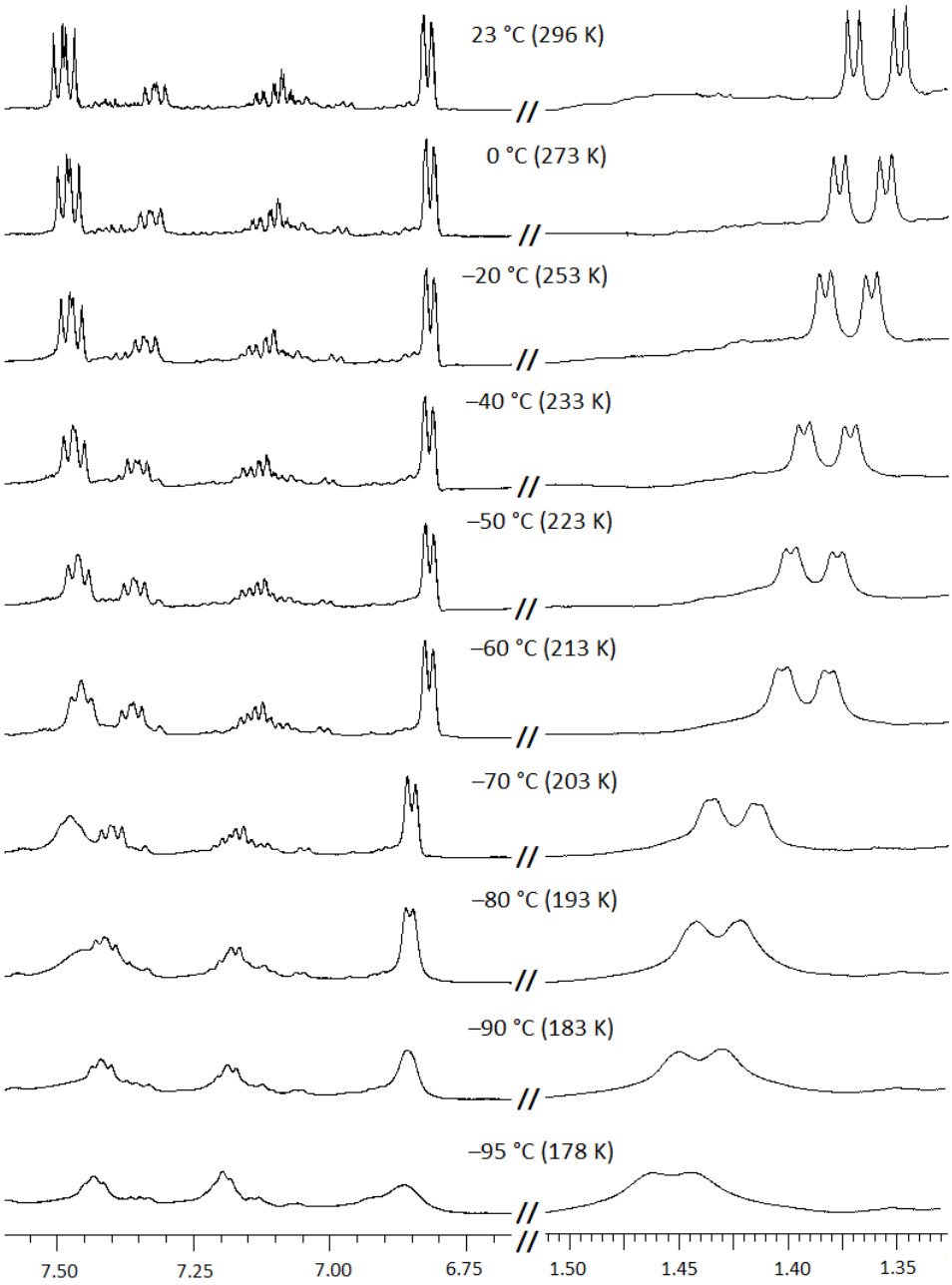


**Figure 2.4**. Variable temperature $^1$H NMR spectra of **4** (500 MHz, $CD_2Cl_2$).

somewhat between 23 °C, –60 °C, and –95 °C (δ 1.36, 1.40 and 1.45). Although decoalescence was not achieved, the increasingly broad signal suggested that a threshold was being approached. The aromatic proton signals (δ 6.80-7.50) exhibited only very modest changes from 23 °C to –60 °C, and then also broadened.

Analogous spectra were recorded using the solvent $CDFCl_2$,[24] which freezes at –135 °C. However, it was not possible to acquire meaningful data at temperatures lower than –100 °C due to the precipitation of **4**. Importantly, the presence of the four-bond phosphorus coupling ($^4J_{HP}$) in the **Me**$_2$PhP $^1$H NMR signals at the high temperature limit (296 K) indicates that phosphine dissociation cannot be a factor in whatever process renders the methyl groups equivalent.

Finally, additional experiments were conducted in efforts to avoid the phosphine ligand scrambling in the final step of Scheme 2.3. First, cross couplings of **2** and **3** were attempted in the absence of the CuCl and *n*-$Bu_4NF$ catalysts. Specifically, $C_6D_5Br$, $BrCH_2CH_2Br$, THF, and $CDCl_3$ solutions were heated at 40-65 °C in NMR tubes in the hopes of effecting thermal $ClSiEt_3$ eliminations. However, no reactions were observed over the course of 48-72 h. Second, the synthesis of the ethynyl complex *trans*-$(C_6F_5)(Me_2PhP)(p\text{-}tol_3P)Pt(C{\equiv}CH)$ was attempted, both from **2** and commercial $LiC{\equiv}CH$ and by the protodesilylation of **3**. It is often possible to deprotonate ethynyl complexes with strong organolithium bases,[25] and the resulting $L_nMC{\equiv}CLi$ species can cleanly react with a variety of electrophiles,[25,26] including transition metal halides.[27] However, the ethynyl complex was always accompanied by a multitude of byproducts.

## 2.3 Discussion

The phosphine ligand scrambling that accompanied the coupling of **2** and **3** was entirely unexpected and in retrospect was likely masked in earlier studies[20,23] in which the phosphine ligands in both reaction components were identical. In work recently submitted for publication, analogous phosphine scrambling has been observed in related condensations of platinum butadiynyl complexes and platinum chloride complexes.[28] Here, PtC≡CC≡CPt species with all six types of phosphine substitution patterns have been isolated and characterized.

On the positive side, these phenomena suggest the possibility of carrying out late stage phosphine substitutions simultaneously with coupling, thereby increasing the scope of available end products without a commensurate increase in intermediates. It is also worth emphasizing that the conversion of **1** to **2** – a thermal phosphine ligand substitution – is slow at room temperature (ca. 20% conversion after 1 day). Enhanced substitution rates are often found with paramagnetic metal complexes.[29] Perhaps the copper catalyst somehow promotes redox equilibria that facilitate scrambling.

In addition to **4** and **5**, two other diplatinum ethynediyl complexes, both of the formula *trans,trans*-(X)($R_3P$)$_2$PtC≡CPt($PR_3$)$_2$(X), have been structurally characterized. One of these, *trans,trans*-(Cl)($Ph_3P$)$_2$PtC≡CPt($PPh_3$)$_2$(Cl) (**6**), has been prepared by a different type of route involving 1,2-dichloroethyne.[30] The other, *trans,trans*-(I)($Me_3P$)$_2$PtC≡CPt($PMe_3$)$_2$(I) (**7**), was synthesized by cross coupling platinum ethynyl and chloride complexes using protocols similar to those in Scheme 2.3 ($HNEt_2$, CuCl).[31]

The crystal structures are shown Figures 2.5 and 2.6. Neither features any potentially diastereotopic groups.

The four $PPh_3$ ligands in **6** clearly make for a more congested PtC≡CPt environment than the four smaller $PMe_3$ ligands **7**. The endgroup orientations can be quantified by taking the angle between the two planes defined the P-Pt-P linkage on one terminus and the platinum atom of the other. These fall in the narrow range 82.3°-89.3°, as indicated in Figures 2.5 and 2.6. When the angle is 90°, the steric separation between the phosphine ligands is maximized.

As is obvious from Figures 2.2 and 2.3, the two triarylphosphines and two aryldialkylphosphines in **4** make for a more congested PtC≡CPt environment than the one triarylphosphine and three aryldialkylphosphines in **5**. In the former, the endgroup/endgroup angle (88.6°) is close to those of **6** and **7**. However, in the latter the angle decreases to 57.6°. Smaller angles are of course consistent with lower endgroup/endgroup steric interactions. Perhaps the large angle in **7**, which has the smallest phosphine ligands, is imposed by crystal packing forces.

With respect to our original plan for establishing atropisomerism in cojoined square planar complexes, two modifications merit consideration. One line of investigation would involve *shorter* bridges between the endgroups. However, most two atom linkers ($N_2$, CN, etc) would be about the same length, and we are not aware of any

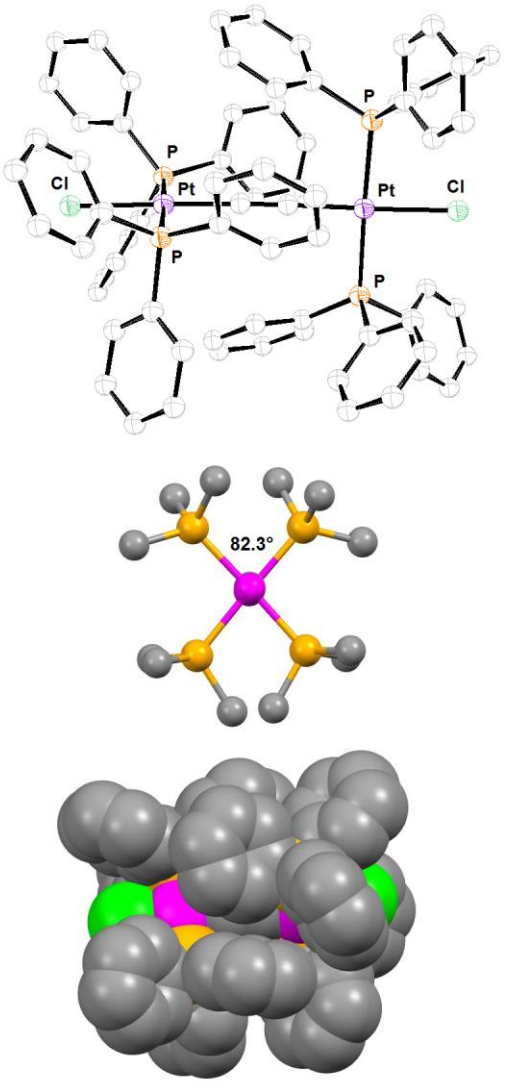


**Figure 2.5**. Thermal ellipsoid (top; 50% probability level), Newman (middle), and space filling (bottom) representations of *trans*,*trans*-(Cl)($Ph_3P$)$_2$PtC≡CPt($PPh_3$)$_2$(Cl) (**6**).

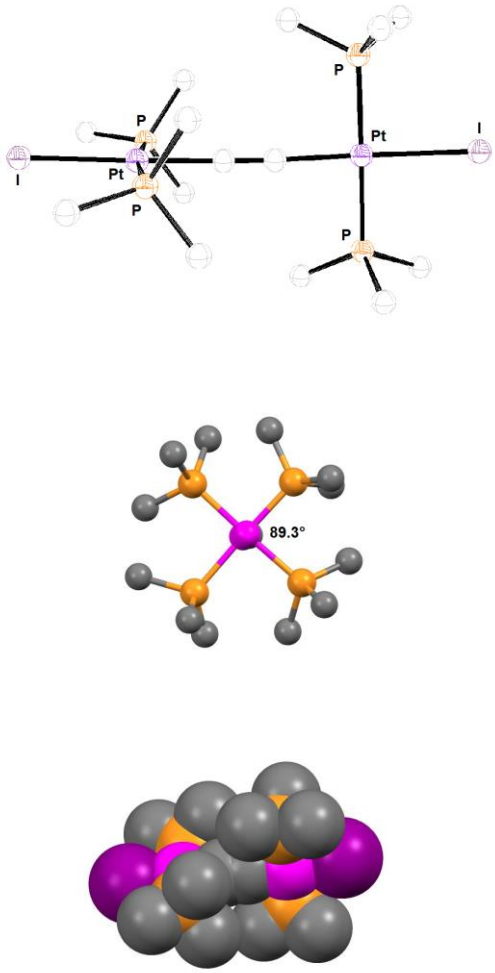


**Figure 2.6**. Thermal ellipsoid (top; 50% probability level), Newman (middle), and space filling (bottom) representations of *trans*,*trans*-(I)($Me_3P$)$_2$PtC≡CPt($PMe_3$)$_2$(I) (**7**).

single atom linkers that would enforce a linear Pt-E-Pt geometry. Alternatively, the covalent radius of nickel is ca. 10% shorter than that of platinum, so dinickel homologs would experience greater endgroup/endgroup interactions. Another approach would be to

employ still bulkier phosphine ligands, such as bis(*t*-butyl) substituted $(t\text{-Bu})_2PPh$ in place of $Me_2PPh$.

In this context, we presume that in **4**, some type of gearing of the phosphorus-carbon substituents on each terminus allows the square planes to rotate by 180°.[32] This interconverts the enantiomers and exchanges the diastereotopic methyl groups. However, it seems from Figure 2.5 that in tetrakis(triarylphosphine) analogs such as **6**, such rotations should have much higher activation barriers. The issue then becomes introducing a single triarylphosphine with groups that will become diastereotopic on each platinum. One possibility would be to append an isopropyl substituent, such as with $(p\text{-}i\text{PrC}_6\text{H}_4)_3\text{P}$. However, this increases the distance between the diastereotopic groups and the axis of chirality, so the methyl signals may become more difficult to differentiate by NMR.[33]

With regard to endgroup rotation, the heterobimetallic ethynediyl complexes *trans*-$(\eta^5\text{-}C_5Me_5)Re(NO)(PPh_3)(C{\equiv}C)Pd(PEt_3)_2(Cl)$ and *trans*-$(\eta^5\text{-}C_5Me_5)Re(NO)(PPh_3)(C{\equiv}C)Rh(PPh_3)_2(CO)$ merit emphasis.[27] These feature chiral pseudotetrahedral rhenium and square planar palladium or rhodium termini. Both compounds – but not the butadiynediyl (C≡CC≡C) analogs – show two $R_3PMPR_3$ $^{31}P$ NMR signals at low temperature, indicating restricted rotation about the ReC≡CPd/Rh linkages. Coalescence occurs upon warming, establishing barriers ($\Delta G^{\ddagger}(T_{coal})$) of 11.7-10.9 kcal/mol. In view of these data, **4** almost certainly represents a "near miss" with respect to similar decoalescence phenomena.

Yet another strategy would be to engineer sufficiently high barriers to endgroup rotation that the atropisomers could be physically separated. The most obvious technique would be "chiral chromatography". The resulting samples would be optically active, rendering NMR probes of atropisomerism unnecessary. The rate of endgroup rotation could be derived (or bounded) from the racemization rate. Such complexes might also be active as enantioselective catalysts, but since most square planar metal catalysts require ligand dissociation steps, there may be problems with configurational stabilities. However, introducing a pendant phosphido ligand (perhaps in place of a $C_6F_5$ group in **4**) could provide a link to a catalytically active metal of any coordination geometry.

In summary, while the title quest remains unconsummated, the data provide a clear road map for refined approaches that should eventually yield atropisomers. Ultimately, this well established type of organic stereoisomerism is certain to have a counterpart in the coordination chemistry of square planar metal complexes.

**2.4 Experimental section**

Reactions were conducted under nitrogen atmospheres. Workups were carried out in air. Chemicals were treated as follows: $CH_2Cl_2$ (for reactions), dried and degassed with a Glass Contour solvent purification system; hexanes (98.5%, Aldrich), $CH_2Cl_2$ (99.5%, EMD; for chromatography), $HNEt_2$ (99.5%, Aldrich), CuCl (99.999%, Acros; stored in glove box), CuI (99.999%, Alfa Aesar; stored in glove box), $Me_2PhP$ (99%, Strem), *p*-$tol_3P$ (95%, TCI), $HC{\equiv}CSiEt_3$ (97%, Strem), *n*-$Bu_4NF$ (Acros), $CDCl_3$, and

$CD_2Cl_2$ (2 × Cambridge Isotope Laboratories), used as received. The solvent $CDFCl_2$ was prepared by a literature procedure.[24]

NMR spectra were recorded at ambient probe temperatures unless noted and referenced as follows ( /ppm): $^1H$, residual internal $CHCl_3$ (7.26); $^{13}C$, internal $CDCl_3$ (77.0); $^{31}P$, external $H_3PO_4$ (0.00). Melting points were recorded with a Stanford Research Systems (SRS) MPA100 (Opti-Melt) automated system. Microanalyses were conducted by Atlantic Microlab.

***trans*-($C_6F_5$)($Me_2PhP$)(*p*-$tol_3P$)Pt(Cl) (2)**. A Schlenk flask was charged with *trans*-($C_6F_5$)(*p*-$tol_3P)_2$Pt(Cl) (**1**,[20] 0.503 g, 0.501 mmol), $Me_2PhP$ (0.279 g, 2.02 mmol), and $CH_2Cl_2$ (15 mL). The mixture was stirred for 3 d. The solvent was removed by rotary evaporation, and the residue was chromatographed (alumina, 3 cm × 15 cm, packed with hexanes, eluted with a $CH_2Cl_2$/hexanes gradient (0:100 to 40:60 v/v)). The solvent was removed from the product containing fractions by oil pump vacuum to give **2** as a white solid (0.285 g, 0.341 mmol, 68%), mp 210 °C. Calcd for $C_{35}H_{32}ClF_5P_2Pt$: C, 50.04; H, 3.84. Found: 50.01; H, 3.82.

NMR ($CDCl_3$, δ in ppm): $^1H$ (500 MHz) 7.51 (m, 2H, *o* to P, Ph), 7.47 (m, 6H, *o* to P, tol), 7.32 (m, 3H, *m*/*p* to P, Ph), 7.11 (d, $^3J_{HH}$ = 8.1 Hz, 6H, *m* to P, tol), 2.34 (s, 9H, $CCH_3$), 1.78 (dd, $^2J_{HP}$ = 10.5 Hz, $^4J_{HP}$ = 2.7 Hz, 6H, $PMe_2$); $^{13}C\{^1H\}$ (125 MHz) 145.9 (dd, $^1J_{CF}$ = 229 Hz, $^2J_{CF}$ = 23 Hz, *o* to Pt), 140.9 (d, $^4J_{CP}$ = 2.3 Hz, *p* to P, tol), 136.8 (dm, $^1J_{CF}$ = 238 Hz, *m*/*p* to Pt), 134.5 (d, $^2J_{CP}$ = 10.4 Hz, *o* to P, tol), 132.9 (dd, $^1J_{CP}$ =

54 Hz, $^{3}J_{CP}$ = 3.1 Hz, *i* to P, Ph), 130.6 (d, $^{2}J_{CP}$ = 9.7 Hz, *o* to P, Ph), 130.3 (d, $^{4}J_{CP}$ = 2.0 Hz, *p* to P, Ph), 128.9 (d, $^{3}J_{CP}$ = 10.8 Hz, *m* to P, tol), 128.4 (d, $^{3}J_{CP}$ = 10.0 Hz, *m* to P, Ph), 126.6 (dd, $^{1}J_{CP}$ = 55.4 Hz, $^{3}J_{CP}$ = 2.7 Hz, *i* to P, tol), 111.1 (t, $^{2}J_{CF}$ = 43.5 Hz *i* to Pt), 21.5 (s, C$\underline{C}$H$_3$), 12.3 (dd, $^{1}J_{CP}$ = 36.6 Hz, $^{3}J_{CP}$ = 1.7 Hz, $^{2}J_{CPt}$ (satellite) = 37.6 Hz, $PMe_2$); $^{31}P\{^{1}H\}$ (202 MHz) 19.49 (d, $^{2}J_{PP}$ = 450 Hz, *p*-tol$_3$P; $^{1}J_{PPt}$ = 2621 Hz[34]), –6.00 (d, $^{2}J_{PP}$ = 450 Hz, $Me_2PhP$; $^{1}J_{PPt}$ = 2614 Hz[34]).

***trans*-($C_6F_5$)($Me_2PhP$)(*p*-tol$_3$P)Pt(C≡CSi$Et_3$) (3)**. A Schlenk flask was charged with **2** (0.114 g, 0.136 mmol), CuI (0.015 g, 0.077 mmol),[22] and $HNEt_2$ (10 mL), and cooled to –45 °C (acetonitrile/$CO_2$). Then HC≡CSi$Et_3$ (1.07 g, 7.82 mmol) was added with stirring. After 3 h, the cold bath was removed. After 2 d, TLC showed that no **2** remained, and three new bands. The solvent was removed by rotary evaporation and the residue was chromatographed (alumina, 3 cm × 25 cm, packed with hexanes, eluted with a $CH_2Cl_2$/hexanes gradient (0:100 to 20:80 v/v)). The solvent was removed from the product containing fractions (middle TLC band) by oil pump vacuum to give **3** as an orange oil (0.079 g, 0.085 mmol, 62%). For $^{31}P\{^{1}H\}$ NMR data and probable structures for the species in the other bands, see the text.

NMR ($CDCl_3$, δ in ppm): $^{1}H$ (500 MHz) 7.61 (m, 2H, *o* to P, Ph), 7.47 (m, 6H, *o* to P, tol), 7.33 (m, 3H, *m*/*p* to P, Ph), 7.06 (d, $^{3}J_{HH}$ = 6.5 Hz, 6H, *m* to P, tol), 2.33 (s, 9H, $CCH_3$), 1.85 (dd, $^{2}J_{HP}$ = 10.6 Hz, $^{4}J_{HP}$ = 2.6 Hz, 6H, $PMe_2$), 0.66 (m, 9H, $CH_3$, $SiEt_3$),

0.20 (m, 6H, $CH_2$, $SiEt_3$); $^{31}P\{^1H\}$ (202 MHz) 14.77 (d, $^2J_{PP}$ = 448 Hz, *p*-$tol_3P$; $^1J_{PPt}$ = 2608 Hz[34]), –14.51 (d, $^2J_{PP}$ = 448 Hz, $Me_2PhP$; $^1J_{PPt}$ = 2598 Hz[34]).

***trans*,*trans*-($C_6F_5$)(*p*-$tol_3P$)($Me_2PhP$)Pt(C≡C)Pt($PPhMe_2$)(P*p*-$tol_3$)($C_6F_5$) (4) and *trans*,*trans*-($C_6F_5$)($Me_2PhP$)$_2$Pt(C≡C)Pt($PPhMe_2$)(P*p*-$tol_3$)($C_6F_5$) (5)**. A Schlenk flask was charged with **2** (0.150 g, 0.179 mmol), $HNEt_2$ (30 mL), and CuCl (0.004 g, 0.04 mmol). The mixture was stirred until a clear solution formed and then cooled to –45 °C. Another Schlenk flask was charged with **3** (0.144 g, 0.155 mmol) and $CH_2Cl_2$ (5 mL). Then *n*-$Bu_4NF$ (1.0 M in THF/5 wt% $H_2O$, 0.03 mL, 0.03 mmol) was added. The solution was stirred for 15 min, cooled to –45 °C, and then transferred to the solution of **2** with stirring. The mixture was allowed to warm to room temperature. After 5 d, the solvent was removed by rotary evaporation and the residue was chromatographed (alumina, 3 cm × 25 cm, packed with hexanes, eluted with a $CH_2Cl_2$/hexanes gradient (0:100 to 30:70 v/v)). The main fraction containing all PtC≡CPt species was collected, and the sample was further purified by preparative TLC (40:60 v/v $CH_2Cl_2$/hexanes). Of the most prominent bands ($R_f$ 0.77, 0.55, 0.50, 0.44, 0.41, 0.32), two (0.55, 0.44) were extracted with $CH_2Cl_2$. The samples were filtered, and the solvents were removed by oil pump vacuum to give **4** as a light yellow solid (0.0059 g, 0.0036 mmol, 2.3%) and **5** as a pale yellow solid (0.0156 g, 0.087 mmol, 5.6%), respectively.

**Data for 4**. mp 190 °C. NMR ($CDCl_3$, δ in ppm): $^1H$ (500 MHz) 7.62 (m, 12H, *o* to P, tol), 7.35 (m, 4H, *o* to P, Ph), 7.13 (m, 6H, *m*/*p* to P, Ph), 6.90 (d, $^3J_{HH}$ = 5.0 Hz,

12H, *m* to P, tol), 2.28 (s, 18H, $CCH_3$), 1.37 (dd, $^2J_{HP}$ = 10.5 Hz, $^4J_{HP}$ = 2.3 Hz, 12H, $PMe_2$); $^{13}C\{^1H\}$ (125 MHz)[35] 147.4 (d, $^1J_{CF}$ = 316.3 Hz, *o* to Pt), 139.8 (d, $^4J_{CP}$ = 2.5 Hz, *p* to P, tol), 134.8 (d, $^2J_{CP}$ = 13.0 Hz, *o* to P, tol), 134.4 (dd, $^1J_{CP}$ = 23.8 Hz,[35] $^3J_{CP}$ = 3.8 Hz,[35] *i* to P, Ph), 130.6 (d, $^2J_{CP}$ = 10.0 Hz, *o* to P, Ph), 129.3 (d, $^4J_{CP}$ = 6.3 Hz,[35] *p* to P, Ph), 128.8 (d, $^3J_{CP}$ = 16.3 Hz,[35] *m* to P, Ph), 128.0 (d, $^3J_{CP}$ = 10.0 Hz, *m* to P, tol), 127.5 (d, $^1J_{CP}$ = 11.3 Hz, *i* to P, tol), 114.6 (t, $^2J_{CF}$ = 40.6 Hz, *i* to Pt), 90.0 (s, Pt*C*≡), 23.2 (s, C$\underline{C}H_3$), 13.8 (dd, $^1J_{CP}$ = 38.8 Hz, $^3J_{CP}$ = 1.8 Hz, $PMe_2$); $^{31}P\{^1H\}$ (202 MHz) 12.72 (d, $^2J_{PP}$ = 428 Hz, *p*-$tol_3P$), –13.57 (d, $^2J_{PP}$ = 428 Hz, $Me_2PhP$).

**Data for 5**. NMR ($CDCl_3$, δ in ppm): $^1H$ (500 MHz) 7.46 (m, 6H, *o* to P, tol), 7.32 (m, 6H, *o* to P, Ph), 7.30 (m, 9H, *m*/*p* to P, Ph), 7.09 (d, $^3J_{HH}$ = 5.0 Hz, 6H, *m*/*p* to P, tol), 2.33 (s, 9H, $CCH_3$), 1.77 (dd, $^2J_{HP}$ = 10.5 Hz, $^4J_{HP}$ = 2.6 Hz, 6H, $PMe_2$), 1.25 (apparent d, $J_{HP}$ = 6.0 Hz, 12H, $PMe_2$); $^{31}P\{^1H\}$ (202 MHz) 15.97 (d, $^2J_{PP}$ = 446 Hz, *p*-$tol_3P$), –8.33 (s, 2$PMe_2Ph$), –9.51 (d, $^2J_{PP}$ = 446 Hz, $Me_2PhP$).

### 2.5 Crystallography

**A.** A $CH_2Cl_2$/hexanes (1:5 v/v) solution of **2** was kept in a refrigerator. After 7 d, data were collected on a colorless thin plate as outlined in Table 2.1. Cell parameters were obtained from 60 data frames using a 0.5° scan and refined with 37445 reflections using the program Cell Now. Integrated intensity information for each reflection was obtained by reduction of the data frames with APEX2.[36] Data were scaled, and

absorption corrections were applied using the program SADABS.[37] The structure was solved by direct methods using SHELXTL (XS) and refined (weighted least squares refinement on $F^2$).[38,39] Non-hydrogen atoms were refined with anisotropic thermal parameters. Hydrogen atoms were placed in idealized positions and were set riding on the parent atoms. PLATON was used to verify the absence of additional symmetry or voids.[40] Olex2 was employed for the final data presentation and structure plots.[39] **B.** A $CH_2Cl_2$/hexanes (1:12 v/v) solution of **4** was kept in a refrigerator. After 30 d, data were collected on a colorless thin plate as outlined in Table 2.1. The structure was solved and refined analogously to that of **2** (60 data frames, 0.5° scan, 72057 reflections). **C.** A $CH_2Cl_2$/hexanes (1:4 v/v) solution of **5** was kept in a refrigerator. After 7 d, data were collected on a colorless thin plate as outlined in Table 2.1. The structure was solved and refined analogously to that of **2** (60 data frames, 0.5° scan, 64243 reflections).

CCDC-1512409 (for **2**), -1512410 (for **4**), and -1512411 (for **5**) contain the supplementary crystallographic data for this paper. These data can be obtained free of charge from The Cambridge Crystallographic Data Centre via www.ccdc.cam.ac.uk/data_request/cif.

Table 2.1 Summary of crystallographic data

| Complex | **2** | **4** | **5** |
|---|---|---|---|
| Empirical formula | $C_{35}H_{32}ClF_5P_2Pt$ | $C_{72}H_{64}F_{10}P_4Pt_2$ | $C_{59}H_{54}F_{10}P_4Pt_2$ |
| Formula weight | 840.08 | 1633.29 | 1467.08 |
| Diffractometer | BRUKER APEX2 | BRUKER APEX2 | BRUKER APEX2 |
| Temperature [K] | 110.15 | 110.15 | 110.15 |
| Wavelength [Å] | 0.71073 | 0.71073 | 0.71073 |
| Crystal system | Monoclinic | Monoclinic | Monoclinic |
| Space group | $P_12_1/c_1$ | $C_12_1/c_1$ | $P_12_1/c_1$ |
| Unit cell dimensions | | | |
| *a* [Å] | 8.5080(17) | 54.510(10) | 12.4743(10) |
| *b* [Å] | 24.712(5) | 10.7037(19) | 28.231(2) |
| *c* [Å] | 16.297(3) | 21.931(4) | 15.8257(13) |
| α [°] | 90 | 90 | 90 |
| β [°] | 104.731(2) | 92.896(2) | 101.4680(10) |
| γ [°] | 90 | 90 | 90 |
| Volume [Å$^3$] | 3313.9(11) | 12780(4) | 5461.9(8) |
| Z | 4 | 8 | 4 |
| $\rho_{calcd}$ [Mg/m$^3$] | 1.684 | 1.698 | 1.784 |
| Absorption coefficient [mm$^{-1}$] | 4.463 | 4.546 | 5.307 |
| F(000) | 1648 | 6416 | 2856 |
| Crystal size[mm$^3$] | 0.56 × 0.54 × 0.32 | 0.32 × 0.06 × 0.04 | 0.20 × 0.19 × 0.16 |
| Θ range of data collection [°] | 1.532 to 27.462 | 1.859 to 27.420 | 1.666 to 27.464 |

Table 2.1 Continued

| Complex | **2** | **4** | **5** |
|---|---|---|---|
| Index ranges | $-11 \le h \le 10$, | $-70 \le h \le 70$, | $-16 \le h \le 16$ |
| | $-31 \le k \le 32$, | $-13 \le k \le 13$, | $-36 \le k \le 36$ |
| | $-21 \le l \le 21$ | $-28 \le l \le 28$ | $-20 \le l \le 20$ |
| Reflections collected | 37445 | 72057 | 64243 |
| Independent reflections | 7540 [R(int) = 0.0840] | 14389 [R(int) = 0.0379] | 12490 [R(int) = 0.0419] |
| Completeness to Θ | 100.0 % (25.242) | 99.8 % (25.242) | 100.0 % (25.242) |
| Max. and min. transmission | 0.7456 and 0.2412 | 0.4305 and 0.1993 | 0.7456 and 0.5461 |
| Data / restraints / parameters | 7540 / 0 / 402 | 14389 / 72 / 803 | 12490 / 0 / 685 |
| Goodness-of-fit on $F^2$ | 1.030 | 1.064 | 1.027 |
| Final R indices [$I>2\sigma(I)$] | | | |
| $R_1$ | 0.0342 | 0.0315 | 0.0243 |
| $wR_2$ | 0.0793 | 0.0689 | 0.0486 |
| R indices (all data) | | | |
| $R_1$ | 0.0404 | 0.0397 | 0.0334 |
| $wR_2$ | 0.0823 | 0.0720 | 0.0513 |
| Largest diff. peak and hole [$e.Å^{-3}$] | 2.332 and –2.567 | 1.959 and –1.603 | 1.466 and –0.680 |

Table 2.2 Key crystallographic bond lengths [Å] and angles [°]

| | **2** | **4** | **5** |
|---|---|---|---|
| Pt(1)-P(1) | 2.2831(10) | 2.2814(11) | 2.2872(9) |
| Pt(1)-P(2) | 2.3003(10) | 2.2810(12) | 2.2877(9) |
| Pt(1)-Cl(1) | 2.3623(11) | - | - |
| Pt(1)-C(1) | 2.014(4) | 2.008(4) | 2.013(3) |
| Pt(1)-C(3) | - | 2.062(4) | 2.076(3) |
| Pt(2)-P(3) | - | 2.2811(10) | 2.2802(8) |
| Pt(2)-P(4) | - | 2.2658(11) | 2.3080(8) |
| Pt(2)-C(2) | - | 2.016(4) | 2.020(3) |
| Pt(2)-C(9)/C(38) | - | 2.068(4) | 2.064(3) |
| C(1)-C(2) | - | 1.213(5) | 1.215(4) |
| P(2)-Pt(1)-P(1) | 175.81(3) | 168.61(4) | 175.88(3) |
| C(1)-Pt(1)-P(1) | 90.05(10) | 89.18(11) | 87.75(9) |
| C(1)-Pt(1)-P(2) | 93.36(10) | 86.00(11) | 88.46(9) |
| C(1)-Pt(1)-C(3)/Cl(1) | 177.51(10) | 175.79(16) | 177.16(13) |
| C(3)/Cl(1)-Pt(1)-P(1) | 87.57(4) | 92.39(11) | 91.18(9) |
| C(3)/Cl(1)-Pt(1)-P(2) | 89.05(4) | 93.14(11) | 92.68(9) |
| P(4)-Pt(2)-P(3) | - | 171.77(4) | 175.02(3) |
| C(2)-Pt(2)-P(3) | - | 88.93(11) | 87.23(9) |
| C(2)-Pt(2)-P(4) | - | 85.22(11) | 89.34(9) |
| C(2)-Pt(2)-C(9)/C(38) | - | 179.39(15) | 178.54(13) |
| C(9)/C(38)-Pt(2)-P(3) | - | 91.64(11) | 92.25(9) |
| C(9)/C(38)-Pt(2)-P(4) | - | 94.23(11) | 91.26(9) |
| C(2)-C(1)-Pt(1) | - | 172.9(3) | 173.7(3) |
| C(1)-C(2)-Pt(2) | - | 175.0(3) | 174.7(3) |

# 3. SYNTHESES AND STRUCTURES OF SQUARE PLANAR DIPLATINUM BUTADIYNEDIYL COMPLEXES WITH TWO DIFFERENT MONOPHOSPHINE LIGANDS ON EACH TERMINUS; PROBING THE FEASIBILITY OF A NEW TYPE OF INORGANIC ATROPISOMERISM

## 3.1 Introduction

There is an extensive literature of complexes in which two square planar platinum(II) fragments cap butadiynediyl or -C≡C-C≡C- moieties. [20,21b,41-43] There is also an extensive literature involving higher homologs with as many as 28 sp carbon atoms. [20,21b,41c,42-46] However, there are a number of interesting properties or phenomena that are uniquely associated with shorter sp carbon bridges. For example, the platinum(II)/platinum(III) radical cations generated by one electron oxidations are much more stable at modest chain lengths.[20,42a,47]

In a recent paper,[48] we described a quest for atropisomers[1,4a,12,16] derived from diplatinum ethynediyl or PtC≡CPt complexes.[31,49] The idea was that with appropriate substitution patterns, as exemplified in Scheme 3.1 with adducts that bear two different *trans* disposed monophosphine ligands on each platinum, it might be possible to separate enantiomers or diastereomers with an axis of chirality. Alternatively, slow interconversion could be established by NMR techniques. To date, these efforts have not resulted in a demonstration of atropisomerism. However, this is likely because the phosphine ligands initially employed were not bulky enough (e.g., X/Y = Ph/Me in **I**).

Promising second generation targets are easily envisioned (e.g., X/Y = Ph/*t*-Bu or *i*-Pr/*o*-$C_6H_4X$).

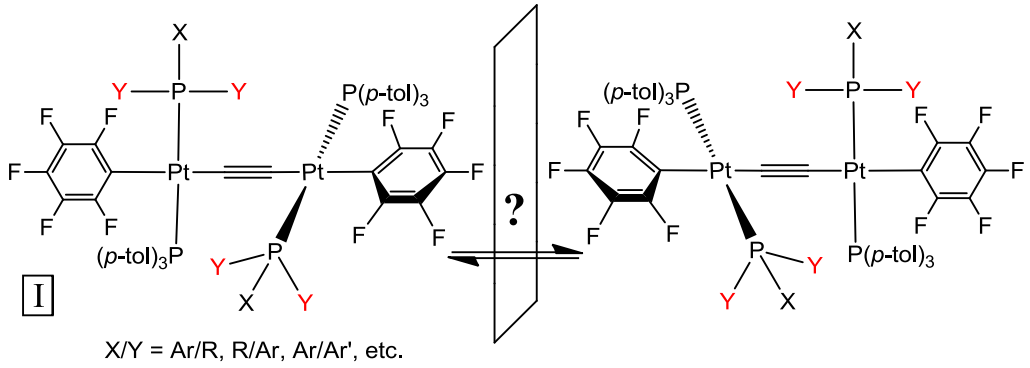


**Scheme 3.1**. Enantiomeric atropisomers derived from diplatinum ethynediyl complexes. The Y groups are diastereotopic and potentially distinguishable by NMR.

In laying the groundwork for these studies, related complexes with longer PtC≡CC≡CPt bridges were also investigated. Although in retrospect there was little chance of detecting atropisomerism in such species, they provided valuable testing grounds for syntheses of coupling partners, such as platinum chloride complexes with the types of monophosphine ligands in Scheme 3.1, *trans*-(Ar)($R_2$PhP)(*p*-$tol_3$P)Pt(Cl).[50] They also revealed problematic phosphine scrambling processes under certain coupling conditions, and "standard" protocols that became unreliable in the presence of bulkier phosphine ligands. Furthermore, several crystal structures that help visualize the magnitudes of the endgroup/endgroup interactions, which must underpin any atropisomerism, could be determined. Accordingly, in this full paper, a detailed account of this previously undisclosed work is presented.

## 3.2 Results

As noted on page vii of this dissertation, some of the results on this section were acquired by Dr. Sandip Dey. However, all of Dr. Dey's data were indepently analyzed and interpreted by the author.

### 3.2.1. Syntheses of monoplatinum complexes *trans*-($C_6F_5$)($R_2$PhP)(*p*-$tol_3$P)Pt(Cl)

The previously reported platinum chloride complex *trans*-($C_6F_5$)(*p*-$tol_3P)_2$Pt(Cl) (**PtCl**)[20] and $Me_2$PhP (1.0 equiv) were combined in $CH_2Cl_2$ at room temperature. As shown in Scheme 3.2 (top), workup gave the monosubstitution product *trans*-($C_6F_5$)($Me_2$PhP)(*p*-$tol_3$P)Pt(Cl) (**Pt'Cl-a**) as a white solid in 89% yield. In some cases, small amounts of **PtCl** remained, or the disubstituted byproduct *trans*-($C_6F_5$)($Me_2$PhP)$_2$Pt(Cl) (**Pt"Cl-a**) was detected (each $\leq$4%). In these cases, **Pt'Cl-a** was purified chromatographically. The identity of **Pt"Cl-a** was confirmed by an independent synthesis from [($C_6F_5$)(tht)Pt($\mu$-Cl)]$_2$ and $Me_2$PhP (73%; Scheme 3.2, bottom). This route has been used to prepare many related platinum bis(phosphine) complexes.[20,21b,45g,i]

Similar reactions were carried out with three other phosphines of the formula $R_2$PhP (R = alkyl or aryl; **b-d** in Scheme 3.2). With the triarylphosphines (*p*-*t*-$BuC_6H_4)_2$PhP and (*p*-$MeOC_6H_4)_2$PhP, no reactions with **PtCl** occurred over the course of 16 h in refluxing $CH_2Cl_2$. However, after 22 h in refluxing toluene, the target complexes *trans*-($C_6F_5$)(*p*-$tol_3$P)((*p*-*t*-$BuC_6H_4)_2$PhP)Pt(Cl) (**Pt'Cl-b**) and *trans*-

$(C_6F_5)(p\text{-tol}_3P)((p\text{-MeOC}_6H_4)_2PhP)Pt(Cl)$ (**Pt'Cl-c**) could be isolated in 29-42% yields following chromatography.

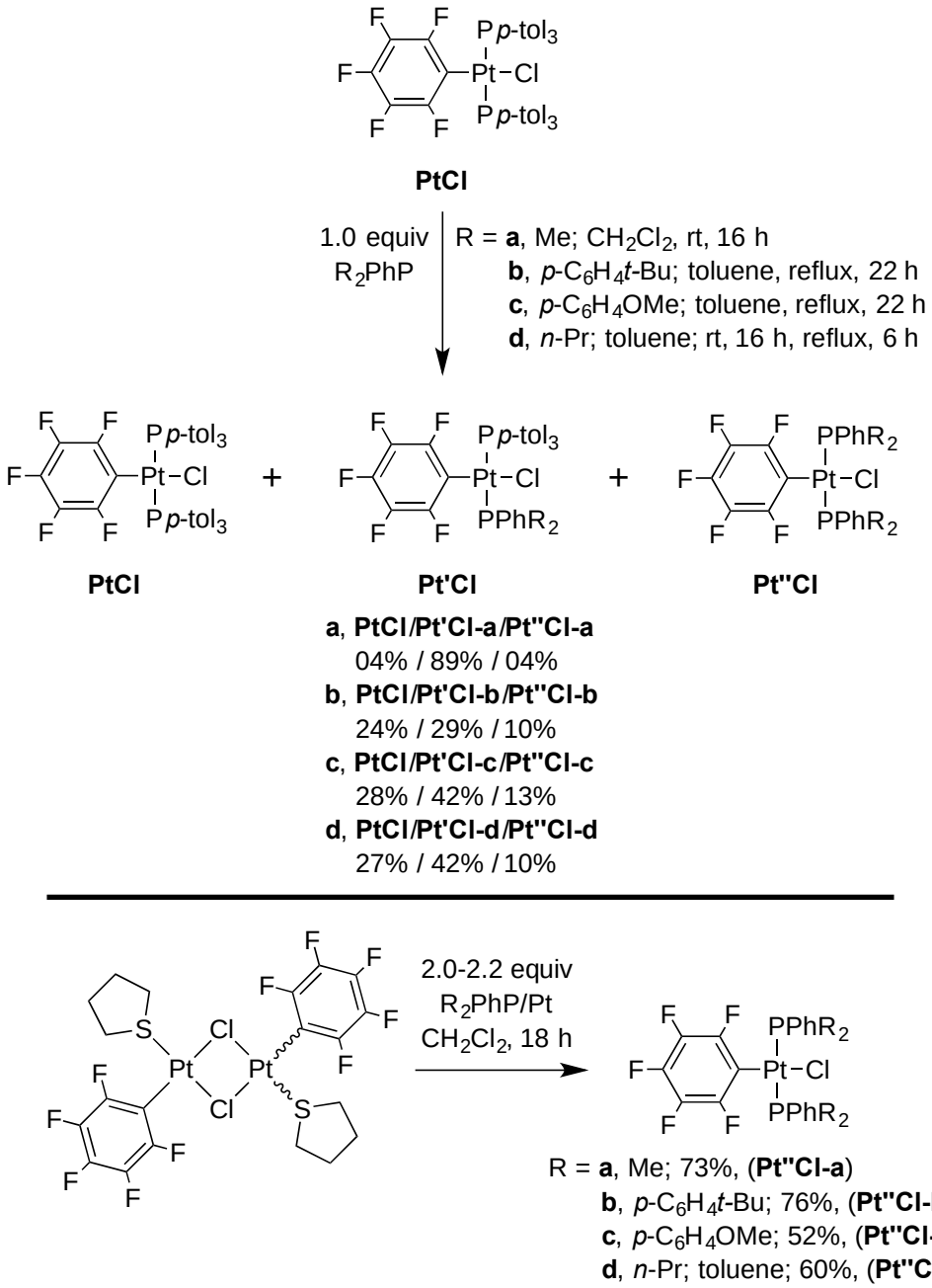


**Scheme 3.2**. Syntheses of monoplatinum complexes *trans*-$(C_6F_5)(R_2PhP)(p\text{-tol}_3P)Pt(Cl)$ (**Pt'Cl**; top) and *trans*-$(C_6F_5)(R_2PhP)_2Pt(Cl)$ (**Pt''Cl**; bottom).

When **PtCl** and *n*-$Pr_2PhP$ were combined in $CH_2Cl_2$ or toluene at room temperature, conversion to *trans*-$(C_6F_5)$(*p*-$tol_3P$)(*n*-$Pr_2PhP$)Pt(Cl) (**Pt'Cl-d**) was slow and incomplete. However, the yield of **Pt'Cl-d** improved to 42% when the sample was refluxed in toluene (6 h). In each of these reactions, smaller amounts of the disubstituted byproducts **Pt"Cl-b-d** were also obtained, as verified by independent syntheses (Scheme 3.2, bottom). Thus, not all of the starting **PtCl** was consumed.

Analogous complexes with the bulkier phosphine *t*-$Bu_2PhP$ were sought, but no reaction took place with **PtCl** in refluxing toluene. Thus, alternative routes were explored as summarized in Scheme 3.3. First, reactions of $[(C_6F_5)(tht)Pt(\mu\text{-}Cl)]_2$ and excess *t*-$Bu_2PhP$ in $CH_2Cl_2$ or refluxing toluene yielded the monophosphine complex $(C_6F_5)$(*t*-$Bu_2PhP$)(tht)Pt(Cl) (**1**) instead of the target bis(phosphine) complex *trans*-$(C_6F_5)$(*t*-$Bu_2PhP)_2$Pt(Cl) (**Pt"Cl-e**; compare to Scheme 3.2, bottom). The stereochemistry depicted in Figure 3.1 was confirmed by a crystal structure (below). Subsequent reactions of **1** with the phosphines $Et_3P$ or *p*-$tol_3P$ in refluxing toluene resulted in *t*-$Bu_2PhP$ displacement. The two-fold substitution products *trans*-$(C_6F_5)(Et_3P)_2$Pt(Cl) or *trans*-$(C_6F_5)$(*p*-$tol_3P)_2$Pt(Cl) (**PtCl**) described earlier[20,21b] were isolated.

Next, the previously reported dichloride complex *trans*-(*t*-$Bu_2PhP)_2Pt(Cl)_2$ (**2**) was synthesized by a slight modification of the literature procedure (Scheme 3.3, bottom).[51] The $^1J_{PPt}$ value (2542 Hz) indicated a *trans* stereochemistry,[52] in accord with a crystal structure.[53] However, subsequent additions of $C_6F_5Li$ (prepared *in situ* from *n*-

BuLi and $C_6F_5Br$)[54] in either 1:1 or 1:2 stoichiometries gave mainly starting material. Up to 20% conversion to a new species could be observed in some experiments, but the properties were not appropriate for the target molecule.

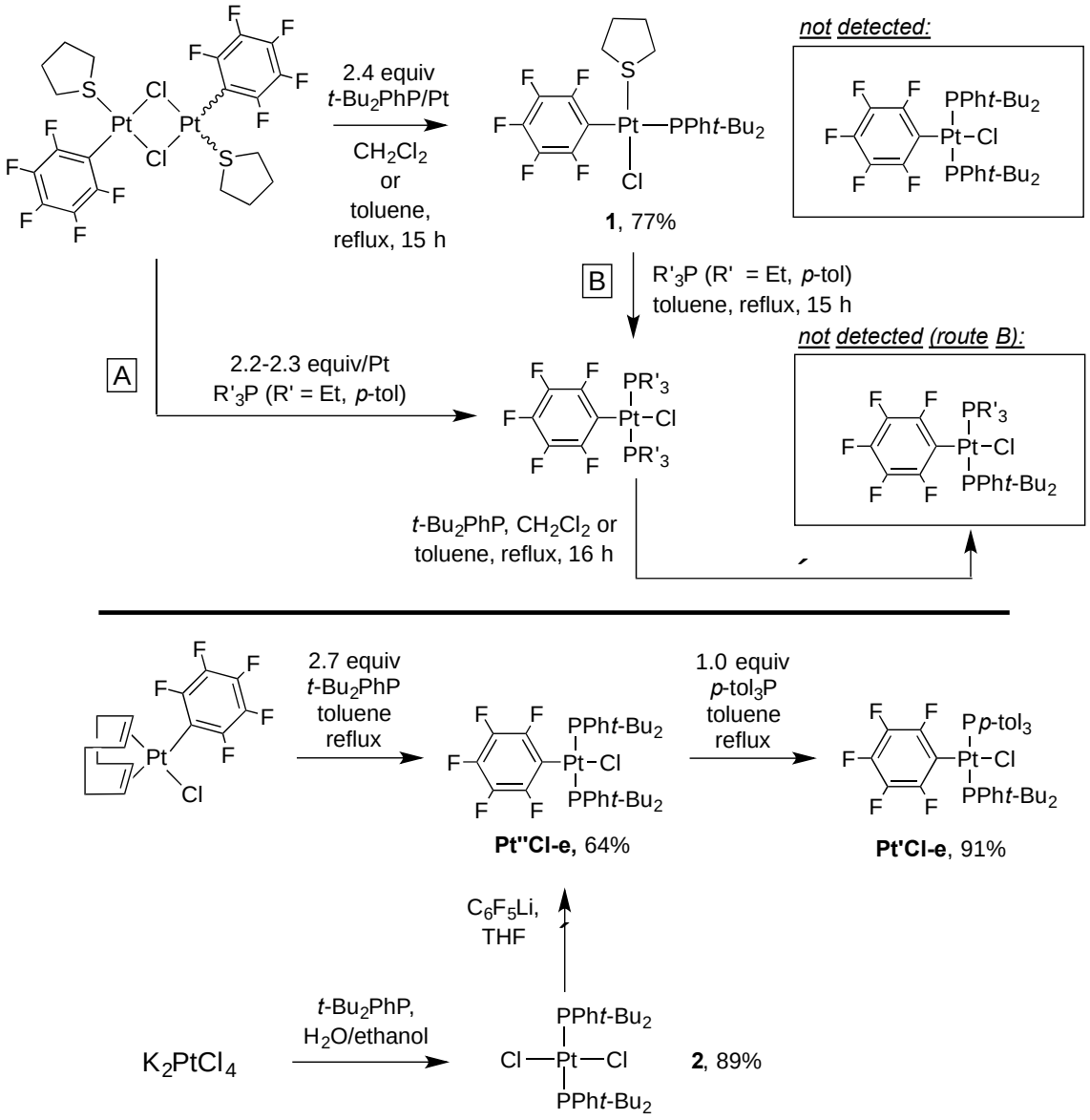


**Scheme 3.3**. Successful and unsuccessful routes to the monoplatinum complexes *trans*-($C_6F_5$)(*t*-$Bu_2$PhP)(*p*-$tol_3$P)Pt(Cl) (**Pt"Cl-e**) and *trans*-($C_6F_5$)(*t*-$Bu_2$PhP)(*p*-$tol_3$P)Pt(Cl) (**Pt'Cl-e**).

Finally, routes involving the previously described cyclooctadiene complex (cod)($C_6F_5$)Pt(Cl) were investigated (Scheme 3.3, bottom).[55] No reaction took place with *t*-$Bu_2$PhP (2.7 equiv) at room temperature, but *trans*-($C_6F_5$)(*t*-$Bu_2$PhP)$_2$Pt(Cl) (**Pt"Cl-e**) formed cleanly in refluxing toluene. A 64% yield was isolated after workup. A subsequent reaction with *p*-$tol_3$P (1.0 equiv) in refluxing toluene gave the target complex **Pt'Cl-e** in 91% yield.

### 3.2.2 Syntheses of butadiynyl complexes *trans*-($C_6F_5$)($R_2$PhP)(*p*-$tol_3$P)Pt(C≡C)$_2$H (**Pt'$C_4$H**)

The next objective was to convert the chloride complexes **Pt'Cl-a-e** to the corresponding butadiynyl complexes. As shown in Scheme 3.4 (top), conditions that were effective in an earlier synthesis of *trans*-($C_6F_5$)(*p*-$tol_3$P)$_2$Pt(C≡C)$_2$H (**Pt$C_4$H**)[20] were applied to **Pt'Cl-a** (excess butadiyne, $HNEt_2$, cat. CuI). A chromatographic workup gave the target complex *trans*-($C_6F_5$)($Me_2$PhP)(*p*-$tol_3$P)Pt(C≡C)$_2$H (**Pt'$C_4$H-a**) in 36% yield, together with lesser amounts of the phosphine scrambling products **Pt$C_4$H** (16%) and **Pt"$C_4$H-a** (10%). In an alternative approach, the butadiynyl complex **Pt$C_4$H** was treated with $Me_2$PhP (1.0 equiv, $CH_2Cl_2$, 18 h). Chromatography gave a comparable product distribution: **Pt'$C_4$H-a**, 30%, **Pt$C_4$H**, 18%, **Pt"$C_4$H-a**, 11%.

When the di(*n*-propyl)phenylphosphine chloride complex **Pt'Cl-d** and butadiyne were similarly reacted, NMR analyses showed the formation of a 92:4:4 mixture of the

target complex **Pt'C$_4$H-d** and the phosphine scrambling products **PtC$_4$H** and **Pt"C$_4$H-d**. Crystallization afforded pure **Pt'C$_4$H-d** in 73% yield. Interestingly, the two complexes with triarylphosphine ligands, **Pt'Cl-b**,**c**, did not give detectable phosphine scrambling. Workups afforded the butadiynyl complexes **Pt'C$_4$H-b**,**c** in 75-77% yields. As summarized in Scheme 3.4 (bottom), all attempts to replace the chloride ligand in **Pt'Cl-e** by alkynyl ligands were unsuccessful. Alternative cross coupling protocols (see also below)[42b] involving *t*-BuOK base and $KPF_6$ gave no reaction.

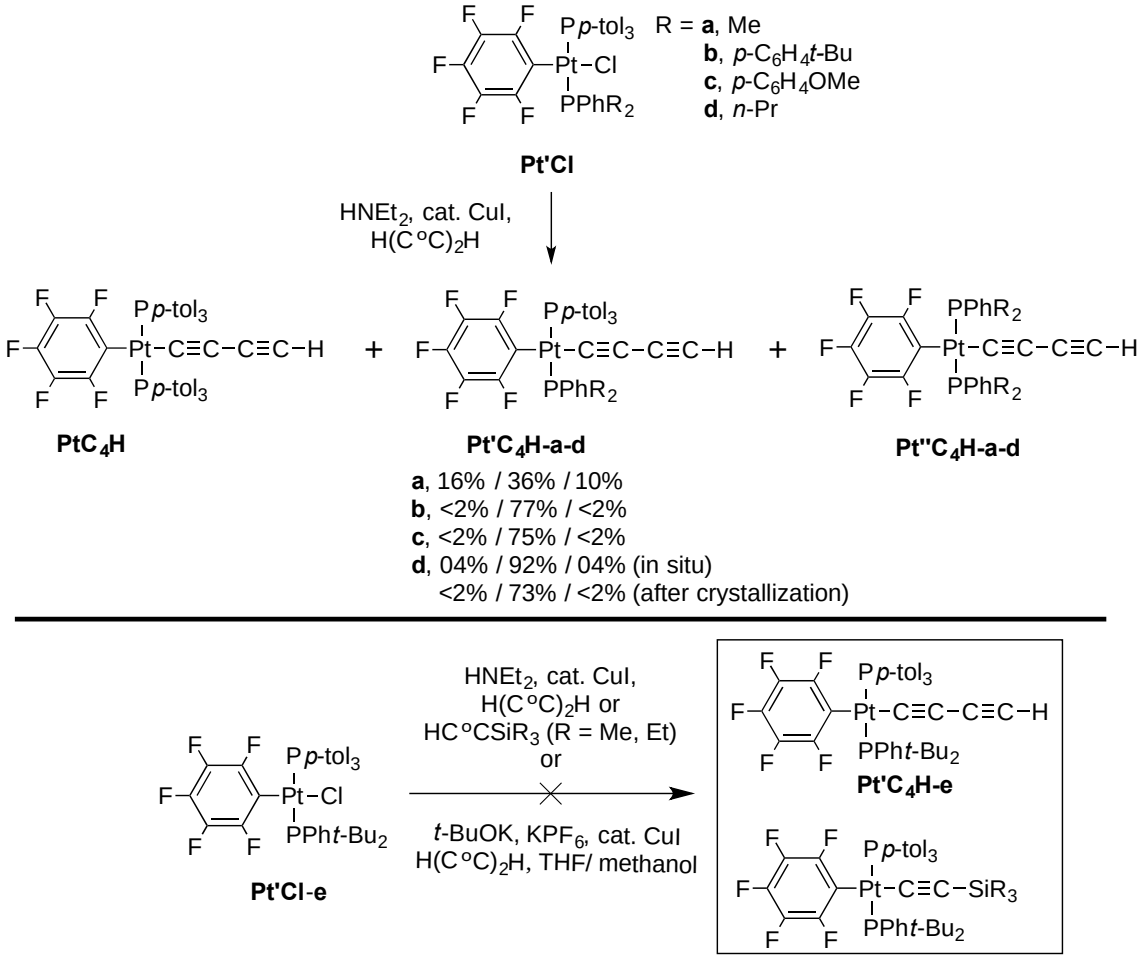


**Scheme 3.4**. Successful and unsuccessful syntheses of monoplatinum butadiynyl and alkynyl complexes.

### 3.2.3 Syntheses of diplatinum butadiynediyl complexes

Numerous diplatinum butadiynediyl complexes have been prepared by Hagihara heterocouplings of platinum butadiynyl and platinum chloride complexes.[20,21b,42b] Thus, as shown in Scheme 3.5, equimolar quantities of the butadiynyl complexes **Pt'C$_4$H-a-c** (see Scheme 3.4) and chloride complexes **Pt'Cl-a-c** (see Scheme 3.2) were combined in $HNEt_2$ in the presence of a catalytic amount of CuCl. After 66-88 h at 45-50 °C, workups gave mixtures of five to six diplatinum butadiynediyl complexes. Although the individual yields were low, they could be separated by silica gel column chromatography.

It quickly became apparent that the many products were derived from scrambling of the phosphine ligands. In our previous applications of Hagihara coupling reactions, all of the phos-phine ligands had been identical, so this phenomenon remained undetected. In accord with nomenclature introduced above, the three possible endgroups could be designated **Pt** ((C$_6$F$_5$)(*p*-tol$_3$P)$_2$Pt), **Pt'** ((C$_6$F$_5$)(*p*-tol$_3$P)(R$_2$PhP)Pt), and **Pt"** ((C$_6$F$_5$)(R$_2$PhP)$_2$Pt). These can in turn code for the six possible products, **PtC$_4$Pt**, **PtC$_4$Pt'**, **PtC$_4$Pt"**, **Pt'C$_4$Pt'**, **Pt'C$_4$Pt"** and **Pt"C$_4$Pt"**.

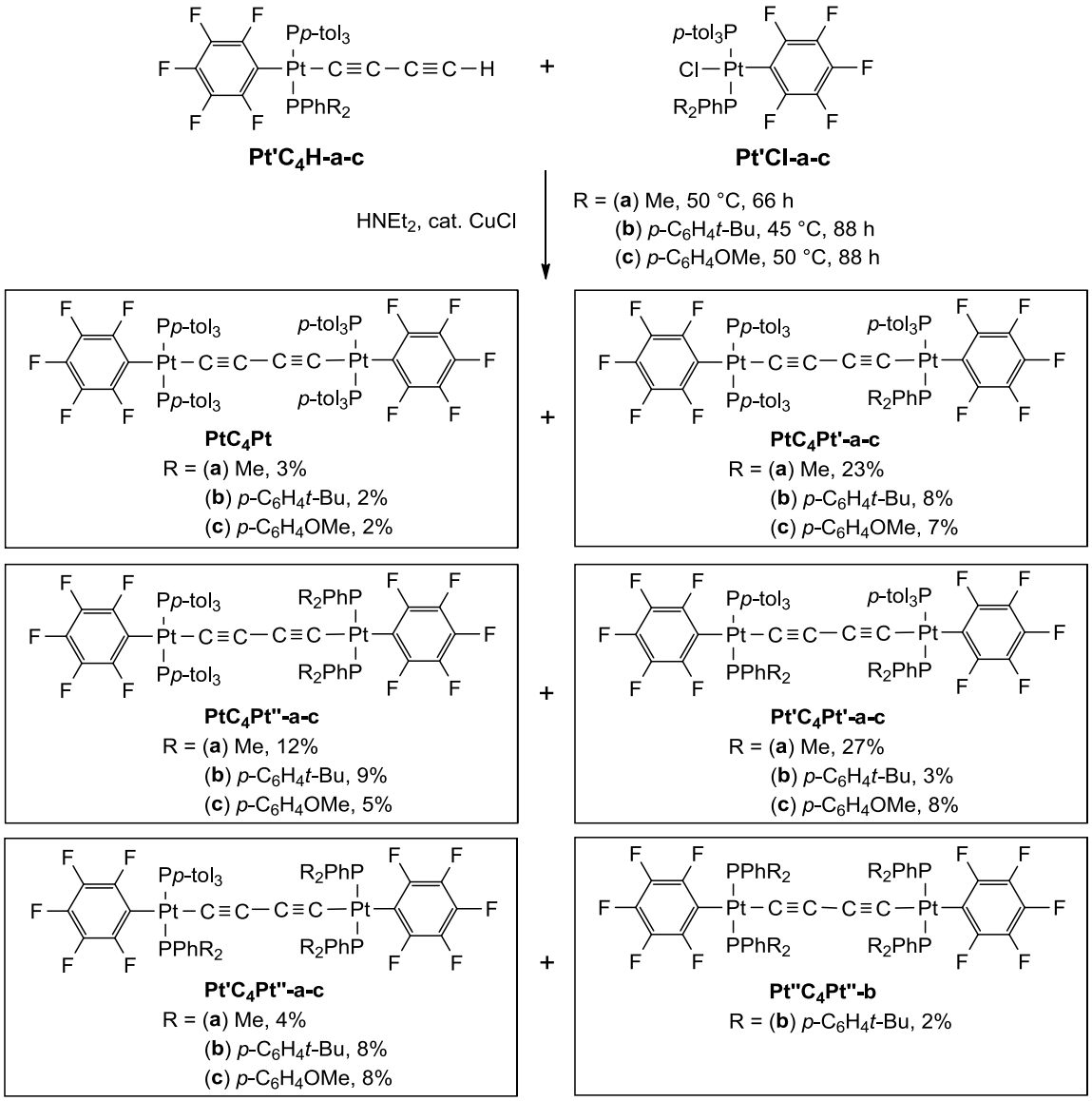


**Scheme 3.5**. Syntheses of diplatinum butadiynyl complexes.

In the case where the phenylphosphine substituents ($R_2$) were Me (**a**), five diplatinum complexes were isolated: **PtC$_4$Pt**, 3%; **PtC$_4$Pt'-a**, 23%; **PtC$_4$Pt''-a**, 12%; **Pt'C$_4$Pt'-a**, 27%; **Pt'C$_4$Pt''-a**, 4%. The $R_f$ values decreased as the number of $Me_2PhP$ ligands increased. All were air stable yellow solids, and were characterized by NMR ($^1$H, $^{13}$C{$^1$H}, $^{31}$P{$^1$H}) and microanalyses, as summarized in the experimental section. The

structures readily followed from the NMR properties, principal details of which are described below.

In the case where the phenylphosphine substituents were *p*-*t*-Bu$C_6H_4$ (**b**), six diplatinum complexes were isolated: **Pt$C_4$Pt**, 2%; **Pt$C_4$Pt'-b**, 8%; **Pt$C_4$Pt"-b**, 9%; **Pt'$C_4$Pt'-b**, 3%; **Pt'$C_4$Pt"-b**, 8%; **Pt"$C_4$Pt"-b**, 2%. In the case where the phenylphosphine substituents were *p*-Me$OC_6H_4$ (**c**), five complexes were isolated as summarized in Scheme 3.5. This coupling was somewhat slower, so a significant amount of unreacted chloride complex **Pt'Cl-c** (26%) was recovered, together with traces of the scrambled analog **PtCl** (1%).

Given these disappointing results, attention was turned to an alternative recipe for cross coupling metal chloride and terminal alkynyl complexes. It had been shown that when THF/methanol solvent mixtures were employed with slight excesses of *t*-BuOK and $KPF_6$ and a catalytic amount of CuCl, diplatinum butadiynediyl complexes could be isolated in good yields.[42b] This protocol was optimized using equimolar quantities of the *p*-$tol_3P$ substituted reaction partners *trans*-$(C_6F_5)(p\text{-}tol_3P)_2Pt(C{\equiv}C)_2H$ (**Pt$C_4$H**) and **PtCl**. As described elsewhere,[56] workup gave the known complex **Pt$C_4$Pt** in 73% yield.

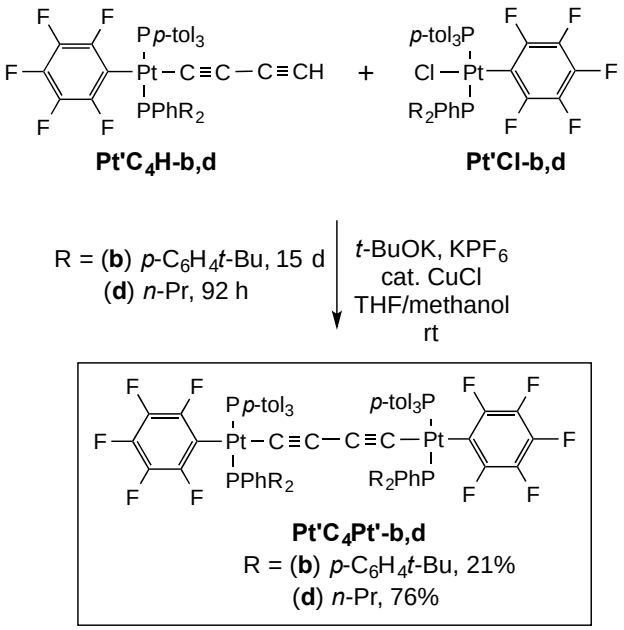


**Scheme 3.6**. Syntheses of diplatinum butadiynyl complexes; alternative cross coupling procedure.

Next, comparable conditions were applied to coupling partners that each contained two different phosphine ligands. As shown in Scheme 3.6, **Pt'C$_4$H-b** and **Pt'Cl-b** were reacted for 15 d at room temperature. Workup gave the target complex **Pt'C$_4$Pt'-b** in 21% yield, as well as traces of **PtC$_4$Pt'-b** and **Pt'C$_4$Pt''-b** (ca. 1% each). Considerable amounts of **Pt'C$_4$H-b** and **Pt'Cl-b** were recovered (19%, 36%). Comparable conversions were realized after 3-4 d at 50 °C. Finally, **Pt'C$_4$H-d** and **Pt'Cl-d** were similarly reacted. Workup after 92 h at room temperature gave the target complex **Pt'C$_4$Pt'-d** in 76% yield after crystallization. No chromatographic purification step was necessary, and no phosphine scrambling byproducts were apparent.

### 3.2.4 NMR properties

Certain NMR features of the preceding complexes merit note. In our earlier paper involving similar diplatinum ethynediyl complexes,[48] no coupling was observed between phosphine ligands on opposite termini (small $^{5}J_{PP}$). The same would be expected for the more widely separated phosphine ligands in the diplatinum butadiynediyl complexes in this study (still smaller $^{7}J_{PP}$). Thus, to a first approximation, their NMR spectra should be "hybrids" of those of the monoplatinum butadiynyl complexes corresponding to each endgroup.

This leads to a hierarchy of complexity. First, there are two "series" of butadiynediyl complexes with identical endgroups, each with two *identical* phosphine ligands: **PtC$_4$Pt** (previously reported) and **Pt"C$_4$Pt"-b** (isolated only in trace quantities). These give much simpler spectra. Next, there are the title complexes with identical endgroups, each with two *different* phosphine ligands: **Pt'C$_4$Pt'-a-d**. The $^{1}$H NMR spectra exhibit the characteristic signals of each phosphine, with only a few cases of resolved second order phenomena. However, the $^{13}$C{$^{1}$H} and $^{31}$P{$^{1}$H} NMR spectra exhibit a variety of second order features as described below. Finally, there are three series of complexes with non-identical endgroups: **PtC$_4$Pt'-a-c**, **PtC$_4$Pt"-a-c**, and **Pt'C$_4$Pt"-a-c**. While in theory these give the most complicated NMR spectra, this is only in an additive sense; they seldom introduce new phenomena not manifested in the other complexes.

With regard to the $^{31}P\{^{1}H\}$ NMR spectra, certain trends in the monoplatinum complexes deserve comment. First, **Pt'Cl-a**,**d** and **Pt'C$_4$H-a**,**d** feature one triarylphosphine ligand and one dialkylphenylphosphine ligand. They exhibit well separated signals ( 18.3 to 20.2, *p*-tol$_3$P; –9.9 to 8.8, R$_2$PPh) and couple as expected ($^{2}J_{PP}$ = 404-450 Hz). However, **Pt'Cl-b**,**c** and **Pt'C$_4$H-b**,**c** feature two similar triarylphosphine ligands.[57] With **Pt'Cl-b** and **Pt'C$_4$H-b**, only one singlet is observed ( 19.8-17.8), presumably due to accidental degeneracy. With **Pt'Cl-c** and **Pt'C$_4$H-c**, two closely spaced singlets are found ( 19.51-19.57, 17.58-17.64).

All of these trends extend to the diplatinum butadiynediyl complexes **Pt'C$_4$Pt'-a-d**. However, when $^{31}P\{^{1}H\}$ NMR spectra of **Pt'C$_4$Pt'-b** were recorded at –80 °C, separate signals for the *p*-tol$_3$P and (*p*-*t*-BuC$_6$H$_4$)$_2$PhP ligands could be observed (δ ($CD_2Cl_2$) 13.79 and 13.91 as opposed to one signal at 14.00 at 22 °C). Importantly, the structures of all four complexes have been confirmed crystallographically (below).

The $^{13}C\{^{1}H\}$ NMR spectra of **Pt'Cl-a**,**d**, **Pt'C$_4$H-a**,**d**, and **Pt'C$_4$Pt'-a**,**d** are unexceptional. However, those of **Pt'Cl-b**,**c**, **Pt'C$_4$H-b**,**c**, and **Pt'C$_4$Pt'-b**,**c** are complicated by numerous "virtual couplings".[58] That of **Pt'C$_4$Pt'-b** features a variety of virtual triplets (typically 5-6 Hz for all aryl carbon atoms that are *o*/*m* to phosphorus). In contrast, that of **Pt'C$_4$Pt'-c** exhibits a corresponding number of doublet of doublets, in which the *J* values are very close to those of the virtual triplets. Other complexes that

exhibit a large number of virtual triplets include **Pt"Cl-a** and **Pt"$C_4$H-a** (nearly all $Me_2PhP$ ligand $^{13}C$ NMR signals, and the $Me_2P$ $^1H$ NMR signal).

Many NMR spectra were recorded at low temperature in hopes of detecting dynamic processes or separate signals for diastereotopic groups as diagrammed in Scheme 3.1. All of these were uninformative. For example, the $^1H$ NMR spectra of **Pt'$C_4$Pt'-a** and **Pt'$C_4$Pt'-c** ($CD_2Cl_2$) did not show any significant changes when cooled to –80 °C. In the case of **Pt'$C_4$Pt'-b**, some $^1H$ NMR peaks became broader, but no decoalescence phenomena were detected. With **Pt'$C_4$Pt'-b**,**c**, the *ipso* carbon atoms of the $(p\text{-}XC_6H_4)_2P$ moieties are potentially diastereotopic, but only broadened $^{13}C\{^1H,^{31}P\}$ signals were observed at –80 °C.

NMR spectra of the more soluble complex **Pt'$C_4$Pt'-d** were recorded in the lower freezing solvent $CDFCl_2$.[24] Some $^1H$ NMR signals merged as the temperature was lowered, but no decoalescence was apparent at –120 °C. The $^{13}C\{^1H\}$ NMR spectrum showed only broadening, and the $^{31}P\{^1H\}$ NMR spectrum was essentially unchanged.

### 3.2.5 Structural properties

Crystal structures were sought as a means of confirming structural assignments, and for gauging endgroup/endgroup interactions in the diplatinum complexes. Single crystals of **1**, **Pt"Cl-e**, **Pt'$C_4$H-a**, **Pt'$C_4$Pt'-a-d**, and **Pt$C_4$Pt"-b** or solvates thereof were grown, and the structures were determined as outlined in Tables 3.1-3.3 and the experimental section. Key metrical parameters are provided in Table 3.3 and Figures 3.1-

3.3. Many other tetraphosphine complexes with $ArPt(C{\equiv}C)_mPtAr$ linkages have been structurally characterized,[20,21b,23,42,45a-c,e-k,n-p] and the bond lengths and angles in Table 3.3 are unexceptional.

The molecular structures are depicted in Figures 3.1-3.8, and additional representations are provided below and in the supplementary material. About half of the lattices contained some type of disorder, which was modeled as detailed in the experimental section. Both **Pt'$C_4$Pt'-a** and **Pt'$C_4$Pt'-d** exhibited centers of inversion at the midpoints of the $C_4$ chains.

For the diplatinum complexes, a measure of the "twist" associated with the square planar endgroups was sought. In one approach, least squares planes were defined using the P-Pt-P linkage on one terminus, and the platinum from the other. For the idealized atropisomers in Scheme 3.1, the angle defined by these two planes would be 90°. As summarized in Table 3.3, the angles between the planes in the crystal structures ranged from 0° for the complexes with an inversion center to 44-51° for the others. When planes defined by the P-Pt-P linkages and the ligating $C_6F_5$ carbon atom ($C_{ipso}$) were employed, the values were very similar.

In the diplatinum complexes, the pentafluorophenyl ligands on each platinum were always sandwiched between two phosphine derived aryl groups. The average centroid-centroid spacing (π stacking distance) for each molecule is given in Table 3.3 (3.60-4.10 Å). This phenomenon has been seen in many other diplatinum polyynediyl complexes bearing pentafluorophenyl and two *trans*-triarylphosphine

ligands,[20,21b,23,45e,j,k] and has been attributed to quadrupolar interactions between the fluorinated and non-fluorinated aryl groups.[59] Other structural features are analyzed in the discussion section.

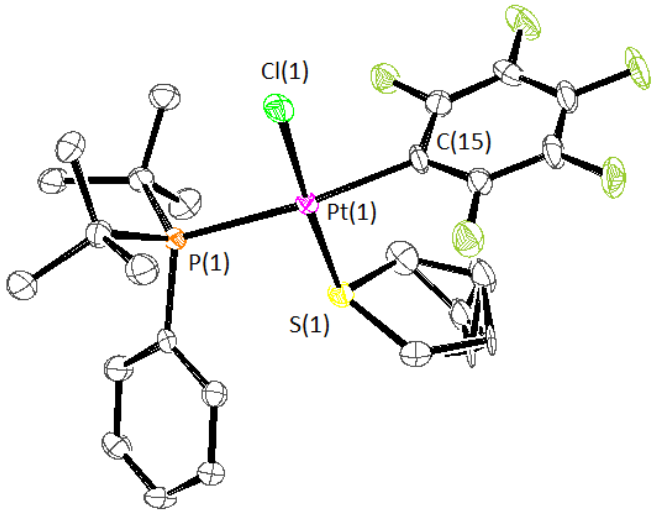


**Figure 3.1**. Molecular structure of **1** with thermal ellipsoids at 50% probability level. Key bond lengths (Å) and angles (°): Pt(1)-C(15), 2.077(8); Pt(1)-S(1), 2.302(2); Pt(1)-Cl(1), 2.342(2); Pt(1)-P(1), 2.365(2); C(15)-Pt(1)-S(1), 90.4(2); C(15)-Pt(1)-Cl(1), 86.5(2); S(1)-Pt(1)-Cl(1), 176.26(7); C(15)-Pt(1)-P(1), 177.9(2); S(1)-Pt(1)-P(1), 88.90(7); Cl(1)-Pt(1)-P(1), 94.35(7).

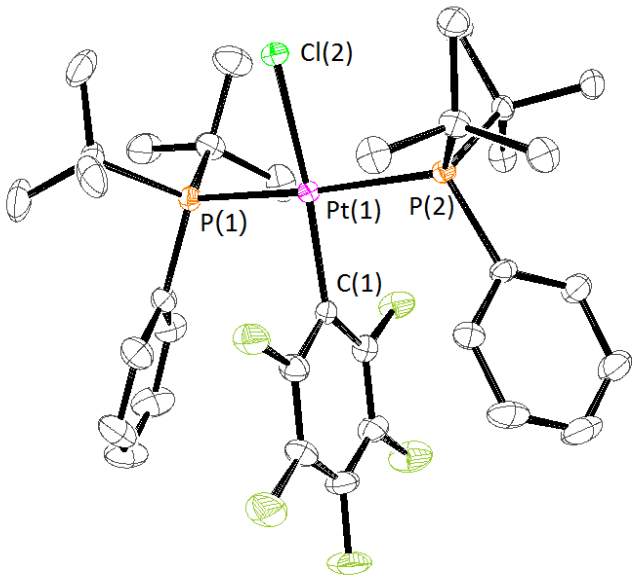


**Figure 3.2**. Molecular structure of **Pt"Cl-e** with thermal ellipsoids at 50% probability level. Key bond lengths (Å) and angles (°): Pt(1)-C(1), 2.020(3); Pt(1)-P(2), 2.3634(8); Pt(1)-P(1), 2.3673(8); Pt(1)-Cl(2), 2.3647(7); C(1)-Pt(1)-P(2), 92.45(8); C(1)-Pt(1)-Cl(2), 168.68(8); P(2)-Pt(1)-Cl(2), 88.52(2); C(1)-Pt(1)-P(1), 90.98(8); P(2)-Pt(1)-P(1), 169.14(3); P(1)-Pt(1)-Cl(2), 90.14(3).

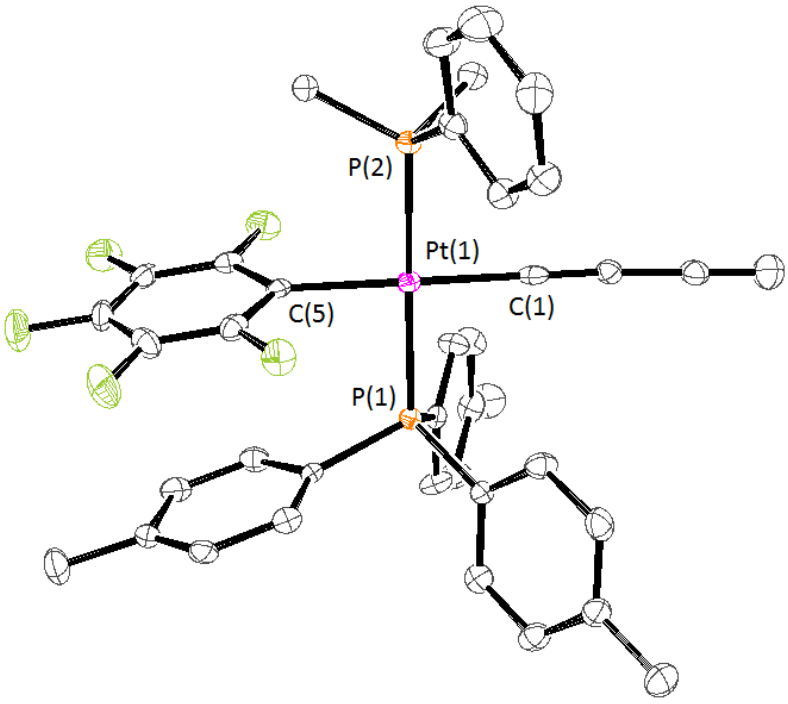


**Figure 3.3**. Molecular structure of **Pt'C$_4$H-a** with thermal ellipsoids at 50% probability level. Key bond lengths (Å) and angles (°): Pt(1)-C(1), 1.993(4); Pt(1)-P(1), 2.3298(13); Pt(1)-P(2), 2.2927(13), Pt(1)-C(5), 2.067(4); C(1)-Pt(1)-P(2), 88.87(11); C(1)-Pt(1)-C(5), 178.05(17); P(2)-Pt(1)-C(5), 91.37(11); C(1)-Pt(1)-P(1), 90.51(11); P(2)-Pt(1)-P(1), 179.30(4); P(1)-Pt(1)-C(5), 89.26(11).

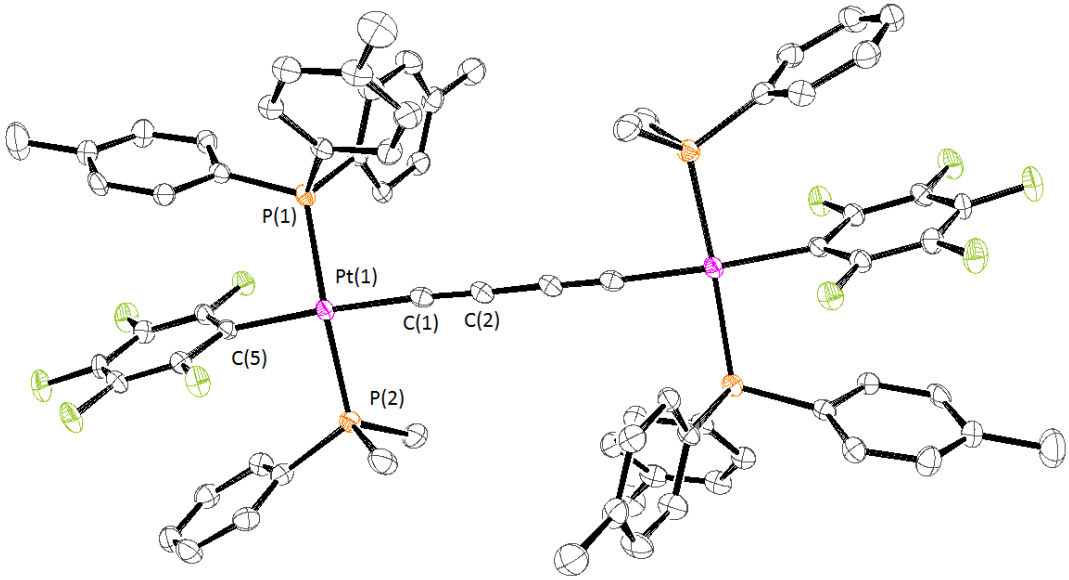


**Figure 3.4**. Molecular structure of **Pt'C$_4$Pt'-a** with thermal ellipsoids at 50% probability level and solvate molecules omitted.

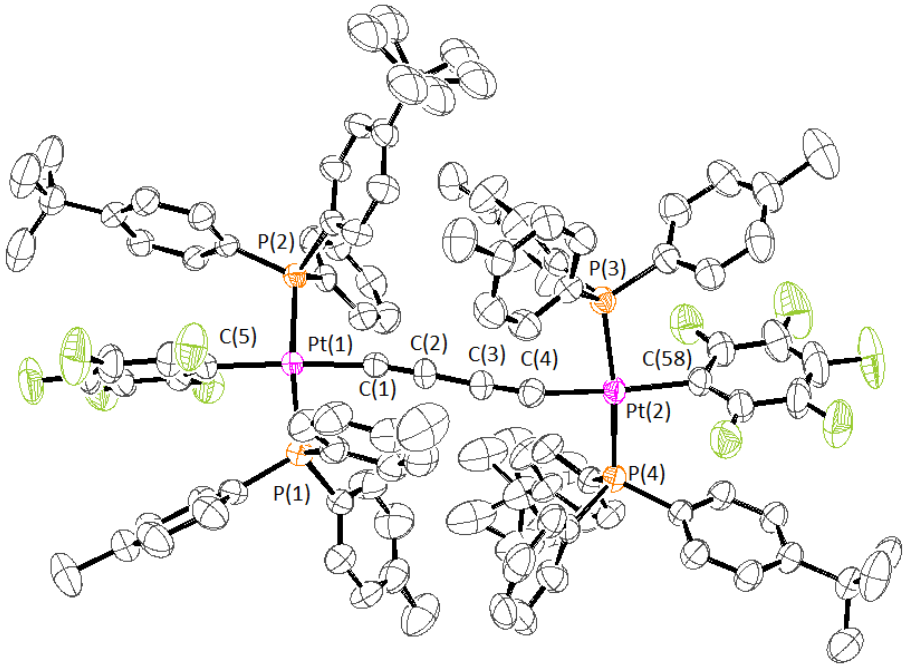


**Figure 3.5**. Molecular structure of **Pt'C$_4$Pt'-b** with thermal ellipsoids at 50% probability level; some *t*-butyl groups are disordered as described in the experimental section.

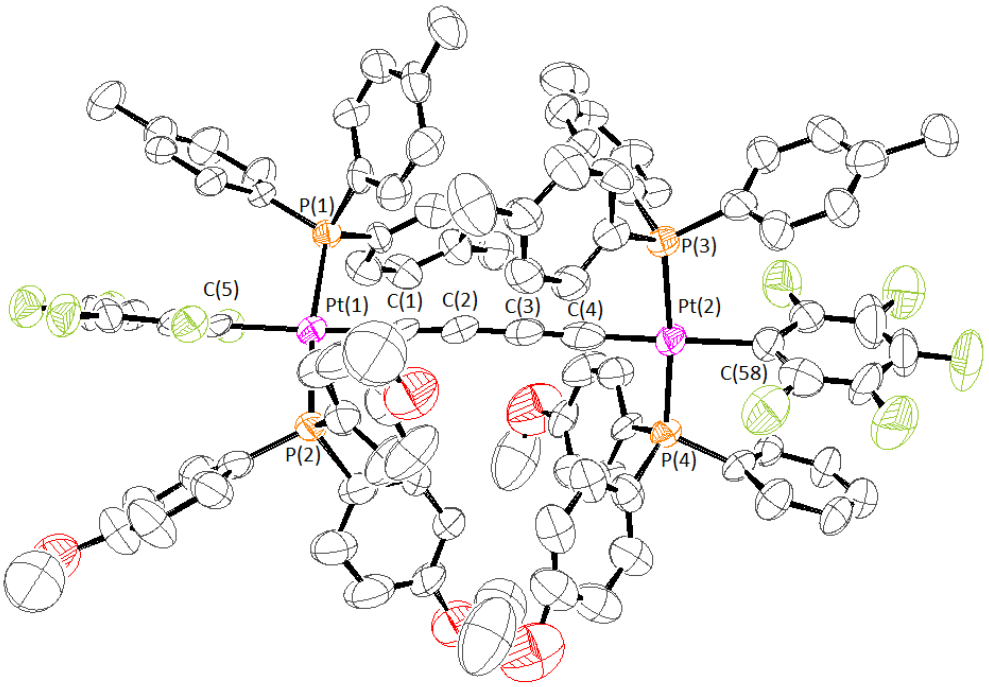


**Figure 3.6**. Molecular structure of **Pt'C$_4$Pt'-c** with thermal ellipsoids at 50% probability level; the methoxy groups are disordered as described in the experimental section.

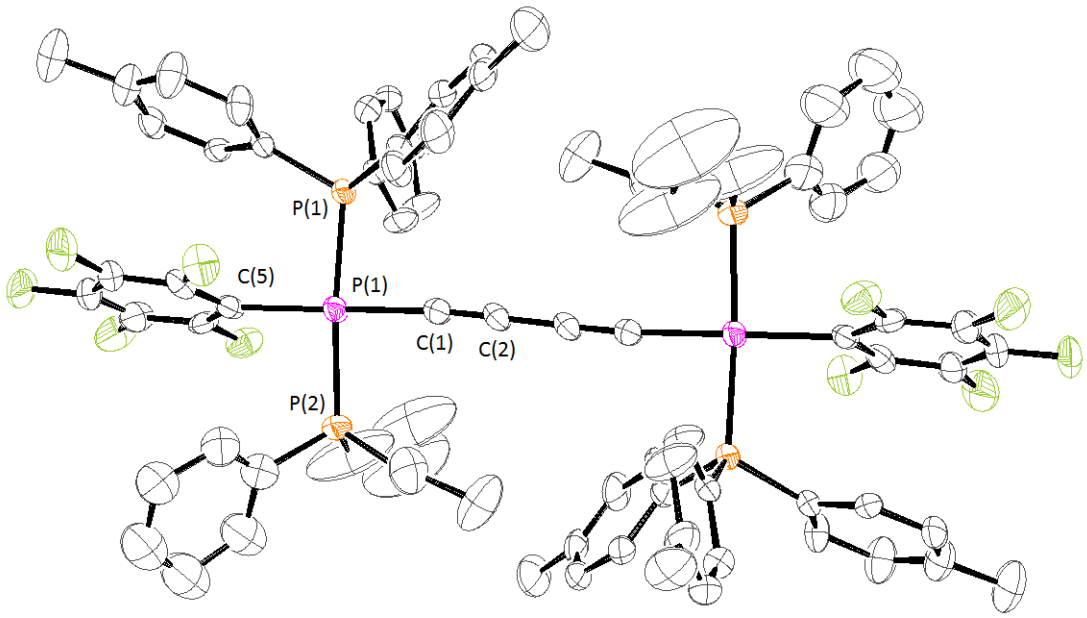


**Figure 3.7.** Molecular structure of **Pt'$C_4$Pt'-d** with thermal ellipsoids at 50% probability level.

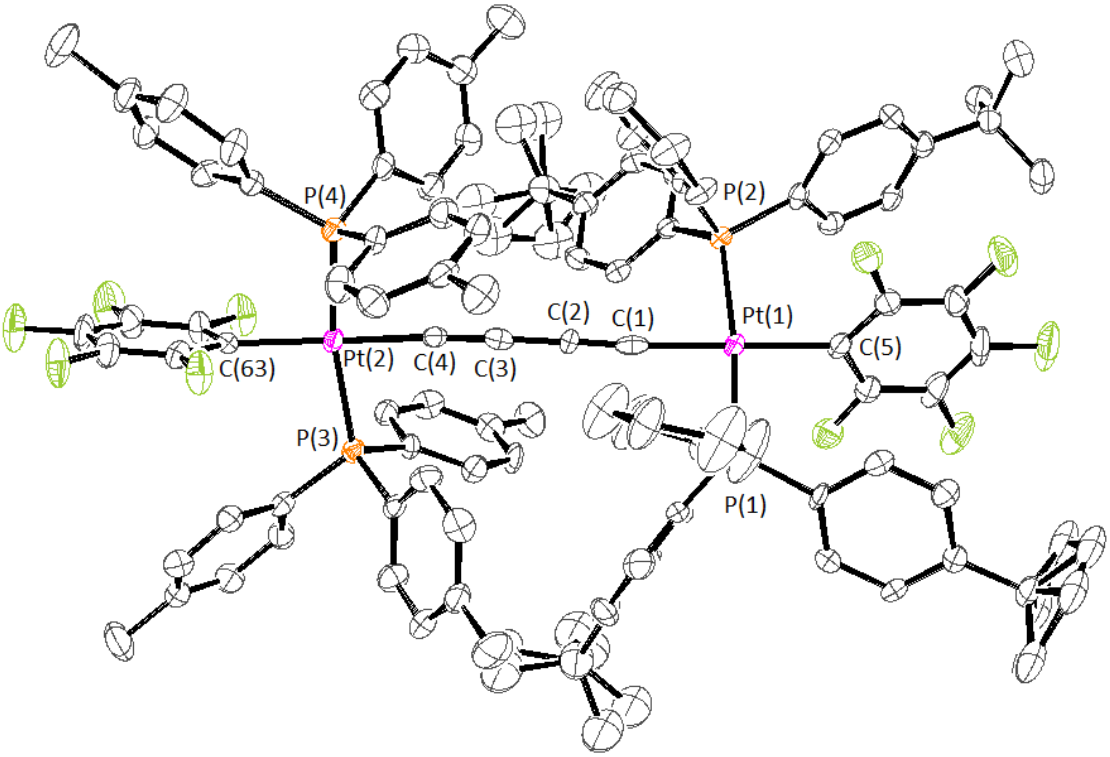


**Figure 3.8**. Molecular structure of **Pt$C_4$Pt"-b** with thermal ellipsoids at 50% probability level and solvate molecules omitted; some *t*-butyl groups are disordered as described in the experimental section.

### 3.2.6 Other characterization

The UV-visible spectra of diplatinum polyynediyl complexes have been extensively analyzed as a function of carbon chain length.[20,23,43a] The $_{max}$ red shifts and becomes more intense, and a series of much weaker bands at still longer wavelengths – representing C≡C vibrational fine structure – become increasingly apparent. Such bands were not detected when we initially characterized **PtC$_4$Pt**.[20] Hence, the UV-visible spectra of representative diplatinum butadiynediyl complexes were recorded at higher concentrations and with special attention to this region. As summarized in Table 3.4, two such bands at 395-387 and 428-422 nm could always be detected. The molar extinction coefficients ($\varepsilon$, $M^{-1}cm^{-1}$) were 500-400 and 120-50, respectively.

## 3.3 Discussion

### 3.3.1. Syntheses

The preceding data reveal a number of synthetic challenges with respect to both the monoplatinum and diplatinum target complexes. For example, Scheme 3.3 illustrates the difficulties associated with introducing two bulky *trans* *t*-Bu$_2$PhP ligands onto a $C_6F_5PtCl$ fragment. Although a route to the adduct **Pt"Cl-e** and the substitution product **Pt'Cl-e** could ultimately be realized, several reactions that worked with less bulky phosphine ligands (Scheme 3.2) were unsuccessful. In the same vein, all efforts to replace the chloride ligand in **Pt'Cl-e** with any type of alkynyl ligand were thwarted (Scheme 3.4).

The phosphine ligand scrambling that accompanied the coupling of **Pt'C$_4$H-a-c** and **Pt'Cl-a-c** (Scheme 3.5) was unexpected. This phenomenon was likely masked in earlier studies, which involved reaction components with a single phosphine ligand.[20,21b,42b] Enhanced substitution rates are often found with paramagnetic metal complexes.[29] Perhaps the copper catalyst somehow promotes redox equilibria that facilitate scrambling. However, very little or no scrambling is found with the alternative copper catalyzed coupling protocol in Scheme 3.6. This recipe was not investigated until a late stage of this project. Otherwise, at least some of the target complexes might have been realized in much higher overall yields.

Nonetheless, ligand labilization such as in Scheme 3.5 can sometimes be turned into an advantage. For example, one could consider the possibility of carrying out late stage phosphine substitutions simultaneously with coupling. This could greatly increase the breadth of end products accessible, without a corresponding increase in intermediates that must be characterized.

### 3.3.2. Structural and dynamic properties

None of the low temperature NMR experiments carried out with the diplatinum butadiynediyl complexes gave any evidence of atropisomerism. Importantly, the many types of NMR couplings observed at ambient temperature (e.g., $^{1}J_{PPt}$, $^{n}J_{HPt}$, $^{n}J_{CPt}$, $^{2}J_{PP}$, certain $^{n}J_{HP}$ and $^{n}J_{CP}$, etc.) exclude the operation of any low energy ligand dissociation

processes. These might provide pathways for interconverting atropisomers and/or exchanging diastereotopic groups (see Scheme 3.1).

This inability to document atropisomerism could have been anticipated if recently published studies with related diplatinum ethynediyl complexes[48] had been carried out first. However, we misjudged the degree of endgroup/endgroup interactions. In this context, Figure 3.9 compares space filling representations of three diplatinum complexes: (1) the butadiynediyl complex *trans*,*trans*-$(C_6F_5)(Et_3P)_2Pt(C{\equiv}C)_2Pt$ $(PEt_3)_2$(*p*-tol),[42b] which has four identical, moderately sized phosphine ligands, $PEt_3$, (2) **Pt'C$_4$Pt'-b**, which has bulkier *p*-$tol_3P$ and $(p\text{-}t\text{-}BuC_6H_4)_2PhP$ ligands on each platinum, and (3) the ethynediyl complex *trans*,*trans*-$(C_6F_5)$(*p*-$tol_3P$)$(Me_2PhP)Pt(C{\equiv}C)Pt$ $(PPhMe_2)$(P*p*-$tol_3$)$(C_6F_5)$ (**Pt'C$_2$Pt'-a**),[48] which has a smaller $Me_2PhP$ ligand and a bulkier *p*-$tol_3P$ ligand on each platinum. The sp carbon chains are highlighted in dark blue.

In the first complex (Figure 3.9, top), the endgroups are well separated and the carbon chain is highly exposed. In the case of **Pt'C$_4$Pt'-b** (Figure 3.9, middle), the phosphine ligands on opposite termini have considerable van der Waals contacts, but the carbon chain remains somewhat visible. With this ligand set, the platinum square planes can apparently rotate by 180°, allowing the interconversion of the types of structures in Scheme 3.1. Concomitant gearing of the aryl groups on the phosphine ligands is required. Space filling representations of all crystallographically characterized complexes are provided in the supplementary material. **Pt'C$_4$Pt'-c** exhibits a slightly higher degree of endgroup/endgroup interactions, but **Pt'C$_4$Pt'-a**,**d** show no van der Waals contacts as all.

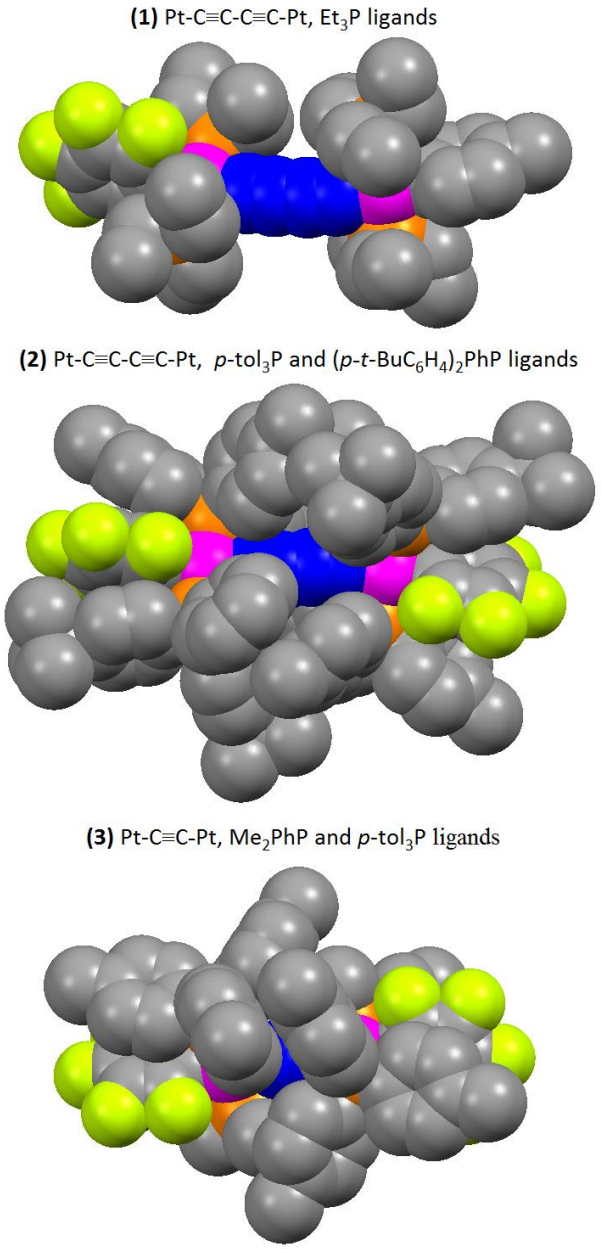


**Figure 3.9**. Representative space filling representations of diplatinum polyynediyl complexes: (1) *trans*,*trans*-$(C_6F_5)(Et_3P)_2Pt(C{\equiv}C)_2Pt(PEt_3)_2$(*p*-tol); (2) **Pt'C$_4$Pt'-b**; (3) *trans*,*trans*-$(C_6F_5)$(*p*-$tol_3P)(Me_2PhP)Pt(C{\equiv}C)Pt(PPhMe_2)(P$*p*-$tol_3)(C_6F_5)$ (**Pt'C$_2$Pt'-a**).

The phosphine ligands on opposite termini in **Pt'C$_2$Pt'-a** (Figure 3.9, bottom) have extensive van der Waals contacts and nearly completely shield the sp carbon chain. However, low temperature NMR spectroscopy still failed to establish atropisomerism,[48]

presumably due to a modest barrier to square plane rotation and/or phosphorus substituent gearing. Nonetheless, we consider this a "near miss", as restricted rotation has been observed about other $MC_2M'$ linkages (where one metal is formally octahedral).[60] Other approaches towards realizing this well established mode of organic stereoisomerism with square planar metal complexes will be pursued in the future. It should also be noted that several other types of atropisomerism have been documented in inorganic and organometallic complexes.[61]

### 3.3.3. Summary

This study has greatly increased the number of diplatinum butadiynediyl complexes in the literature, particularly with regard to less symmetrically substituted systems. This was assisted by an unanticipated phosphine ligand scrambling process (Scheme 3.5), which proves avoidable under modified reaction conditions (Scheme 3.6). These complexes and their precursors exhibit a wealth of fascinating NMR and structural properties. While the diplatinum complexes remain insufficiently congested for any dynamic processes or atropisomerism to be observed, other applications can be anticipated (e.g., improved stabilities of mixed valence Pt(II)/Pt(III) cation radicals)[20,42a] and will be investigated in due course.

## 3.4 Experimental section

Reactions were conducted under inert atmospheres. Workups were carried out in air. Toluene and $CH_2Cl_2$ used for reactions were dried and degassed with a Glass

Contour solvent purification system; other solvents were used as received from common commercial sources. The following reagents were used as received: CuCl (99.999%, Aldrich), CuI (99.999%, Aldrich), $KPF_6$ (99.9%, Aldrich), *t*-BuOK (97.0%, TCI), $Cl_2PhP$ (98%, Fluka), $Me_2PhP$ (99%, Strem), *n*-$Pr_2PhP$ (98%, Aldrich), *t*-$Bu_2PhP$ (95%, Aldrich), (*p*-$MeOC_6H_4)_2PhP$ (95%, Alfa Aeser), *p*-$tol_3P$ (95%, TCI) and $K_2PtCl_4$ (99.8%, Aldrich).

NMR spectra were recorded at ambient probe temperature unless noted using a Varian instrument operating at 500.00 ($^1H$), 125.65 ($^{13}C\{^1H\}$), or 202.28 ($^{31}P\{^1H\}$) MHz and referenced as follows ( /ppm): $^1H$, residual internal $CHCl_3$ (7.26); $^{13}C$, internal $CDCl_3$ (77.2); $^{31}P$, external $H_3PO_4$ (0.00). UV/visible spectra were recorded on a Shimadzu UV-1800 spectrophotometer. Melting points were recorded using a Stanford Research Systems (SRS) MPA100 (Opti-Melt) automated melting point system. Microanalyses were conducted by Atlantic Microlab.

***trans*-($C_6F_5$)($Me_2PhP$)(*p*-$tol_3P$)Pt(Cl) (Pt'Cl-a).**[50] A Schlenk flask was charged with *trans*-($C_6F_5$)(*p*-$tol_3P)_2$Pt(Cl) (**PtCl**;[20] 3.170 g, 3.150 mmol), $Me_2PhP$ (0.450 mL, 3.150 mmol) and $CH_2Cl_2$ (140 mL). The mixture was stirred for 16 h. The solvent was removed by rotary evaporation. The residue was washed with hexane (2 × 20 mL) and dried by oil pump vacuum to give **Pt'Cl-a** as a white powder (2.344 g, 2.790 mmol, 89%), mp 210 °C. Calcd for $C_{35}H_{32}ClF_5P_2Pt$ (840.06): C, 50.04; H, 3.84. Found: 50.01; H, 3.82.

NMR (δ, $CDCl_3$): $^1$H 7.53 (m, 2H, *o* to P, Ph), 7.47 (dd, $^3J_{HH}$ = 9.8 Hz, $^3J_{HP}$ = 11.4 Hz, 6H, *o* to P, tol), 7.33 (m, 3H, *m*/*p* to P, Ph), 7.11 (dd, $^3J_{HH}$ = 8.1 Hz, $^4J_{HP}$ = 1.8 Hz, 6H, *m* to P, tol), 2.35 (s, 9H, $CH_3$, tol), 1.79 (dd, $^2J_{HP}$ = 10.5 Hz, $^4J_{HP}$ = 2.7 Hz, $^3J_{HPt}$ = 36.9 Hz, 6H, $PMe_2$); $^{13}C\{^1H\}$ 145.9 (dd, $^1J_{CF}$ = 229 Hz, $^2J_{CF}$ = 23 Hz, *o* to Pt, $C_6F_5$), 140.9 (d, $^4J_{CP}$ = 2.3 Hz, *p* to P, tol), 136.8 (dm, $^1J_{CF}$ = 238 Hz, *m*/*p* to Pt, $C_6F_5$), 134.5 (d, $^2J_{CP}$ = 10.4 Hz, *o* to P, tol), 132.9 (dd, $^1J_{CP}$ = 54 Hz, $^3J_{CP}$ = 3.1 Hz, *i* to P, Ph), 130.6 (d, $^2J_{CP}$ = 9.7 Hz, *o* to P, Ph), 130.3 (d, $^4J_{CP}$ = 2.0 Hz, *p* to P, Ph), 128.9 (d, $^3J_{CP}$ = 10.8 Hz, *m* to P, tol), 128.4 (d, $^3J_{CP}$ = 10.0 Hz, *m* to P, Ph), 126.6 (dd, $^1J_{CP}$ = 55.4 Hz, $^3J_{CP}$ = 2.7 Hz, $^2J_{CPt}$ = 25.8 Hz,[65] *i* to P, tol), 111.1 (t, $^2J_{CF}$ = 43.5 Hz, *i* to Pt, $C_6F_5$), 21.5 (s, $CH_3$, tol), 12.3 (dd, $^1J_{CP}$ = 36.6 Hz, $^3J_{CP}$ = 1.7 Hz, $^2J_{CPt}$ = 37.6 Hz,[65] $PMe_2$); $^{31}P\{^1H\}$ 20.2 (d, $^2J_{PP}$ = 450 Hz, $^1J_{PPt}$ = 2624 Hz,[65] *p*-$tol_3P$), –5.5 (d, $^2J_{PP}$ = 450 Hz, $^1J_{PPt}$ = 2620 Hz,[65] $PMe_2Ph$).

***trans*-$(C_6F_5)(Me_2PhP)_2Pt(Cl)$ (Pt"Cl-a).** A Schlenk flask was charged with $[(C_6F_5)(tht)Pt(\mu\text{-}Cl)]_2$ (1.010 g, 1.040 mmol),[62] $Me_2PhP$ (0.60 mL, 4.20 mmol), and $CH_2Cl_2$ (70 mL). The solution was stirred for 18 h and filtered through a celite/decolorizing charcoal/glass frit assembly. The solvent was removed by rotary evaporation. The residue was washed with methanol (2 × 20 mL) and dried by oil pump vacuum to give **Pt"Cl-a** as a white powder (0.433 g, 0.643 mmol, 31%). The solvent was removed from the washes by rotary evaporation. The residue was recrystallized from

methanol/hexane mixture to yield another crop of **Pt"Cl-a** (0.585 g, 0.868 mmol, 42% or 73% total).

NMR (δ, $CDCl_3$): $^1H$ 7.44 (m, 4H, *o* to P), 7.32 (m, 6H, *m*/*p* to P), 1.73 (virtual t,[66] $^2J_{HP}$ = 3.9 Hz, $^3J_{HPt}$ = 27.9 Hz, 12H, Me); $^{13}C\{^1H\}$ 146.3 (dd, $^1J_{CF}$ = 228 Hz, $^2J_{CF}$ = 26 Hz, $^2J_{CPt}$ = 76 Hz,[65] *o* to Pt, $C_6F_5$), 136.6 (dm, $^1J_{CF}$ = 247 Hz, *m*/*p* to Pt, $C_6F_5$), 132.6 (virtual t,[66] $^1J_{CP}$ = 28.1 Hz, $^2J_{CPt}$ = 33.2 Hz,[65] *i* to P), 130.4 (virtual t,[66] $^2J_{CP}$ = 5.8 Hz, *o* to P), 130.3 (s, *p* to P), 128.4 (virtual t,[66] $^3J_{CP}$ = 5.1 Hz, *m* to P), 108.1 (t, $^2J_{CF}$ = 43.5 Hz, *i* to Pt, $C_6F_5$), 12.2 (virtual t,[66] $^1J_{CP}$ = 18.9 Hz, $^2J_{CPt}$ = 35.8 Hz,[65] $PMe_2$); $^{31}P\{^1H\}$ –5.5 (s, $^1J_{PPt}$ = 2520 Hz[65]).

***trans*-($C_6F_5$)(*p*-$tol_3P$)((*p*-*t*-$BuC_6H_4)_2PhP$)Pt(Cl) (Pt'Cl-b).** A Schlenk flask was charged with **PtCl** (6.186 g, 6.147 mmol),[20] (*p*-*t*-$BuC_6H_4)_2PhP$ (2.302 g, 6.147 mmol),[63] and toluene (150 mL). The solution was refluxed for 22 h. The solvent was removed by rotary evaporation and oil pump vacuum. The residue was washed with hexane (3 × 30 mL, leaving 5.213 g) and chromatographed on a silica gel column (3.8 × 42 cm, 8:1 v/v toluene/hexane). The solvent was removed from the product containing fractions by rotary evaporation and oil pump vacuum to give **Pt'Cl-b** (1.906 g, 1.771 mmol, 29%), **PtCl** (1.475 g, 1.466 mmol, 24%), and an unknown complex (0.121 g) as white solids. A fourth fraction contained mainly *trans*-($C_6F_5$)((*p*-*t*-$BuC_6H_4)_2PhP)_2Pt(Cl)$ (**Pt"Cl-b**, ~10%), together with the unknown complex and a second one.

Date for **Pt'Cl-b.** dec pt 249 °C. Calcd. for $C_{53}H_{52}ClF_5P_2Pt$ (1076.46): C 59.14, H 4.87. Found: C 59.31, H 4.86. NMR (δ, $CDCl_3$): $^1$H 7.88-7.78 (m, 2H, *o* to P, Ph), 7.60-7.47 (m, 10H, *o* to P, tol+$C_6H_4$), 7.40-7.33 (m, 3H, *m/p* to P, Ph), 7.30 (d, $^3J_{HH}$ = 8.4 Hz, 4H, *m* to P, $C_6H_4$), 7.13 (d, $^3J_{HH}$ = 7.8 Hz, 6H, *m* to P, tol), 2.36 (s, 9H, $CH_3$, tol), 1.30 (s, 18H, $C(CH_3)_3$); $^{13}C\{^1H\}$ 153.9 (s, *p* to P, $C_6H_4$), 145.3 (dd, $^1J_{CF}$ = 225 Hz, $^2J_{CF}$ = 22 Hz, *o* to Pt, $C_6F_5$), 141.0 (s, *p* to P, tol), 136.3 (dm, $^1J_{CF}$ = 245 Hz, *m/p* to Pt, $C_6F_5$), 135.0 (virtual t,[66] $^2J_{CP}$ = 6.3 Hz, *o* to P, Ph), 134.6 (virtual t,[66] $^2J_{CP}$ = 6.3 Hz, *o* to P, tol), 134.3 (virtual t,[66] $^2J_{CP}$ = 6.3 Hz, *o* to P, $C_6H_4$), 130.7 (s, *p* to P, Ph), 130.2 (dd, $^1J_{CP}$ = 30.9 Hz, $^3J_{CP}$ = 26.5 Hz, *i* to P, Ph), 128.9 (virtual t,[66] $^3J_{CP}$ = 5.7 Hz, *m* to P, tol), 128.2 (virtual t,[66] $^3J_{CP}$ = 5.6 Hz, *m* to P, Ph), 126.7 (dd, $^1J_{CP}$ = 31.7 Hz, $^3J_{CP}$ = 27.5 Hz, *i* to P, tol), 126.6 (dd, $^1J_{CP}$ = 31.8 Hz, $^3J_{CP}$ = 27.2 Hz, *i* to P, $C_6H_4$), 125.1 (virtual t,[66] $^3J_{CP}$ = 5.6 Hz, *m* to P, $C_6H_4$), 114.5 (t, $^2J_{CF}$ = 45.4 Hz, *i* to Pt, $C_6F_5$), 34.9 (s, *C*$(CH_3)_3$), 31.2 (s, $CH_3$); 21.5 (s, $CH_3$, tol); $^{31}P\{^1H\}$ 19.8 (s, $^1J_{PPt}$ = 2726 Hz[65]).

***trans*-$(C_6F_5)((p\text{-}t\text{-}BuC_6H_4)_2PhP)_2Pt(Cl)$ (Pt"Cl-b).** A Schlenk flask was charged with $[(C_6F_5)(tht)Pt(\mu\text{-}Cl)]_2$ (0.129 g, 0.132 mmol),[62] $(p\text{-}t\text{-}BuC_6H_4)_2PhP$ (0.218 g, 0.582 mmol),[63] and $CH_2Cl_2$ (20 mL). The solution was stirred for 16 h and filtered through a celite/decolorizing charcoal/glass frit assembly. The solvent was removed by rotary evaporation. The residue was washed with cold methanol (2 × 10 mL) and dried by oil pump vacuum to give **Pt"Cl-b** as a white powder (0.231 g, 0.201 mmol, 76%).

NMR (δ, $CDCl_3$): $^1H$ 7.91-7.80 (m, 4H, *o* to P, Ph), 7.56-7.46 (m, 8H, *o* to P, $C_6H_4$), 7.44-7.36 (m, 6H, *m*/*p* to P, Ph), 7.28 (d, $^3J_{HH}$ = 8.4 Hz, 8H, *m* to P, $C_6H_4$), 1.29 (s, 36H, $CH_3$); $^{31}P\{^1H\}$ 19.7 (s, $^1J_{PPt}$ = 2731 Hz[65]).

***trans*-($C_6F_5$)(*p*-$tol_3P$)((*p*-$MeOC_6H_4)_2PhP$)Pt(Cl) (Pt'Cl-c).** A Schlenk flask was charged with **PtCl** (5.032 g, 5.000 mmol),[20] (*p*-$MeOC_6H_4)_2PhP$ (1.612 g, 5.000 mmol), and toluene (120 mL). The solution was refluxed for 22 h. The solvent was removed by rotary evaporation and oil pump vacuum. The residue was washed with hexane (3 × 50 mL) and chromatographed on a silica gel column (3.8 × 42 cm), using 50:50 v/v $CH_2Cl_2$/hexane to elute **PtCl**, 80:20 v/v $CH_2Cl_2$/hexane to elute **Pt'Cl-c**, and 40:60 v/v ethyl acetate/hexane to elute *trans*-($C_6F_5$)((*p*-$MeOC_6H_4)_2PhP)_2$Pt(Cl) (**Pt"Cl-c**). The solvent was removed from the fractions by rotary evaporation and oil pump vacuum to give **PtCl** (1.406 g, 1.397 mmol, 28%), **Pt'Cl-c** (2.149 g, 2.098 mmol, 42%) and **Pt"Cl-c** (0.643 g, 0.616 mmol, 13%) as white solids.

Data for **Pt'Cl-c**. mp 215 °C. Calcd for $C_{47}H_{40}ClF_5O_2P_2Pt$ (1024.30): C, 55.11; H, 3.94. Found: 55.06; H, 3.95. NMR (δ, $CDCl_3$): $^1H$ 7.71-7.61 (m, 4H, *o* to P, $C_6H_4$), 7.59-7.42 (m, 8H, *o* to P, tol+Ph), 7.37-7.29 (m, 1H, *p* to P, Ph), 7.26 (d, $^3J_{HH}$ = 7.2 Hz, 2H, *m* to P, Ph), 7.13 (d, $^3J_{HH}$ = 7.5 Hz, 6H, *m* to P, tol), 6.88 (d, $^3J_{HH}$ = 8.1 Hz, 4H, *m* to P, $C_6H_4$), 3.83 (s, 6H, $OCH_3$), 2.36 (s, 9H, $CH_3$, tol); $^{13}C\{^1H\}$ 161.5 (s, *p* to P, $C_6H_4$), 145.2 (dd, $^1J_{CF}$ = 225 Hz, $^2J_{CF}$ = 20 Hz, *o* to Pt, $C_6F_5$), 140.9 (s, *p* to P, tol), 136.5 (dm, $^1J_{CF}$ = 238 Hz, *m*/*p* to Pt, $C_6F_5$), 136.4 (virtual t,[66] $^2J_{CP}$ = 6.9 Hz, *o* to P, $C_6H_4$), 134.4

(virtual t,[66] $^{2}J_{CP}$ = 6.3 Hz, *o* to P, tol), 133.7 (virtual t,[66] $^{2}J_{CP}$ = 5.9 Hz, *o* to P, Ph), 131.0 (dd, $^{1}J_{CP}$ = 33.9 Hz, $^{3}J_{CP}$ = 23.9 Hz, *i* to P, Ph), 130.2 (s, *p* to P, Ph), 128.8 (virtual t,[66] $^{3}J_{CP}$ = 5.5 Hz, *m* to P, tol), 127.8 (virtual t,[66] $^{3}J_{CP}$ = 5.2 Hz, *m* to P, Ph), 126.5 (dd, $^{1}J_{CP}$ = 34.4 Hz, $^{3}J_{CP}$ = 24.7 Hz, *i* to P, tol), 120.5 (dd, $^{1}J_{CP}$ = 36.6 Hz, $^{3}J_{CP}$ = 25.9 Hz, *i* to P, $C_6H_4$), 114.5 (br, *i* to Pt, $C_6F_5$), 113.8 (dd, $^{3}J_{CP}$ = 6.6 Hz, $^{5}J_{CP}$ = 5.1 Hz, *m* to P, $C_6H_4$), 55.4 (s, $OCH_3$), 21.4 (s, $CH_3$, tol); $^{31}P\{^{1}H\}$ 19.565, 19.506 (2 × s, $^{1}J_{PPt}$ = 2723 Hz[65]).

***trans*-($C_6F_5$)((*p*-$MeOC_6H_4$)$_2$PhP)$_2$Pt(Cl) (Pt"Cl-c).** A Schlenk flask was charged with [($C_6F_5$)(tht)Pt($\mu$-Cl)]$_2$ (0.140 g, 0.144 mmol),[62] (*p*-$MeOC_6H_4$)$_2$PhP (0.210 g, 0.652 mmol), and $CH_2Cl_2$ (25 mL). The solution was stirred for 16 h and filtered through a celite/decolorizing charcoal/glass frit assembly. The solvent was removed by rotary evaporation. The residue was washed with methanol (2 × 2 mL) and recrystallized from dichloromethane/hexane/methanol to give **Pt"Cl-c** as a white powder (0.155 g, 0.149 mmol, 52%).

NMR (δ, $CDCl_3$): $^{1}H$ 7.71-7.60 (m, 8H, *o* to P, $C_6H_4$), 7.54-7.43 (m, 4H, *o* to P, Ph), 7.38-7.30 (m, 6H, *p* to P, Ph), 7.26 (d, $^{3}J_{HH}$ = 7.5 Hz, 4H, *m* to P, Ph), 6.88 (d, $^{3}J_{HH}$ = 8.7 Hz, 8H, *m* to P, $C_6H_4$), 3.83 (s, 12H, $OCH_3$); $^{31}P\{^{1}H\}$ 19.2 (s, $^{1}J_{PPt}$ = 2716 Hz[65]).

***trans*-($C_6F_5$)(*p*-$tol_3$P)(*n*-$Pr_2$PhP)Pt(Cl) (Pt'Cl-d).** A Schlenk flask was charged with **PtCl** (6.167 g, 6.128 mmol),[20] *n*-$Pr_2$PhP (1.30 mL, 6.190 mmol), and toluene (120 mL). The solution was stirred for 16 h and then refluxed for 6 h. The solvent was

removed by rotary evaporation and oil pump vacuum. The residue was washed with hexane (3 × 60 mL). Only unreacted **PtCl** remained (1.096 g, 1.089 mmol, 18%). The solvent was removed from the combined washes by rotary evaporation and oil pump vacuum. The residue was chromatographed on a silica gel column (6.4 × 43 cm) using 50:50 v/v $CHCl_3$/hexane to elute displaced *p*-$tol_3P$, 55:45 v/v $CHCl_3$ /hexane to elute **Pt"Cl-d**, 60:40 v/v $CHCl_3$/hexane to elute **Pt'Cl-d**, and 80:20 v/v $CHCl_3$/hexane to elute **PtCl**. The solvent was removed from the fractions by rotary evaporation and oil pump vacuum to give **Pt"Cl-d** (0.481 g, 0.612 mmol, 10%), **Pt'Cl-d** (2.295 g, 2.561 mmol, 42%), and **PtCl** (0.511 g, 0.508 mmol, 9% or 27% including the residue isolated above).

Data for **Pt'Cl-d**. NMR (δ, $CDCl_3$): $^1$H 7.47 (dd, $^3J_{HP}$ = 11.0 Hz, $^3J_{HH}$ = 8.0 Hz, 6H, *o* to P, tol; overlapped with m, 2H, *o* to P, Ph), 7.35-7.28 (m, 3H, *m*/*p* to P, Ph), 7.10 (dd, $^3J_{HH}$ = 8.0 Hz, $^4J_{HP}$ = 2.0 Hz, 6H, *m* to P, tol), 2.35 (s, 9H, $CH_3$, tol), 2.29-1.95 (m, 4H, $PCH_2$), 1.79-1.39 (m, 4H, $PCH_2CH_2$), 1.01 (dt, $^3J_{HH}$ = 7.5 Hz, $^4J_{HP}$ = 0.5 Hz, 6H, $PCH_2CH_2CH_3$); $^{13}C\{^1H\}$ 145.8 (dd, $^1J_{CF}$ = 226 Hz, $^2J_{CF}$ = 19 Hz, *o* to Pt, $C_6F_5$), 140.8 (d, $^4J_{CP}$ = 2.5 Hz, *p* to P, tol), 136.6 (dm, $^1J_{CF}$ = 256 Hz, *m*/*p* to Pt, $C_6F_5$), 134.4 (dd, $^2J_{CP}$ = 11.1 Hz, $^4J_{CP}$ = 1.1 Hz, *o* to P, tol), 131.3 (d, $^2J_{CP}$ = 8.8 Hz, *o* to P, Ph), 130.6 (dd, $^1J_{CP}$ = 50.0 Hz, $^3J_{CP}$ = 2.6 Hz, *i* to P, Ph), 130.0 (d, $^4J_{CP}$ = 2.4 Hz, *p* to P, Ph), 128.8 (d, $^3J_{CP}$ = 10.9 Hz, *m* to P, tol), 128.2 (d, $^3J_{CP}$ = 9.8 Hz, *m* to P, Ph), 126.6 (dd, $^1J_{CP}$ = 55.0 Hz, $^3J_{CP}$ = 3.0 Hz, *i* to P, tol), 111.1 (t, $^2J_{CF}$ = 43.8 Hz, *i* to Pt, $C_6F_5$), 24.9 (dd, $^1J_{CP}$ = 32.0 Hz, $^3J_{CP}$ = 1.9 Hz, $PCH_2$), 21.4 (d, $^5J_{CP}$ = 1.1 Hz, $CH_3$, tol), 17.7 (s, $PCH_2CH_2$),

15.9 (d, $^{3}J_{CP}$ = 14.7 Hz, $PCH_2CH_2CH_3$); $^{31}P\{^{1}H\}$ 20.2 (d, $^{2}J_{PP}$ = 434 Hz, $^{1}J_{PPt}$ = 2624 Hz,[65] *p*-$tol_3P$), 8.8 (d, $^{2}J_{PP}$ = 434 Hz, $^{1}J_{PPt}$ = 2629 Hz,[65] *n*-$Pr_2PhP$).

***trans*-$(C_6F_5)$(*n*-$Pr_2PhP)_2Pt(Cl)$ (Pt"Cl-d).** A Schlenk flask was charged with $[(C_6F_5)(tht)Pt(\mu\text{-}Cl)]_2$ (0.130 g, 0.134 mmol),[62] *n*-$Pr_2PhP$ (0.13 mL, 0.619 mmol) and $CH_2Cl_2$ (25 mL). The solution was stirred for 16 h and filtered through a celite/decolorizing charcoal/glass frit assembly. The solvent was removed by rotary evaporation. The residue was recrystallized from hexane to give **Pt"Cl-d** as a white powder (0.125 g, 0.159 mmol, 60%).

NMR (δ, $CDCl_3$): $^{1}H$ 7.43-7.37 (m, 4H, *o* to P), 7.29 (d, $^{4}J_{HP}$ = 7.0 Hz, 4H, *m* to P, overlapped with m, 2H, *p* to P), 2.21-1.90 (m, 8H, $PCH_2$), 1.71-1.33 (m, 8H, $PCH_2CH_2$), 0.98 (t, $^{3}J_{HH}$ = 7.5 Hz, 12 H, $PCH_2CH_2CH_3$); $^{31}P\{^{1}H\}$ 8.7 (s, $^{1}J_{PPt}$ = 2534 Hz[65]).

**$(C_6F_5)$(*t*-$Bu_2PhP$)(tht)Pt(Cl) (1).**[67] A Schlenk flask was charged with $[(C_6F_5)(tht)Pt(\mu\text{-}Cl)]_2$ (0.986 g, 1.015 mmol),[62] *t*-$Bu_2PhP$ (1.16 mL, 4.816 mmol), and $CH_2Cl_2$ (75 mL). The solution was stirred for 16 h and filtered through a celite/decolorizing charcoal/glass frit assembly. The solvent was removed by rotary evaporation. The residue was washed with cold methanol (2 × 10 mL). Recrystallization from $CH_2Cl_2$/hexane gave colorless crystals of **1** (1.099 g, 1.552 mmol, 77%).

NMR (δ, $CDCl_3$): $^{1}H$ 7.99-7.88 (m, 4H, *o* to P), 7.52-7.43 (d, 6H, *m*/*p* to P), 3.04, 2.71 (each br, 4H, $SCH_2$), 1.59 (d, 18H, $^{3}J_{HP}$ = 13.5 Hz, $C(CH_3)_3$), 1.42 (br, 4H,

$SCH_2\mathit{CH}_2$) ; $^{13}C\{^1H\}$[68] 146.7 (dd, $^1J_{CF}$ = 222 Hz, $^2J_{CF}$ = 22 Hz, *o* to Pt, $C_6F_5$), 137.6 (dm, $^1J_{CF}$ = 243 Hz, *m*/*p* to Pt, $C_6F_5$), 135.2 (d, $^2J_{CP}$ = 8.4 Hz, *o* to P), 131.2 (d, $^1J_{CP}$ = 35.3 Hz, *i* to P), 130.3 (d, $^4J_{CP}$ = 2.0 Hz, *p* to P), 127.9 (d, $^3J_{CP}$ = 8.7 Hz, *m* to P), 39.4 (s, $SCH_2$), 37.5 (d, $^1J_{CP}$ = 18.6 Hz, $^2J_{CPt}$ = 17.7 Hz,[65] $\mathit{C}(CH_3)_3$), 30.9 (d, $^2J_{CP}$ = 3.0 Hz, $CH_3$), 29.8 (s, $^3J_{CPt}$ = 15.9 Hz,[65] $SCH_2\mathit{CH}_2$); $^{31}P\{^1H\}$ (see Figure B-4) 42.0 (apparent septet, $^4J_{PF}$ = 34.8 Hz, $^1J_{PPt}$ = 2330 Hz[65]).

***trans*-($t$-$Bu_2PhP)_2Pt(Cl)_2$ (2).**[51,53] A Schlenk flask was charged with $K_2PtCl_4$ (1.299 g, 3.130 mmol) and deoxygenated $H_2O$ (10 mL). Another Schlenk flask was charged with $t$-$Bu_2PhP$ (1.50 mL, 6.295 mmol) and ethanol (10 mL). The ethanol solution was transferred via cannula to the aqueous solution. The resulting pink suspension was stirred. After 1 d, the yellow precipitate was washed with $H_2O$, ethanol, hexane and diethyl ether, and dried in vacuum to give previously reported **2** (1.968 g, 2.769 mmol, 89%).

NMR (δ, $CDCl_3$): $^1H$ 7.94 (br, 4H, *o* to P, Ph), 7.42-7.30 (m, 6H, *m*/*p* to P, Ph), 1.61 (virtual t,[66] $^3J_{HP}$ = 6.8 Hz, 36H, $C(CH_3)_3$); $^{31}P\{^1H\}$ 42.8 (s, $^1J_{PPt}$ = 2542 Hz[65]).

***trans*-($C_6F_5$)($t$-$Bu_2PhP)_2Pt(Cl)$ (Pt"Cl-e).** A Schlenk flask was charged with (cod)($C_6F_5$)Pt(Cl) (2.797 g, 5.530 mmol),[55] $t$-$Bu_2PhP$ (3.50 mL, 14.689 mmol) and toluene (120 mL). The solution was refluxed for 48 h. The solvent was removed by rotary evaporation and oil pump vacuum. The residue was washed with ethanol (2 × 25 mL) and

hexane (2 × 25 mL) and dried by oil pump vacuum to give **Pt"Cl-e** as a white solid (2.980 g, 3.538 mmol, 64%).

NMR (δ, $CDCl_3$): $^1$H 7.90 (br, s, 4H, *o* to P, Ph), 7.24-7.08 (m, 6H, *m*/*p* to P, Ph), 1.58 (t, $^3J_{HP}$ = 6.0 Hz, 36H, $C(CH_3)_3$); $^{31}P\{^1H\}$ 41.8 (br s, $^1J_{PPt}$ = 2668 Hz).

***trans*-($C_6F_5$)(*p*-$tol_3P$)(*t*-$Bu_2PhP$)Pt(Cl) (Pt'Cl-e).** A Schlenk flask was charged with **Pt"Cl-e** (2.815 g, 3.342 mmol), *p*-$tol_3P$ (1.025 g, 3.368 mmol) and toluene (120 mL). The solution was refluxed for 14 h. The solvent was removed by rotary evaporation. The residue was washed with methanol (2 × 30 mL), ethanol (20 mL) and hexane (20 mL) to give **Pt'Cl-e** as a white powder (2.800 g, 3.029 mmol, 91%).

NMR (δ, $CDCl_3$): $^1$H 7.87-7.80 (m, 2H, *o* to P, Ph), 7.52 (dd, $^3J_{HP}$ = 11.0 Hz, $^3J_{HH}$ = 8.0 Hz, 6H, *o* to P, tol), 7.28-7.21 (m, 3H, *m*/*p* to P, Ph), 7.11 (d, $^3J_{HH}$ = 8.0 Hz, $^4J_{HP}$ = 2.0 Hz, 6H, *m* to P, tol), 2.35 (s, 9H, $CH_3$, tol) 1.52 (d, $^3J_{HP}$ = 14.0 Hz, 18H, $C(CH_3)_3$); $^{13}C\{^1H\}$ 146.2 (dd, $^1J_{CF}$ = 222 Hz, $^2J_{CF}$ = 20 Hz, *o* to Pt, $C_6F_5$), 140.8 (d, $^4J_{CP}$ = 2.4 Hz, *p* to P, tol), 136.8 (dm, $^1J_{CF}$ = 254 Hz, *m*/*p* to Pt, $C_6F_5$), 135.5 (d, $^2J_{CP}$ = 7.9 Hz, *o* to P, Ph), 134.6 (d, $^2J_{CP}$ = 10.7 Hz, *o* to P, tol), 130.1 (d, $^1J_{CP}$ = 38.3 Hz, *i* to P, Ph), 129.6 (d, $^4J_{CP}$ = 1.6 Hz, *p* to P, Ph), 128.7 (d, $^3J_{CP}$ = 11.2 Hz, *m* to P, tol), 126.7 (d, $^3J_{CP}$ = 9.0 Hz, *m* to P, Ph), 126.7 (dd, $^1J_{CP}$ = 58.3 Hz, $^3J_{CP}$ = 1.8 Hz, *i* to P, tol), 111.0 (t, $^2J_{CF}$ = 40.2 Hz, *i* to Pt, $C_6F_5$), 37.6 (dd, $^1J_{CP}$ = 17.8 Hz, $^3J_{CP}$ = 3.0 Hz, *C*($CH_3$)), 31.5 (s,

$CH_3$); 21.5 (s, $CH_3$, tol); $^{31}P\{^1H\}$ 50.2 (d, $^2J_{PP}$ = 421 Hz, $^1J_{PPt}$ = 2711 Hz,[65] *t*-$Bu_2PhP$), 18.5 (d, $^2J_{PP}$ = 421 Hz, $^1J_{PPt}$ = 2689 Hz,[65] *p*-$tol_3P$).

***trans*-($C_6F_5$)($Me_2PhP$)(*p*-$tol_3P$)$Pt(C{\equiv}C)_2H$ (Pt'$C_4H$-a). Synthesis A.** A Schlenk flask was charged with *trans*-($C_6F_5$)(*p*-$tol_3P)_2Pt(C{\equiv}C)_2H$ (**Pt$C_4H$**;[20] 0.822 g, 0.806 mmol), $Me_2PhP$ (0.115 mL, 0.811 mmol), and $CH_2Cl_2$ (60 mL). The solution was stirred for 18 h. The solvent was removed by oil pump vacuum. The residue was washed with hexane (2 × 20 mL). A $^{31}P\{^1H\}$ NMR spectrum of the washes showed signals for *p*-$tol_3P$, *p*-$tol_3PO$, and smaller quantities of platinum complexes (~10%). The residue was chromatographed on a silica gel column (2.5 × 30 cm, packed in hexane, eluted with 1:1 v/v $CH_2Cl_2$/hexane). The solvent was removed from the product containing fractions by rotary evaporation and oil pump vacuum to give **Pt$C_4H$** as an off-white solid (0.148 g, 0.145 mmol, 18%), **Pt'$C_4H$-a** as pale yellow solid (0.206 g, 0.242 mmol, 30%), and *trans*-($C_6F_5$)($Me_2PhP)_2Pt(C{\equiv}C)_2H$ (**Pt"$C_4H$-a**) as a pale yellow solid (0.061 g, 0.089 mmol, 11%).

Data for **Pt'$C_4H$-a**. mp 128 °C. Calcd for $C_{39}H_{33}F_5P_2Pt$ (853.71): C, 54.87; H, 3.90. Found: 54.66; H, 3.90. NMR (δ, $CDCl_3$): $^1H$ 7.53 (m, 2H, *o* to P, Ph), 7.45 (dd, $^3J_{HH}$ = 8.3 Hz, $^3J_{HP}$ = 11.6 Hz, 6H, *o* to P, tol), 7.35 (m, 3H, *m*/*p* to P, Ph), 7.11 (dd, $^3J_{HH}$ = 7.8 Hz, $^4J_{HP}$ = 1.8 Hz, 6H, *m* to P, tol), 2.36 (s, 9H, $CH_3$, tol), 1.88 (dd, $^2J_{HP}$ = 10.5 Hz, $^4J_{HP}$ = 2.7 Hz, $^3J_{HPt}$ = 44.4 Hz,[65] 6H, $PMe_2$), 1.69 (t, $^6J_{HP}$ = 1.0 Hz, $^5J_{HPt}$ =

9.3 Hz,[65] 1H, ≡CH); $^{13}C\{^{1}H\}$ 146.4 (dd, $^{1}J_{CF}$ = 228 Hz, $^{2}J_{CF}$ = 22 Hz, *o* to Pt, $C_6F_5$), 140.9 (d, $^{4}J_{CP}$ = 2.3 Hz, *p* to P, tol), 136.9 (dm, $^{1}J_{CF}$ = 230 Hz, *m*/*p* to Pt, $C_6F_5$), 134.4 (d, $^{2}J_{CP}$ = 10 Hz, $^{3}J_{CPt}$ = 31 Hz,[65] *o* to P, tol), 133.5 (dd, $^{1}J_{CP}$ = 54.4 Hz, $^{3}J_{CP}$ = 3.1 Hz, $^{2}J_{CPt}$ = 28.9 Hz,[65] *i* to P, Ph), 130.7 (d, $^{2}J_{CP}$ = 9.7 Hz, $^{3}J_{CPt}$ = 28.2 Hz,[65] *o* to P, Ph), 130.4 (d, $^{4}J_{CP}$ = 2.3 Hz, *p* to P, Ph), 128.9 (d, $^{3}J_{CP}$ = 11.1 Hz, *m* to P, tol), 128.4 (d, $^{3}J_{CP}$ = 10.4 Hz, *m* to P, Ph), 127.4 (dd, $^{1}J_{CP}$ = 56.8 Hz, $^{3}J_{CP}$ = 2.6 Hz, $^{2}J_{CPt}$ = 27.2 Hz,[65] *i* to P, tol), 124.5 (t, $^{2}J_{CF}$ = 52 Hz, *i* to Pt, $C_6F_5$), 99.5 (br, $^{1}J_{CPt}$ = 1011 Hz,[65] Pt*C*≡C), 92.7 (s, $^{2}J_{CPt}$ = 278 Hz,[65] PtC≡*C*), 72.4 (t, $^{4}J_{CP}$ = 2.3 Hz, $^{3}J_{CPt}$ = 36.7 Hz,[65] PtC≡C*C*), 60.1 (s, PtC≡CC≡*C*), 21.5 (s, $CH_3$, tol), 14.4 (dd, $^{1}J_{CP}$ = 37.6 Hz, $^{3}J_{CP}$ = 1.7 Hz, $^{2}J_{CPt}$ = 45.3 Hz,[65] $PMe_2$); $^{31}P\{^{1}H\}$ 18.3 (d, $^{2}J_{PP}$ = 419 Hz, $^{1}J_{PPt}$ = 2556 Hz,[65] *p*-$tol_3P$), –9.9 (d, $^{2}J_{PP}$ = 419 Hz, $^{1}J_{PPt}$ = 2529 Hz,[65] $Me_2PhP$).

Data for **Pt"$C_4$H-a.** NMR (δ, $CDCl_3$): $^{1}H$ 7.44 (m, 4H, *o* to P, Ph), 7.34 (t, $^{3}J_{HP}$ = 0.9 Hz, 4H, *m* to P, Ph), 7.32 (m, 2H, *p* to P, Ph), 1.82 (virtual t,[66] $^{2}J_{HP}$ = 3.9 Hz, $^{3}J_{HPt}$ = 33 Hz, 12H, $PMe_2$; ≡CH signal not observed); $^{13}C\{^{1}H\}$[68] 146.7 (dd, $^{1}J_{CF}$ = 216 Hz, $^{2}J_{CF}$ = 28 Hz, *o* to Pt, $C_6F_5$), 136.8 (dm, $^{1}J_{CF}$ = 258 Hz, *m*/*p* to Pt, $C_6F_5$), 133.2 (virtual t,[66] $^{1}J_{CP}$ = 28.6 Hz, *i* to P), 130.6 (virtual t,[66] $^{2}J_{CP}$ = 5.8 Hz, *o* to P), 130.4 (s, *p* to P), 128.5 (virtual t,[66] $^{3}J_{CP}$ = 5.1 Hz, *m* to P), 100.2 (br, Pt*C*≡C), 90.3 (s, $^{2}J_{CPt}$ = 256 Hz,[65] PtC≡*C*), 72.2 (s, PtC≡C*C*), 60.2 (s, PtC≡CC≡*C*), 14.3 (virtual t,[66] $^{1}J_{CP}$ = 19.8 Hz, $^{2}J_{CPt}$ = 44.3 Hz,[65] $PMe_2$); $^{31}P\{^{1}H\}$ –9.9 (s, $^{1}J_{PPt}$ = 2426 Hz[65]).

**Synthesis B.** A Schlenk flask was charged with **Pt'Cl-a** (0.791 g, 0.942 mmol), CuI (0.040 g, 0.21 mmol), $CH_2Cl_2$ (6 mL), and $HNEt_2$ (50 mL), and cooled to –45 °C ($CO_2$/$CH_3CN$). Then butadiyne (1.7 M in THF, 10.5 mL, 17.5 mmol)[64] was added with stirring. The cold bath was allowed to warm to room temperature (ca. 3 h). After an additional 16 h, the solvent was removed by oil pump vacuum. The residue was extracted with toluene (3 × 20 mL). The combined extracts were filtered through a neutral alumina column (7 cm, packed in toluene). The solvent was removed by rotary evaporation and oil pump vacuum. The residue was washed with ethanol (20 mL) and dried by oil pump vacuum (total mass 0.5015 g). Analysis by $^{31}P\{^1H\}$ NMR established the following product quantities: **Pt'$C_4$H-a** (0.2835 g, 0.332 mmol, 36%), **Pt$C_4$H** (0.154 g, 0.151 mmol, 16%), **Pt"$C_4$H-a** (0.064 g, 0.093 mmol, 10%).

***trans*-($C_6F_5$)(*p*-$tol_3P$)((*p*-*t*-Bu$C_6H_4$)$_2$PhP)Pt($C{\equiv}C)_2$H (Pt'$C_4$H-b).** A Schlenk flask was charged with **Pt'Cl-b** (0.539 g, 0.501 mmol), CuI (0.020 g, 0.11 mmol), $CH_2Cl_2$ (4 mL) and $HNEt_2$ (40 mL), and cooled to –45 °C ($CO_2$/$CH_3CN$). Then butadiyne (2.14 M in THF, 4.2 mL, 9.0 mmol)[64] was added with stirring. The cold bath was allowed to warm at 10 °C (ca. 6 h). The cold bath was removed, and after an additional 1 h, the solvent was removed by oil pump vacuum. The residue was extracted with toluene (3 × 25 mL). The combined extracts were filtered through a neutral alumina column (2.5 × 7 cm, packed in toluene). The solvent was removed by rotary evaporation to give **Pt'$C_4$H-b** as an off-white solid (0.418 g, 0.384 mmol, 77%), dec pt 149 °C. Calcd for ($C_{57}H_{53}F_5P_2Pt$)·($CH_2Cl_2$) (1175.03): C, 59.29; H, 4.72. Found: 59.16; H, 4.72.

NMR (δ, $CDCl_3$): $^1H$ 7.85-7.73 (m, 2H, *o* to P, Ph), 7.62-7.41 (m, 10H, *o* to P, tol+$C_6H_4$), 7.43-7.34 (m, 3H, *m*/*p* to P, Ph), 7.29 (d, $^3J_{HH}$ = 8.4 Hz, 4H, *m* to P, $C_6H_4$), 7.12 (d, $^3J_{HH}$ = 7.8 Hz, 6H, *m* to P, tol), 5.31 (s, 2H, $CH_2Cl_2$), 2.35 (s, 9H, $CH_3$, tol), 1.47 (t, $^6J_{HP}$ = 0.9 Hz, 1H, ≡CH); 1.29 (s, 18H, $C(CH_3)_3$); $^{13}C\{^1H\}$ 154.0 (s, *p* to P, $C_6H_4$), 146.0 (dd, $^1J_{CF}$ = 226 Hz, $^2J_{CF}$ = 23 Hz, *o* to Pt, $C_6F_5$), 141.0 (s, *p* to P, tol), 136.5 (dm, $^1J_{CF}$ = 254 Hz, *m*/*p* to Pt, $C_6F_5$), 134.9 (virtual t,[66] $^2J_{CP}$ = 6.4 Hz, *o* to P, Ph), 134.6 (virtual t,[66] $^2J_{CP}$ = 6.4 Hz, *o* to P, tol), 134.3 (virtual t,[66] $^2J_{CP}$ = 6.4 Hz, *o* to P, $C_6H_4$), 131.1 (virtual t,[66] $^1J_{CP}$ = 29.3 Hz, *i* to P, Ph), 130.7 (s, *p* to P, Ph), 128.9 (virtual t,[66] $^3J_{CP}$ = 5.6 Hz, *m* to P, tol), 128.2 (virtual t,[66] $^3J_{CP}$ = 5.5 Hz, *m* to P, Ph), 127.5 (virtual t,[66] $^1J_{CP}$ = 30.2 Hz, *i* to P, tol), 127.2 (virtual t,[66] $^1J_{CP}$ = 30.0 Hz, *i* to P, $C_6H_4$), 125.1 (virtual t,[66] $^3J_{CP}$ = 5.5 Hz, *m* to P, $C_6H_4$), 98.1 (s, $^1J_{CPt}$ = 993 Hz,[65] Pt*C*≡C), 95.3 (s, $^2J_{CPt}$ = 265 Hz,[65] PtC≡*C*), 72.7 (t, $^4J_{CP}$ = 2.5 Hz, $^3J_{CPt}$ = 36.2 Hz,[65] PtC≡C*C*), 59.9 (s, PtC≡CC≡*C*), 53.7 (s, $CH_2Cl_2$), 34.9 (s, *C*$(CH_3)_3$), 31.3 (s, $CH_3$); 21.5 (s, $CH_3$, tol); $^{31}P\{^1H\}$ 17.8 (s, $^1J_{PPt}$ = 2656 Hz[65]).

***trans*-($C_6F_5$)(*p*-$tol_3P$)((*p*-$MeOC_6H_4)_2PhP$)Pt($C{\equiv}C)_2H$ (Pt'$C_4$H-c).** Complex **Pt'Cl-c** (1.317 g, 1.286 mmol), CuI (0.051 g, 0.268 mmol), $CH_2Cl_2$ (10 mL), $HNEt_2$ (80 mL), and butadiyne (2.14 M in THF, 15 mL, 32.1 mmol)[64] were combined in a procedure analogous to that for **Pt'$C_4$H-b**. A similar workup (toluene extraction 3 × 40 mL) gave

**Pt'$C_4$H-c** as an off-white solid (0.999 g, 0.962 mmol, 75%), mp 138 °C. Calcd for $C_{51}H_{41}F_5O_2P_2Pt$ (1037.92): C, 59.02; H, 3.98. Found: 58.93; H, 3.98.

NMR (δ, $CDCl_3$): $^1$H 7.66-7.56 (m, 4H, *o* to P, $C_6H_4$), 7.55-7.41 (m, 8H, *o* to P, tol+Ph), 7.36-7.29 (m, 1H, *p* to P, Ph), 7.26 (d, $^3J_{HH}$ = 5.4 Hz, 2H, *m* to P, Ph), 7.12 (d, $^3J_{HH}$ = 7.5 Hz, 6H, *m* to P, tol), 6.87 (d, $^3J_{HH}$ = 9.0 Hz, 4H, *m* to P, $C_6H_4$), 3.84 (s, 6H, $OCH_3$), 2.36 (s, 9H, $CH_3$, tol), 1.49 (t, $^6J_{HP}$ = 0.9 Hz, 1H, ≡CH); $^{13}$C{$^1$H} 161.6 (s, *p* to P, $C_6H_4$), 145.9 (dd, $^1J_{CF}$ = 225 Hz, $^2J_{CF}$ = 24 Hz, *o* to Pt, $C_6F_5$), 140.9 (s, *p* to P, tol), 136.7 (dm, $^1J_{CF}$ = 238 Hz, *m*/*p* to Pt, $C_6F_5$), 136.4 (dd, $^2J_{CP}$ = 7.9 Hz, $^4J_{CP}$ = 6.3 Hz, *o* to P, $C_6H_4$), 134.4 (dd, $^2J_{CP}$ = 7.0 Hz, $^4J_{CP}$ = 5.8 Hz, *o* to P, tol), 133.8 (dd, $^2J_{CP}$ = 6.7 Hz, $^4J_{CP}$ = 5.5 Hz, *o* to P, Ph), 131.8 (dd, $^1J_{CP}$ = 34.4 Hz, $^3J_{CP}$ = 24.5 Hz, *i* to P, Ph), 130.3 (s, *p* to P, Ph), 128.8 (dd, $^3J_{CP}$ = 6.6 Hz, $^5J_{CP}$ = 4.6 Hz, *m* to P, tol), 127.9 (dd, $^3J_{CP}$ = 6.2 Hz, $^5J_{CP}$ = 4.4 Hz, *m* to P, Ph), 127.4 (dd, $^1J_{CP}$ = 35.1 Hz, $^3J_{CP}$ = 25.3 Hz, $^2J_{CPt}$ = 26.4 Hz,[65] *i* to P, tol), 121.4 (dd, $^1J_{CP}$ = 37.2 Hz, $^3J_{CP}$ = 26.4 Hz, $^2J_{CPt}$ = 27.9 Hz,[65] *i* to P, $C_6H_4$), 113.8 (dd, $^3J_{CP}$ = 6.9 Hz, $^5J_{CP}$ = 5.0 Hz, *m* to P, $C_6H_4$), 98.0 (s, $^1J_{CPt}$ = 989 Hz,[65] Pt*C*≡C), 95.2 (s, $^2J_{CPt}$ = 267 Hz,[65] PtC≡*C*), 72.6 (t, $^4J_{CP}$ = 2.5 Hz, $^3J_{CPt}$ = 34.5 Hz,[65] PtC≡C*C*), 60.1 (s, PtC≡CC≡*C*), 55.4 (s, $OCH_3$), 21.5 (s, $CH_3$, tol); $^{31}$P{$^1$H} 17.64, 17.58 (2 × s, $^1J_{PPt}$ = 2647 Hz[65]).

***trans*-($C_6F_5$)(*p*-$tol_3$P)(*n*-$Pr_2$PhP)Pt(C≡C)$_2$H (Pt'$C_4$H-d).** Complex **Pt'Cl-d** (1.214 g, 1.355 mmol), CuI (0.053 g, 0.278 mmol), $CH_2Cl_2$ (10 mL), $HNEt_2$ (90 mL),

and butadiyne (3.98 M in THF, 6.1 mL, 24.4 mmol)[64] were combined in a procedure analogous to that for **Pt'$C_4$H-c**. A similar workup gave a residue that was recrystallized from hexane to give **Pt'$C_4$H-d** as an off-white solid (0.898 g, 0.987 mmol, 73%), mp 54 °C. Calcd for $C_{43}H_{41}F_5P_2Pt$ (909.81): C, 56.77; H, 4.54. Found: 56.52; H, 4.64.

NMR (δ, $CDCl_3$): $^1$H 7.53-7.47 (m, 2H, *o* to P, Ph), 7.44 (dd, $^3J_{HP}$ = 11.0 Hz, $^3J_{HH}$ = 8.0 Hz, 6H, *o* to P, tol), 7.37-7.30 (m, 3H, *m*/*p* to P, Ph), 7.10 (dd, $^3J_{HH}$ = 8.0 Hz, $^4J_{HP}$ = 2.0 Hz, 6H, *m* to P, tol), 2.35 (s, 9H, $CH_3$, tol), 2.31-2.08 (m, 4H, $PCH_2$), 1.65 (t, $^6J_{HP}$ = 1.0 Hz, 1H, ≡CH), 1.76-1.62, 1.53-1.39 (2 × m, 2H/2H, $PCH_2CH_2$), 1.02 (dt, $^3J_{HH}$ = 7.3 Hz, $^4J_{HP}$ = 1.0 Hz, 6H, $PCH_2CH_2CH_3$); $^{13}C\{^1H\}$ 146.5 (dd, $^1J_{CF}$ = 224 Hz, $^2J_{CF}$ = 23 Hz, *o* to Pt, $C_6F_5$), 140.9 (d, $^4J_{CP}$ = 2.4 Hz, *p* to P, tol), 136.9 (dm, $^1J_{CF}$ = 248 Hz, *m*/*p* to Pt, $C_6F_5$), 134.4 (dd, $^2J_{CP}$ = 11.3 Hz, $^4J_{CP}$ = 1.1 Hz, $^3J_{CPt}$ = 20.1 Hz,[65] *o* to P, tol), 131.5 (d, $^2J_{CP}$ = 9.4 Hz,$^3J_{CPt}$ = 17.8 Hz,[65] *o* to P, Ph), 131.3 (dd, $^1J_{CP}$ = 51.6 Hz, $^3J_{CP}$ = 2.6 Hz, *i* to P, Ph), 130.2 (d, $^4J_{CP}$ = 2.3 Hz, *p* to P, Ph), 128.8 (d, $^3J_{CP}$ = 11.1 Hz, *m* to P, tol), 128.2 (d, $^3J_{CP}$ = 9.9 Hz, *m* to P, Ph), 127.5 (dd, $^1J_{CP}$ = 56.4 Hz, $^3J_{CP}$ = 2.9 Hz, $^3J_{CPt}$ = 26.4 Hz,[65] *i* to P, tol), 124.4 (t, $^2J_{CF}$ = 53 Hz, *i* to Pt, $C_6F_5$), 98.6 (br, $^1J_{CPt}$ = 1000 Hz,[65] Pt*C*≡C), 92.7 (s, $^2J_{CPt}$ = 274 Hz,[65] PtC≡*C*), 72.6 (t, $^4J_{CP}$ = 2.4 Hz, $^3J_{CPt}$ = 34.9 Hz,[65] PtC≡C*C*), 59.9 (s, PtC≡CC≡*C*), 27.0 (dd, $^1J_{CP}$ = 33.3 Hz, $^3J_{CP}$ = 1.8 Hz, $^2J_{CPt}$ = 33.5 Hz,[65] $PCH_2$), 21.5 (d, $^5J_{CP}$ = 1.3 Hz, $CH_3$, tol), 18.0 (s, $^3J_{CPt}$ = 23.5 Hz,[65]

$PCH_2CH_2$), 16.1 (d, $^3J_{CP}$ = 15.0 Hz, $PCH_2CH_2CH_3$); $^{31}P\{^1H\}$ 18.5 (d, $^2J_{PP}$ = 404 Hz, $^1J_{PPt}$ = 2556 Hz,[65] *p*-$tol_3P$), 6.0 (d, $^2J_{PP}$ = 404 Hz, $^1J_{PPt}$ = 2546 Hz,[65] *n*-$Pr_2PhP$).

***trans*,*trans*-($C_6F_5$)(*p*-$tol_3P$)($Me_2PhP$)Pt(C≡C)$_2$Pt($PPhMe_2$)(P*p*-$tol_3$)($C_6F_5$)**

(**Pt'$C_4$Pt'-a**). A Schlenk flask was charged with **Pt'Cl-a** (0.354 g, 0.421 mmol), **Pt'$C_4$H-a** (0.359 g, 0.420 mmol), CuCl (0.016 g, 0.166 mmol), and $HNEt_2$ (60 mL). The mixture was stirred for 65 h at 50 °C. After cooling, the solvent was removed by oil pump vacuum, and the residue extracted with toluene (3 × 20 mL). The combined extracts were filtered through a neutral alumina column (8 cm, packed in toluene). The solvent was removed by rotary evaporation. The residue was chromatographed on a silica gel column (2.5 × 40 cm, 40:60 v/v $CH_2Cl_2$/hexane). The solvent was removed from the product containing fractions by rotary evaporation and oil pump vacuum to give five complexes as yellow solids: *trans*,*trans*-($C_6F_5$)(*p*-$tol_3P$)$_2$Pt(C≡C)$_2$Pt(P*p*-$tol_3$)$_2$($C_6F_5$) (**PtC$_4$Pt**,[20] 0.021 g, 0.011 mmol, 3%), *trans*,*trans*-($C_6F_5$)(*p*-$tol_3P$)$_2$Pt(C≡C)$_2$Pt(P*p*-$tol_3$)($PPhMe_2$)($C_6F_5$) (**PtC$_4$Pt'-a**, 0.169 g, 0.0928 mmol, 23%), *trans*,*trans*-($C_6F_5$)(*p*-$tol_3P$)$_2$Pt(C≡C)$_2$Pt($PPhMe_2$)$_2$($C_6F_5$) (**PtC$_4$Pt"-a**, 0.079 g, 0.048 mmol, 12%), *trans*,*trans*-($C_6F_5$)(*p*-$tol_3P$)($Me_2PhP$)Pt(C≡C)$_2$Pt($PPhMe_2$)(P*p*-$tol_3$)($C_6F_5$) (**Pt'C$_4$Pt'-a**, 0.184 g, 0.111 mmol, 27%), and *trans*,*trans*-($C_6F_5$)(*p*-$tol_3P$)($Me_2PhP$)Pt(C≡C)$_2$Pt($PPhMe_2$)$_2$($C_6F_5$) (**Pt'C$_4$Pt"-a**, 0.022 g, 0.015 mmol, 4%).

Data for **PtC$_4$Pt.**[20] NMR (δ, $CDCl_3$): $^1H$ 7.42 (m, 24H, *o* to P), 6.88 (d, $^3J_{HH}$ = 7.8 Hz, 24H, *m* to P), 2.28 (s, 36H, $CH_3$); $^{31}P\{^1H\}$ 16.4 (s, $^1J_{PPt}$ = 2713 Hz[65]).

Data for **PtC$_4$Pt'-a.** mp 132 °C. Calcd for $C_{87}H_{74}F_{10}P_4Pt_2$ (1823.58): C, 57.30; H, 4.09. Found: 57.15; H, 4.22. NMR (δ, $CDCl_3$): $^1$H 7.53 (m, 12H, *o* to P, tol, **Pt**), 7.37 (dd, $^3J_{HH}$ = 8.3 Hz, $^3J_{HP}$ = 11.2 Hz, 6H, *o* to P, tol, **Pt'**), 7.31-7.21 (m, 3H, *o*/*p* to P, Ph), 7.16-7.10 (m, 2H, *m* to P, Ph), 7.00 (d, $^3J_{HH}$ = 7.8 Hz, 12H, *m* to P, tol, **Pt**), 6.90 (dd, $^3J_{HH}$ = 8.4 Hz, $^4J_{HP}$ = 2.1 Hz, 6H, *m* to P, tol, **Pt'**), 2.30 (s, 18H, $CH_3$, tol, **Pt**), 2.28 (s, 9H, $CH_3$, tol, **Pt'**), 1.54 (dd, $^2J_{HP}$ = 10.5 Hz, $^4J_{HP}$ = 2.7 Hz, $^3J_{HPt}$= 44.4 Hz,[65] 6H, $PMe_2$); $^{13}C\{^1H\}$[68,69] 146.4 (dd, $^1J_{CF}$ = 223 Hz, $^2J_{CF}$ = 26 Hz, *o* to **Pt'**, $C_6F_5$), 146.1 (dd, $^1J_{CF}$ = 222 Hz, $^2J_{CF}$ = 24 Hz, *o* to **Pt**, $C_6F_5$), 140.3 (s, *p* to P, tol, **Pt**), 140.1 (d, $^4J_{CP}$ = 2.3 Hz, *p* to P, tol, **Pt'**), 136.4 (dm, $^1J_{CF}$ = 267 Hz, *m*/*p* to **Pt**/**Pt'**, $C_6F_5$), 134.7 (virtual t,[66] $^2J_{CP}$ = 6.3 Hz, *o* to P, tol, **Pt**), 134.5 (d, $^2J_{CP}$ = 11.5 Hz, *o* to P, tol, **Pt'**), 134.5 (dd, $^1J_{CP}$ = 59 Hz, $^3J_{CP}$ = 3.2 Hz, *i* to P, Ph), 130.2 (d, $^2J_{CP}$ = 9.1 Hz, *o* to P, Ph), 129.6 (d, $^4J_{CP}$ = 2.4 Hz, *p* to P, Ph), 128.5 (d, $^3J_{CP}$ = 10.7 Hz, *m* to P, tol, **Pt'**), 128.5 (virtual t,[66] $^3J_{CP}$ = 5.4 Hz, *m* to P, tol, **Pt**), 128.3 (virtual t,[66] $^1J_{CP}$ = 29.6 Hz, *i* to P, tol, **Pt**), 128.3 (dd, $^1J_{CP}$ = 55.4 Hz, $^3J_{CP}$ = 2.3 Hz, *i* to P, tol, **Pt'**), 128.0 (d, $^3J_{CP}$ = 10.0 Hz, *m* to P, Ph), 102.8 (s, $^3J_{CP}$ = 31.5 Hz, $^2J_{CPt}$ = 266 Hz,[65] PtC≡*C*), 100.8 (s, $^3J_{CP}$ = 33.8 Hz, $^2J_{CPt}$ = 273 Hz,[65] Pt'C≡*C*), 88.8 (br, $^1J_{CPt}$ = 960 Hz,[65] PtC/Pt'C), 21.5 (s, $CH_3$, tol, **Pt**), 21.4 (s, $CH_3$, tol, **Pt'**), 13.7 (dd, $^1J_{CP}$ = 38.2 Hz, $^3J_{CP}$ = 2.0 Hz, $^2J_{CPt}$ = 49.4 Hz,[65] $PMe_2$); $^{31}P\{^1H\}$ 17.0 (s, $^1J_{PPt}$ = 2714 Hz,[65] *p*-$tol_3P$, **Pt**), 15.9 (d, $^2J_{PP}$ = 436 Hz, $^1J_{PPt}$ = 2620 Hz,[65] *p*-$tol_3P$, **Pt'**), –10.7 (d, $^2J_{PP}$ = 436 Hz, $^1J_{PPt}$ = 2554 Hz,[65] $Me_2PhP$, **Pt'**).

Data for **PtC$_4$Pt"-a.** mp 101 °C. Calcd for $C_{74}H_{64}F_{10}P_4Pt_2$ (1657.38): C, 53.63; H, 3.89. Found: 53.82; H, 3.87. NMR (δ, $CDCl_3$): $^1$H 7.55 (m, 12H, *o* to P, tol), 7.20 (m, 6H, *o*/*p* to P, Ph), 7.12 (d, 4H, $^3J_{HH}$ = 7.2 Hz, *m* to P, Ph), 7.08 (d, $^3J_{HH}$ = 7.8 Hz, 12H, *m* to P, tol), 2.36 (s, 18H, $CH_3$, tol), 1.55 (virtual t,[66] $^2J_{HP}$ = 3.6 Hz, $^3J_{HPt}$ = 31.8 Hz, 12H, PMe); $^{13}$C{$^1$H} 146.8 (dd, $^1J_{CF}$ = 229 Hz, $^2J_{CF}$ = 28 Hz, *o* to **Pt"**, $C_6F_5$), 146.1 (dd, $^1J_{CF}$ = 221 Hz, $^2J_{CF}$ = 25 Hz, *o* to **Pt**, $C_6F_5$), 140.4 (s, *p* to P, tol), 136.5 (dm, $^1J_{CF}$ = 266 Hz, *m*/*p* to **Pt/Pt"**, $C_6F_5$), 134.7 (virtual t,[66] $^2J_{CP}$ = 6.3 Hz, *o* to P, tol), 134.1 (virtual t,[66] $^1J_{CP}$ = 27.0 Hz, *i* to P, Ph), 130.2 (virtual t,[66] $^2J_{CP}$ = 5.4 Hz, *o* to P, Ph), 129.7 (s, *p* to P, Ph), 128.6 (virtual t,[66] $^3J_{CP}$ = 5.7 Hz, *m* to P, tol), 128.2 (virtual t,[66] $^1J_{CP}$ = 29.9 Hz, *i* to P, tol), 128.1 (virtual t,[66] $^3J_{CP}$ = 5.1 Hz, *m* to P, Ph), 124.8 (br, *i* to **Pt**, $C_6F_5$), 123.0 (br, *i* to **Pt"**, $C_6F_5$), 101.5 (s, $^3J_{CP}$ = 34.7 Hz, $^2J_{CPt}$ = 260 Hz,[65] PtC≡*C*), 97.5 (s, $^3J_{CP}$ = 33.2 Hz, $^2J_{CPt}$ = 286 Hz,[65] Pt"C≡*C*), 89.1 (s, $^1J_{CPt}$ = 968 Hz,[65] Pt"C), 88.9 (s, $^1J_{CPt}$ = 959 Hz,[65] PtC), 21.6 (s, $CH_3$, tol), 14.0 (virtual t,[66] $^1J_{CP}$ = 19.8 Hz, $^2J_{CPt}$ = 44.2 Hz,[65] $PMe_2$); $^{31}$P{$^1$H} 17.5 (s, $^1J_{PPt}$ = 2712 Hz,[65] P(*p*-tol)$_3$), –10.8 (s, $^1J_{PPt}$ = 2458 Hz,[65] $Me_2PhP$).

Data for **Pt'C$_4$Pt'-a.** mp 194 °C. Calcd for $(C_{74}H_{64}F_{10}P_4Pt_2)\cdot(CH_2Cl_2)_2$ (1827.20): C, 49.96; H, 3.75. Found: 50.29; H, 3.70. NMR (δ, $CDCl_3$): $^1$H 7.46 (dd, $^3J_{HH}$ = 8.1 Hz, $^3J_{HP}$ = 11.1 Hz, 12H, *o* to P, tol, overlapped with m, 2H, *o* to P, Ph), 7.17-7.31 (m, 6H, *m*/*p* to P, Ph), 7.02 (d, $^3J_{HH}$ = 7.8 Hz, 12H, *m* to P, tol), 2.31 (s, 18H, $CH_3$, tol), 1.73 (dd, $^2J_{HP}$ = 10.5 Hz, $^4J_{HP}$ = 2.7 Hz, $^3J_{HPt}$ = 45 Hz, 12H, $PMe_2$); $^{13}$C{$^1$H} 146.5 (dd,

$^{1}J_{CF}$ = 223 Hz, $^{2}J_{CF}$ = 20 Hz, *o* to Pt, $C_6F_5$), 140.3 (d, $^{4}J_{CP}$ = 2.4 Hz, *p* to P, tol), 136.4 (dm, $^{1}J_{CF}$ = 282 Hz, *m*/*p* to Pt, $C_6F_5$), 134.6 (d, $^{2}J_{CP}$ = 11.1 Hz, *o* to P, tol), 134.4 (dd, $^{1}J_{CP}$ = 53 Hz, $^{3}J_{CP}$ = 3.1 Hz, *i* to P, Ph), 130.5 (d, $^{2}J_{CP}$ = 9.7 Hz, *o* to P, Ph), 129.8 (d, $^{4}J_{CP}$ = 2.4 Hz, *p* to P, Ph), 128.6 (d, $^{3}J_{CP}$ = 10.7 Hz, *m* to P, tol), 128.1 (d, $^{3}J_{CP}$ = 10.4 Hz, *m* to P, Ph), 128.2 (dd, $^{1}J_{CP}$ = 55.4 Hz, $^{3}J_{CP}$ = 2.7 Hz, $^{2}J_{CPt}$ = 26.2 Hz,[65] *i* to P, tol), 126.1 (t, $^{2}J_{CF}$ = 50.4 Hz, *i* to Pt, $C_6F_5$), 99.6 (s, $^{3}J_{CP}$ = 33.9 Hz, $^{2}J_{CPt}$ = 275 Hz,[65] PtC≡*C*), 90.0 (s, $^{1}J_{CPt}$ = 971 Hz,[65] Pt*C*), 21.5 (s, $CH_3$, tol), 14.2 (dd, $^{1}J_{CP}$ = 37.9 Hz, $^{3}J_{CP}$ = 2.0 Hz, $^{2}J_{CPt}$ = 45.0 Hz,[65] $PMe_2$); $^{31}P\{^{1}H\}$ 16.8 (d, $^{2}J_{PP}$ = 435 Hz, $^{1}J_{PPt}$ = 2610 Hz,[65] P(*p*-tol)$_3$), –10.8 (d, $^{2}J_{PP}$ = 435 Hz, $^{1}J_{PPt}$ = 2570 Hz,[65] $Me_2PhP$).

Data for **Pt'$C_4$Pt"-a.** NMR (δ, $CDCl_3$): $^{1}H$ 7.50 (dd, $^{3}J_{HH}$ = 8.0 Hz, $^{3}J_{HP}$ = 11.1 Hz, 6H, *o* to P, tol, **Pt'**, overlapped with m, 2H, *o* to P, Ph, **Pt'**), 7.32 (m, 6H, *o*/*p* to P, Ph, **Pt"**), 7.22 (m, 3H, *m*/*p* to P, Ph, **Pt'**), 7.12 (d, $^{3}J_{HH}$ = 8.4 Hz, 4H, *m* to P, Ph, **Pt"**), 7.07 (d, $^{3}J_{HH}$ = 8.1 Hz, 6H, *m* to P, tol), 2.33 (s, 9H, $CH_3$, tol), 1.88 (dd, $^{2}J_{HP}$ = 10.5 Hz, $^{4}J_{HP}$ = 2.7 Hz, $^{3}J_{HPt}$ = 45 Hz,[65] 6H, $PMe_2$, **Pt'**), 1.70 (virtual t,[66] $^{2}J_{HP}$ = 3.3 Hz, $^{3}J_{HPt}$ = 32.4 Hz,[65] 12H, $PMe_2$, **Pt"**); $^{31}P\{^{1}H\}$ 18.0 (d, $^{2}J_{PP}$ = 433 Hz, $^{1}J_{PPt}$ = 2595 Hz,[65] *p*-tol$_3$P), –10.2 (d, $^{2}J_{PP}$ = 433 Hz, $^{1}J_{PPt}$ = 2576 Hz,[65] $Me_2PhP$, **Pt'**), –10.4 (s, $^{1}J_{PPt}$ = 2459 Hz,[65] $Me_2PhP$, **Pt"**).

***trans*,*trans*-($C_6F_5$)(*p*-tol$_3$P)((*p*-*t*-Bu$C_6H_4$)$_2$PhP)Pt(C≡C)$_2$Pt(PPh(*p*-$C_6H_4$*t*-Bu)$_2$)(P*p*-tol$_3$)($C_6F_5$) (Pt'$C_4$Pt'-b). Synthesis A**. A Schlenk flask was charged with

**Pt'Cl-b** (0.286 g, 0.266 mmol), **Pt'$C_4$H-b** (0.289 g, 0.266 mmol), CuCl (0.014 g, 0.141 mmol), and $HNEt_2$ (60 mL). The mixture was stirred for 88 h at 45 °C. After cooling, the solvent was removed by oil pump vacuum, and the residue extracted with toluene (3 × 25 mL). The combined extracts were filtered through a neutral alumina column (8 cm, packed in toluene). The solvent was removed by rotary evaporation. The residue was chromatographed on a silica gel column (3.8 × 43 cm, 30:70 v/v $CH_2Cl_2$/hexane). The solvent was removed from the product containing fractions by rotary evaporation and oil pump vacuum to give three pure complexes as yellow solids: *trans*, *trans*-($C_6F_5$)((*p*-*t*-Bu$C_6H_4$)$_2$PhP)$_2$Pt(C≡C)$_2$Pt(PPh(*p*-$C_6H_4$*t*-Bu)$_2$)$_2$($C_6F_5$) (**Pt"$C_4$Pt"-b**, 0.010 g, 0.005 mmol, 2%), *trans*,*trans*-($C_6F_5$)(*p*-$tol_3$P)((*p*-*t*-Bu$C_6H_4$)$_2$PhP)Pt(C≡C)$_2$Pt(PPh(*p*-$C_6H_4$*t*-Bu)$_2$)$_2$($C_6F_5$) (**Pt'$C_4$Pt"-b**, 0.036 g, 0.016 mmol, 6%) and **Pt$C_4$Pt** (0.009 g, 0.005 mmol, 2%). Other fractions contained mixtures of three additional complexes. One of these (0.055 g) was chromatographed on a silica gel column (2.5 × 42 cm, 18:82 v/v ethyl acetate/hexane). The solvent was removed from the product containing fractions by rotary evaporation and oil pump vacuum to give *trans*,*trans*-($C_6F_5$)(*p*-$tol_3$P)$_2$Pt(C≡C)$_2$Pt(PPh(*p*-$C_6H_4$*t*-Bu)$_2$)$_2$($C_6F_5$) (**Pt$C_4$Pt"-b**, 0.015 g, 0.007 mmol, 3%) and *trans*,*trans*-($C_6F_5$)(*p*-$tol_3$P)$_2$Pt(C≡C)$_2$Pt(PPh(*p*-$C_6H_4$*t*-Bu)$_2$)(P*p*-$tol_3$)($C_6F_5$) (**Pt$C_4$Pt'-b**, 0.039 g, 0.019 mmol, 8%). Another fraction (0.064 g) was chromatographed on a silica gel column (2.5 × 43 cm, 12:88 v/v ethyl acetate/hexane). The solvent was removed from the product containing fractions by rotary evaporation and oil pump vacuum to give **Pt'$C_4$Pt"-b** (0.010 g, 0.005 mmol, 2%) and a mixture of **Pt'$C_4$Pt'-b** and

**PtC$_4$Pt"-b** (0.050 g). NMR analysis of the mixture indicated 3% and 6% yields of **Pt'C$_4$Pt'-b** and **PtC$_4$Pt"-b**, respectively (a total of 0.046 g, 0.021 mmol, 8% for the latter).

Data for **Pt"C$_4$Pt"-b**. dec pt 205 °C. NMR (δ, $CDCl_3$): $^1$H 7.75-7.67 (m, 8H, *o* to P, Ph), 7.44-7.35 (m, 16H, *o* to P, $C_6H_4$), 7.13 (d, $^3J_{HH}$ = 8.4 Hz, 16H, *m* to P, $C_6H_4$), 7.06 (m, 4H, *p* to P, Ph), 6.93 (m, 8H, *m* to P, Ph), 1.26 (s, 72H, $C(CH_3)_3$); $^{31}$P{$^1$H} 16.0 (s, $^1J_{PPt}$ = 2715 Hz[65]).

Data for **Pt'C$_4$Pt"-b.** dec pt 182 °C. Calcd for $C_{115}H_{114}F_{10}P_4Pt_2$(2200.19): C 62.78; H 5.22. Found: C 62.76, H 5.26. NMR (δ, $CDCl_3$): $^1$H 7.77-7.66 (m, 6H, *o* to P, Ph), 7.48-7.36 (m, 18H, *o* to P, tol+$C_6H_4$), 7.14 (d, $^3J_{HH}$ = 8.4 Hz, 12H, *m* to P, $C_6H_4$, overlapped with m, 6H, *p* to P, Ph), 7.03-6.90 (m, 6H, *m* to P, Ph), 6.83 (d, $^3J_{HH}$ = 7.8 Hz, 6H, *m* to P, tol), 2.25 (s, 9H, $CH_3$, tol), 1.27 (s, 18H, $C(CH_3)_3$, **Pt'**), 1.26 (s, 36H, $C(CH_3)_3$, **Pt"**); $^{13}$C{$^1$H}[68] 153.1 (s, *p* to P, $C_6H_4$, **Pt'** and **Pt"**), 146.0 (dd, $^1J_{CF}$ = 222 Hz, $^2J_{CF}$ = 24 Hz, *o* to Pt, $C_6F_5$), 139.9 (s, *p* to P, tol), 136.8 (dm, $^1J_{CF}$ = 235 Hz, *m*/*p* to Pt, $C_6F_5$), 135.02 (virtual t,[66] $^2J_{CP}$ = 6.3 Hz, *o* to P, Ph, **Pt"**), 135.00 (virtual t,[66] $^2J_{CP}$ = 6.2 Hz, *o* to P, Ph, **Pt'**), 134.6 (virtual t,[66] $^2J_{CP}$ = 6.3 Hz, *o* to P, tol), 134.43 (virtual t,[66] $^2J_{CP}$ = 5.8 Hz, *o* to P, $C_6H_4$, **Pt'**), 134.35 (virtual t,[66] $^2J_{CP}$ = 6.0 Hz, *o* to P, $C_6H_4$, **Pt"**), 131.6 (dd, $^1J_{CP}$= 30.6 Hz, $^3J_{CP}$ = 28.2 Hz, *i* to P, Ph, **Pt'**), 131.5 (virtual t,[66] $^1J_{CP}$ = 29.0 Hz, *i* to P, Ph, **Pt"**), 129.8 (s, *p* to P, Ph, **Pt'** and **Pt"**), 128.3 (virtual t,[66] $^3J_{CP}$ = 5.4 Hz, *m*

to P, tol), 127.52 (virtual t,[66] $^3J_{CP}$ = 5.0 Hz, *m* to P, Ph, **Pt'**), 127.47 (virtual t,[66] $^3J_{CP}$ = 5.4 Hz, *m* to P, Ph, **Pt"**), 124.6 (virtual t,[66] $^3J_{CP}$ = 5.4 Hz, *m* to P, $C_6H_4$, **Pt'** and **Pt"**), 104.4 (s, $^2J_{CPt}$ = 271 Hz,[65] PtC≡*C*), 104.2 (s, $^2J_{CPt}$ = 271 Hz,[65] PtC≡*C*), 87.0 (s, $^1J_{CPt}$ = 952 Hz,[65] Pt*C*), 34.8 (s, *C*$(CH_3)_3$), 31.38 (s, C(*C*$H_3)_3$, **Pt'**), 31.36 (s, C(*C*$H_3)_3$, **Pt"**), 21.5 (s, $CH_3$, tol); $^{31}P\{^1H\}$[70] 16.35 (s, $^1J_{PPt}$ = 2713 Hz[65]), 16.16 (s, $^1J_{PPt}$ = 2712 Hz[65]**)**.

Data for **Pt$C_4$Pt"-b.** NMR (δ, $CDCl_3$): $^1H$ (see Figure B-5)[71] 7.75-7.65 (m, 4H, *o* to P, Ph), 7.48-7.35 (m, 20H, *o* to P, tol+$C_6H_4$), 7.14 (d, $^3J_{HH}$ = 7.5 Hz, 8H, *m* to P, $C_6H_4$, overlapped with m, 4H, *p* to P, Ph), 7.04-6.92 (m, 4H, *m* to P, Ph), 6.84 (dd, $^3J_{HH}$ = 7.8 Hz, $^4J_{HP}$ = 2.4 Hz, 12H, *m* to P, tol), 2.260, 2.251 (2 × s, 9H/9H, $CH_3$, tol), 1.264, 1.259 (2 × s, 18H/18H, $C(CH_3)_3$); $^{31}P\{^1H\}$ (see Figure B-6)[71] 16.2 (apparent t, $J_{PP}$ = 17.2 Hz, $^1J_{PPt}$ = 2715 Hz[65]). MS (MALDI, THAP matrix, m/z for the most intense peak of the isotope envelope): 2130 ($M^+$, 46%), 2153 ($M+Na^+$, 74%), 2169 ($M+K^+$, 35%), and other peaks.

Data for **Pt$C_4$Pt'-b.** dec pt 155 °C. Calcd for $C_{105}H_{94}F_{10}P_4Pt_2$ (2059.86): C, 61.22; H, 4.60. Found: C 61.27, H 4.73; NMR (δ, $CDCl_3$): $^1H$ 7.75-7.65 (m, 2H, *o* to P, Ph), 7.49-7.35 (m, 18H, *o* to P, tol+$C_6H_4$), 7.14 (d, $^3J_{HH}$ = 8.4 Hz, 4H, *m* to P, $C_6H_4$, overlapped with m, 2H, *p* to P, Ph), 7.02 (t, $^3J_{HH}$ = 7.6 Hz, 2H, *m* to P, Ph), 6.87 (d, $^3J_{HH}$ = 7.8 Hz, 18H, *m* to P, tol), 2.27 (s, 27H, $CH_3$, tol), 1.27 (s, 18H, $C(CH_3)_3$); $^{13}C\{^1H\}$[68] 153.3 (s, *p* to P, $C_6H_4$, **Pt'** and **Pt"**), 146.1 (dd, $^1J_{CF}$ = 223 Hz, $^2J_{CF}$ = 23 Hz, *o* to **Pt'**,

$C_6F_5$), 140.04 (s, *p* to P, tol, **Pt'**), 140.00 (s, *p* to P, tol, **Pt**), 136.7 (dm, $^1J_{CF}$ = 218 Hz, *m*/*p* to **Pt'**, $C_6F_5$), 135.1 (virtual t,[66] $^2J_{CP}$ = 6.7 Hz, *o* to P, Ph), 134.7 (virtual t,[66] $^2J_{CP}$ = 6.2 Hz, *o* to P, tol, **Pt**/**Pt'**), 134.5 (virtual t,[66] $^2J_{CP}$ = 6.1 Hz, *o* to P, $C_6H_4$), 131.7 (virtual t,[66] $^1J_{CP}$ = 30 Hz, *i* to P, Ph), 129.9 (s, *p* to P, Ph), 128.4 (virtual t,[66] $^3J_{CP}$ = 5.6 Hz, *m* to P, tol), 128.38 (virtual t,[66] $^1J_{CP}$ = 29.7 Hz, *i* to P, tol, **Pt**), 128.35 (virtual t,[66] $^1J_{CP}$ = 29.6 Hz, *i* to P, tol, **Pt'**), 128.1 (virtual t,[66] $^1J_{CP}$ = 30.1 Hz, *i* to P, $C_6H_4$), 127.5 (virtual t,[66] $^3J_{CP}$ = 5.4 Hz, *m* to P, Ph), 124.6 (virtual t,[66] $^3J_{CP}$= 5.4 Hz, *m* to P, $C_6H_4$), 104.4, 104.2 (2 × s, $^2J_{CPt}$ = 259/259 Hz,[65] PtC≡*C*), 86.84, 86.60 (2 × s, $^1J_{CPt}$ = 970/965 Hz,[65] Pt*C*), 34.8 (s, *C*$(CH_3)_3$), 31.3 (s, $CH_3$), 21.4 (s, $CH_3$, tol); $^{31}P\{^1H\}$ 16.29 (s, $^1J_{PPt}$ = 2711 Hz,[65] **Pt**), 16.17 (s, $^1J_{PPt}$ = 2712 Hz,[65] **Pt'**).

**Synthesis B**. A Schlenk flask was charged with **Pt'Cl-b** (0.913 g, 0.848 mmol), **Pt'$C_4$H-b** (0.925 g, 0.848 mmol), CuCl (0.019 g, 0.194 mmol), *t*-BuOK (0.118 g, 1.048 mmol), $KPF_6$ (0.188 g, 1.023 mmol), THF (70 mL), and methanol (50 mL) with stirring. After 15 d, the solvent was removed by rotary evaporation and oil pump vacuum. The residue was extracted with $CH_2Cl_2$ (3 × 25 mL). The extract was filtered through a alumina/celite pad (2.5 × 5 cm). The solvent was removed by rotary evaporation and oil pump vacuum. The residue was chromatographed on a silica gel column (3.8 × 44 cm, 3:1 v/v toluene/hexane). The solvent was removed from the product containing fractions by rotary evaporation and oil pump vacuum to give two pure complexes, **Pt'$C_4$Pt''-b** (0.020 g, 0.009 mmol, 2%) and **Pt'Cl-b** (0.320 g, 0.297 mmol, 36%), as yellow and white

solids, respectively. The other fractions were mixtures, and one that was rich in diplatinum products was chromatographed on a silica gel column (3.8 × 43 cm, 1:1 v/v chloroform/hexane). The solvent was removed from the product containing fractions by rotary evaporation and oil pump vacuum to give three pure complexes, **Pt'C$_4$H-b** (0.171 g, 0.157 mmol, 19%), **Pt'C$_4$Pt'-b** (0.379 g, 0.178 mmol, 21%) and **PtC$_4$Pt'-b** (0.014 g, 0.007 mmol, 1%).

Data for **Pt'C$_4$Pt'-b**. dec pt 165 °C. Calcd for $C_{110}H_{104}F_{10}P_4Pt_2$ (2130.09): C 62.03, H 4.92; found: C 62.13, H 4.96; NMR (δ, $CDCl_3$): $^1$H 7.75-7.64 (m, 4H, *o* to P, Ph), 7.49-7.35 (m, 20H, *o* to P, tol+$C_6H_4$), 7.14 (d, $^3J_{HH}$ = 8.7 Hz, 8H, *m* to P, $C_6H_4$, overlapped with m, 4H, *p* to P, Ph), 7.05-6.95 (m, 4H, *m* to P, Ph), 6.83 (d, $^3J_{HH}$ = 7.8 Hz, 12H, *m* to P, tol), 2.25 (s, 18H, $CH_3$, tol), 1.26 (s, 36H, $C(CH_3)_3$); $^{13}C\{^1H\}$[68] 153.2 (s, *p* to P, $C_6H_4$, **Pt'** and **Pt"**), 146.1 (dd, $^1J_{CF}$ = 221 Hz, $^2J_{CF}$ = 21 Hz, *o* to **Pt'**, $C_6F_5$), 140.0 (s, *p* to P, tol), 136.3 (dm, $^1J_{CF}$ = 254 Hz, *m*/*p* to **Pt'**, $C_6F_5$), 135.0 (virtual t,[66] $^2J_{CP}$ = 6.3 Hz, *o* to P, Ph), 134.6 (virtual t,[66] $^2J_{CP}$ = 6.3 Hz, *o* to P, tol), 134.4 (virtual t,[66] $^2J_{CP}$ = 5.9 Hz, *o* to P, $C_6H_4$), 131.7 (dd, $^1J_{CP}$ = 31.0 Hz, $^3J_{CP}$ = 27.6 Hz, *i* to P, Ph), 129.9 (s, *p* to P, Ph), 128.3 (virtual t,[66] $^3J_{CP}$ = 5.5 Hz, *m* to P, tol), 128.3 (dd, $^1J_{CP}$ = 31.0 Hz, $^3J_{CP}$ = 28.4 Hz, *i* to P, tol), 128.1 (dd, $^1J_{CP}$ = 31.2 Hz, $^3J_{CP}$ = 27.8 Hz, *i* to P, $C_6H_4$), 127.5 (virtual t,[66] $^3J_{CP}$ = 5.5 Hz, *m* to P, Ph), 124.6 (virtual t,[66] $^3J_{CP}$ = 5.2 Hz, *m* to P, $C_6H_4$), 104.3 (s, $^2J_{CPt}$ = 254 Hz,[65] PtC≡*C*), 86.8 (br s, $^1J_{CPt}$ = 967 Hz,[65] Pt*C*), 34.9 (s, *C*$(CH_3)_3$),

31.4 (s, $CH_3$), 21.5 (s, $CH_3$, tol); $^{31}P\{^1H\}$ (see also Figure B-1) 16.4 (s, $^1J_{PPt}$ = 2711 Hz[65]).

***trans*,*trans*-($C_6F_5$)(*p*-$tol_3P$)((*p*-$MeOC_6H_4)_2PhP$)Pt(C≡C)$_2$Pt(PPh(*p*-$C_6H_4OMe)_2$)(P*p*-$tol_3$)($C_6F_5$) (Pt'$C_4$Pt'-c).** A Schlenk flask was charged with **Pt'Cl-c** (0.747 g, 0.729 mmol), **Pt'$C_4$H-c** (0.688 g, 0.663 mmol), CuCl (0.026 g, 0.263 mmol), and $HNEt_2$ (120 mL). The mixture was stirred for 88 h at 50 °C. After cooling, the solvent was removed by rotary evaporation. The maroon residue was chromatographed on a silica gel column (3.8 × 42 cm) using 40:60 v/v $CH_2Cl_2$/hexane to elute **Pt$C_4$Pt** (0.022 g, 0.011 mmol, 2%), 50:50 v/v $CH_2Cl_2$/hexane to elute *trans*, *trans*-($C_6F_5$)(*p*-$tol_3P)_2$Pt(C≡C)$_2$Pt(P*p*-$tol_3$)(PPh(*p*-$C_6H_4OMe)_2)_2$($C_6F_5$) (**Pt$C_4$Pt'-c**, 0.084 g, 0.042 mmol, 7%) and **PtCl** (0.111 g, 0.108 mmol, 16%), 60:40 v/v $CH_2Cl_2$/hexane to elute an unknown complex (0.062 g), *trans*,*trans*-($C_6F_5$)(*p*-$tol_3P)_2$Pt(C≡C)$_2$Pt(PPh(*p*-$C_6H_4OMe)_2)_2$($C_6F_5$) (**Pt$C_4$Pt''-c**, 0.059 g, 0.029 mmol, 5%), and *trans*,*trans*-($C_6F_5$)(*p*-$tol_3P$)((*p*-$MeOC_6H_4)_2PhP$)Pt(C≡C)$_2$Pt(PPh(*p*-$C_6H_4OMe)_2$)(P*p*-$tol_3$)($C_6F_5$) (**Pt'$C_4$Pt'-c**, 0.111 g, 0.055 mmol, 8%), 70:30 v/v $CH_2Cl_2$/hexane to elute **Pt'Cl-c** (0.199 g, 0.185 mmol, 26%), and 75:20 v/v $CH_2Cl_2$/hexane to elute *trans*,*trans*-($C_6F_5$)(*p*-$tol_3P$)((*p*-$MeOC_6H_4)_2PhP$)Pt(C≡C)$_2$Pt(PPh(*p*-$C_6H_4OMe)_2)_2$($C_6F_5$) (**Pt'$C_4$Pt''-c**, 0.098 g, 0.048 mmol, 8%) and a second unknown complex (0.059 g).

Data for **Pt$C_4$Pt'-c.** NMR (δ, $CDCl_3$): $^1H$ 7.57-7.35 (m, 24H, *o* to P, Ph+tol+$C_6H_4$), 7.16 (t, $^3J_{HH}$ = 7.8 Hz, 1H, *p* to P, Ph), 7.03 (t, $^3J_{HH}$ = 7.5 Hz, 2H, *m* to P,

Ph), 6.88 (d, $^3J_{HH}$ = 7.8 Hz, 18H, *m* to P, tol), 6.62 (d, $^3J_{HH}$ = 8.7 Hz, 4H, *m* to P, $C_6H_4$), 3.73 (s, 6H, $OCH_3$), 2.28 (s, 27H, $CH_3$, tol); $^{31}P\{^1H\}$ 16.35 (s, $^1J_{PPt}$ = 2711 Hz,[65] *p*-tol$_3$P, **Pt**), 16.24, 16.17 (2 × s, $^1J_{PPt}$ = 2707 Hz,[65] *p*-tol$_3$P, (*p*-MeO$C_6H_4$)$_2$PhP, **Pt'**).

Data for **PtC$_4$Pt"-c.** dec pt 184 °C. Calcd for $C_{98}H_{80}F_{10}O_4P_4Pt_2$ (2025.68): C, 58.11; H, 3.98. Found: 58.10; H, 3.98. NMR (δ, $CDCl_3$): $^1H$ 7.54-7.36 (m, 24H, *o* to P, Ph+tol+$C_6H_4$), 7.18 (t, $^3J_{HH}$ = 7.2 Hz, 2H, *p* to P, Ph), 7.03 (t, $^3J_{HH}$ = 7.5 Hz, 4H, *m* to P, Ph), 6.90 (d, $^3J_{HH}$ = 7.8 Hz, 12H, *m* to P, tol), 6.63 (d, $^3J_{HH}$ = 9.0 Hz, 8H, *m* to P, $C_6H_4$), 3.73 (s, 12H, $OCH_3$), 2.29 (s, 18H, $CH_3$, tol); $^{13}C\{^1H\}$[68] 161.1 (s, *p* to P, $C_6H_4$, **Pt'** and **Pt"**), 146.1 (dm, $^1J_{CF}$ = 229 Hz, *o* to **Pt/Pt"**, $C_6F_5$), 140.0 (s, *p* to P, tol), 136.4 (virtual t,[66] $^2J_{CP}$ = 6.9 Hz, *o* to P, $C_6H_4$), 136.3 (dm, $^1J_{CF}$ = 261 Hz, *m*/*p* to **Pt/Pt"**, $C_6F_5$), 134.6 (virtual t,[66] $^2J_{CP}$ = 6.3 Hz, *o* to P, tol), 134.0 (virtual t,[66] $^2J_{CP}$ = 6.1 Hz, *o* to P, Ph), 132.4 (virtual t,[66] $^1J_{CP}$ = 29.0 Hz, *i* to P, Ph), 129.7 (s, *p* to P, Ph), 128.3 (virtual t,[66] $^3J_{CP}$ = 5.5 Hz, *m* to P, tol), 128.3 (virtual t,[66] $^1J_{CP}$ = 29.6 Hz, *i* to P, tol), 127.4 (virtual t,[66] $^3J_{CP}$ = 5.4 Hz, *m* to P, Ph), 122.2 (virtual t,[66] $^1J_{CP}$ = 31.3 Hz, *i* to P, $C_6H_4$), 113.3 (virtual t,[66] $^3J_{CP}$ = 5.8 Hz, *m* to P, $C_6H_4$), 104.1, 103.8 (2 × s, $^2J_{CPt}$ = 275 Hz,[65] PtC≡*C*), 86.9 (br s, $^1J_{CPt}$ = 951 Hz,[65] Pt*C*≡C), 55.4 (s, $OCH_3$), 21.5 (s, $CH_3$, tol); $^{31}P\{^1H\}$ 16.30 (s, $^1J_{PPt}$ = 2710 Hz,[65] P*p*-tol$_3$), 15.92 (s, $^1J_{PPt}$ = 2698 Hz,[65] (*p*-MeO$C_6H_4$)$_2$PhP).

Data for **Pt'C$_4$Pt'-c.** mp 128 °C. Calcd for $C_{98}H_{80}F_{10}O_4P_4Pt_2$ (2025.68): C, 58.11; H, 3.98. Found: 58.28; H, 3.89. NMR (δ, $CDCl_3$): $^1H$ 7.55-7.36 (m, 24H, *o* to P,

Ph+tol+$C_6H_4$), 7.18 (t, $^3J_{HH}$ = 7.2 Hz, 2H, *p* to P, Ph), 7.04 (t, $^3J_{HH}$ = 7.2 Hz, 4H, *m* to P, Ph), 6.89 (d, $^3J_{HH}$ = 7.8 Hz, 12H, *m* to P, tol), 6.65 (d, $^3J_{HH}$ = 8.7 Hz, 8H, *m* to P, $C_6H_4$), 3.74 (s, 12H, $OCH_3$), 2.29 (s, 18H, $CH_3$); $^{13}C\{^1H\}$[68] 161.1 (s, *p* to P, $C_6H_4$, **Pt'** and **Pt"**), 146.1 (dd, $^1J_{CF}$ = 223 Hz, $^2J_{CF}$ = 23 Hz, *o* to Pt, $C_6F_5$), 140.1 (s, *p* to P, tol), 136.4 (virtual t,[66] $^2J_{CP}$ = 7.5 Hz, *o* to P, $C_6H_4$), 136.4 (dm, $^1J_{CF}$ = 258 Hz, *m*/*p* to Pt, $C_6F_5$), 134.6 (virtual t,[66] $^2J_{CP}$ = 6.8 Hz, *o* to P, tol), 134.0 (virtual t,[66] $^2J_{CP}$ = 6.5 Hz, *o* to P, Ph), 132.4 (dd, $^1J_{CP}$ = 33.4 Hz, $^3J_{CP}$ = 24.8 Hz, *i* to P, Ph), 129.7 (s, *p* to P, Ph), 128.4 (dd, $^3J_{CP}$ = 6.1 Hz, $^5J_{CP}$ = 4.8 Hz, *m* to P, tol), 128.3 (dd, $^1J_{CP}$ = 33.9 Hz, $^3J_{CP}$ = 25.4 Hz, *i* to P, tol), 127.4 (dd, $^3J_{CP}$ = 5.9 Hz, $^5J_{CP}$ = 4.6 Hz, *m* to P, Ph), 122.2 (dd, $^1J_{CP}$ = 36.0 Hz, $^3J_{CP}$ = 26.8 Hz, *i* to P, $C_6H_4$), 113.3 (dd, $^3J_{CP}$ = 6.6 Hz, $^5J_{CP}$ = 5.4 Hz, *m* to P, $C_6H_4$), 103.9 (s, $^2J_{CPt}$ = 264 Hz,[65] PtC≡*C*), 86.8 (s, $^1J_{CPt}$ = 966 Hz,[65] Pt*C*≡C), 55.4 (s, $OCH_3$), 21.5 (s, $CH_3$, tol); $^{31}P\{^1H\}$ 16.17, 16.14 (2 × s, $^1J_{PPt}$ = 2704 Hz[65]).

Data for **Pt'$C_4$Pt"-c.** mp 119 °C. Calcd for $C_{97}H_{78}F_{10}O_6P_4Pt_2$ (2043.73): C, 57.01; H, 3.85. Found: 57.13; H, 3.86. NMR (δ, $CDCl_3$): $^1H$ 7.57-7.37 (m, 24H, *o* to P, Ph+tol+$C_6H_4$), 7.19 (t, $^3J_{HH}$ = 7.5 Hz, 3H, *p* to P, Ph), 7.05 (t, $^3J_{HH}$ = 7.2 Hz, 6H, *m* to P, Ph), 6.91 (d, $^3J_{HH}$ = 7.8 Hz, 6H, *m* to P, tol), 6.66 (d, $^3J_{HH}$ = 9.0 Hz, 4H, *m* to P, $C_6H_4$, **Pt'**), 6.65 (d, $^3J_{HH}$ = 8.7 Hz, 8H, *m* to P, $C_6H_4$, **Pt"**), 3.75 (s, 6H, $OCH_3$, **Pt'**), 3.74 (s, 12H, $OCH_3$, **Pt"**), 2.30 (s, 9H, $CH_3$); $^{13}C\{^1H\}$[68] 161.1 (s, *p* to P, $C_6H_4$, **Pt'** and **Pt"**), 146.1 (dd, $^1J_{CF}$ = 223 Hz, $^2J_{CF}$ = 24 Hz, *o* to **Pt'/Pt"**, $C_6F_5$), 140.1 (s, *p* to P, tol), 136.4

(virtual t,[66] $^{2}J_{CP}$ = 6.9 Hz, *o* to P, $C_6H_4$, **Pt'** and **Pt"**), 136.3 (dm, $^{1}J_{CF}$ = 261 Hz, *m*/*p* to **Pt'**/**Pt"**, $C_6F_5$), 134.6 (virtual t,[66] $^{2}J_{CP}$ = 6.3 Hz, *o* to P, tol), 134.0 (virtual t,[66] $^{2}J_{CP}$ = 6.1 Hz, *o* to P, Ph, **Pt'** and **Pt"**), 132.4 (virtual t,[66] $^{1}J_{CP}$ = 29.0 Hz, *i* to P, Ph, **Pt"**), 132.4 (dd, $^{1}J_{CP}$ = 33.3 Hz, $^{3}J_{CP}$ = 25.0 Hz, *i* to P, Ph, **Pt'**), 129.7 (s, *p* to P, Ph, **Pt'** and **Pt"**), 128.4 (virtual t,[66] $^{3}J_{CP}$ = 5.5 Hz, *m* to P, tol), 128.3 (dd, $^{1}J_{CP}$ = 33.6 Hz, $^{3}J_{CP}$ = 25.7 Hz, *i* to P, tol), 127.5 (virtual t,[66] $^{3}J_{CP}$ = 5.4 Hz, *m* to P, Ph, **Pt'** and **Pt"**), 122.2 (dd, $^{1}J_{CP}$ = 35.9 Hz, $^{3}J_{CP}$ = 27.0 Hz, *i* to P, $C_6H_4$, **Pt'**), 122.2 (virtual t,[66] $^{1}J_{CP}$ = 31.3 Hz, *i* to P, $C_6H_4$, **Pt"**), 113.3 (virtual t,[66] $^{3}J_{CP}$ = 5.7 Hz, *m* to P, $C_6H_4$, **Pt'** and **Pt"**), 103.8, 103.7 (2 × s, $^{2}J_{CPt}$ = 265/265 Hz,[65] PtC≡*C*), 87.0 (s, $^{1}J_{CPt}$ = 963 Hz,[65] Pt*C*≡C), 55.39 (s, $OCH_3$, **Pt'**), 55.37 (s, $OCH_3$, **Pt"**), 21.5 (s, $CH_3$, tol); $^{31}P\{^{1}H\}$ 16.19, 16.15 (2 × s, $^{1}J_{PPt}$ = 2703 Hz,[65] *p*-$tol_3P$, (*p*-$MeOC_6H_4)_2PhP$, **Pt'**), 15.94 (s, $^{1}J_{PPt}$ = 2696 Hz,[65] (*p*-$MeOC_6H_4)_2PhP$, **Pt"**).

***trans*,*trans*-(C$_6$F$_5$)(*p*-tol$_3$P)(*n*-Pr$_2$PhP)Pt(C≡C)$_2$Pt(PPh*n*-Pr$_2$)(P*p*-tol$_3$)(C$_6$F$_5$) (Pt'C$_4$Pt'-d).** A Schlenk flask was charged with **Pt'Cl-d** (0.876 g, 0.977 mmol), **Pt'C$_4$H-d** (0.888 g, 0.976 mmol), CuCl (0.021 g, 0.212 mmol), *t*-BuOK (0.146 g, 1.301 mmol), $KPF_6$ (0.239 g, 1.298 mmol), THF (70 mL), and methanol (50 mL) with stirring. After 92 h, the solvent was removed by rotary evaporation and oil pump vacuum. The residue was extracted with $CH_2Cl_2$ (3 × 25 mL). The extract was filtered through an alumina/celite pad (2.5 × 4 cm). The solvent was removed by rotary evaporation and oil pump vacuum. The residue was recrystallized twice from $CH_2Cl_2$ to yield pale yellow crystals of

**Pt'$C_4$Pt'-d** (1.312 g, 0.741 mmol, 76%), dec pt 214 °C. Calcd for $C_{82}H_{80}F_{10}P_4Pt_2$ (1769.62): C, 55.66; H, 4.56. Found: 55.88; H, 4.72.

NMR (δ, $CDCl_3$): $^1$H (see also Figures S3.2 and S3.3) 7.46 (dd, $^3J_{HP}$ = 11.0 Hz, $^3J_{HH}$ = 8.0 Hz, 12H, *o* to P, tol), 7.41-7.34 (m, 4H, *o* to P, Ph), 7.27-7.21 (m, 2H, *p* to P, Ph), 7.20-7.15 (m, 4H, *m* to P, Ph), 6.99 (dd, $^3J_{HH}$ = 8.0 Hz, $^4J_{HP}$ = 2.0 Hz, 12H, *m* to P, tol), 2.31 (s, 18H, $CH_3$, tol), 2.20-2.08, 2.07-1.93 (2 × m, 4H/4H, $PCH_2$), 1.67-1.53, 1.47-1.33 (2 × m, 4H/4H, $PCH_2CH_2$), 0.87 (t, $^3J_{HH}$ = 7.5 Hz, 12H, $PCH_2CH_2CH_3$); $^{13}$C{$^1$H} 146.5 (dd, $^1J_{CF}$ = 224 Hz, $^2J_{CF}$ = 25 Hz, *o* to Pt, $C_6F_5$), 140.2 (d, $^4J_{CP}$ = 2.4 Hz, *p* to P, tol), 136.6 (dm, $^1J_{CF}$ = 249 Hz, *m*/*p* to Pt, $C_6F_5$), 134.6 (d, $^2J_{CP}$ = 11.2 Hz, *o* to P, tol), 132.1 (dd, $^1J_{CP}$ = 49.1 Hz, $^3J_{CP}$ = 2.8 Hz, *i* to P, Ph), 131.3 (d, $^2J_{CP}$ = 8.8 Hz, *o* to P, Ph), 129.5 (d, $^4J_{CP}$ = 1.9 Hz, *p* to P, Ph), 128.5 (d, $^3J_{CP}$ = 10.8 Hz, *m* to P, tol), 128.4 (dd, $^1J_{CP}$ = 54.9 Hz, $^3J_{CP}$ = 3.0 Hz, *i* to P, tol), 127.9 (d, $^3J_{CP}$ = 9.7 Hz, *m* to P, Ph), 126.4 (t, $^2J_{CF}$ = 52.3 Hz, *i* to Pt, $C_6F_5$), 99.9 (s, $^2J_{CPt}$ = 267.6 Hz,[65] PtC≡*C*), 87.9 (br, $^1J_{CPt}$ = 971 Hz,[65] Pt*C*≡C), 26.9 (dd, $^1J_{CP}$ = 33.5 Hz, $^3J_{CP}$ = 1.3 Hz, $PCH_2$), 21.4 (d, $^5J_{CP}$ = 1.1 Hz, $CH_3$, tol), 18.0 (s, $PCH_2CH_2$), 16.0 (d, $^3J_{CP}$ = 14.8 Hz, $PCH_2CH_2CH_3$); $^{31}$P{$^1$H} 17.6 (d, $^2J_{PP}$ = 421 Hz, $^1J_{PPt}$ = 2620 Hz,[65] *p*-$tol_3P$), 6.0 (d, $^1J_{PPt}$ = 2590 Hz,[65] $^2J_{PP}$ = 421 Hz, *n*-$Pr_2PhP$).

### 3.5 Crystallography

Colorless crystals of **1** and **Pt'Cl-e** were grown from $CH_2Cl_2$/hexane at room temperature. Pale yellow crystals of **Pt'$C_4$H-a** were grown from $CH_2Cl_2$/acetone/hexane at –5 °C. Pale yellow crystals of **Pt'$C_4$Pt'-a**·$2CH_2Cl_2$ were grown from $CH_2Cl_2$/hexane –5 °C. Orange-brown crystals of **Pt$C_4$Pt''-b**·$C_7H_8$ were grown from toluene/ethanol at room temperature. Yellow crystals of **Pt'$C_4$Pt'-b** could be grown analogously, or from toluene/hexane at –15 °C (identical unit cells). Yellow crystals of **Pt'$C_4$Pt'-c** were grown from $CH_2Cl_2$/ethanol mixture at room temperature. Pale yellow crystals of **Pt'$C_4$Pt'-d** were grown from $CH_2Cl_2$ at –15 °C.

For all the data in Tables 3.1 and 3.2, integrated intensity information for each reflection was obtained by reduction of the data frames with the program APEX2[37] or SAINTplus[72]. The integration method employed a three dimensional profiling algorithm, and all data were corrected for Lorentz and polarization factors, as well as crystal decay effects. These data were merged and scaled to produce suitable data sets. The program SADABS[73] was employed for absorption corrections. Structures were solved using SHELXTL (SHELXS).[38] All non-hydrogen atoms were refined with anisotropic thermal parameters. Carbon bound hydrogen atoms were placed in idealized positions (C-H = 0.96 Å, $U_{iso}(H) = 1.2 \times U_{iso}(C)$. The structures were refined (weighted least squares/$F^2$) to convergence.[38]

With **1**, the thermal parameters of the $SC_4H_8$ carbon atoms (C(45) to C(48)) indicated disorder, which could be modeled. The R factor (6.5%) and significant

unaccounted electron densities near Pt(1) in the Fourier difference map (~6.4, 2.4, 1.8, and 1.6 eÅ$^{-3}$; distance from Pt(1) to highest *q*1 peak ca. 1.0 Å; distances between *q*1, *q*2, *q*3, and *q*4 all about 2.1 Å) suggested a "whole-molecule-disorder". Using O-fit in XP, the whole-molecule-disorder was modeled and refined, decreasing the R factor to 4.7%. There were two possible configurations for the disorder with the $C_6F_5$ ligands occupying opposite ends: one with both $SC_4H_8$ ligands and hence both Cl ligands occupying the same side, and the other with these ligands occupying opposite sides. Both models were refined, but the resulting R factors were very close and did not differentiate between them. The occupancy of the molecule with Pt(1) refined to 0.93, and that with Pt(1A) refined to 0.07. Considering the highly biased ratio, the refinement was carried out with the molecule with the minor occupancy fully rigid.

With **Pt'Cl-e**, systematic reflection conditions suggested the noncentrosymmetric space group $P2_12_12_1$. This assignment was further supported by statistical tests. With **Pt'$C_4$Pt'-a**·$2CH_2Cl_2$, there were no complications although the inversion center at the midpoint of the sp carbon chain is noteworthy.

With **Pt$C_4$Pt"-b**·$C_7H_8$, the combination of the Cu source and the multi-wire detector on the GADDS diffractometer employed restricted the 2θ angle to 120°. This precluded attaining the resolution recommended by the CHECK-CIF protocol. Some *t*-Bu groups were disordered, but their occupancies could be modeled (73:27 for C(60/61/62) vs. C(60A/61A/62A); 46:54 for C(50/51/52) vs. C(50A/51A/52A); 24:76 for C(34/35/36) vs. C(34A/35A/36A)). Under the conditions employed, data collection could only be carried out to 93% completion.

With **Pt'$C_4$Pt'-b**, data were collected at the lowest temperature possible with the instrument (−60 °C, 213 K). Some *t*-Bu groups were disordered, but their occupancies could be modeled (61:39 for C(102/103/104) vs. C(130/131/132); 55:45 for C(49/50/51) vs. C(49A/C50A/C51A)). The fluorine atoms also exhibited elongated displacement parameters, suggesting a wagging of the $C_6F_5$ groups. No attempts were made to model this disorder.

With **Pt'$C_4$Pt'-c**, two methoxy groups were disordered over three sites: O(1)-C(38), O(2) -C(48), O(3)-C(51). As a result, one hydrogen on the phenyl group associated with this disorder is not modeled (the formula shows one less hydrogen). Some of the thermal parameters associated with the other methoxy groups are larger, but attempts to model additional disorder did not give lower R factors. The same limitations as with **Pt$C_4$Pt"-b** precluded attaining the resolution recommended by the CHECK-CIF protocol.

With **Pt'$C_4$Pt'-d**, which exhibited an inversion center at the midpoint of the sp carbon chain, four carbon atoms of the phenyl group (C(34) to C(37)) and three of one *n*-propyl group (C(38) to C(40)) showed elongated thermal ellipsoids, indicating disorder. However, efforts to model this disorder did not improve the refinement.

CCDC 1515530, 1515531, 1515532, 1515534, 1515535, 1515537, 1515538 and 1515536 contain the supplementary crystallographic data for **1**, **Pt"Cl-e**, **Pt'$C_4$H-a**, **Pt'$C_4$Pt'-a-d**, and **Pt$C_4$Pt"-b**. These data can be obtained free of charge from The Cambridge Crystallographic Data Centre via www.ccdc. cam.ac.uk/data_request/cif .

**Table 3.1** Summary of crystallographic data for monoplatinum complexes.

| Complex | **1** | **Pt'Cl-e** | **Pt'$C_4$H-a** |
|---|---|---|---|
| empirical formula | $C_{48}H_{62}Cl_2F_{10}P_2Pt_2S_2$ | $C_{34}H_{46}ClF_5P_2Pt$ | $C_{39}H_{33}F_5P_2Pt$ |
| formula weight | 1416.12 | 842.19 | 853.68 |
| temperature K | 110(2) | 110(2) | 110(2) |
| Diffractometer | Bruker D8 GADDS | Bruker Apex 2 | Bruker Smart |
| wavelength Å | 0.71073 | 0.71073 | 0.71073 |
| crystal system | monoclinic | orthorhombic | triclinic |
| space group | $P2_{1/n}$ | $P2_12_12_1$ | $P\bar{1}$ |
| unit cell dimensions | | | |
| *a* Å | 13.403(8) | 12.1059(15) | 9.502(5) |
| *b* Å | 16.599(10) | 14.2630(18) | 11.234(5) |
| *c* Å | 24.219(15) | 20.214(2) | 16.775(8) |
| α° | 90 | 90 | 82.188(6) |
| β° | 102.724(8) | 90 | 83.654(6) |
| γ° | 90 | 90 | 73.939(6) |
| Volume (Å$^3$) | 5256(6) | 3490.3(7) | 1699.8(14) |
| *Z* | 4 | 4 | 2 |
| $\rho_{calcd}$ Mg·m$^{-3}$) | 1.790 | 1.603 | 1.668 |
| μ mm$^{-1}$/F(000) | 5.627/2768 | 4.238/1680 | 4.277/840 |
| Crystal size mm$^3$ | 0.05 × 0.04 × 0.03 | 0.60 × 0.40 × 0.10 | 0.35 × 0.15 × 0.15 |
| θ range of data collection ° | 1.50 to 28.76 | 2.43 to 27.50 | 1.23 to 27.76 |
| index ranges | $-18 \le h \le 17$ | $-15 \le h \le 15$ | $-12 \le h \le 12$ |
| | $-22 \le k \le 21$ | $-18 \le k \le 18$ | $-14 \le k \le 14$ |
| | $-32 \le l \le 32$ | $-25 \le l \le 26$ | $-21 \le l \le 21$ |
| reflections collected/independent | 58195/12840 | 39178/7918 | 19785/7793 |
| data/restraints/parameters | 12840 / 123 / 610 | 7918 / 0 / 400 | 7793 / 0 / 423 |
| goodness of fit on $F^2$ | 1.073 | 1.073 | 1.012 |
| final R indices I>2σ(I) | *R*1 = 0.0468, | *R*1 = 0.0192, | *R*1 = 0.0359, |
| | *w*R2= 0.0999 | *w*R2= 0.0399 | *w*R2= 0.0712 |
| R indices (all data) | *R*1 = 0.0823, | *R*1 = 0.0210, | *R*1 = 0.0452, |
| | *w*R2= 0.1155 | *w*R2= 0.0404 | *w*R2= 0.0743 |
| largest diff. peak and hole eÅ$^{-3}$ | 2.735 and –2.208 | 0.878 and –0.386 | 2.250 and –2.234 |

**Table 3.2** Summary of crystallographic data for diplatinum complexes.

| Complex | **Pt'$C_4$Pt'-a**·$2CH_2Cl_2$ | **Pt'$C_4$Pt'-b** | **Pt'$C_4$Pt'-c** | **Pt'$C_4$Pt'-d** | **Pt$C_4$Pt''-b**·$C_7H_8$ |
|---|---|---|---|---|---|
| empirical formula | $C_{76}H_{68}Cl_4F_{10}P_4Pt_2$ | $C_{110}H_{104}F_{10}P_4Pt_2$ | $C_{98}H_{79}F_{10}O_4P_4Pt_2$* | $C_{82}H_{80}F_{10}P_4Pt_2$ | $C_{117}H_{112}F_{10}P_4Pt_2$ |
| formula weight | 1827.16 | 2129.99 | 2024.67 | 1769.52 | 2222.13 |
| temperature K | 110(2) | 213(2) | 110(2) | 110(2) | 110(2) |
| diffractometer | Bruker Apex 2 | Bruker Apex 2 | Bruker D8 GADDS | Bruker D8 GADDS | Bruker D8 GADDS |
| wavelength Å | 0.71073 | 0.71073 | 1.54178 | 1.54178 | 1.54178 |
| crystal system | monoclinic | monoclinic | triclinic | monoclinic | triclinic |
| space group | *P*2(1)/c | *P*2(1)/n | *P*-1 | *P*2/n | *P*-1 |
| unit cell dimensions | | | | | |
| *a* Å | 13.8673(12) | 15.376(8) | 14.276(6) | 15.1018(6) | 14.3804(7) |
| *b* Å | 20.4887(18) | 31.668(15) | 15.175(2) | 13.6152(6) | 14.8720(7) |
| *c* Å | 14.6707(13) | 20.056(10) | 20.880(3) | 18.0925(9) | 24.5452(12) |
| α° | 90 | 90 | 81.953(7) | 90 | 99.639(3) |
| β° | 117.9260(10) | 94.529(7) | 83.809(8) | 96.814(3) | 92.688(3) |
| γ° | 90 | 90 | 72.767(8) | 90 | 100.460(3) |
| Volume ($Å^3$) | 3682.9(6) | 9736(8) | 4267.4(11) | 3693.8(3) | 5073.1(4) |
| Z | 2 | 4 | 2 | 2 | 2 |
| $\rho_{calcd}$ Mg $m^{-3}$) | 1.648 | 1.453 | 1.576 | 1.591 | 1.453 |
| μ $mm^{-1}$/F(000) | 4.094/1796 | 3.003/4280 | 7.376/2010 | 8.378/1756 | 6.225/2234 |
| crystal size $mm^3$ | 0.15 × 0.14 × 0.05 | 0.25 × 0.12 × 0.10 | 0.10 × 0.09 × 0.03 | 0.15 × 0.07 × 0.03 | 0.15 × 0.12 × 0.02 |
| θ range of data collection ° | 2.53 to 28.81 | 2.06 to 27.50 | 2.14 to 57.50 | 3.25 to 61.43 | 1.83 to 60.00 |
| index ranges | $-18 \le h \le 18$ | $-19 \le h \le 19$ | $-15 \le h \le 15$ | $-17 \le h \le 17$ | $-15 \le h \le 15$ |
| | $-27 \le k \le 26$ | $-41 \le k \le 41$ | $-16 \le k \le 16$ | $-15 \le k \le 15$ | $-16 \le k \le 16$ |
| | $-19 \le l \le 19$ | $-26 \le l \le 26$ | $-22 \le l \le 22$ | $-20 \le l \le 20$ | $-27 \le l \le 27$ |
| reflections collected/independent | 42642/9026 | 113592/22325 | 33184/10958 | 23951/5676 | 37606/14105 |
| data/restraints/parameters | 9026/0/438 | 22325/12/1120 | 10958/70/1051 | 5676/65/442 | 14105/18/1199 |
| goodness of fit on $F^2$ | 1.051 | 1.031 | 1.044 | 1.015 | 1.042 |
| final R indices I>2σ(I) | *R*1 = 0.0349, | *R*1 = 0.0396, | *R*1 = 0.0579, | *R*1 = 0.0368, | *R*1 = 0.0380, |
| | *w*R2= 0.0699 | *w*R2= 0.0889 | *w*R2= 0.1251 | *w*R2= 0.0917 | *w*R2= 0.0916 |
| R indices (all data) | *R*1 = 0.0536, | *R*1 = 0.0705, | *R*1 = 0.0989, | *R*1 = 0.0533, | *R*1 = 0.0565, |
| | *w*R2= 0.0755 | *w*R2= 0.0994 | *w*R2= 0.1362 | *w*R2= 0.0982 | *w*R2= 0.0964 |
| largest diff. peak and hole $eÅ^{-3}$ | 1.278 and −1.128 | 1.461 and −1.024 | 1.444 and −1.176 | 1.072 and −0.978 | 1.786 and −1.146 |

**Table 3.3** Key interatomic distances (Å) and bond or plane/plane angles (°) in diplatinum complexes.

| | **Pt'C$_4$Pt'-a**·2CH$_2$Cl$_2$ | **Pt'C$_4$Pt'-b** | **Pt'C$_4$Pt'-c** | **Pt'C$_4$Pt'-d** | **PtC$_4$Pt''-b**·C$_7$H$_8$ |
|---|---|---|---|---|---|
| Pt(1)-C(1) | 1.990(4) | 1.995(4) | 1.966(12) | 2.021(7) | 1.994(7) |
| C(1)≡C(2) | 1.219(5) | 1.195(5) | 1.247(15) | 1.186(9) | 1.216(8) |
| C(2)-C(3)[a] | 1.376(7) | 1.381(6) | 1.393(18) | 1.392(13) | 1.366(9) |
| C(3)≡C(4)[a] | 1.219(5) | 1.215(6) | 1.274(17) | 1.186(9) | 1.238(8) |
| C(4)-Pt(2)[a] | 1.990(4) | 1.979(4) | 1.912(16) | 2.021(7) | 1.973(6) |
| Pt(1)-C$_{ipso}$ | 2.061(4) | 2.071(4) | 2.068(11) | 2.089(6) | 2.074(4) |
| Pt(2)-C$_{ipso}$[a] | 2.061(4) | 2.072(4) | 2.082(12) | 2.089(6) | 2.071(6) |
| Pt(1)-P(1) | 2.3101(10) | 2.3048(14) | 2.308(3) | 2.3130(16) | 2.2971(15) |
| Pt(1)-P(2) | 2.2932(11) | 2.3059(14) | 2.315(3) | 2.3007(17) | 2.2980(15) |
| Pt(2)-P(3)[a] | 2.3101(10) | 2.3138(14) | 2.297(3) | 2.3130(16) | 2.3044(15) |
| Pt(2)-P(4)[a] | 2.2932(11) | 2.2998(14) | 2.299(3) | 2.3007(17) | 2.2905(15) |
| Av. C$_{sp}$≡C$_{sp}$ | 1.219 | 1.205 | 1.274 | 1.186 | 1.227 |
| Pt···Pt | 7.792 | 7.729 | 7.764 | 7.792 | 7.779 |
| sum of bond lengths, Pt(1) to Pt(2) | 7.797 | 7.765 | 7.792 | 7.806 | 7.787 |
| Pt(1)-C(1)-C(2) | 176.8(3) | 171.0(4) | 178.1(10) | 174.0(6) | 175.5(5) |
| C(1)-C(2)-C(3)[a] | 178.4(5) | 178.0(5) | 176.5(13) | 177.8(9) | 178.4(7) |
| C(2)-C(3)-C(4)[a] | 178.4(5) | 175.7(5) | 174.0(15) | 177.8(9) | 178.0(6) |
| C(3)-C(4)-Pt(2)[a] | 176.8(3) | 169.6(4) | 175.0(11) | 174.0(6) | 176.3(5) |
| avg. π stacking[b] | 3.603 | 3.708 | 3.734 | 4.098 | 4.042 |
| (P1-Pt1-P2)Pt2 vs. (P3-Pt2-P4)Pt1[c] | 0 | 44.18 | 51.30 | 0 | 46.07 |
| (C$_{ipso}$-P1-Pt1-P2) vs. (P3-Pt2-P4-C$_{ipso}$)[c] | 0 | 43.67 | 51.71 | 0 | 48.46 |

[a] To facilitate comparisons, some atoms of **Pt'C$_4$Pt'-a**·2CH$_2$Cl$_2$ and **Pt'C$_4$Pt'-d**, both of which exhibit inversion centers, have been renumbered from those in the cif files. [b] Distance between the centroids of the C$_6$F$_5$ and aryl rings; average of four values. [c] Angle between planes defined by these atoms.

**Table 3.4** UV-visible data for diplatinum butadiynediyl complexes *trans*,*trans*-($C_6F_5$)(*p*-$tol_3P$)($R_3P$)Pt(C≡C)$_2$Pt($PR_3$)(P*p*-$tol_3$)($C_6F_5$) in $CH_2Cl_2$.

| Complex | $R_3P$ | (nm) [$\varepsilon$ ($M^{-1}cm^{-1}$) ] |
|---|---|---|
| **Pt'$C_4$Pt'-a** | $Me_2PhP$ | 321 [24900], 344 [19500], 388 [560], 422 [79] |
| **Pt'$C_4$Pt'-b** | (*p*-*t*-Bu$C_6H_4$)$_2$PhP | 293 [16700], 330 [18900], 351 [14700], 393 [470], 427 [80] |
| **Pt'$C_4$Pt'-c** | (*p*-MeO$C_6H_4$)$_2$PhP | 311 [12800], 330 [16500], 351 [12600], 392 [470], 427 [120] |
| **Pt'$C_4$Pt'-d** | *n*-$Pr_2$PhP | 306 [15000], 322 [20000], 344 [15000], 387 [400], 422 [50] |
| **Pt$C_4$Pt** | *p*-$tol_3P$ | 328 [37000], 351 [12600], 395[500], 428 [90][a] |

[a] Reported in reference 20: 330 [17000], 350 [13200].

# 4. EXPLORING THE FEASIBILITY OF DIELS-ALDER FUNCTIONALIZATION OF POLYYNE CHAINS TO ACHIEVE GRAPHENE-LIKE STRUCTURES

## 4.1 Introduction

Nowadays, there is an increased interest in allotropes of carbon among numerous research groups.[74] Many molecular and polymeric allotropes have already been isolated, but the one-dimensional *sp*-hybridized species "carbyne", remains the least characterized.[75] Importantly, many investigators now pay much attention to the synthesis and detailed physical and chemical characterization of metal capped polyynediyl complexes $L_mM(C{\equiv}C)_nML_m$, motivated by a variety of fundamental and applied objectives, ranging from models for "carbyne" to applications in molecular electronics.[76]

Graphene is one of the crystalline forms of carbon, in which carbon atoms are arranged in a regular hexagonal pattern.[77] It can be described as a one-atom thick layer of graphite and is always prepared "top down" from graphite.[78] However, to our knowledge there has been comparatively little consideration given to "bottom up" syntheses,[79] for which a long polyyne would be a possible template.

My objective is to explore the feasibility of Diels-Alder functionalization of polyyne chains to achieve graphene-like structures. It would be a novel way to construct graphene from polyynes by the "bottom up" approach. The overall plan depicted in Scheme 4.1 is arbitrarily illustrated with a platinum capped carbyne model. We seek to

establish the feasibility of the necessary steps one at a time. We will first test whether the *sp* carbon chains undergo Diels-Alder cycloadditions with *o*-xylylene,[80] a very reactive but easy-to-generate species. Multiple cycloadditions/aromatizations and subsequent dehydrogenation would lead to a simple two-dimensional conjugated aromatic network. At some stage, solubility will likely be diminished and we will need to switch to characterization methods used for graphene itself.

A further theme that readily emerges from this analysis is the use of structurally authenticated bis(polyynediyl) systems in which two *sp* chains bridge the same extended endgroups.[81] Such assemblies can be viewed as multistranded molecular wires. As shown in Scheme 4.1 (bottom), multiple cycloadditions/aromatizations and subsequent dehydrogenation would lead to the growing of truly graphene-like assemblies.

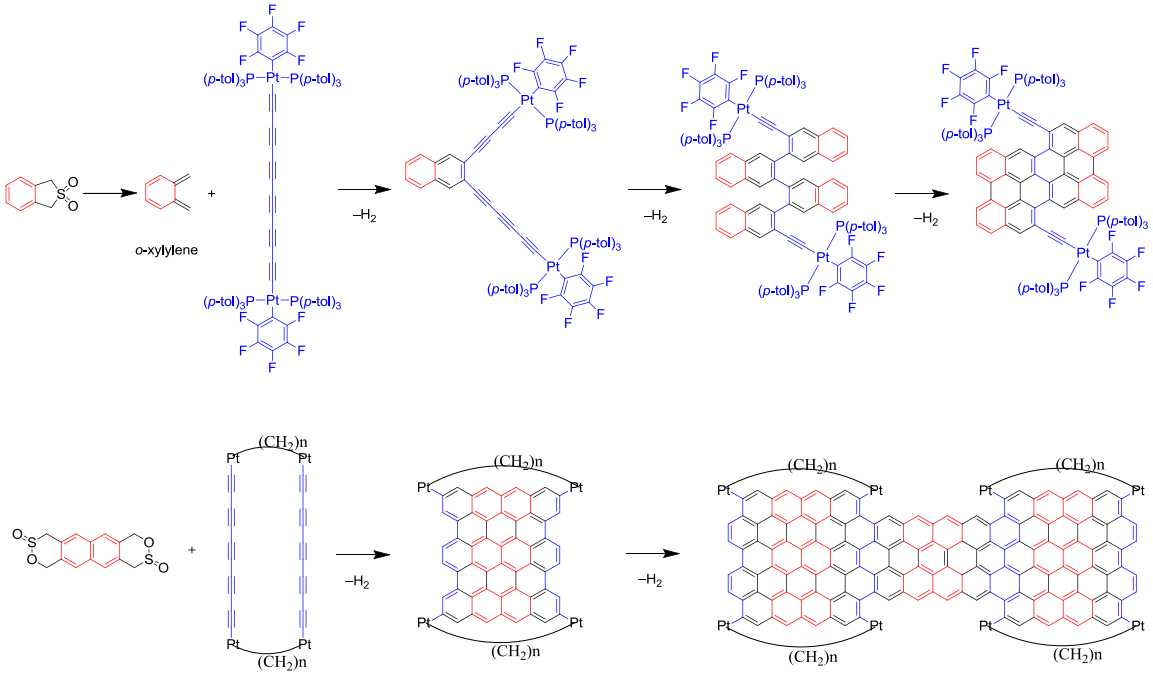


**Scheme 4.1**. Overall plan to explore the feasibility of Diels-Alder functionalization of polyyne chains to achieve graphene-like structures.

## 4.2 Results

### 4.2.1 Synthesis of platinum capped polyyne precursor

Scheme 4.2 summarizes previously reported syntheses of several monoplatinum and diplatinum polyyne species, including **PtC$_6$TES**, **PtC$_{10}$TES**, **PtC$_6$Pt**, **PtC$_8$Pt**, **PtC$_{10}$Pt**, **PtC$_{12}$Pt**, where **Pt** = *trans*-(C$_6$F$_5$)(*p*-tol$_3$P)$_2$Pt and **TES** = SiEt$_3$. All sequences start with the monoplatinum bis(phosphine) chloride complex *trans*-(C$_6$F$_5$)(*p*-tol$_3$P)$_2$PtCl (**PtCl**).[20] Coupling of **PtCl** with butadiyne, catalyzed by CuI in the presence of HNEt$_2$, leads to the formation of *trans*-(C$_6$F$_5$)(*p*-tol$_3$P)$_2$Pt(C≡C)$_2$H (**PtC$_4$H**, 80%).[20]

For the further chain extension, the reactions of **PtC$_4$H** with Et$_3$SiC≡CH (**TESC$_2$H**) or Et$_3$Si(C≡C)$_2$H (**TESC$_4$H**) were carried out.[20] The products then undergo homocoupling or cross coupling with **PtCl** to give the desired one dimensional *sp*-hybridized **PtC$_x$Pt** chains.[20]

As briefly illustrated in Scheme 4.2, the cross coupling of **PtC$_4$H** and **TESC$_2$H** (ca. 30 fold excess) resulted in the formation of **PtC$_6$TES** (45%).[20] **PtC$_6$TES** and **TESC$_4$H** (ca. 20 fold excess) were coupled and gave the desired complex **PtC$_{10}$TES** (53%); in an initial step (*in situ*), the triethylsilyl group of the platinum complex is replaced by a hydrogen atom. After the homocoupling of **PtC$_4$H** and **PtC$_6$TES**, **PtC$_8$Pt** (97%) and **PtC$_{12}$Pt** (80%) were isolated.[20] The cross coupling of **PtCl** with **PtC$_6$TES** or **PtC$_{10}$TES** leads to the formation of **PtC$_6$Pt** (35%) or **PtC$_{10}$Pt** (77%).[20]

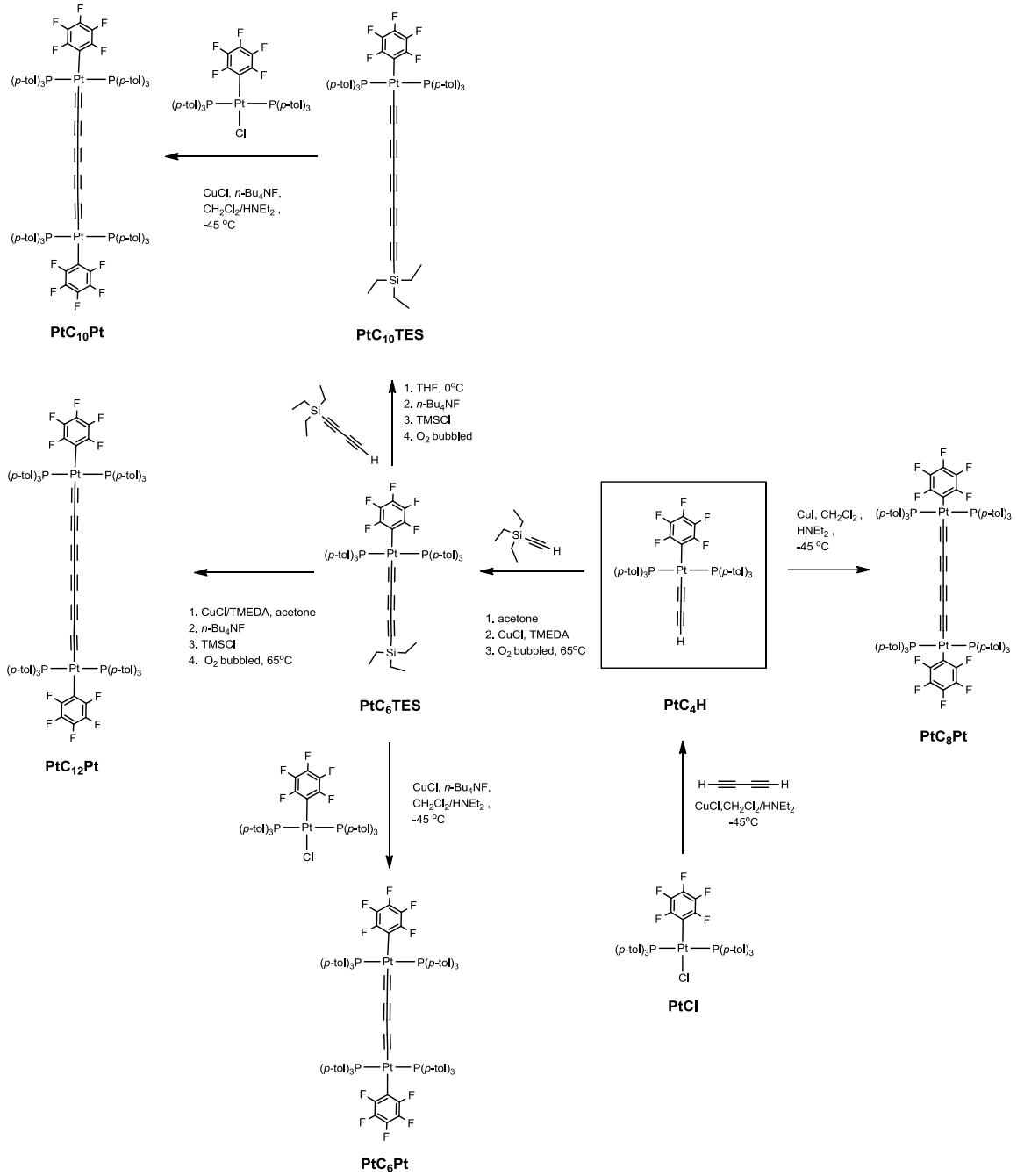


**Scheme 4.2**. Syntheses of the diplatinum carbon chain complexes **PtC$_x$Pt**.

### 4.2.2 Exploring the feasibility of Diels-Alder functionalization of polyyne chains

The elusive intermediate o-quinodimethane (*o*-QDM), also named *o*-xylylene, has attracted much attention from both theoretical and synthetic chemists over the past 50 years. As a *cisoid*-diene with a strong driving force of aromatization, *o*-xylylene has a remarkable Diels-Alder reactivity and is often used as building blocks in the syntheses of cyclic organic compounds or polymeric materials by inter- or intramolecular [4 + 2] trapping. The readily available precursor 1,3-dihydrobenzo[c]thiophene-2,2-dioxide, depicted in Schemes 4.1 and 4.3, is known to extrude $SO_2$ at ca. 180 °C.[82] The isomer 1,4-dihydro-2,3-benzoxathiin-3-oxide (see Scheme 4.4 below) is known to require lower thermolysis temperatures for the cheletropic elimination of $SO_2$. Thus, *o*-xylylene can be obtained at temperatures as low as 80 °C.[83]

In order to test the feasibility of Diels-Alder cycloadditions of the *sp* carbon chains with *o*-xylylene, and to determine the conditions required for dehydrogenation of the newly formed 6-membered rings to benzenoid systems, a solution of platinum capped polyyne precursor and 1,3-dihydrobenzo[*c*]thiophene-2,2-dioxide (ca. 9 fold excess) in the high boiling solvent 1,2,4-trichlorobenzene was kept in the dark under nitrogen at 160 °C overnight. The crude reaction mixture was assayed by mass spectrometry (MALDI), and some peaks suggested the formation of the target complexes. They are discussed below.

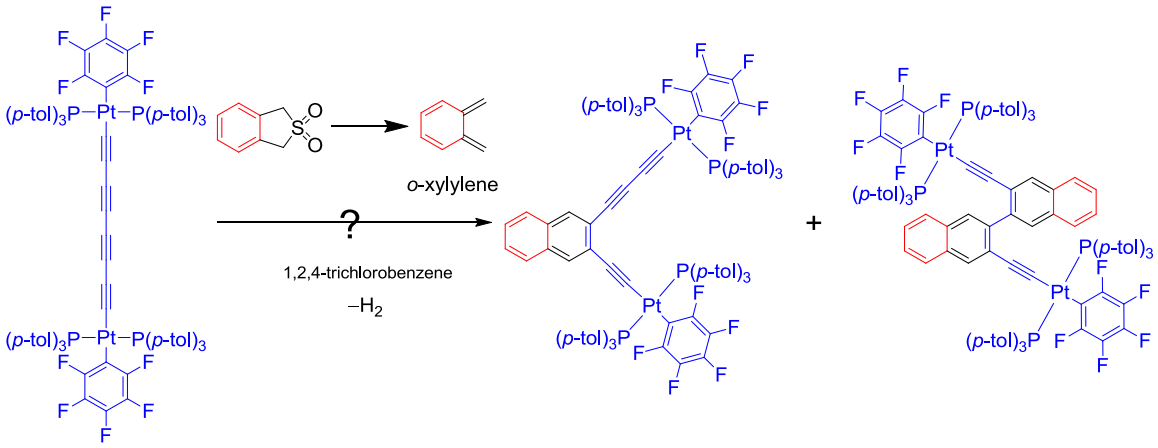


**Scheme 4.3**. Overall plan to explore the feasibility of Diels-Alder functionalization of **PtC$_8$Pt** to achieve graphene-like structures.

Though transition metal capped polyynes exhibit much better stabilities, long polyynes still slowly decompose at room temperature. This situation gets even worse at high temperature and forces me to seek new approaches under milder conditions. Another route was sought and a solution of platinum capped polyyne precursor in toluene was combined with 1,4-dihydro-2,3-benzoxathiin-3-oxide (ca. 3 fold excess) as shown in Scheme 4.4. The mixture was heated to 100 °C under nitrogen in the dark. After 1 d, a chromatographic workup (alumina) gave a brown solid. The mass spectrum (MALDI) was then investigated and some peaks were consistent with the target cycloadduct. These data are analyzed below. Importantly, in all of these cases efforts to obtain a well defined pure product by chromatography were unsuccessful.

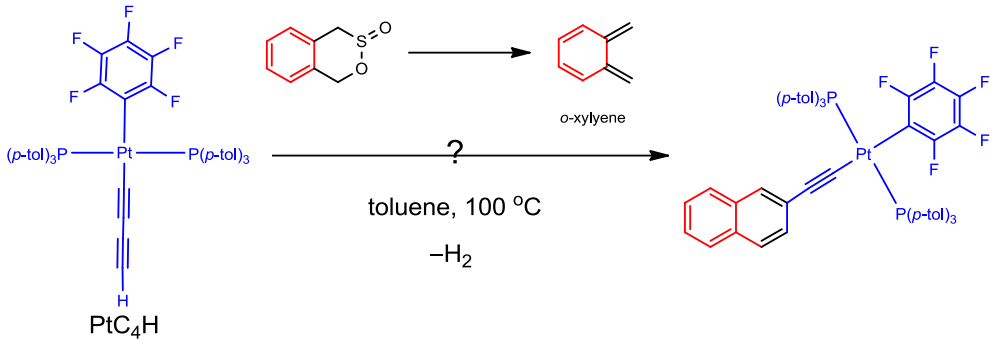


**Scheme 4.4**. Overall plan to explore the feasibility of Diels-Alder functionalization of **$PtC_4H$** to achieve graphene-like structures.

From a similar reaction (see **method C**, experimental section), a crystalline product was obtained. The structure was solved as summarized in Table 4.2 and the experimental section. The molecular structure in Figure 4.1 shows that the carbon rich ligand had been substituted by a bromide ligand, apparently from the '-dibromo-*o*-xylene precursor to *o*-xylylene used in that experiment. This new compound was not of particular interest in the context of this study. Nonetheless the key metrical parameters are given in the caption of Figure 4.1. A related chloride complex with fluorous phosphine ligands has also been structurally characterized.[84]

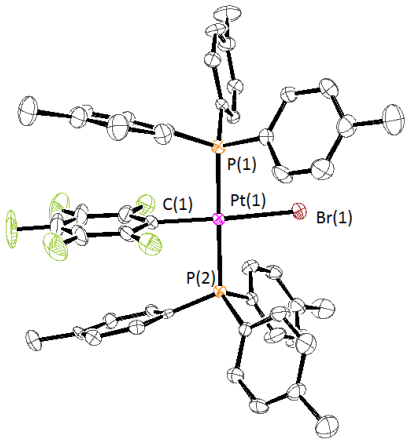


**Figure 4.1**. Molecular structure of **PtBr** with thermal ellipsoids at 50% probability level. Key bond lengths (Å) and angles (°): Pt(1)-C(1), 2.017(4); Pt(1)-P(1), 2.3087(11); Pt(1)-P(2), 2.3137(11); Pt(1)-Br(1), 2.4879(5); P(2)-Pt(1)-P(1), 174.54(4); C(1)-Pt(1)-P(1), 90.08(12); C(1)-Pt(1)-P(2), 90.34(12); C(1)-Pt(1)-Br(1), 174.00(12); Br(1)-Pt(1)-P(1), 89.48(3); Br(1)-Pt(1)-P(2), 90.66(3).

### 4.2.3 Combining *o*-carborane and polyyne chains

In recent decades there has been much interest in carboranes, which are icosahedral cluster compounds consisting of 10 boron atoms and 2 carbon atoms.[85] This reflects their impact in the fields of medicinal chemistry and materials science, which in turn derives from their somewhat nontraditional bonding structures, rich boron content, high thermal or chemical stabilities, the 3c-2e$^-$ bonds and consequent three-dimensional delocalization of skeletal electrons, and the resulting electron-deficient cage systems, which makes them attractive targets for incorporation into conjugated polymeric systems.[86] Additionally, the special reactivity and electron-withdrawing nature of carboranes are widely recognized as three-dimensional aromaticity.[87]

Previously, alkynes like (*p*-I$C_6H_4$)(C≡C)(*p*-$C_6H_4$I) have been shown to react with $B_{10}H_{14}$·2[$S(CH_3)_2$] at 80-85 °C in toluene to give 1,2-bis(4-iodophenyl)-*o*-carborane (see Scheme 4.5).[85a] Accordingly, the polyynes **TESC$_4$TES**, **TESC$_8$TES**, or **PtC$_8$Pt** were combined with $B_{10}H_{14}$·2[$S(CH_3)_2$][87] (1.2 eq.) in refluxing toluene. However, chromatographic workups did not give any well defined products.

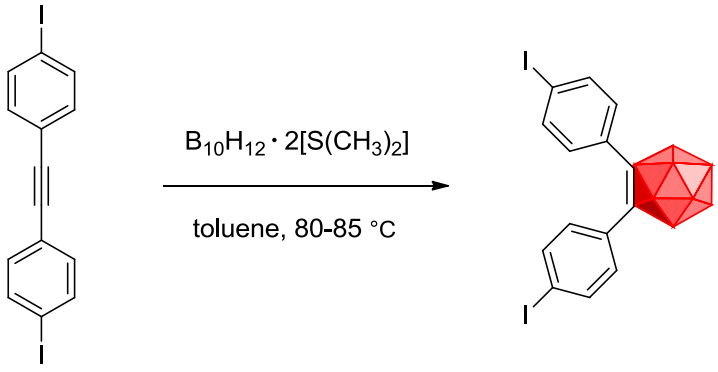


**Scheme 4.5**. Synthesis of 1,2-bis(4-iodophenyl)-*o*-carborane.

### 4.2.4 Cobalt catalyzed [2+2+2] cyclolotrimerizations invovling polyyne chains

The transition metal-catalyzed [2+2+2] cycloaddition reaction is an expedient way to prepare six-membered ring systems, such as benzenes, pyridines, and cyclohexadienes, starting from alkynes, nitriles, and alkenes.[88] In this aspect, cobalt complexes are widely used as catalysts, which provide extensive levels of chemo-, regio-, and diastereoselectivity. [CpCo(CO)(dimethyl fumarate)] is a new easy-to-handle air-stable complex that catalyzes various [2+2+2] cycloadditions without the need for solvent purification.[89]

This air-stable complex was evaluated as a catalyst for the intramolecular [2+2+2] cycloaddition (cyclotrimerization) of the polyynes **PtC$_4$H**, **TESC$_8$TES**, **PtC$_6$Pt**, and **PtC$_8$Pt** under "classical" conditions (in refluxing toluene for several hours, either in the dark or under ambient lighting).[89] Unfortunately, no trimeric species could be detected after the reaction.

## 4.3 Discussion

The reactions of the platnium complexes mentioned above (**PtC$_4$H**, **PtC$_6$TES**, **PtC$_6$Pt**, **PtC$_8$Pt**, **PtC$_{10}$Pt**, **PtC$_{12}$Pt**) and o-xylylene (generated from either 1,3-dihydrobenzo[c]thiophene-2,2-dioxide or 1,4-dihydro-2,3-benzoxathiin-3-oxide) were analyzed from the standpoint of the formation of cycloadducts using mass spectrometric evidence. The conclusions are summarized in Table 4.1.

As noted above, the generation of *o*-xylylene from 1,3-dihydrobenzo[c]thiophene-2,2-dioxide requires a very high thermolysis temperature (>160 °C), which might lead to the decomposition of partially platinum capped polyynes (**PtC$_4$H**, dec pt. 171 °C).[20] Nonetheless, the formation of **PtC$_8$Pt** adducts were evidenced by some mass spectrum peaks (2142 ([**PtC$_8$Pt**+*o*-xylylene]$^+$; 2244, [**PtC$_8$Pt**+2(*o*-xylylene)]$^+$; 2342, [**PtC$_8$Pt**+3(*o*-xylylene)]$^+$), which are shown in Figures 4.4-4.7. However, 1,4-dihydro-2,3-benzoxathiin-3-oxide can generate *o*-xylylene at temperatures as low as 80 °C, and the formation of **PtC$_4$H** or **PtC$_6$TES** adducts were indicated by certain mass spectrum peaks (1121, [**PtC$_4$H**+*o*-xylylene]$^+$; 1261, ([**PtC$_6$TES**+*o*-xylylene]$^+$), which are shown in Figures 4.2-4.4. With regard to the fully platinum capped polyynes (**PtC$_6$Pt**, **PtC$_8$Pt**, **PtC$_{10}$Pt**, **PtC$_{12}$Pt**), 80 °C appears to be insufficient for their activation. In these reactions, only dimers which formed from *o*-xylylene and unreacted diplatinum starting materials were detected. Possibly the two bulky endgroups retard the bimolecular rate constant, at least until a certain threshold *sp* carbon chain length is realized.

**Table 4.1**. Diels-Alder cycloadditions of other platinum capped polyyne precursors.

| Run | Pt capped precursor | Proposed Cycloaddition Product[a] |
|---|---|---|
| 1 | 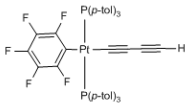 | 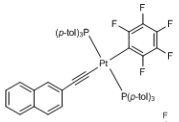 |
| 2 | 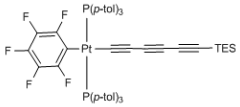 | 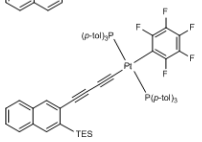 |
| 3 | 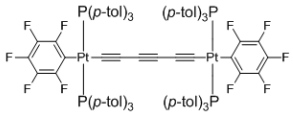 | None[b] |
| 4 | 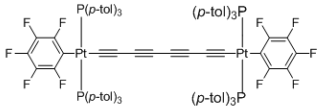 | 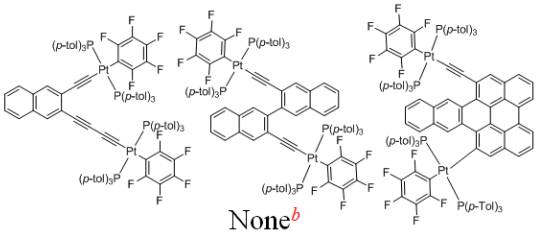 |
| 5 | 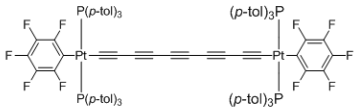 | None[b] |
| 6 | 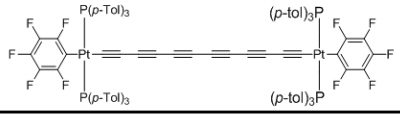 | None[b] |

[a]Consistent with peaks observed by mass spectrometry.

[b]None of the peaks on the mass spectra fit a cycloaddition product.

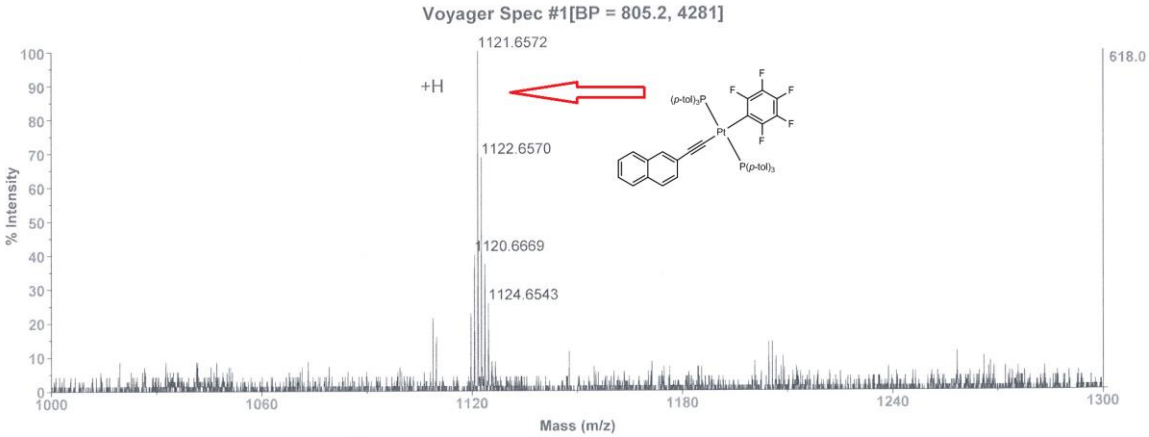


**Figure 4.2.** Mass spectrum of proposed product from coupling reactions between 1,4-dihydro-2,3-benzoxathiin-3-oxide and **$PtC_4H$**.

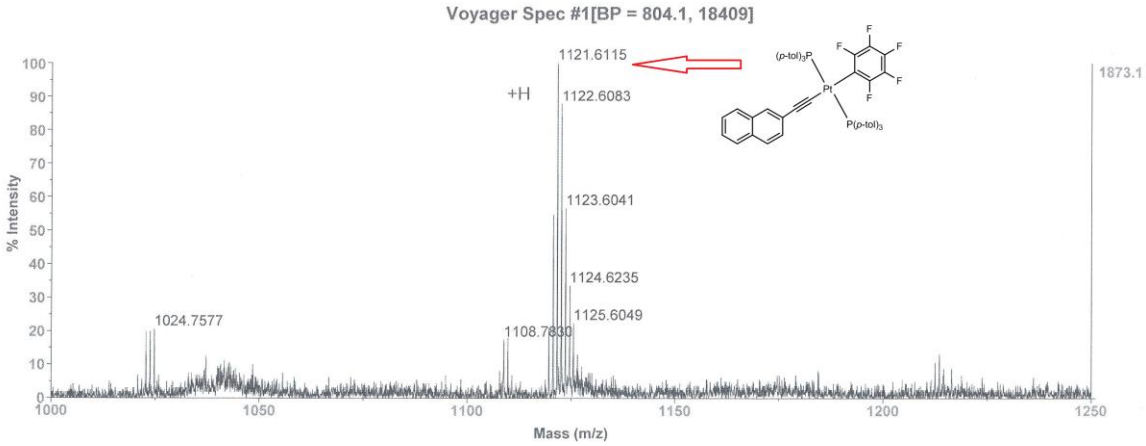


**Figure 4.3.** Mass spectrum of proposed product from coupling reactions between 1,4-dihydro-2,3-benzoxathiin-3-oxide and **PtC$_4$H**.

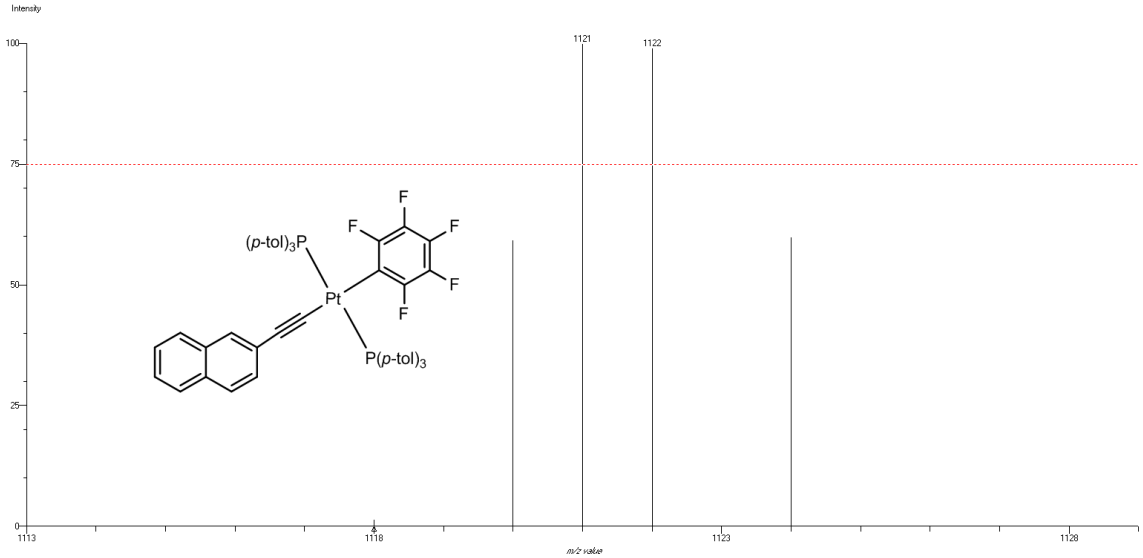


**Figure 4.4.** Simulation of molecular ions of proposed product from coupling between 1,4-dihydro-2,3-benzoxathiin-3-oxide and **PtC$_4$H** (See Figures 4.2 and 4.3).

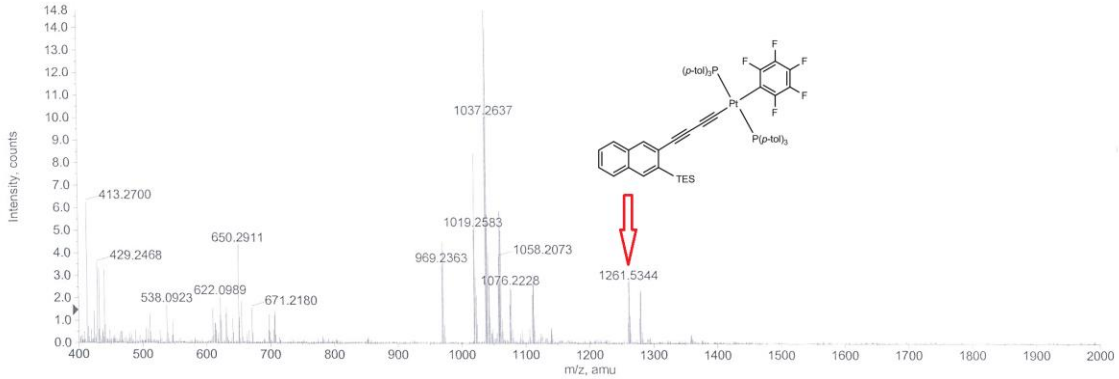


**Figure 4.5.** Mass spectrum of proposed product from coupling reactions between 1,4-dihydro-2,3-benzoxathiin-3-oxide and **PtC$_6$TES**.

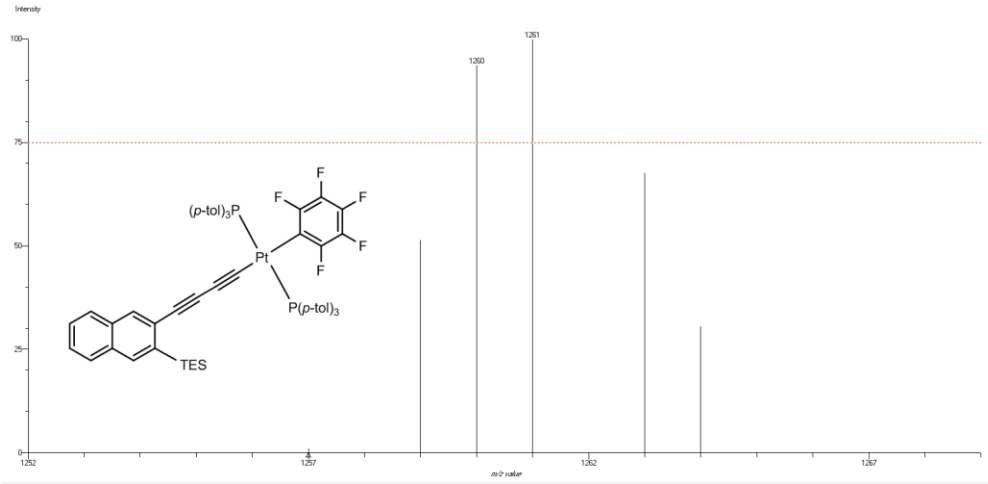


**Figure 4.6.** Simulation of molecular ions of proposed product from coupling between 1,4-dihydro-2,3-benzoxathiin-3-oxide and **PtC$_6$TES** (see Figure 4.5).

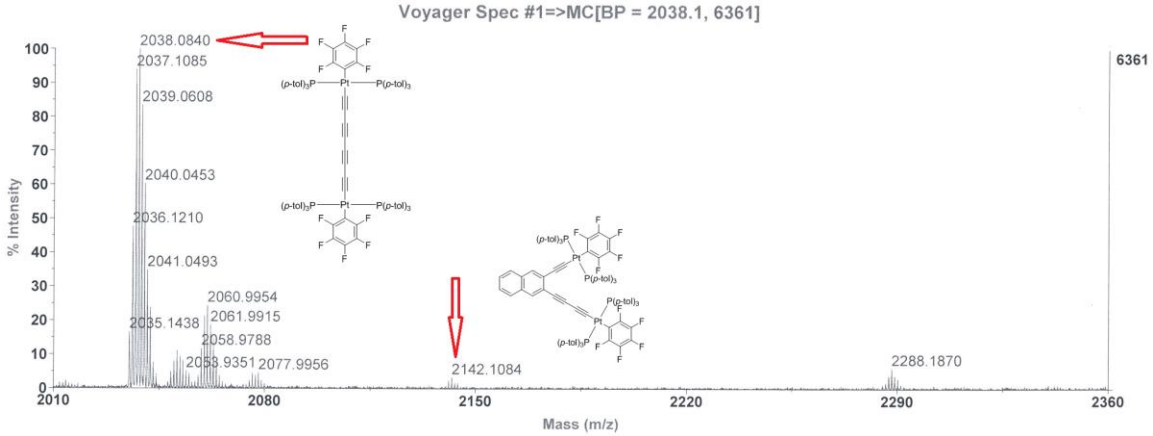


**Figure 4.7.** Mass spectrum of proposed product from coupling reactions between 1,3-dihydrobenzo[c]thiophene-2,2-dioxide and **PtC$_8$Pt**.

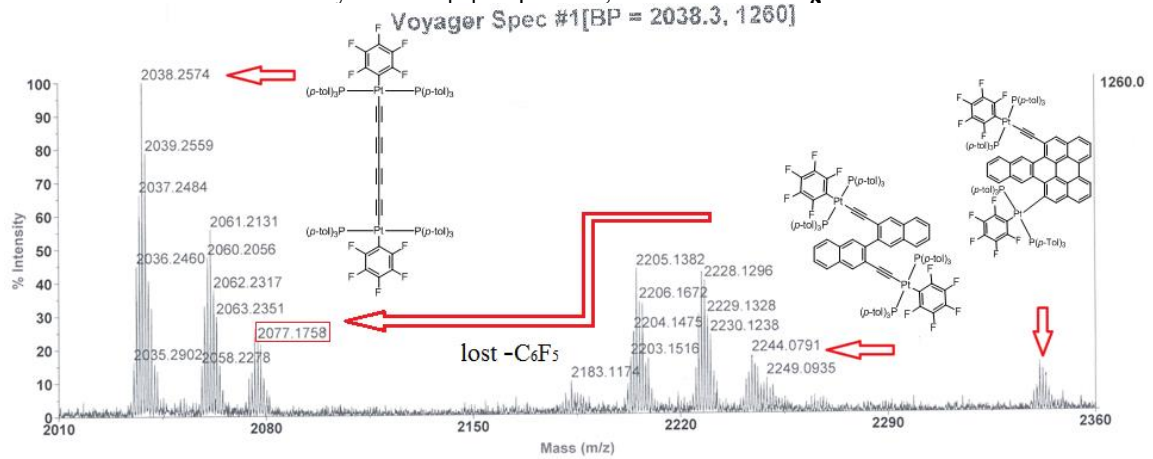


**Figure 4.8.** Mass spectrum of proposed product from coupling reactions between 1,3-dihydrobenzo[c]thiophene-2,2-dioxide and **PtC$_8$Pt**.

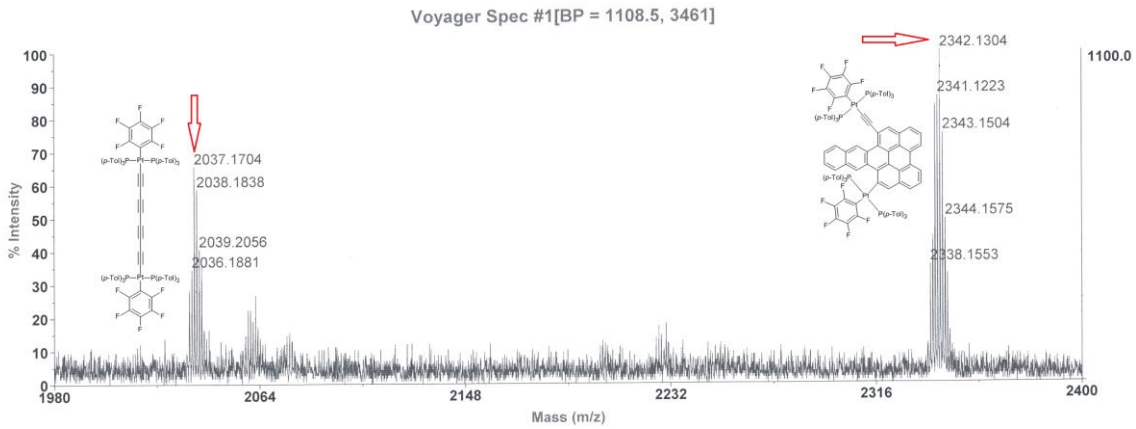


**Figure 4.9.** Mass spectrum of proposed product from coupling reactions between 1,3-dihydrobenzo[c]thiophene-2,2-dioxide and **PtC$_8$Pt**.

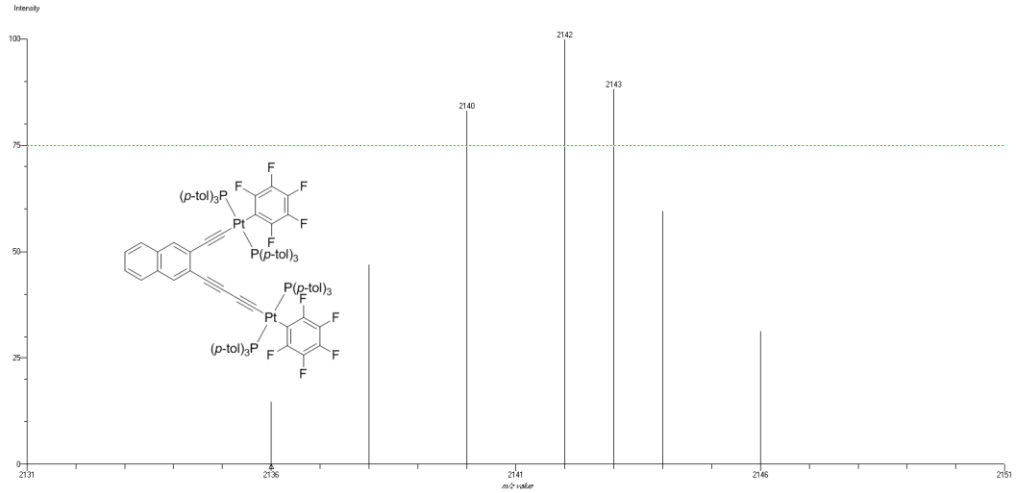


**Figure 4.10.** Simulation of molecular ions of proposed product from 1:1 coupling between 1,3-dihydrobenzo[c]thiophene-2,2-dioxide and **PtC$_8$Pt** (see Figure 4.7).

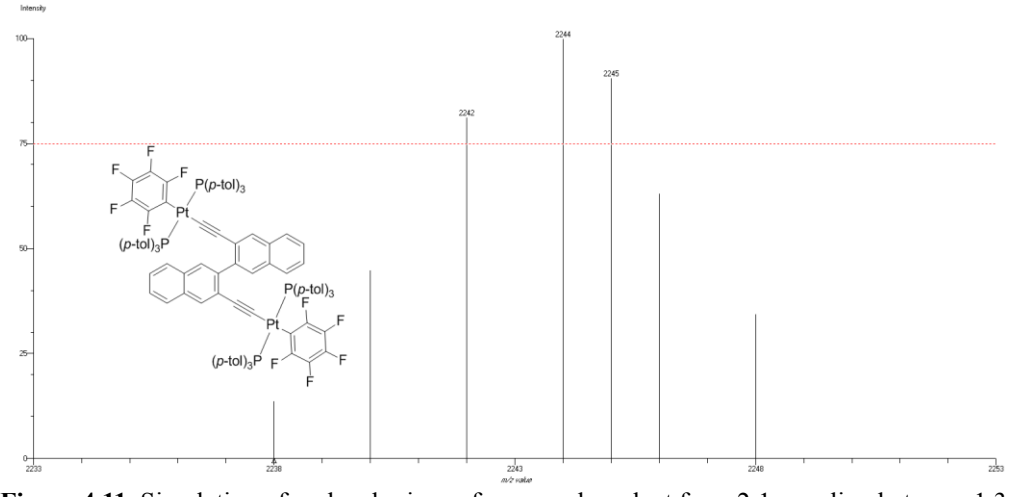


**Figure 4.11.** Simulation of molecular ions of proposed product from 2:1 coupling between 1,3-dihydrobenzo[c]thiophene-2,2-dioxide and **PtC$_8$Pt** (see Figure 4.8).

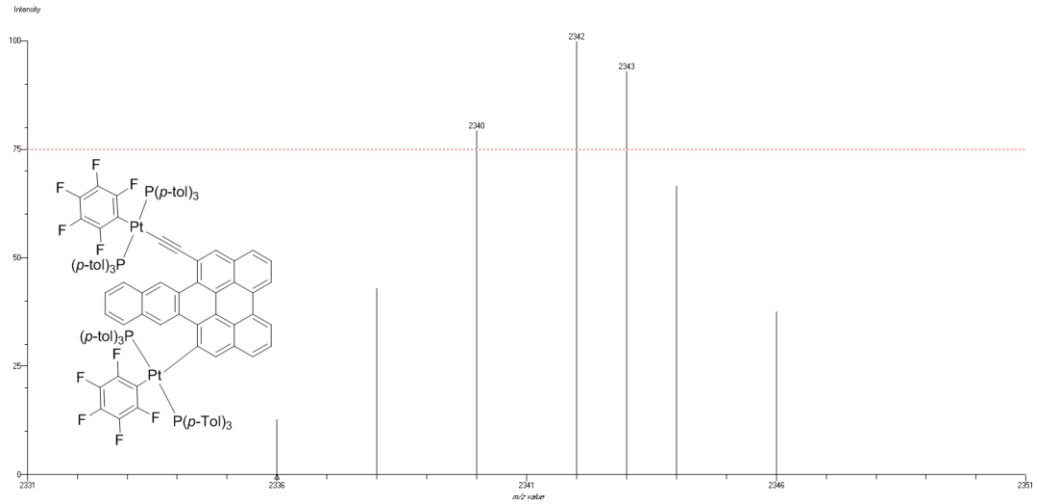


**Figure 4.12.** Simulation of molecular ions of proposed product from 3:1 coupling between 1,3-dihydrobenzo[c]thiophene-2,2-dioxide and **PtC$_8$Pt** (see Figures 4.8 and 4.9).

As detailed in the experimental section, no tractable products could be isolated from the reactions between $B_{10}H_{12}{\cdot}2[S(CH_3)_2]$ and **TESC$_4$TES**, **TESC$_8$TES**, or **PtC$_8$Pt**. In the last case, a considerable amount of **PtC$_8$Pt** was recovered. In all of the efforts directed at catalysis of intermolecular [2+2+2] cycloadditions with [CpCo(CO)(dimethyl fumarate)], the polyyne was almost always recovered (**PtC$_4$H**, **TESC$_8$TES**, **PtC$_6$Pt**, **PtC$_8$Pt**). This, the unsaturated substrates selected for this study seem to be very inert towards reactions that convert the alkyne linkages to cyclic compounds.

The proposed mechanism for intermolecular [2+2+2] cycloaddition catalyzed by [CpCo(CO)(dimethyl fumarate)] is depicted in Scheme 4.6. The first step generates a reactive bis(alkyne) species from the stable precursor molecules. The alkyne ligands couple to yield a metallacyclopentadiene. Next, the unsaturated metallacycle react with another alkyne reactant in an insertion or cycloaddition reaction, followed by elimination from the metal center to furnish the final products, benzene derivatives. Based upon the above investigation, the main barrier that stops intermolecular [2+2+2] cycloaddition

might be the bulky end groups connected to the triple bond: the very bulky end groups on the platinum capped polyynes hinder the initial coordination to the cobalt metal center or the further coordination to the cobalt metal center. The net result is that no trimer is formed.

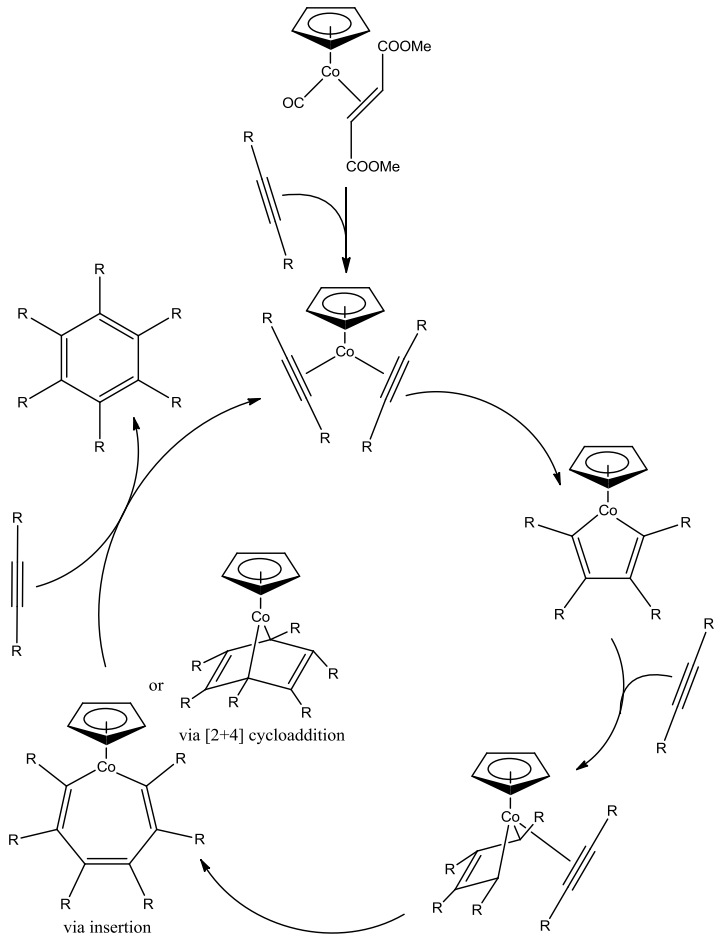


**Scheme 4.6**. Proposed mechanism for [2+2+2] cycloaddition catalyzed by [CpCo(CO)(dimethyl fumarate)].

Before concluding, it should be emphasized that monoplatnium complexes of the formula **PtC$_x$H** ($x$ = 4, 6, 8, 10) do undergo "click chemistry", or copper(I) catalyzed 3+2 cycloadditions of benzyl azide, as illustrated for a typical case in Scheme 4.7.[90] Thus, it is not unrealistic to expect cycloaddition chemistry from the above families of polyynes.

However, the overall body of results indicates that they are much less reactive than many other types of alkynyl compounds.

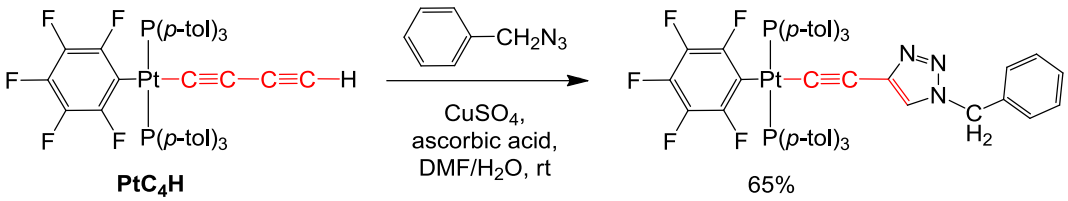


**Scheme 4.7**. A click cycloaddition of **$PtC_4H$**.

## 4.4 Summary

In summary, the feasibility of the Diels-Alder functionalization of polyyne chains was evidenced by the reactions of (a) monoplatnium complexes (**$PtC_4H$**, **$PtC_6TES$)** and o-xylylene (generated from 1,4-dihydro-2,3-benzoxathiin-3-oxide), and (b) diplatnium complex **$PtC_8Pt$** and o-xylylene (generated from 1,3-dihydrobenzo[c]thiophene-2,2-dioxide). Alternative cyclofunctionalizations involving the polyynes **$TESC_4TES$**, **$TESC_8TES$**, or **$PtC_8Pt$**, and $B_{10}H_{14}{\cdot}2[S(CH_3)_2]$ were attempted in refluxing toluene. However, chromatographic workups did not give any well defined products. Finally, a catalyst [CpCo(CO)(dimethyl fumarate)] that was effective in many [2+2+2] cycloaddition reactions was applied to the polyynes **$PtC_4H$**, **$TESC_8TES$**, **$PtC_6Pt$**, and **$PtC_8Pt$** under "classical" conditions (refluxing toluene for several hours, either in the dark or under ambient lighting). However, no trimeric species could be detected afterwards. It is concluded that the steric congestion in these polyynes must be reduced,

for example by lengthening the sp carbon chain, so that any interference to cycloaddition from the bulky endgroups is minimized.

### 4.5 Experimental section

Reactions were conducted under inert atmospheres. Workups were carried out in air unless noted. Chemicals were treated as follows: $CH_2Cl_2$ and toluene (for reactions), dried and degassed with a Glass Contour solvent purification system; hexanes (98.5%, Aldrich), $CH_2Cl_2$ (99.5%, EMD; for chromatography), $HNEt_2$ (99.5%, Aldrich), acetone (99.5%, Aldrich), toluene (99.5%, EMD), ethyl acetate (99.8%, Aldrich), ethanol (99.8%, Aldrich), benzene (99.8%, Aldrich), THF (99%, BDH), DMF (99%, Aldrich), methanol (99.9%, BDH), ether (99%, BDH), heptane (99%, Aldrich), 1,2,4-trichlorobenzene (99%, Aldrich), AcOH (99.85%, Aldrich), CuCl (99.999%, Acros), CuI (99.999%, Alfa Aesar), TMSCl (98+%, Alfa Aesar), TMEDA (99%, Acros), **TESC$_2$H** ($HC{\equiv}CSiEt_3$, 97%, Strem), benzyltriethylammonium chloride (99%, Aldrich), *n*-$Bu_4NBr$ (98%, Alfa Aesar), $H_2O_2$ (Aldrich), *α,α′*-dibromo-*o*-xylene (95%, TCI), sodium sulfide nonahydrate (Aldrich), rongalite (95%, TCI), decaborane (technical grade, Aldrich), dimethylsulfide (99%, Aldrich), dimethyl fumarate (99%, Acros), $CpCo(CO)_2$ (technical grade, Aldrich), *n*-$Bu_4NF$ (Acros), diphenylacetylene (99%, Acros), zinc (99.9%, Alfa Aesar), $CDCl_3$ (Cambridge Isotope Laboratories), used as received. The precursors *trans*-$(C_6F_5)(p\text{-}tol_3P)_2Pt(Cl)$ (**PtCl**),[20] **TESC$_4$TES**,[91] **TESC$_8$TES**,[91] **TESC$_4$H**,[91] and butadiyne[64] were prepared according to the literature.

NMR spectra were recorded at ambient probe temperature unless noted using a Varian instrument operating at 500.00 ($^{1}$H), 125.65 ($^{13}$C{$^{1}$H}), 202.28 ($^{31}$P{$^{1}$H}) or 470.35 ($^{19}$F{$^{1}$H}) MHz and referenced as follows ( /ppm): $^{1}$H, residual internal $CHCl_3$ (7.26); $^{13}$C, internal $CDCl_3$ (77.2); $^{31}$P, external $H_3PO_4$ (0.00); $^{19}$F, internal $C_6F_6$ (–162.4).

***trans*-$(C_6F_5)$(*p*-$tol_3P)_2Pt(C{\equiv}C)_2H$ ($PtC_4H$).**[20] A Schlenk flask was charged with **PtCl** (1.944 g, 1.933 mmol),[20] CuI (0.083 g, 0.44 mmol), $CH_2Cl_2$ (15 mL), and $HNEt_2$ (110 mL), and cooled to –45 °C ($CO_2$/$CH_3CN$). Then butadiyne (in THF, 11.6 mL, 49.9 mmol) was added with stirring. The cold bath was allowed to warm to room temperature (ca. 3 h). After an additional 3 h, the solvent was removed by oil pump vacuum. The residue was extracted with toluene (3 × 25 mL). The combined extracts were filtered through a neutral alumina column (10 cm, packed in toluene). The solvent was removed by rotary evaporation. The residue was washed with ethanol (25 mL) and dried by oil pump vacuum to give **$PtC_4H$** as an off-white solid (1.589 g, 1.559 mmol, 80%).

NMR (δ, $CDCl_3$): $^{1}$H 7.49-7.45 (m, 12H, *o* to P), 7.09 (d, $^{3}J_{HH}$ = 7.9 Hz, 12H, *m* to P), 2.33 (s, 18H, $CH_3$ *p* to P), 1.53 (s, 1H, ≡CH); $^{31}$P{$^{1}$H} 18.05 (s, $^{1}J_{PPt}$ = 2658 Hz[65]).

***trans*-$(C_6F_5)$(*p*-$tol_3P)_2Pt(C{\equiv}C)_3SiEt_3$ ($PtC_6TES$).**[20] A three-neck flask was charged with **$PtC_4H$** (2.455 g, 2.409 mmol), **$TESC_2H$** (2.638 g, 18.84 mmol), and acetone (150 mL), and fitted with a gas dispersion tube and a condenser cooled with

chilled water. A Schlenk flask was charged with CuCl (0.630 g, 6.36 mmol) and acetone (150 mL), and TMEDA (0.400 mL, 2.67 mmol) was added with stirring. After 45 min, stirring was halted, and a green solid separated from a blue supernatant. Then $O_2$ was bubbled through the three-neck flask with stirring, and the solution was heated to 65 °C. After 15 min, the blue supernatant was added in portions. After 3 h, the solvent was removed by rotary evaporation. The residue was extracted with hexanes (3 × 50 mL) and then benzene (3 × 50 mL). The solvent was removed from the extracts by rotary evaporation and oil pump vacuum. The yellow powder was chromatographed on a silica gel column (20 cm, 10:90 v/v $CH_2Cl_2$/hexanes to elute **PtC$_6$TES**, 30:70 v/v $CH_2Cl_2$/hexanes to elute byproduct **PtC$_8$Pt** (0.5122 g, 0.2516 mmol, 10%)). The first band was taken to dryness by oil pump vacuum to give **PtC$_6$TES** as a yellow powder (1.248 g, 1.08 mmol, 45%).

NMR (δ, $CDCl_3$): $^1$H 7.48-7.44 (m, 12H, *o* to P), 7.10 (d, $^3J_{HH}$ = 7.6 Hz, 12H, *m* to P), 2.35 (s, 18H, $CH_3$, *p* to P), 0.91 (t, $^3J_{HH}$ = 7.9 Hz, 9H, $CH_2CH_3$), 0.51 (q, $^3J_{HH}$ = 7.9 Hz, 6H, $SiCH_2$); $^{13}$C{$^1$H} 145.7 (dd, $^1J_{CF}$ = 226 Hz, $^2J_{CF}$ = 19.4 Hz, *o* to Pt), 140.8 (s, *p* to P), 137.9-135.9 (m, *p* to Pt), 137.3-135.2 (m, *m* to Pt), 134.2 (virtual t,[92] $^2J_{CP}$ = 6.4 Hz, *o* to P), 128.6 (virtual t,[92] $^3J_{CP}$ = 5.5 Hz, *m* to P), 127.1 (virtual t,[92] $^1J_{CP}$ = 30.3 Hz, *i* to P), 103.67 (br s, Pt*C*≡C), 95.37 (s, PtC≡*C*), 91.19 (s, SiC≡*C*), 80.33 (s, Si*C*≡C), 66.10, 55.89 (2 × s, PtC≡C*C*≡*C*Si), 21.3 (s, $CH_3$, *p* to P), 7.3 (s, *C*$H_2$$CH_3$), 4.3 (s, $^1J_{CSi}$ = 56.7 Hz,[93] $SiCH_2$); $^{19}$F{$^1$H} −117.66 to −117.77 (m, $^3J_{FPt}$ = 292 Hz,[65] 2F, *o* to Pt),

–164.91 to –165.05 (m, 2F, *m* to Pt), –165.34 (t, $^3J_{FF}$ = 19.4 Hz, 1F, *p* to Pt); $^{31}P\{^1H\}$ 18.06 (s, $^1J_{PPt}$ = 2638 Hz[65]).

***trans*-($C_6F_5$)(*p*-$tol_3P$)$_2$Pt(C≡C)$_5$$SiEt_3$ ($PtC_{10}TES$).**[20] A three necked flask was fitted with a gas dispersion tube, charged with **$PtC_6TES$** (0.388 g, 0.335 mmol) and THF (40 mL), and cooled to 0 °C. Then wet *n*-$Bu_4NF$ (1.0 M in THF, 5 wt% water, 0.10 mL, 0.10 mmol) was added with stirring. After 10 min (TLC, silica gel, 1:9 v/v ethyl acetate/hexanes, showed no remaining educts), TMSCl (0.10 mL, 1.2 mmol) and cold acetone (0 °C, 90 mL) were added followed by **$TESC_4H$** (1.066 g, 6.485 mmol). Then $O_2$ was bubbled through the mixture and the CuCl/TMEDA suspension (7 mL) was added with stirring. After 40 min (TLC showed no remaining educts), hexanes (90 mL) were added. The dark green suspension was filtered through a pad of silica gel (3 × 10 cm, packed in 1:1 v/v acetone/hexanes), which was rinsed (1:1 v/v acetone/hexanes) until the filtrate became colorless. The solvents were removed from the filtrate by rotary evaporation at 20 °C and the red brown residue was dried by oil pump vacuum and chromatographed on a silica gel column (3.5 × 30 cm, packed in hexanes, eluted with 1:2 v/v $CH_2Cl_2$/hexanes). The solvents were removed from the product containing fractions by rotary evaporation and oil pump vacuum to give **$PtC_{10}TES$** as an orange-yellow solid (0.213 g, 0.177 mmol, 53%) and **$PtC_{12}Pt$** as a yellow-orange solid (0.051g, 0.025 mmol, 7.5%).

NMR (δ, $CDCl_3$): $^1H$ 7.52-7.48 (m, 12H, *o* to P), 7.15 (d, $^3J_{HH}$ = 7.8 Hz, 12H, *m* to P), 2.38 (s, 18H, $CH_3$, *p* to P), 1.00 (t, $^3J_{HH}$ = 7.9 Hz, 9H, C$H_2$$CH_3$), 0.64 (q, $^3J_{HH}$ =

7.9 Hz, 6H, $SiCH_2$); $^{13}C\{^1H\}$ 145.7 (dd, $^1J_{CF}$ = 224 Hz, $^2J_{CF}$ = 19.3 Hz, *o* to Pt), 141.0 (s, *p* to P), 137.9-136.1 (dm, $^1J_{CF}$ = 236 Hz, *p* to Pt), 137.5-135.3 (m, *m* to Pt), 134.2 (virtual t,[92] $^2J_{CP}$ = 6.3 Hz, *o* to P), 128.7 (virtual t,[92] $^3J_{CP}$ = 5.5 Hz, *m* to P), 126.8 (virtual t,[92] $^1J_{CP}$ = 30.4 Hz, *i* to P), 108.02 (br s, $^1J_{CPt}$ = 1001 Hz,[65] Pt*C*≡C), 95.01 (s, $^2J_{CPt}$ = 260 Hz,[65] PtC≡*C*), 89.60 (s, SiC≡*C*), 84.71 (s, $^1J_{CSi}$ = 73.8 Hz,[93] Si*C*≡C), 66.61, 64.94, 63.07, 60.26, 59.50, 56.48 (6 × s, PtC≡C(*C*≡*C*)$_3$Si), 21.3 (s, $CH_3$, *p* to P), 7.3 (s, *C*$H_2$$CH_3$), 4.1 (s, $^1J_{CSi}$ = 56.8 Hz,[93] $SiCH_2$); $^{19}F\{^1H\}$ −117.62 to −117.94 (m, $^3J_{FPt}$ = 292 Hz,[65] 2F, *o* to Pt), −164.93 to −165.65 (m, 2F, *m* to Pt), −165.33 (t, $^3J_{FF}$ = 19.4 Hz, 1F, *p* to Pt); $^{31}P\{^1H\}$ 18.02 (s, $^1J_{PPt}$ = 2615 Hz[65]).

***trans,trans*-($C_6F_5$)(*p*-$tol_3P$)$_2$Pt(C≡C)$_3$Pt(*p*-$tol_3P$)$_2$($C_6F_5$) (PtC$_6$Pt).**[20] A Schlenk flask was charged with **PtCl** (0.5073 g, 0.5045 mmol), $HNEt_2$ (200 mL), and CuCl (0.04 g, 0.4 mmol). The mixture was stirred until a clear solution formed and was then cooled to −45 °C. Another Schlenk flask was charged with **PtC$_6$TES** (0.5012 g, 0.4332 mmol) and $CH_2Cl_2$ (20 mL). Then *n*-$Bu_4NF$ (1.0 M in THF/5 wt% $H_2O$, 0.10 mL, 0.10 mmol) was added. The solution was stirred for 15 min, cooled to −45 °C, and transferred via cannula to the solution of **PtCl** with stirring. The mixture was allowed to warm to room temperature. After 5 d, the solvent was removed by oil pump vacuum. The residue was extracted with hexanes (3 × 50 mL) and toluene (3 × 50 mL). The extracts were passed in sequence through a neutral alumina column (15 cm, packed in hexanes). The solvent was removed from the toluene extracts by rotary evaporation and oil pump vacuum. The

residue was chromatographed on a silica gel column (15 cm, 40:60 v/v $CH_2Cl_2$/hexanes). The yellow band was taken to dryness by oil pump vacuum to give **PtC$_6$Pt** as a yellow powder (0.3028 g, 0.1505 mmol, 35%). The sample was recrystallized from $CHCl_3$/methanol.

NMR (δ, $CDCl_3$): $^1$H 7.44 (m, 24H, *o* to P), 7.06 (d, $^3J_{HH}$ = 7.8 Hz, 24H, *m* to P), 2.29 (s, 36H, $CH_3$); $^{13}C\{^1H\}$ 145.7 (dd, $^1J_{CF}$ = 226 Hz, $^2J_{CF}$ = 22 Hz, *o* to Pt), 140.4 (s, *p* to P), 137.0 (dm, $^1J_{CF}$ = 235 Hz, *p* to Pt), 136.5 (dm, $^1J_{CF}$ = 249 Hz, *m* to Pt), 134.2 (virtual t,[92] $^2J_{CP}$ = 6.5 Hz, *o* to P), 128.7 (virtual t,[92] $^3J_{CP}$ = 5.5 Hz, *m* to P), 126.8 (virtual t,[92] $^1J_{CP}$ = 30.5 Hz, i to P), 98.4 (s, PtC≡*C*), 95.8 (br s, Pt*C*≡C), 61.1 (s, PtC≡C*C*), 21.3 (s, $CH_3$). MS:[94] 2014 ($PtC_6Pt^+$, 10%), 970 ($[(C_6F_5)(p\text{-}tol_3P)_2Pt]^+$, 40%), 803 ($[(p\text{-}tol_3P)_2Pt]^+$, 100%).

***trans,trans*-(C$_6$F$_5$)(*p*-tol$_3$P)$_2$Pt(C≡C)$_4$Pt(*p*-tol$_3$P)$_2$(C$_6$F$_5$) (PtC$_8$Pt).**[20] A three-neck flask was charged with **PtC$_4$H** (1.035 g, 1.016 mmol) and acetone (25 mL), and fitted with a gas dispersion tube and a condenser. A Schlenk flask was charged with CuCl (0.015 g, 0.15 mmol) and acetone (6 mL), and TMEDA (0.010 mL, 0.060 mmol) was added with stirring. After 30 min, stirring was halted, and a green solid separated from a blue supernatant. Then $O_2$ was bubbled through the three-neck flask with stirring, and the solution was heated to 65 °C. After 10 min, the blue supernatant was added in portions. After 1.5 h, the solvent was removed by rotary evaporation. The residue was extracted with toluene (2 × 20 mL). The combined extracts were filtered through a neutral alumina

column (7 cm, packed in toluene). The solvent was removed by rotary evaporation. Ethanol (20 mL) was added, and the yellow powder was collected by filtration and dried by oil pump vacuum to give **PtC$_8$Pt** as a yellow soild (1.005 g, 0.4936 mmol, 97%).

NMR (δ, $CDCl_3$): $^1$H 7.43 (m, 24H, *o* to P), 7.06 (d, $^3J_{HH}$ = 7.8 Hz, 24H, *m* to P), 2.33 (s, 36H, $CH_3$); $^{13}C\{^1H\}$ 145.7 (dd, $^1J_{CF}$ = 225 Hz, $^2J_{CF}$ = 22 Hz, *o* to Pt), 140.6 (s, *p* to P), 136.8 (dm, $^1J_{CF}$ = 240 Hz, *p* to Pt), 136.6 (dm, $^1J_{CF}$ = 248 Hz, *m* to Pt), 134.2 (virtual t,[92] $^2J_{CP}$ = 6.2 Hz, *o* to P), 128.6 (virtual t,[92] $^3J_{CP}$ = 5.4 Hz, *m* to P), 127.2 (virtual t,[92] $^1J_{CP}$ = 30.2 Hz, *i* to P), 100.6 (s, $^1J_{CPt}$ = 998 Hz,[65] Pt*C*≡C), 96.7 (s, $^2J_{CPt}$ = 265 Hz,[65] PtC≡*C*), 64.1 (s, PtC≡C*C*), 58.1 (s, PtC≡CC≡*C*), 21.3 (s, $CH_3$); $^{19}F\{^1H\}$ –117.54 (m, $^3J_{FPt}$ = 292 Hz,[65] *o* to Pt), –165.31 (m, *m* to Pt), –165.89 (t, $^3J_{FF}$ = 19.3 Hz, *p* to Pt).

***trans,trans*-(C$_6$F$_5$)(*p*-tol$_3$P)$_2$Pt(C≡C)$_5$Pt(*p*-tol$_3$P)$_2$(C$_6$F$_5$) (PtC$_{10}$Pt).**[20] A Schlenk flask was charged with **PtCl** (0.5042 g, 0.5014 mmol), $HNEt_2$ (200 mL), and CuCl (0.04 g, 0.4 mmol). The mixture was stirred until a clear solution formed and was then cooled to –45 °C. Another Schlenk flask was charged with **PtC$_{10}$TES** (0.2813 g, 0.2334 mmol) and $CH_2Cl_2$ (20 mL). Then *n*-$Bu_4NF$ (1.0 M in THF/5 wt% $H_2O$, 0.10 mL, 0.10 mmol) was added. The solution was stirred for 15 min, cooled to –45 °C, and transferred via cannula to the solution of **PtCl** with stirring. The mixture was allowed to warm to room temperature. After 5 d, the solvent was removed by oil pump vacuum. The residue was extracted with hexanes (3 × 50 mL) and toluene (3 × 50 mL). The extracts

were passed in sequence through a neutral alumina column (15 cm, packed in hexanes). The solvent was removed from the toluene extracts by rotary evaporation and oil pump vacuum. The residue was chromatographed on a silica gel column (15 cm, 40:60 v/v $CH_2Cl_2$/hexanes). The yellow band was taken to dryness by oil pump vacuum to give **PtC$_{10}$Pt** as a yellow powder (0.3708 g, 0.1800 mmol, 77%). The sample was recrystallized from $CHCl_3$/methanol.

NMR (δ, $CDCl_3$): $^1$H 7.43 (m, 12H, *o* to P), 7.10 (d, $^3J_{HH}$ = 8.0 Hz, 12H, *m* to P), 2.34 (s, 18H, $CH_3$, tol), 0.93 (t, $^3J_{HH}$ = 7.8 Hz, 9H, $CH_2CH_3$), 0.63 (q, $^3J_{HH}$ = 7.8 Hz, 6 H, $CH_2CH_3$); $^{31}$P{$^1$H} 18.0 (s, $^1J_{PPt}$ = 2611 Hz[65]).

***trans,trans*-(C$_6$F$_5$)(*p*-tol$_3$P)$_2$Pt(C≡C)$_6$Pt(*p*-tol$_3$P)$_2$(C$_6$F$_5$) (PtC$_{12}$Pt).**[20] A three-neck flask was charged with **PtC$_6$TES** (0.1007 g, 0.08704 mmol) and acetone (25 mL), and fitted with a gas dispersion tube and a condenser. A Schlenk flask was charged with CuCl (0.100 g, 1.01 mmol) and acetone (30 mL), and TMEDA (0.060 mL, 0.40 mmol) was added with stirring. After 30 min, stirring was halted, and a green solid separated from a blue supernatant. Then *n*-$Bu_4NF$ (1.0M in THF/5 wt% $H_2O$, 0.020 mL, 0.020 mmol) was added to the solution of **PtC$_6$TES** with stirring. After 20 min, TMSCl (0.011 mL, 0.086 mmol) was added. Then $O_2$ was bubbled through the solution. After 10 min, the blue supernatant was added in portions. The flask was transferred to an oil bath, which was heated to 65 °C (ca. 10 min). After 3 h, the solvent was removed by rotary evaporation. The residue was extracted with hexanes (3 × 10 mL), which was passed through a neutral alumina column (10 cm, packed in hexanes) and discarded, and then

with benzene (3 × 10 mL), which was filtered through the same column. The solvent was removed by rotary evaporation. Methanol (20 mL) was added, and the yellow powder was collected by filtration and dried by oil pump vacuum to give **$PtC_{12}Pt$** (0.073 g, 0.035 mmol, 80%) as an orange solid.

NMR (δ, $CDCl_3$): $^1H$ 7.43 (m, 24H, *o* to P), 7.09 (d, $^3J_{HH}$ = 7.8 Hz, 24H, *m* to P), 2.34 (s, 36H, $CH_3$); $^{13}C\{^1H\}$ 145.7 (dd, $^1J_{CF}$ = 226 Hz, $^2J_{CF}$ = 22 Hz, *o* to Pt), 140.9 (s, *p* to P), 136.6 (dm, $^1J_{CF}$ = 240 Hz, *p* to Pt), 136.8 ($^1J_{CF}$ = 248 Hz, *m* to Pt), 134.2 (virtual t,[92] $^2J_{CP}$ = 6.5 Hz, *o* to P), 128.7 (virtual t,[92] $^3J_{CP}$ = 5.5 Hz, *m* to P), 126.9 (virtual t,[92] $^1J_{CP}$ = 29.4 Hz, *i* to P), 106.5 (s, Pt*C*≡C), 95.5 (s, PtC≡*C*), 65.7 (s, PtC≡C*C*), 63.0, 61.0, 57.1 (3 × s, middle C≡C), 21.3 ppm (s, $CH_3$); MS:[94] 2085 ($PtC_{12}Pt^+$, 5%).

**1,3-Dihydrobenzo[c]thiophene.**[82] A mixture of *α,α′*-dibromo-*o*-xylene (13.22 g, 0.050 mol) and benzene (50 mL) was stirred until the dibromide dissolved completely. Then a solution of sodium sulfide nonahydrate (24.10 g, 0.100 mol) in water (20 mL) and benzyltriethylammonium chloride (0.05 g) were added. The mixture was stirred for 30 h at 20 °C, and then steam distilled. Benzene distilled off first, and then the 1,3-dihydrobenzo[c]thiophene was collected under a water layer. The product was separated and cooled in the refrigerator giving a brown sticky oil (4.124 g, 30.32 mmol, 61%) that was used without additional purification.

NMR (δ, $CDCl_3$): $^1H$ 7.14 (s, 4H, Ph), 4.45 (s, 4H, $CH_2$).

**1,3-Dihydrobenzo[c]thiophene-2,2-dioxide.**[82] A mixture of 1,3-dihydrobenzo[c]thiophene (4.083 g, 30.02 mmol) and glacial AcOH (25 mL) was cooled

in an ice bath at 5 °C, and a solution of 30% $H_2O_2$ (7 mL) was added dropwise over 1 h. Then the mixture was stirred for 1 h at 20 °C and 3 h at 95 °C. The mixture was cooled, and the crystals that precipitated were collected by filtration, washed with water, dried in air, and recrystallized from EtOH to give 1,3-dihydrobenzo[c]thiophene-2,2-dioxide as orange needles (4.513 g, 26.86 mmol, 90%).

NMR (δ, $CDCl_3$): $^1$H 7.25 (s, 4H, Ph), 4.34 (s, 4H, $CH_2$).

**1,4-Dihydro-2,3-benzoxathiin-3-oxide.**[83] A suspension of sodium hydroxymethane-sulfinate (rongalite) (3.027 g, 25.65 mmol) was stirred with a solution of *α,α′*-dibromo-*o*-xylene (3.172 g, 12.02 mmol) and *n*-$Bu_4NBr$ (2 mmol) in DMF (20 mL). Then water (150 mL) was added, and the solids were removed by filtration. The filtrate was extracted with ether. The ether solution was dried (anhydrous magnesium sulfate), and the solvent was removed by rotary evaporation to give 1,4-dihydro-2,3-benzoxathiin-3-oxide as a colorless oil (1.774 g, 10.56 mmol, 88%).

NMR (δ, $CDCl_3$): $^1$H 7.42-7.20 (m, 4H), 5.32 (d, $^2J_{HH}$ = 13.8 Hz, 1H), 4.97 (d, $^2J_{HH}$ = 13.9 Hz, 1H), 4.41 (d, $^2J_{HH}$ = 15.0 Hz, 1H), 3.55 (d, $^2J_{HH}$ = 14.9 Hz, 1H).

**$B_{10}H_{12}$·2[$S(CH_3)_2$].**[87] Decaborane (0.3919 g, 3.21 mmol) and dimethylsulfide (2.53 mL, 33.5 mmol, 10 fold excess) were added to a 10 mL round bottom flask fitted with a condensor under nitrogen. The resulting solution was refluxed for 6 h, cooled to room temperature, and allowed to sit under nitrogen for 24 h, after which time white crystals had grown. The product crystals were collected by filtration, washed with heptane (3 × 30 mL), and dried under vacuum (0.6661 g, 2.708 mmol, 84%). **Note:**

**Decaborane and dimethylsulfide both have potent, unpleasant aromas and the product $B_{10}H_{12}\cdot 2[S(CH_3)_2]$ was even more noxious.**

**[CpCo(CO)(dimethyl fumarate)].**[89] A solution of dimethyl fumarate (0.0476 g, 0.3302 mmol), $CpCo(CO)_2$ (0.060 mL, 0.4 mmol), and toluene (30 mL) was flushed with nitrogen and refluxed for 3 h under ambient lighting. The mixture was concentrated under reduced pressure and the residue was chromatographed on an alumina column (3 cm × 15 cm, packed with hexanes, eluted with $CH_2Cl_2$/hexanes 0:1 to 4:6 v/v). The solvent was removed from the product containing fractions to give [CpCo(CO)(dimethyl fumarate)] as a red solid (0.0938 g, 0.317 mmol, 96%).

NMR (δ, $CDCl_3$): $^1$H 4.99 (s, 5H, Cp), 3.86 (d, $^3J_{HH}$ = 10.3 Hz, 1H), 3.71 (s, 3H), 3.61 (s, 3H), 3.28 (d, $^3J_{HH}$ = 10.3 Hz, 1H); $^{13}C\{^1H\}$ 199.2 (CO), 176.2 (C=O), 175.6 (C=O), 87.2 (Cp), 51.5 ($CH_3$), 51.4 ($CH_3$), 38.2 (CH), 37.1(CH).

**Attempted Diels-Alder cycloaddition of $PtC_4H$. (A)** A Schlenk flask was charged with **$PtC_4H$** (0.1022 g, 1.003 mmol), 1,4-dihydro-2,3-benzoxathiin-3-oxide (0.0526 g, 0.313 mmol), and toluene (40 mL), and was flushed with nitrogen. The mixture was stirred at 110 °C while covered with aluminum foil. After 48 h, the mixture was cooled and the solvent was removed by rotary evaporation. The crude residue was chromatographed on an alumina column (3 cm × 25 cm, packed with hexanes, eluted with $CH_2Cl_2$/hexanes 0:1 to 1:1 v/v). The fractions were assayed by mass spectrometry (MALDI), and as discussed in chapter 4.4, some peaks were consistent with the target molecule. **(B)** A Schlenk flask was charged with **$PtC_4H$**, 1,3-dihydrobenzo[*c*]thiophene-

2,2-dioxide (ca. 9 fold excess), and 1,2,4-trichlorobenzene (20 mL), flushed with nitrogen, and kept at 160 °C in the dark for 1 d. The mixture was cooled to room temperature and chromatographed on an alumina column (3 cm × 25 cm, packed with hexanes, eluted with $CH_2Cl_2$/hexanes 0:1 to 3:7 v/v). The fractions were checked by mass spectrometry (MALDI), and as discussed in chapter 4.4, no target product was detected. **(C)** A Schlenk flask was charged with **PtC$_4$H** (0.1329 g, 0.1231 mmol), *α,α′*-dibromo-*o*-xylene (ca. 2 fold excess), and THF (20 mL), flushed with nitrogen, and kept in an ultrasound bath (42 kHz) with zinc dust (0.0070 g, 0.1072 mmol) in the dark.[95] After 1 h, the solvent was removed by rotary evaporation and the residue was chromatographed on an alumina column (3 cm × 25 cm, packed with hexanes, eluted with $CH_2Cl_2$/hexanes 0:1 to 3:7 v/v). An off-white solid was collected (ca. 60% yield). A single crystal was obtained by the slow evaporation of a $CH_2Cl_2$/hexanes solution (1:3, v/v). The structure proved to be *trans*-($C_6F_5$)(*p*-tol$_3$P)$_2$PtBr as described below.

MS:[94] 1121 ([**PtC$_4$H**+*o*-xylylene]$^+$, 20%), 1019 (**PtC$_4$H**$^+$, 5%), 970 ([($C_6F_5$)(*p*-tol$_3$P)$_2$Pt]$^+$, 10%), 803 ([(*p*-tol$_3$P)$_2$Pt]$^+$, 100%).

**Attempted Diels-Alder cycloaddition of PtC$_6$TES. (A)** A Schlenk flask was charged with **PtC$_6$TES** (0.1233 g, 0.1066 mmol), 1,4-dihydro-2,3-benzoxathiin-3-oxide (0.0542 g, 0.322 mmol), and toluene (40 mL), and was flushed with nitrogen. The mixture was stirred at 100 °C while covered with aluminum foil for 48 h. After cooling, the solvent was removed by rotary evaporation and the residue was chromatographed on an alumina column (alumina, 3 cm × 25 cm, packed with hexanes, eluted with

$CH_2Cl_2$/hexanes 0:1 to 1:1 v/v). The fractions were assayed by mass spectrometry (MALDI), and as discussed in chapter 4.4, some peaks were consistent with the target molecule. **(B)** A Schlenk flask was charged with **PtC$_6$TES**, 1,3-dihydrobenzo[*c*]thiophene-2,2-dioxide (ca. 9 fold excess), and 1,2,4-trichlorobenzene (20 mL), flushed with nitrogen, and heated to 180 °C in the dark. After 1 d, the mixture was chromatographed on an alumina column (3 cm × 25 cm, packed with hexanes, eluted with $CH_2Cl_2$/hexanes 0:1 to 3:7 v/v). The fractions were checked by mass spectrometry (MALDI), and as discussed in chapter 4.4, no target product was detected.

MS:[94] 1261 ([**PtC$_6$TES**+*o*-xylylene]$^+$, 80%), 970 ([$(C_6F_5)$(*p*-tol$_3$P)$_2$Pt]$^+$, 100%).

**Attempted Diels-Alder cycloaddition of PtC$_8$Pt. (A)** A Schlenk flask was charged with **PtC$_8$Pt**, 1,4-dihydro-2,3-benzoxathiin-3-oxide (ca. 3 fold excess), and toluene (25 mL), flushed with nitrogen, and kept at 100 °C in the dark. After 1 d, the solvent was removed by rotary evaporation and the residue was chromatographed on an alumina column (alumina, 3 cm × 25 cm, packed with hexanes, eluted with $CH_2Cl_2$/hexanes 0:1 to 3:7 v/v). The fractions were checked by mass spectometry (MALDI), and as discussed in chapter 4.4, no target product was detected. **(B)** A Schlenk flask was charged with **PtC$_8$Pt**, 1,3-dihydrobenzo[*c*]thiophene-2,2-dioxide (ca. 9 fold excess), and 1,2,4-trichlorobenzene (20 mL), flushed with nitrogen, and kept at 180 °C in the dark. After 1 d, the mixture was cooled and chromatographed on an alumina column (3 cm × 25 cm, packed with hexanes, eluted with $CH_2Cl_2$/hexanes 0:1 to 3:7 v/v). The 1,2,4-trichlorobenzene eluted with hexanes, and unreacted **PtC$_8$Pt** with $CH_2Cl_2$. A final

elution with methanol gave a yellow solid. The fractions were assayed by mass spectometry (MALDI), and as discussed in chapter 4.4, some peaks were consistent with the target molecule.

(a) MS:[94] 2142 ([**PtC$_8$Pt**+*o*-xylylene]$^+$, 5%), 2038 (**PtC$_8$Pt**$^+$, 100%) .

(b) MS:[94] 2342 ([**PtC$_8$Pt**+3(*o*-xylylene)]$^+$, 15%), 2244 ([**PtC$_8$Pt**+2(*o*-xylylene)]$^+$, 20%), 2038 (**PtC$_8$Pt**$^+$, 100%).

(c) MS:[94] 2342 ([**PtC$_8$Pt**+3(*o*-xylylene)]$^+$, 100%), 2038 (**PtC$_8$Pt**$^+$, 70%).

**Attempted Diels-Alder cycloaddition of PtC$_{10}$Pt.** A Schlenk flask was charged with **PtC$_{10}$Pt**, 1,4-dihydro-2,3-benzoxathiin-3-oxide (ca. 3 fold excess), and toluene (25 mL), flushed with nitrogen, and kept at 100 °C in the dark. After 1 d, the solvent was removed by rotary evaporation and the residue was chromatographed on an alumina column (3 cm × 25 cm, packed with hexanes, eluted with $CH_2Cl_2$/hexanes 0:1 to 3:7 v/v). The fractions were checked by mass spectrometry (MALDI), and as discussed in chapter 4.4, no target product was detected. **(B)** A Schlenk flask was charged with **PtC$_{10}$Pt**, 1,3-dihydrobenzo[*c*]thiophene-2,2-dioxide (ca. 9 fold excess), and 1,2,4-trichlorobenzene (20 mL), flushed with nitrogen, and kept at 160 °C in the dark. After 1 d, the mixture was cooled and chromatographed on an alumina column (3 cm × 25 cm, packed with hexanes, eluted with $CH_2Cl_2$/hexanes 0:1 to 3:7 v/v). The fractions were checked by mass spectrometry (MALDI), and as discussed in chapter 4.4, no target product was detected.

**Attempted Diels-Alder cycloaddition of $PtC_{12}Pt$.** A Schlenk flask was charged with **$PtC_{12}Pt$**, 1,4-dihydro-2,3-benzoxathiin-3-oxide (ca. 3 fold excess), and toluene (25 mL), flushed with nitrogen, and kept at 100 °C in the dark. After 1 d, the solvent was removed by rotary evaporation and the residue was chromatographed on an alumina column (3 cm × 25 cm, packed with hexanes, eluted with $CH_2Cl_2$/hexanes 0:1 to 3:7 v/v). The fractions were checked by mass spectrometry (MALDI), and as discussed in chapter 4.4, no target product was detected. **(B)** A Schlenk flask was charged with **$PtC_{12}Pt$**, 1,3-dihydrobenzo[*c*]thiophene-2,2-dioxide (ca. 9 fold excess), and 1,2,4-trichlorobenzene (20 mL), flushed with nitrogen, and kept at 160 °C in the dark. After 1 d, the mixture was cooled and chromatographed on an alumina column (3 cm × 25 cm, packed with hexanes, eluted with $CH_2Cl_2$/hexanes 0:1 to 3:7 v/v). The fractions were checked by mass spectrometry (MALDI), and as discussed in chapter 4.4, no target product was detected.

**Attempted Diels-Alder cycloaddition of diphenylacetylene** A Schlenk flask was charged with diphenylacetylene (0.1522 g, 0.8551 mmol), 1,4-dihydro-2,3-benzoxathiin-3-oxide (0.5032 g, 2.995 mmol), and toluene (40 mL), and was flushed with nitrogen. After 3 h, another portion of 1,4-dihydro-2,3-benzoxathiin-3-oxide (0.5102 g, 3.037 mmol) was added with stirring. The mixture was stirred at 120 °C in the dark (flask covered with aluminum foil). After 24 h, the mixture was cooled and filtered. The solvent was removed from the filtrate by rotary evaporation. The residue was washed with toluene (25 mL) and dried by oil pump vacuum to give an off-white solid. This unknown

material looked like rubber and did not dissolve in water, toluene, hexanes, $CH_2Cl_2$, petroleum ether, DMF, or DMSO at room temperature.

**Addition of TESC$_4$TES and B$_{10}$H$_{12}$·2[S(CH$_3$)$_2$]. TESC$_4$TES** (0.0486 g, 0.175 mmol, 1.0 eq.) and $B_{10}H_{12}$·2[$S(CH_3)_2$] (0.0499 g, 0.203 mmol, 1.2 eq.) were combined in a round bottom flask fitted with a condenser under nitrogen. Then dry toluene (15 mL) was injected via syringe to give a dark red-tan mixture. The mixture was refluxed for 24 h, affording a dark red supernatant with a small amount of precipitate. The mixture was concentrated by rotary evaporation and chromatographed on an alumina column (3 cm × 15 cm, packed with hexanes, eluted with $CH_2Cl_2$/hexanes 0:1 to 3:7 v/v). The solvent was removed from the colored fractions. A $^1$H NMR spectrum of the residue did not show the usual broad peaks indicative of an *o*-carborane (δ 1.60-3.70).[96]

**Addition of TESC$_8$TES and B$_{10}$H$_{12}$·2[S(CH$_3$)$_2$]. TESC$_8$TES** (0.0534 g, 0.164 mmol, 1.0 eq.) and $B_{10}H_{12}$·2[$S(CH_3)_2$] (0.0502 g, 0.204 mmol, 1.2 eq.) were combined in a round bottom flask fitted with a condenser under nitrogen. Then dry toluene (10 mL) was injected via syringe to give a dark red-tan mixture. The mixture was refluxed for 24 h, affording a dark red supernatant with a small amount of precipitate. The mixture was concentrated by rotary evaporation and chromatographed on an alumina column (3 cm × 15 cm, packed with hexanes, eluted with $CH_2Cl_2$/hexanes 0:1 to 3:7 v/v). The solvent was removed from the colored fractions. A $^1$H NMR spectrum of the residue did not show the usual broad peaks indicative of an *o*-carborane (δ 1.60-3.70).[96]

**Addition of $PtC_8Pt$ and $B_{10}H_{12}\cdot 2[S(CH_3)_2]$. $PtC_8Pt$** (0.2863 g, 0.1406 mmol, 1.0 eq.) and $B_{10}H_{12}\cdot 2[S(CH_3)_2]$ (0.0336 g, 0.137 mmol, 1.0 eq.) were combined in a round bottom flask fitted with a condenser under nitrogen. Then dry toluene (20 mL) was injected via syringe to give an brownish-tan mixture. The reaction was refluxed for 3 d, affording a dark brown supernatant with a small amount of precipitate. The mixture was concentrated by rotary evaporation and chromatographed on an alumina column (3 cm × 15 cm, packed with hexanes, eluted with $CH_2Cl_2$/hexanes 0:1 to 3:7 v/v). The mixture showed a strong new TLC spot that fluoresced yellow against a handheld UV lamp. However, this was not found again in any of the fractions from the column. Most of the **$PtC_8Pt$** (0.2528 g, 0.1241 mmol, 88%) was recovered.

**Attempted [2+2+2] cycloaddition of $PtC_4H$.** A solution of [CpCo(CO)(dimethyl fumarate)] (0.0053 g, 0.018 mmol), **$PtC_4H$** (0.1507 g, 0.1479 mmol), and toluene (10 mL) was refluxed for 6 h, both in the dark and under ambient lighting. The mixture was concentrated under reduced pressure and the residue was chromatographed on an alumina column (3 cm × 15 cm, packed with hexanes, eluted with $CH_2Cl_2$/hexanes 0:1 to 3:7 v/v). Most of the **$PtC_4H$** (0.1236 g, 0.1213 mmol, 82%) was recovered.

**Attempted [2+2+2] cycloaddition of $TESC_8TES$.** A solution of [CpCo(CO)(dimethyl fumarate)] (0.0088 g, 0.030 mmol), **$TESC_8TES$** (0.2007 g, 0.6156 mmol), and toluene (10 mL) was refluxed overnight in the dark. A light yellow TLC band was found as shown in Figure 4.13. The mixture was concentrated under reduced pressure and the residue was chromatographed on an alumina column (3 cm × 15 cm,

packed with hexanes, eluted with $CH_2Cl_2$/hexanes 0:1 to 3:7 v/v). However, the TLC band was not found in any of the fractions from the column.

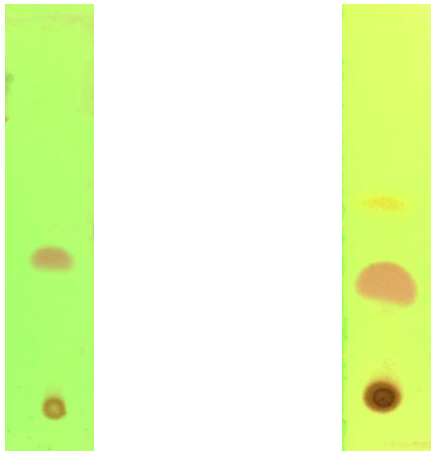

Before reaction; After reaction.

**Figure 4.13**. TLC data.

**Attempted [2+2+2] cycloaddition of $PtC_6Pt$.** A solution of [CpCo(CO)(dimethyl fumarate)] (0.0038 g, 0.013 mmol), **$PtC_6Pt$** (0.2177 g, 0.1082 mmol), and toluene (30 mL) was refluxed for 6 h both in the dark and under ambient lighting. The mixture was concentrated under reduced pressure and the residue was chromatographed on an alumina column (3 cm × 15 cm, packed with hexanes, eluted with $CH_2Cl_2$/hexanes 0:1 to 3:7 v/v). Most of the **$PtC_6Pt$** (0.1611 g, 0.080 mmol, 74%) was recovered.

**Attempted [2+2+2] cycloaddition of $PtC_8Pt$.** A solution of [CpCo(CO)(dimethyl fumarate)] (0.0048 g, 0.016 mmol), **$PtC_8Pt$** (0.2471 g, 0.1213 mmol), and toluene (30 mL) was refluxed for 6 h both in the dark and under ambient lighting. The mixture was concentrated under reduced pressure and the residue was chromatographed on an alumina column (3 cm × 15 cm, packed with hexanes, eluted

with $CH_2Cl_2$/hexanes 0:1 to 3:7 v/v). Most of the **PtC$_8$Pt** (0.2026 g, 0.0995 mmol, 82%) was recovered.

### 4.6 Crystallography

A $CH_2Cl_2$/hexanes (1:3 v/v) solution of the product from the attempted Diels-Alder cycloaddition of **PtC$_4$H** (method C) was kept in the dark. After 7 d, data were collected on a colorless thin plate per Table 4.2. Cell parameters were obtained from 180 data frames using a 0.5° scan and refined with 133166 reflections using the program Cell Now.[97] Integrated intensity information for each reflection was obtained by reduction of the data frames with APEX2.[36] Data were scaled, and absorption corrections were applied using the program SADABS.[37] The structure was solved by direct methods using XT/XS and refined (weighted least squares refinement on $F^2$).[38,39] Non-hydrogen atoms were refined with anisotropic thermal parameters. Hydrogen atoms were placed in idealized positions and were set riding on the parent atoms. PLATON was used to verify the absence of additional symmetry or voids.[40] Olex2 was employed for the final data presentation and structure plots.[39]

**Table 4.2.** Summary of crystallographic data

| Complex | **PtBr** |
|---|---|
| Empirical formula | $C_{48}H_{42}BrF_5P_2Pt$ |
| Formula weight | 1050.75 |
| Diffractometer | BRUKER GADDS |
| Temperature [K] | 110.15 |
| Wavelength [Å] | 1.54178 |
| Crystal system | Orthorhombic |
| Space group | P*bcn* |
| Unit cell dimensions | |
| *a* [Å] | 31.3544(13) |
| *b* [Å] | 12.2773(5) |
| *c* [Å] | 25.2388(10) |
| α [°] | 90 |
| β [°] | 90 |
| γ [°] | 90 |
| Volume [Å$^3$] | 9715.6(7) |
| Z | 8 |
| $\rho_{calcd}$ [mg/m$^3$] | 1.437 |
| Absorption coefficient [mm$^{-1}$] | 7.394 |
| F(000) | 4144 |
| Crystal size[mm$^3$] | 0.08 × 0.07 × 0.04 |
| Θ range of data collection [°] | 1.41 to 60.81 |
| Index ranges | $-35 \le h \le 35$,<br>$-13 \le k \le 13$,<br>$-28 \le l \le 28$ |
| Reflections collected | 133166 |
| Independent reflections | 7317 [R(int) = 0.0589] |
| Completeness to Θ | 83.0 % (67.679) |
| Max. and min. transmission | 0.7519 and 0.4638 |
| Data / restraints / parameters | 7317 / 0 / 520 |
| Goodness-of-fit on F$^2$ | 1.038 |
| Final R indices [I>2σ(I)] | |
| $R_1$ | 0.0276 |
| $wR_2$ | 0.0885 |
| R indices (all data) | |
| $R_1$ | 0.0342 |
| $wR_2$ | 0.0981 |
| Largest diff. peak and hole [e.Å$^{-3}$] | 0.575 and −1.595 |

# 5. SUMMARY AND CONCLUSIONS

## 5.1 Summary

Section 1 briefly introduces the concepts of atropisomerism and graphene. The work in this dissertation mainly sets out results of investigations to prepare inorganic atropisomers derived from square planar metal complexes.

Section 2 described the syntheses and structural characterizations of sterically congested diplatinum ethynediyl adducts, such as *trans*,*trans*-($C_6F_5$)(*p*-$tol_3$P)($Me_2$PhP)-Pt(C≡C)Pt(PPh$Me_2$)(P*p*-$tol_3$)($C_6F_5$), which feature two different phosphine ligands on each platinum endgroup. Interestingly, the square planes are nearly perpendicular in the crystal. The low temperature $^1$H NMR spectra were further studied in hope of observing separate signals for the $\underline{Me}_2$PhP groups which would indicate a diastereotopic relationship and provide strong evidence for the first atropisomers based upon cojoined square planar complexes. Although the conditions appear conducive to atropisomerism, apparently rotation about the PtC≡CPt linkage remains rapid on the NMR time scale.

Section 3 extended the chemistry of section 2 to include square planar diplatinum butadiynediyl complexes. The heterocoupling of platinum chloride and butadiynyl complexes (cat. CuI, $HNEt_2$) gives the target complexes, but with scrambling of the two unlike phosphine ligands on each precursor over all four positions (5-6 isomers). These are separated and structurally characterized, but low temperature NMR spectra do not reveal any dynamic processes.

The goal of section 4 was to investigate the reactivity of the C≡C of the platinum capped polyyne chains by various cycloaddition processes: (1) the feasibility of Diels-Alder functionalization of polyyne chains to achieve graphene-like structures; (2) the combination with attractive *o*-carboranes; (3) the intramolecular [2+2+2] cycloaddition (cyclotrimerization) catalyzed by [CpCo(CO)(dimethyl fumarate)].

**5.2 Conclusions**

The studies in this dissertation have carefully investigated the scope of atropisomerism based upon cojoined square planar complexes. In the present case, P*p*-$tol_3$ and $PPhMe_2$ are quite "similar" phosphines, with respective Tolman cone angles of 145° and 122° (Δ = 23°, from a range extending from 101 to 212°), and respective Tolman electronic parameters of 2066.7 and 2064.8 $cm^{-1}$ (Δ = 1.9 $cm^{-1}$, from a range extending from 2056 to 2110 $cm^{-1}$). Future studies could focus on more different and complementary phosphanes, like $P(OR)_3$, $PMe_2(NR_2)$, $P(NR_2)_3$ and $PMe_2(OR)$. The ligand scrambling might be facilitated by a relative electron deficiency of the Pt(II) centers brought about by the $C_6F_5$ ligands. Any way to disfavor ligand dissociation should prove beneficial, such as enhancing/tuning the electron donating character of the phosphine ligands, or enhancing their mutual affinity across the metal through push-pull electronic complementarity. For this purpose as well, more complementary phosphanes like $P(OR)_3$, $PMe_2(NR_2)$, $P(NR_2)_3$ and $PMe_2(OR)$, could be selected. Another way to solve the ligand scrambling could be addressed by using *trans*-chelating ligands with

optimal bridge length between the two phosphorus atoms or using dissymmetrical pincer ligands connecting the two phosphorus moieties to the Ar ligand at the *meta* positions. Finally, a more in depth study into shortening the metal-metal distance could be the next step. In this context, the replacement of Pt(II) by Ni(II) could be considered. The metal fragment might be changed to one that could accept a mono-atomic spacer, such as a carbon or $C_1$ ligand :C:. Here, the bonding might resemble that of an allene, which can also exhibit axial chirality.

## REFERENCES

(1) Bringmann, G.; Mortimer, A. J. P.; Keller, P. A.; Gresser, M. J.; Garner, J.; Breuning, B. *Angew. Chem., Int. Ed.* **2005**, *44*, 5384-5427; *Angew. Chem.* **2005**, *117*, 5518-5563.

(2) Ōki, M. *Top. Stereochem.* **1984**, *14*, 1-81.

(3) Fukuyama, Y.; Asakawa, Y. *J. Chem. Soc. Perkin Trans. 1* **1991**, 2737-2741.

(4) (a) Clayden, J.; Moran, W. J.; Edwards, P. J.; LaPlante, S. R. *Angew. Chem. Int. Ed.* **2009**, *48*, 6398-6401; *Angew. Chem.* **2009**, *121*, 6516-6520. (b) Joncour, A.; Décor, A.; Thoret, S.; Chiaroni, A.; Baudoin, O. *Angew. Chem. Int. Ed.* **2006**, *45*, 4149-4152; *Angew. Chem.* **2006**, *118*, 4255-4258.

(5) https://www.chem.wisc.edu/areas/reich/handouts/NMR-Spectra/NMR-1,1-dibromo-2,2-bis(chloromethyl)cyclopropane.pdf.

(6) Li, Z.; Chen, L.; Meng, S.; Guo, L.; Huang, J.; Liu, Y.; Wang, W.; Chen, X. *Phys. Rev. B* **2015**, *91*, 094429.

(7) Denis, P. A.; Iribarne, F. *J. Phys. Chem. C* **2013**, *117*, 19048-19055.

(8) Yamada, Y.; Murota, K.; Fujita, R.; Kim, J.; Watanabe, A.; Nakamura, M.; Sato, S.; Hata, K.; Ercius, P.; Ciston, J.; Song, C. Y.; Kim, K.; Regan, W.; Gannett, W.; Zettl, A. *J. Am. Chem. Soc.* **2014**, *136*, 2232-2235.

(9) Eftekhari, A.; Jafarkhani, P. *J. Phys. Chem. C* **2013**, *117*, 25845-25851.

(10) Yamada, Y.; Yasuda, H.; Murota, K.; Nakamura, M.; Sodesawa, T.; Sato, S. *J. Mater. Sci.* **2013**, *48*, 8171-8198.

(11) Yamada, Y.; Kim, J.; Matsuo, S.; Sato, S. *Carbon* **2014**, *70*, 59-74.

(12) Eliel, E. L.; Wilen, S. H. *Stereochemistry of Organic Compounds*; John Wiley & Sons: New York, 1994; Chapter 14.

(13) (a) Hu, N.-X.; Xie, S.; Popovic, Z.; Ong, B.; Hor, A.-M. *J. Am. Chem. Soc.* **1999**, *121*, 5097-5098. (b) Lloyd-Williams, P.; Giralt, E. *Chem. Soc. Rev.* **2001**, *30*, 145-157. (b) Burns, N. Z.; Krylova, I. N.; Hannoush, R. N.; Baran, P. S. *J. Am. Chem. Soc.* **2009**, *131*, 9172-9173.

(14) (a) McCarthy, M.; Guiry, P. J. *Tetrahedron* **2001**, *57*, 3809-3844. (b) Tang, W.; Zhang, X. *Chem. Rev.* **2003**, *103*, 3029-3069. (c) Walsh, P. J.; Lurain, A. E.; Balsells, J. *Chem. Rev.* **2003**, *103*, 3297-3344. (d) Guan, Y.; Ding, Z.; Wulff, W. D. *Chem. Eur. J.* **2013**, *19*, 15565-15571 and earlier work cited therein.

(15) (a) Bringmann, G.; Gulder, T.; Gulder, T. A. M.; Breuning, M. *Chem. Rev.* **2011**, *111*, 563-639. (b) Zask, A.; Murphy, J.; Ellestad, G. A. *Chirality* **2013**, *25*, 265-274. (c) Smyth, J. E.; Butler, N. M.; Keller, P. A. *Nat. Prod. Rep.* **2015**, *32*, 1562-1583. (d) Smith, D. E.; Marquez, I.; Lokensgard, M. E.; Rheingold, A. L.; Hecht, D. A.; Gustafson, J. L. *Angew. Chem., Int. Ed.* **2015**, *54*, 11754-11759; *Angew. Chem.* **2015**, *127*, 11920-11925.

(16) Kumarasamy, E.; Raghunathan, R.; Sibi, M. P.; Sivaguru, J. *Chem. Rev.* **2015**, *115*, 11239-11300.

(17) (a) Andrew, R. E.; Ferdani, D. W.; Ohlin, C. A.; Chaplin, A. B. *Organometallics* **2015**, *34*, 913-917. (b) Williams, K. M.; Cerasino, L.; Intini, F. P.;

Natile, G.; Marzilli, L. G. *Inorg. Chem.* **1998**, *37*, 5260-5268. (c) Albéniz, A. C.; Casado, A. L.; Espinet, P. *Organometallics* **1997**, *16*, 5416-5423.

(18) (a) Fraser, R. R.; Champagne, P. J. *Can. J. Chem.* **1976**, *54*, 3809-3811. (b) Whiteker, G. T.; Harrison, A. M.; Abatjoglou, A. G. *J. Chem. Soc.*, *Chem. Commun.* **1995**, *17*, 1805-1806. (c) Coleman, R. S.; Gurrala, S. R. *Org. Lett.* **2004**, *6*, 4025-4028. (d) Bott, G.; Field, L. D.; Sternhell, S. *J. Am. Chem. Soc.* **1980**, *102*, 5618-5626.

(19) (a) Hartwig, J. F. *Organotransition Metal Chemistry – From Bonding to Catalysis*; University Science Books: Mill Valley, California, 2009; Chapter 5.3.1. (b) Crabtree, R. H. *The Organometallic Chemistry of the Transition Metals*, Wiley Interscience: Hoboken, 2005; Chapters 6-9. (c) Birch, A. J.; Williamson, D. H. *Organic Reactions*; John Wiley & Sons: New York, 1976; Chapter 1 (see pp 7-40).

(20) Mohr, W.; Stahl, J.; Hampel, F.; Gladysz, J. A. *Chem. Eur. J.* **2003**, *9*, 3324-3340.

(21) (a) Bohling, J. C.; Peters, T. B.; Arif, A. M.; Hampel, F.; Gladysz, J. A., in *Coordination Chemistry at the Turn of the Century*; Ondrejovič, G.; Sirota, A. Eds.; Slovak Technical University Press: Bratislava, Slovakia, 1999; pp 47-52. (b) Stahl, J.; Bohling, J. C.; Peters, T. B.; de Quadras, L.; Gladysz, J. A. *Pure Appl. Chem.* **2008**, *80*, 459-474.

(22) Due to the variable quality of laboratory CuI (older samples are commonly discolored), higher loadings (20-50 mol%) are often used to ensure successful coupling reactions.

(23) Zheng, Q.; Bohling, J. C.; Peters, T. B.; Frisch, A. C.; Hampel, F.; Gladysz, J. A. *Chem. Eur. J.* **2006**, *12*, 6486-6505.

(24) Siegel, J. S.; Anet, F. A. L. *J. Org. Chem.* **1988**, *53*, 2629-2630.

(25) (a) Ramsden, J. A.; Weng, W.; Gladysz, J. A. *Organometallics* **1992**, *11*, 3635-3645. (b) Kawata, Y.; Sato, M. *Organometallics* **1997**, *16*, 1093-1096. (c) Dahlenburg, L.; Weiß, A.; Bock, M.; Zahl, A. *J. Organomet. Chem.* **1997**, *541*, 465-471.

(26) (a) Weng, W.; Ramsden, J. A.; Arif, A. M.; Gladysz, J. A. *J. Am. Chem. Soc.* **1993**, *115*, 3824-3825. (b) Weng, W.; Arif, A. M.; Gladysz, J. A. *Angew. Chem., Int. Ed. Engl.* **1993**, *32*, 891-892; *Angew. Chem.* **1993**, *105*, 937-939. (c) Falloon, S. B.; Weng, W.; Arif, A. M.; Gladysz, J. A. *Organometallics* **1997**, *16*, 2008-2015. (d) Bartik, T.; Weng, W.; Ramsden, J. A.; Szafert, S.; Falloon S. B.; Arif, A. M.; Gladysz, J. A. *J. Am. Chem. Soc.* **1998**, *120*, 11071-11081.

(27) (a) Ramsden, J. A.; Weng, W.; Arif, A. M.; Gladysz, J. A. *J. Am. Chem. Soc.* **1992**, *114*, 5890-5891. (b) Weng, W.; Bartik, T.; Brady, M.; Bartik, B.; Ramsden, J. A.; Arif, A. M.; Gladysz, J. A. *J. Am. Chem. Soc.* **1995**, *117*, 11922-11931.

(28) Dey, S.; Zhang, T.; Bhuvanesh, N.; Gladysz, J. A. manuscript in preparation.

(29) Trogler, W. C. *Int. J. Chem. Kinet.* **1987**, *19*, 1025-1047.

(30) Sünkel, K.; Birk, U.; Robl, C. *Organometallics* **1994**, *13*, 1679-1687.

(31) Ogawa, H.; Onitsuka, K.; Joh, T.; Takahashi, S. *Organometallics* **1988**, *7*, 2257-2260.

(32) With respect to gearing, a reviewer has noted that rotation about the platinum-phosphorus and phosphorus-$C_{ipso}$ bonds in **4** and **5** is rapid on the NMR time scale.

(33) Two phosphine ligands in **4**, *p*-$tol_3P$ and $Me_2PhP$, have rather similar Tolman cone angles (145° and 122°, or $\Delta$ = 23° of a range from 101° to 212°) and Tolman electronic parameters (2066.7 $cm^{-1}$ and 2064.8 $cm^{-1}$ or $\Delta$ = 2 $cm^{-1}$ of a range from 2056 $cm^{-1}$ to 2110 $cm^{-1}$). See Tolman, C. A. *Chem. Rev.* **1977**, *77*, 315.

(34) This coupling represents a satellite (d, $^{195}Pt$ = 33.8%) as is not reflected in the peak multiplicity given.

(35) Due to insufficient signal/noise, the $C_6F_5$ $^{13}C$ NMR signals "*o*/*m* to Pt" could not be observed, and the $J_{CP}$ values for most PhP resonances are not as accurate as other $J_{CP}$ values.

(36) APEX2, Program for Data Collection on Area Detectors, BRUKER AXS Inc., 5465 East Cheryl Parkway, Madison, WI 53711-5373 USA.

(37) Sheldrick, G. M.; SADABS, version 2008/1. Program for Absorption Correction for Data from Area Detector Frames, University of Göttingen, Germany, **2008**.

(38) SHELXTL, Sheldrick, G. M. Acta Cryst. **2008**, *A64*, 112-122.

(39) Dolomanov, O. V.; Bourhis, L. J., Gildea, R. J.; Howard, J. A. K.; Puschmann, H. *J. Appl. Cryst.* **2009***, 42*, 339-341.

(40) Spek, A. L. *J. Appl. Cryst.* **2003**, *36,* 7-13.

(41) (a) Klein, A.; Klinkhammer, K.-W.; Scheiring, T. *J. Organomet. Chem.* **1999**, *578*, 128-135. (b) Müller, C.; Lachicotte, R. J.; Jones, W. D. *Organometallics* **2002**, *21,* 1190-1196. (c) Yam, V. W.-W.; Wong, K. M.-C.; Zhu, N. *Angew. Chem., Int. Ed.* **2003**, *42*, 1400-1403; *Angew. Chem.* **2003**, *115*, 1438-1441.

(42) (a) Owen, G. R.; Stahl, J.; Hampel, F.; Gladysz, J. A. *Chem. Eur. J.* **2008**, *14*, 73-87. (b) de Quadras, L.; Shelton, A. H.; Kuhn, H.; Hampel, F.; Schanze, K. S.; Gladysz, J. A. *Organometallics* **2008**, *27*, 4979-4991. (c) Owen, G. R.; Gauthier, S.; Weisbach, N.; Hampel, F.; Bhuvanesh, N.; Gladysz, J. A. *Dalton Trans.* **2010**, 5260-5271.

(43) Computational studies: (a) Zhuravlev, F.; Gladysz, J. A. *Chem. Eur. J.* **2004**, *10*, 6510-6522. (b) Samoc, M.; Humphrey, M. G.; Dalton, G. T.; Gladysz, J. A.; Zheng, Q.; Yelkov, Y.; Ågren, H.; Norman, P. *Inorg. Chem.* **2008**, *47*, 9946-9957.

(44) Takahashi, S.; Murata, E.; Sonogashira, K.; Hagihara, N. *J. Polym. Sci. Polym. Chem. Ed.* **1980**, *18*, 661-669.

(45) (a) Peters, T. B.; Bohling, J. C.; Arif, A. M.; Gladysz, J. A. *Organometallics* **1999**, *18*, 3261-3263. (b) Mohr, W.; Stahl, J.; Hampel, F.; Gladysz, J. A. *Inorg. Chem.* **2001**, *40,* 3263-3264. (c) Stahl, J.; Bohling, J. C.; Bauer, E. B.; Peters, T. B.; Mohr, W.; Martín-Alvarez, J. M.; Hampel, F.; Gladysz, J. A. *Angew. Chem., Int. Ed.* **2002**, *41*, 1871-1876; *Angew. Chem.* **2002**, *114*, 1951-1957. (d) Zheng, Q.; Hampel, F.; Gladysz, J. A. *Organometallics* **2004**, *23*, 5896-5899. (e) Owen, G. R.; Stahl, J.; Hampel, F.; Gladysz, J. A. *Organometallics* **2004**, *23*, 5889-5892. (f) Zheng, Q.; Gladysz, J. A. *J. Am. Chem. Soc.* **2005**, *127*, 10508-10509. (g) de Quadras, L.; Hampel, F.; Gladysz, J. A. *Dalton Transactions* **2006**, 2929-2933. (h) de Quadras, L.; Stahl, J.; Zhuravlev, F.;

Gladysz, J. A. *J. Organomet. Chem.* **2007**, *692*, 1859-1870. (i) de Quadras, L.; Bauer, E. B.; Stahl, J.; Zhuravlev, F.; Hampel, F.; Gladysz, J. A. *New. J. Chem.* **2007**, *31*, 1594-1604. (j) Stahl, J.; Mohr, W.; de Quadras, L.; Peters, T. B.; Bohling, J. C.; Martín-Alvarez, J. M.; Owen, G. R.; Hampel, F.; Gladysz, J. A. *J. Am. Chem. Soc.* **2007**, *129*, 8282-8295. (k) de Quadras, L.; Bauer, E. B.; Mohr, W.; Bohling, J. C.; Peters, T. B.; Martín-Alvarez, J. M.; Hampel, F.; Gladysz, J. A. *J. Am. Chem. Soc.* **2007**, *129*, 8296-8309. (l) Farley, R.; Zheng, Q.; Gladysz, J. A.; Schanze, K. S. *Inorg. Chem.* **2008**, *47*, 2955-2963. (m) Ballmann, S.; Hieringer, W.; Secker, D.; Zheng, Q.; Gladysz, J. A.; Görling, A.; Weber, H. B. *ChemPhysChem* **2010**, *11*, 2256-2260. (n) Weisbach, N.; Baranová, Z.; Gauthier, S.; Reibenspies, J. H.; Gladysz, J. A. *Chem. Commun*. **2012**, *48*, 7562-7564. (o) Sahnoune, H.; Baranová, Z.; Bhuvanesh, N.; Gladysz, J. A.; Halet, J.-F. *Organometallics*, **2013**, *32*, 6360-6367. (p) Baranová, Z.; Amini, H.; Bhuvanesh, N.; Gladysz, J. A. *Organometallics* **2014**, *33*, 6746-6749. (q) Li, Y.; Winkel, R. W.; Weisbach, N.; Gladysz, J. A.; Schanze, K. S. *J. Phys. Chem. A*. **2014**, *115*, 10333-10339.

(46) (a) Szafert, S.; Gladysz, J. A. *Chem. Rev.* **2003**, *103*, 4175-4205. (b) Szafert, S.; Gladysz, J. A. *Chem. Rev.* **2006**, 106, PR1–PR33.

(47) For other metal polyynediyl complexes that exhibit more stable radical cations at shorter sp chain lengths, see (a) Brady, M.; Weng, W.; Zhou, Y.; Seyler, J. W.; Amoroso, A. J.; Arif, A. M.; Böhme, M.; Frenking, G.; Gladysz, J. A. *J. Am. Chem. Soc.* **1997**, *119*, 775-788. (b) Meyer, W. E.; Amoroso, A. J.; Horn, C. R.; Jaeger, M.; Gladysz, J. A. *Organometallics* **2001**, *20*, 1115-1127.

(48) Zhang, T.; Bhuvanesh, N.; Gladysz, J. A. *Eur. J. Inorg. Chem.* **2017**, *2017*, in press. DOI: 10.1002/ejic.201601307.

(49) (a) Ogawa, H.; Joh, T.; Takahashi, S.; Sonogashira, K. *J. Chem. Soc., Chem. Commun.* **1985**, 1220-1221. (b) Berenguer, J. R.; Forniés, J.; Lalinde, E.; Martínez, F. *Organometallics* **1995**, *14*, 2532-2537. (c) Griffith, C. S.; Koutsantonis, G. A. *Aust. J. Chem.* **2012**, *65*, 698-722.

(50) Throughout this dissertation, the descriptor *trans* refers to the orientation of the two phosphine ligands at platinum.

(51) Cheney A. J.; Mann, B. E.; Shaw, B. L.; Salde, R. M. *J. Chem. Soc. A* **1971**, 3833-3842.

(52) Grim, S. O.; Keiter, R. L.; McFarlane, W. *Inorg. Chem*. **1967**, *6*, 1133-1137.

(53) DiMeglio, C. M.; Luck, L. A.; Rithner, C. D.; Rheingold, A. L.; Elcesser, W. L.; Hubbard, J. L.; Bushweller, C. H. *J. Phys. Chem*. **1990**, *94*, 6255-6263.

(54) Usón, R.; Forniés, J.; Martinez, F.; Tomás, M. *J. Chem. Soc., Dalton Trans.* **1980**, 888-894.

(55) (a) Deacon, G. B.; Nelson-Reed, K. T. *J. Organomet. Chem*. **1987**, *322*, 257-268. (b) Better results were obtained when this compound was synthesized by a procedure previously applied to *p*-tol or *p*-$C_6H_4OMe$ analogs: Shekhar, S.; Hartwig, J. F. *J. Am. Chem. Soc.* **2004**, *126*, 13016-13027.

(56) Dey, S. final research report, Texas A&M University, 2011.

(57) The ligands *p*-$tol_3P$, $(p\text{-}t\text{-}BuC_6H_4)_2PhP$, and $(p\text{-}MeOC_6H_4)_2PhP$ would be expected to have similar steric and electronic properties. One manifestation of the latter is

the close correspondence of the average of the values for the three *para* substituents (–0.14, –0.10, –0.19, respectively; data from Smith, M. B.; March, J. *March's Advanced Organic Chemistry*; John Wiley & Sons: New York, 2007; Table 9.4).

(58) Hersh, W. H. *J. Chem. Educ.* **1997**, *74*, 1485-1488.

(59) (a) Ponzini, F.; Zagha, R.; Hardcastle, K.; Siegel, J. S. *Angew. Chem. Int. Ed.* **2000**, *39*, 2323-2325; *Angew. Chem.* **2000**, *112*, 2413-2415. (b) Blanchard, M. D.; Hughes, R. P. Concolino, T. E.; Rheingold, A. L. *Chem. Mater.* **2000**, *12*, 1604-1610. (c) Adams, H.; Jimenez Blanco, J.-L.; Chessari, G.; Hunter, C. A.; Low, C. M. R.; Sanderson, J. M.; Vinter, J. G. *Chem. Eur. J.* **2001**, *7*, 3494-3503. (d) Gung, B. W.; Amicangelo, J. C. *J. Org. Chem.* **2006**, *71*, 9261-9270.

(60) (a) Ramsden, J. A.; Weng, W.; Arif, A. M.; Gladysz, J. A. *J. Am. Chem. Soc.* **1992**, *114*, 5890-5891. (b) Weng, W.; Bartik, T.; Brady, M.; Bartik, B.; Ramsden, J. A.; Arif, A. M.; Gladysz, J. A. *J. Am. Chem. Soc.* **1995**, *117*, 11922-11931.

(61) (a) Albéniz, A. C.; Casado, A. L.; Espinet, P. *Organometallics* **1997**, *16*, 5416-5423. (b) Zanini, M. L.; Meneghetti, M. R.; Ebeling, G.; Livotto, P. R.; Rominger, F.; Dupont, J. *Inorg. Chim. Acta* **2003**, *350*, 527-536. (c) Andrew, R. E.; Ferdani, D. W.; Ohlin, C. A.; Chaplin, A. B. *Organometallics* **2015**, *34*, 913-917.

(62) Eaborn, C.; Odell, K. J.; Pidcock, A. *J. Chem. Soc., Dalton Trans.* **1978**, *4*, 357-368.

(63) Caron, L.; Canipelle, M.; Tilloy, S.; Bricout, H.; Monflier, E. *Tetrahedron Lett.* **2001**, *42*, 8837-8840.

(64) Verkruijsse, H. D.; Brandsma, L. *Synth. Commun.* **1991**, *21*, 657-659.

(65) This coupling represents a satellite (d, $^{195}Pt$ = 33.8%) as is not reflected in the peak multiplicity given.

(66) There are many non-first-order couplings evident in the NMR spectra, especially with complexes with different triarylphosphine ligands on the same platinum, as further discussed in the text. In some cases, virtual triplets are observed, and in other cases doublet of doublets with nearly the same *J* values as the triplets. In both cases, the *J* values represent the apparent couplings between adjacent peaks and not the mathematically rigorously coupling constants.[21]

(67) (a) The phosphorus and sulfur donor ligands in **1** are *cis*. (b) tht = tetrahydrothiophene.

(68) One or more of the arene signals *ipso* to phosphorus (P) or platinum (Pt) were not observed.

(69) This spectrum was recorded using single crystals grown from acetone/diethyl ether/$CH_2Cl_2$/hexane. Signals (δ) for acetone (207.2, 31.1), diethyl ether (66.0, 15.5), and $CH_2Cl_2$ (53.7) were apparent.

(70) The signal intensities are similar and do not allow an unambiguous assignment (theory, 2:1:1).

(71) Although the NMR spectra of **PtC$_4$Pt"-b** exhibits some unusual non-first order features, the structural assignment is unequivocal, as evidenced by the mass spectrum and crystallographic data (Figure 3.8).

(72) SAINT (Version 7). "Program for Data Integration from Area Detector Frames", Bruker–Nonius Inc., 5465 East Cheryl Parkway, Madison, WI 53711-5373 USA.

(73) Paul, F.; Lapinte, C. in *Unusual Structures and Physical Properties in Organometallic Chemistry* (Eds.: Gielen, M.; Willem, R.; Wrackmeyer, B.), Wiley, New York, **2002**, 220-291.

(74) (a) Trinh, C.; Kirlikovali, K. O.; Bartynski, A. N.; Tassone, C. J.; Toney, M. F.; Burkhard, G. F.; McGehee, M. D.; Djurovich, P. I.; Thompson, M. E. *J. Am. Chem. Soc.* **2013**, *135*, 11920-11928. (b) Cerón, M. R.; Izquierdo, M.; Aghabali, A.; Valdez, J. A.; Ghiassi, K. B.; Olmstead, M. M.; Balch, A. L.; Wudl, F.; Echegoyen, L. *J. Am. Chem. Soc.* **2015**, *137*, 7502-7508. (c) Chan, B.; Kawashima, Y.; Katouda, M.; Nakajima, T.; Hirao, K. *J. Am. Chem. Soc.* **2016**, *138,* 1420-1429.

(75) (a) Bruce, M. I. *Coord. Chem. Rev.* **1997**, *166*, 91-119. (b) Low, P. J.; Bruce, M. I. *Adv. Organomet. Chem.* **2001**, *48*, 71-288. (c) Paul, F.; Lapinte, C. *Unusual Structures and Physical Properties in Organometallic Chemistry* (Eds.: Gielen, M.; Willem, R.; Wrackmeyer, B.); John Wiley & Sons: New York, 2002; chap. 6.

(76) (a) Woodworth, B. E.; White, P. S.; Templeton, J. L.; Kenan, W. R. *J. Am. Chem. Soc.* **1997,** *119,* 828-829. (b) ALQaisi, S. M.; Galat, K. J.; Chai, M.; Ray, D. G.; Rinaldi, P. L.; Tessier, C. A.; Youngs, W. J. *J. Am. Chem. Soc.* **1998**, *120*, 12149-12150. (c) Bruce, M. I.; Low, P. J.; Costuas, K.; Halet, J.-F.; Best, S. P.; Heath, G. A. *J. Am. Chem. Soc.* **2000,** *122,* 1949-1962. (d) Che, C.-M.; Chao, H.-Y.; Miskowski, V. M.; Li, Y.; Cheung, K.-K. *J. Am. Chem. Soc.* **2001,** *123,* 4985-4991. (e) Zhao, L.; Mak, T. C. W.

*J. Am. Chem. Soc.* **2004**, *126*, 6852-6853. (f) Semenov, S. N.; Blacque, O.; Fox, T.; Venkatesan, K.; Berke, H. *J. Am. Chem. Soc.* **2010**, *132*, 3115-3127. (g) Semenov, S. N.; Taghipourian, S. F.; Blacque, O.; Fox, T.; Venkatesan, K.; Berke, H. *J. Am. Chem. Soc.* **2010**, *132*, 7584-7585.

(77) Cooper, D. R.; D'Anjou, B.; Ghattamaneni, N.; Harack, B.; Hilke, M.; Horth, A.; Majlis, N.; Massicotte, M.; Vandsburger, L.;Whiteway, E.; Yu, V. *ISRN Condens. Matter Phys.* ***2012****, 1-56.*

(78) Viculis, L. M.; Mack, J. J.; Mayer, O. M.; Hahn, H. T.; Kaner, R. B. *J. Mater. Chem.* **2005**, *15*, 974-978.

(79) (a) Cai, J.; Ruffieux, P.; Jaafar, R.; Bieri, M.; Braun, T.; Blankenburg, S.; Muoth, M.; Seitsonen, A. P.; Saleh, M.; Feng, X.; Müllen, K.; Fasel, R. *Nature* **2010**, *466*, 470-473. (b) Tang, L.; Li, X.; Ji, R.; Teng, K. S.; Tai, G.; Ye, J.; Wei, C.; Lau, S. P. *J. Mater. Chem.* **2012**, *22*, 5676-5683. (c) Tour, J. M. *Chem. Mater.* **2014**, *26*, 163-171. (d) Simonov, K. A.; Vinogradov, N. A.; Vinogradov, A. S.; Generalov, A. V.; Zagrebina, E. M.; Mårtensson, N.; Cafolla, A. A.; Carpy, T.; Cunniffe, J. P.; Preobrajenski, A. B. *J. Phys. Chem. C* **2014**, *118*, 12532-12540. (e) Schwab, M. G.; Narita, A.; Osella, S.; Hu, Y.; Maghsoumi, A.; Mavrinsky, A.; Pisula, W.; Castiglioni, C.; Tommasini, M.; Beljonne, D.; Feng, X.; Millen, K. *Chem. Asian J.* **2015**, *10*, 2134-2138. (f) Yang, W.; Lucotti, A.; Tommasini, M.; Chalifoux, W. A. *J. Am. Chem. Soc.* **2016**, *138*, 9137-9144.

(80) (a) Charlton, J. L.; Alauddin, M. M. *Tetrahedron* **1987**, *43*, 2873-2889. (b) Segura, J.; Martín, N. *Chem. Rev.* **1999**, *99*, 3199-3246.

(81) Owen, G. R.; Gauthier, S.; Weisbach, N.; Hampel, F.; Bhuvanesh, N.; Gladysz, J. A. *Dalton Trans.* **2010**, *39*, 5260-5271.

(82) (a) Tashbaev, G. A. *Russ. Chem. Bull., Int. Ed.* **2005**, *54*, 428-431. (b) Ostrowski, S.; Wyrębek, P. *Tetrahedron Lett.* **2006**, *47*, 8437-8440.

(83) (a) Hoey, M. D.; Dittmer, D. C. *J. Org. Chem.* **1991**, *56*, 1947-1948. (b) Meng, X.; Zhang, W.; Tan, Z.; Du, C.; Li, C.; Bo, Z.; Li, Y.; Yang, X.; Zhen, M.; Jiang, F.; Zheng, J.; Wang, T.; Jiang, L.; Shu, C.; Wang, C. *Chem. Commun.* **2012**, *48*, 425-427.

(84) Clough, M. C.; Fiedler, T.; Bhuvanesh, N.; Gladysz, J. A. *J. Organomet. Chem.* **2016**, *812*, 34-42.

(85) (a) Fox, M. A.; Howard, J. A. K.; MacBride, J. A. H.; Mackinnon, A.; Wade, K. *J. Organomet. Chem.* **2003**, *680*, 155-164. (b) Kokado, K.; Chujo, Y. *Macromolecules* **2009**, *42*, 1418-1420. (c) Kokado, K.; Tokoro, Y.; Chujo, Y. *Macromolecules* **2009**, *42*, 2925-2930. (d) Kaleta, J.; Janoušek, Z.; Nečas, M.; Mazal, C. *Organometallics* **2015**, *34*, 967-972.

(86) (a) Williams, R. E. *Chem. Rev.* **1992**, *92*, 177-207. (b) Lamrani, M.; Hamasaki, R.; Mitsuishi, M.; Miyashita, T.; Yamamoto, Y. *Chem. Commun.* **2000**, 1595-1595. (c) Hamasaki, R.; Ito, M.; Lamrani, M.; Mitsuishi, M.; Miyashita, T.; Yamamoto, Y. *J. Mater. Chem.* **2003**, *13*, 21-26. (d) Endo, Y.; Sawabe, T.; Taoda, Y. *J. Am. Chem. Soc.* **2000**, *122*, 180-181.

(87) Peterson, J. J.; Werre, M.; Simon, Y. C.; Coughlin, E. B.; Carter, K. R. *Macromolecules* **2009**, *42*, 8594-8598.

(88) (a) Agenet, N.; Gandon, V.; Buisine, O.; Slowinski, F.; Aubert, C.; Malacria, M. *Organic Reactions Vol. 68* (Ed.: RajanBabu, T. V.); John Wiley & Sons: Hoboken, 2007; pp. 1-302. (b) Heller, B.; Hapke, M. *Chem. Soc. Rev.* **2007**, *36*, 1085-1094.

(89) Geny, A.; Agenet, N.; Iannazzo, L.; Malacria, M.; Aubert, C.; Gandon, V. *Angew. Chem., Int. Ed.* **2009**, *48*, 1810-1813; *Angew. Chem.* **2009**, *121*, 1842-1845.

(90) Gauthier, S.; Weisbach, N.; Bhuvanesh, N; Gladysz, J. A *Organometallics* **2009**, *28*, 5597-5599.

(91) Eastmond, R.; Johnson, T. R.; Walton, D. R. M. *Tetrahedron* **1972**, *28*, 4601-4616.

(92) The *J* values represent the apparent couplings between adjacent peaks and not the mathematically rigorously coupling constants. Siegel, J. S.; Anet, F. A. L. *J. Org. Chem.* **1988**, *53*, 2629-2630.

(93) This coupling represents a satellite (d, $^{29}$Si = 4.67%), and is not reflected in the peak multiplicity given.

(94) MALDI (THAP matrix); m/z for the most intense peak of the isotope envelope; relative intensities are for the specified mass range.

(95) Han, B. H.; Boudjouk, P. *J. Org. Chem.* **1982**, *47*, 751-752.

(96) Kokado, K; Chujo, Y. *Dalton Trans.* **2011**, *40*, 1919-1923.

(97) Sheldrick, G. M. "Cell_Now (version 2008/1): Program for Obtaining Unit Cell Constants from Single Crystal Data": University of Göttingen, Germany.

# APPENDIX A

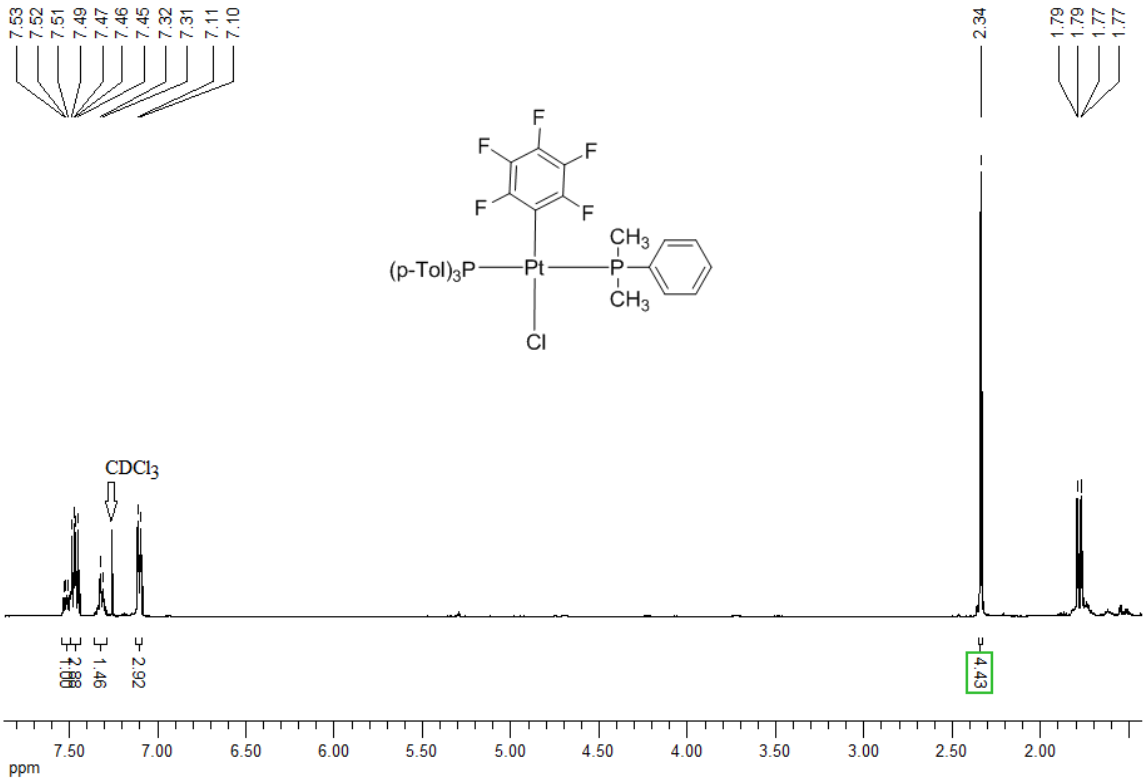


**Figure A-1.** $^{1}$H NMR spectrum of **2** (500 MHz, $CDCl_3$).

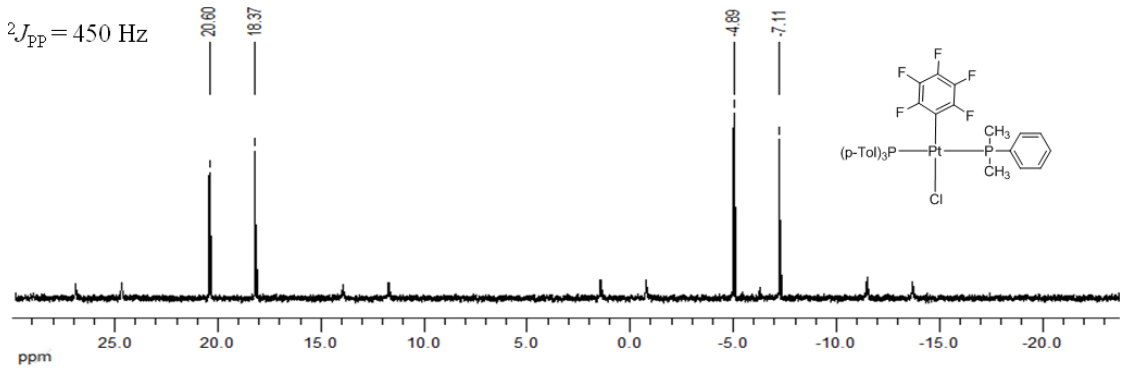


**Figure A-2.** $^{31}$P{$^{1}$H} NMR spectrum of **2** (202 MHz, $CDCl_3$).

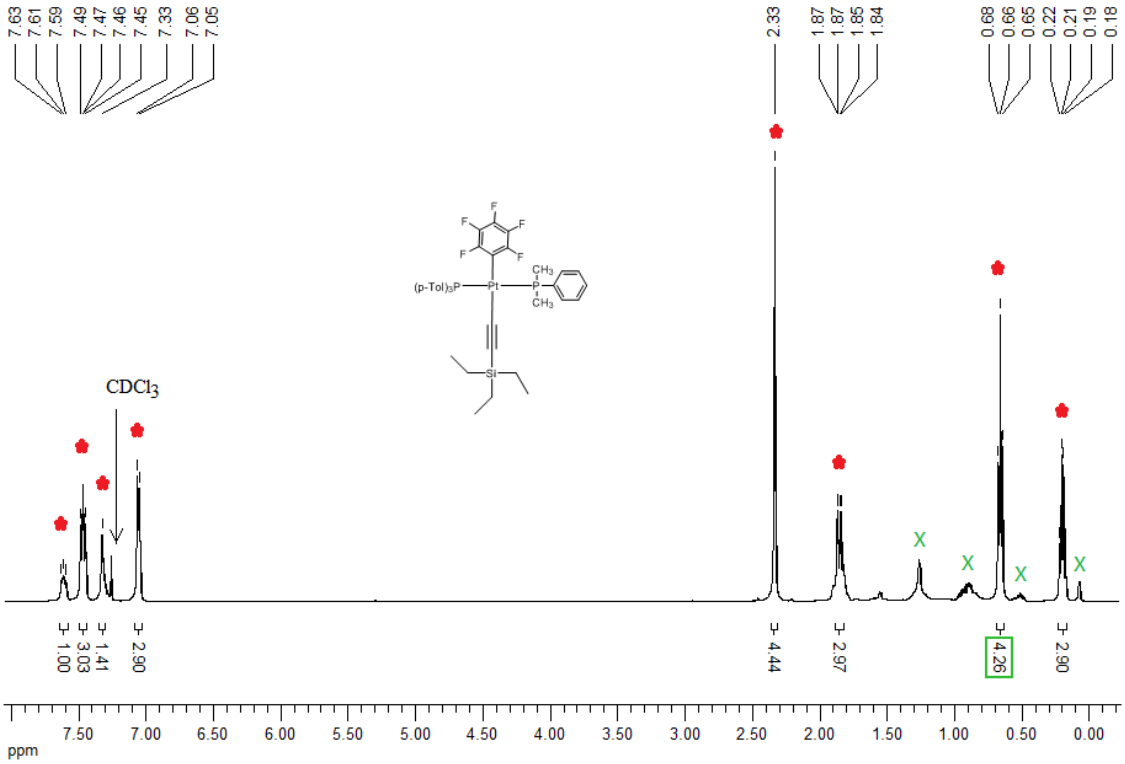


**Figure A-3.** $^{1}$H NMR spectrum of **3** (500 MHz, $CDCl_3$; × = impurity peak).

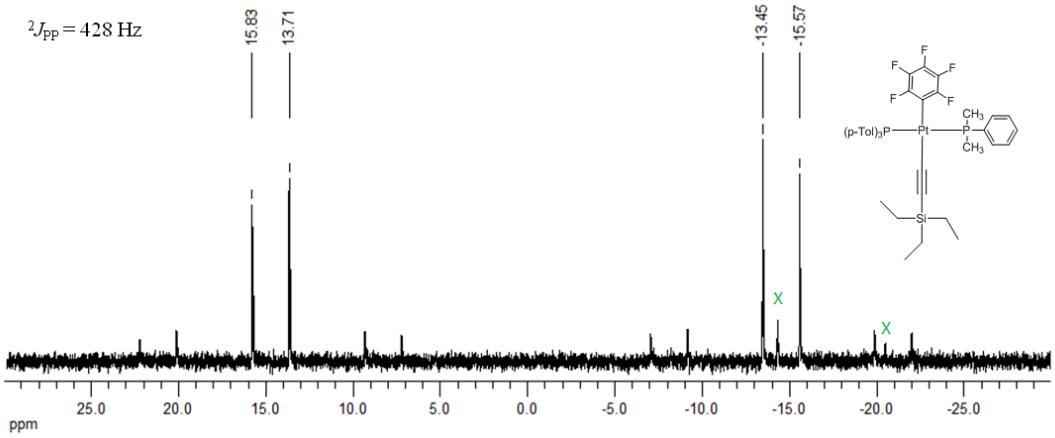


**Figure A-4.** $^{31}P\{^{1}H\}$ NMR spectrum of **3** (202 MHz, $CDCl_3$; × = impurity peak).

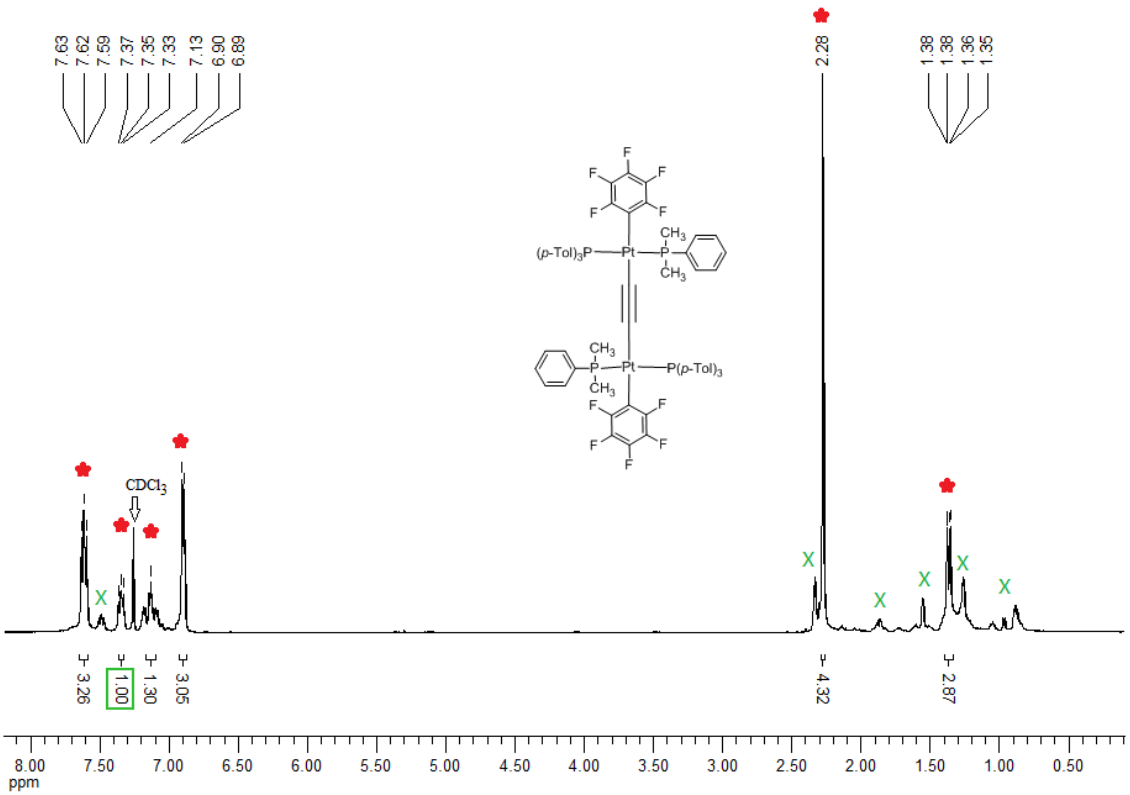


**Figure A-5.** $^{1}$H NMR spectrum of **4** (500 MHz, $CDCl_3$; × = impurity peak).

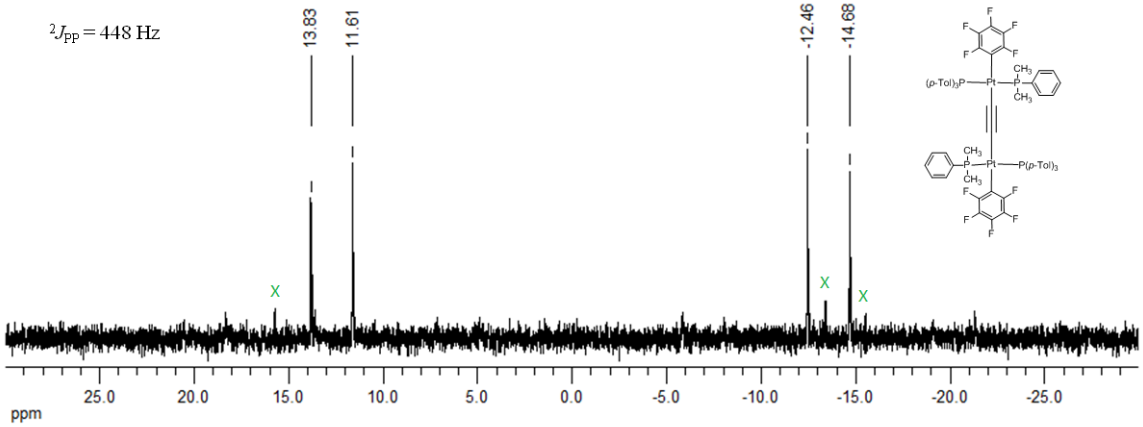


**Figure A-6.** $^{31}P\{^{1}H\}$ NMR spectrum of **4** (202 MHz, $CDCl_3$; × = impurity peak).

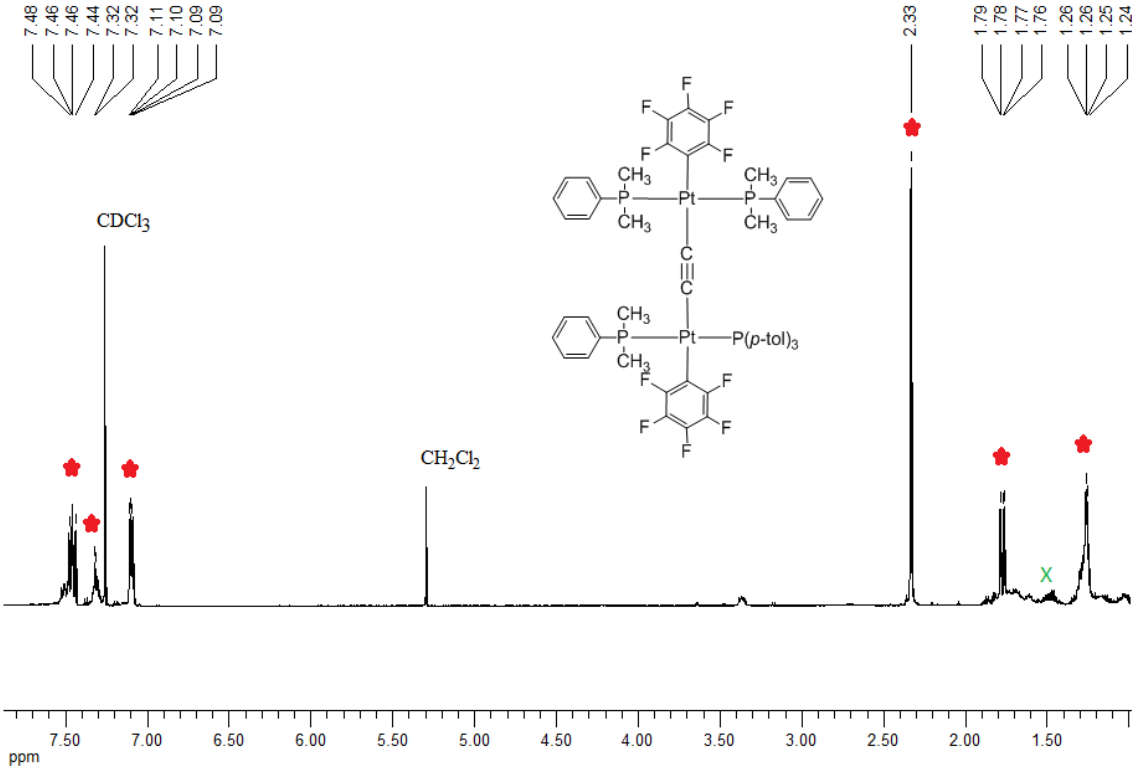


**Figure A-7.** $^{1}$H NMR spectrum of **5** (500 MHz, $CDCl_3$; × = impurity peak).

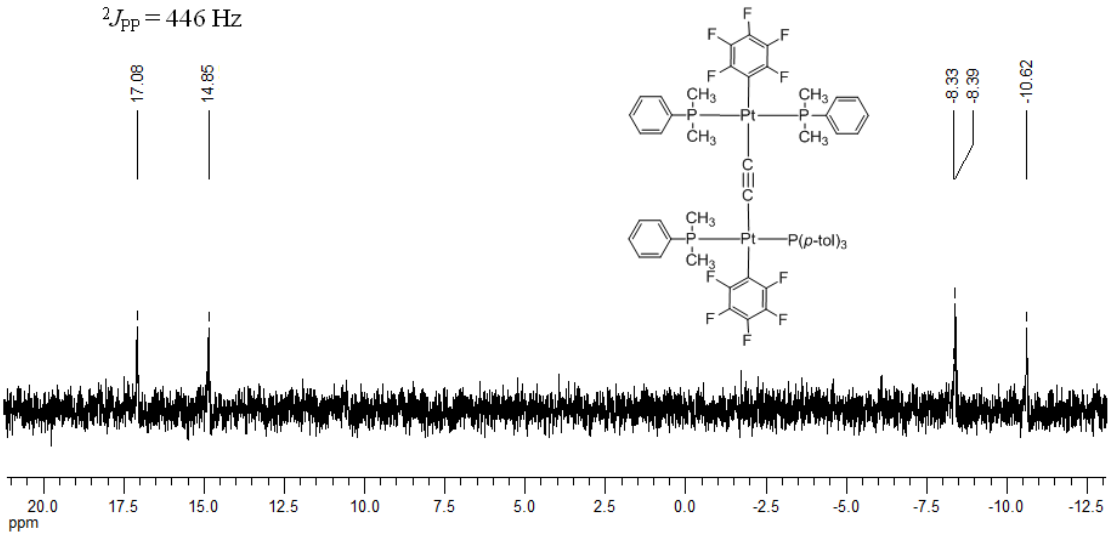


**Figure A-8.** $^{31}P\{^{1}H\}$ NMR spectrum of **5** (202 MHz, $CDCl_3$).

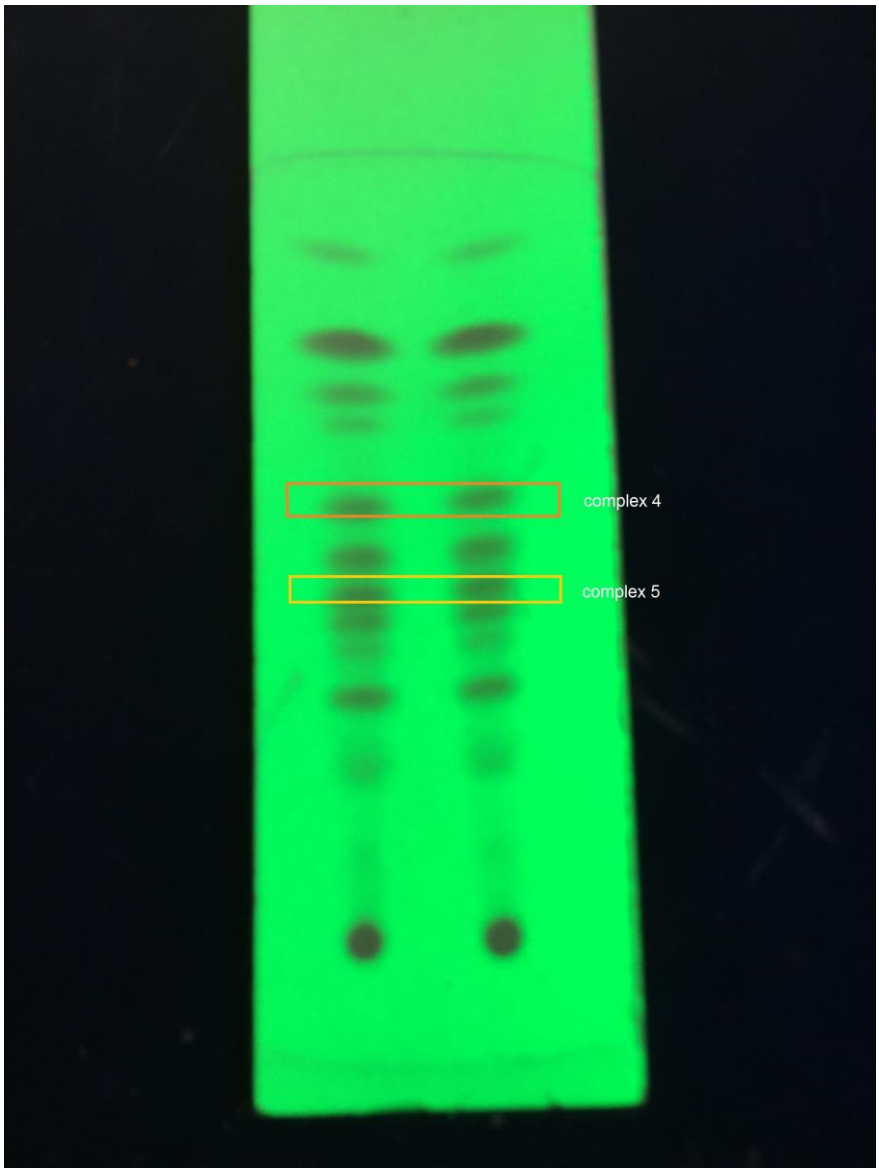


**Figure A-9.** TLC plate associated with the synthesis of **4** and **5** (experimental section).

# APPENDIX B

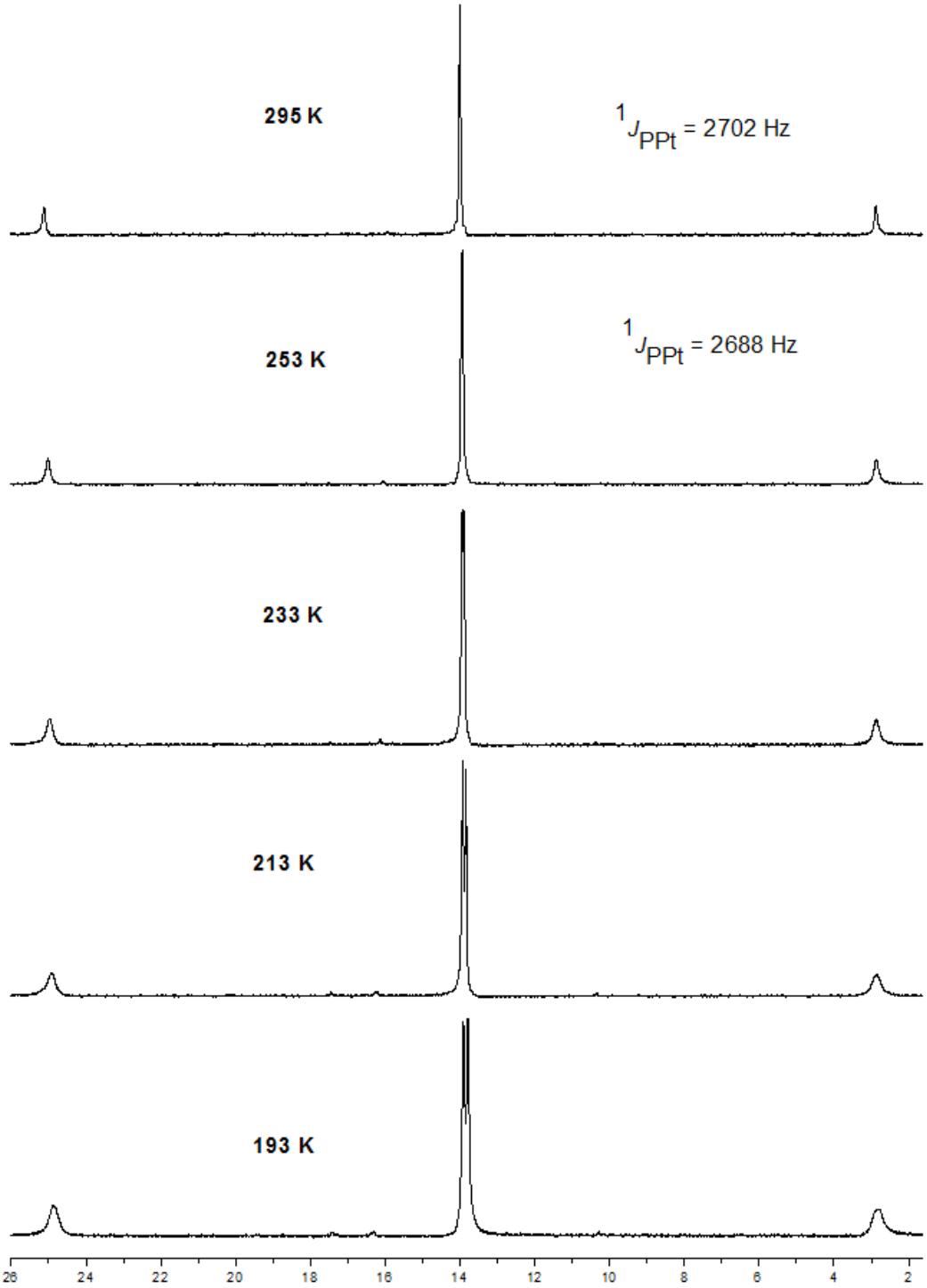


**Figure B-1.** Variable temperature $^{31}P\{^1H\}$ NMR spectra of **Pt'C$_4$Pt'-b** ($CD_2Cl_2$) showing the lifting of the chemical shift degeneracy of the *p*-tol$_3$P and (*p*-*t*-Bu$C_6H_4$)$_2$PhP ligands.

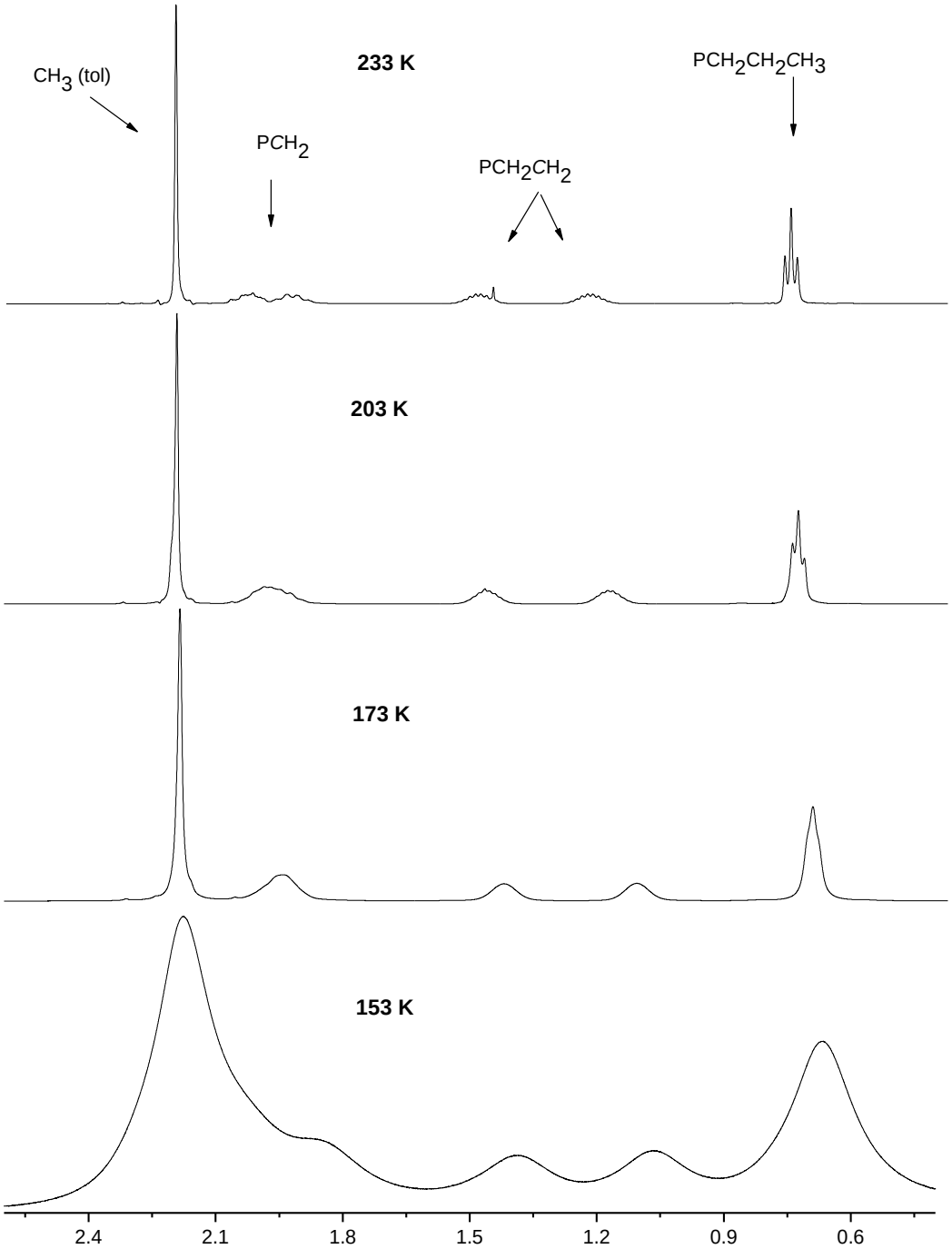


**Figure B-2.** Variable temperature $^{1}$H NMR spectra of **Pt'C$_4$Pt'-d** (partial, $CDFCl_2$).

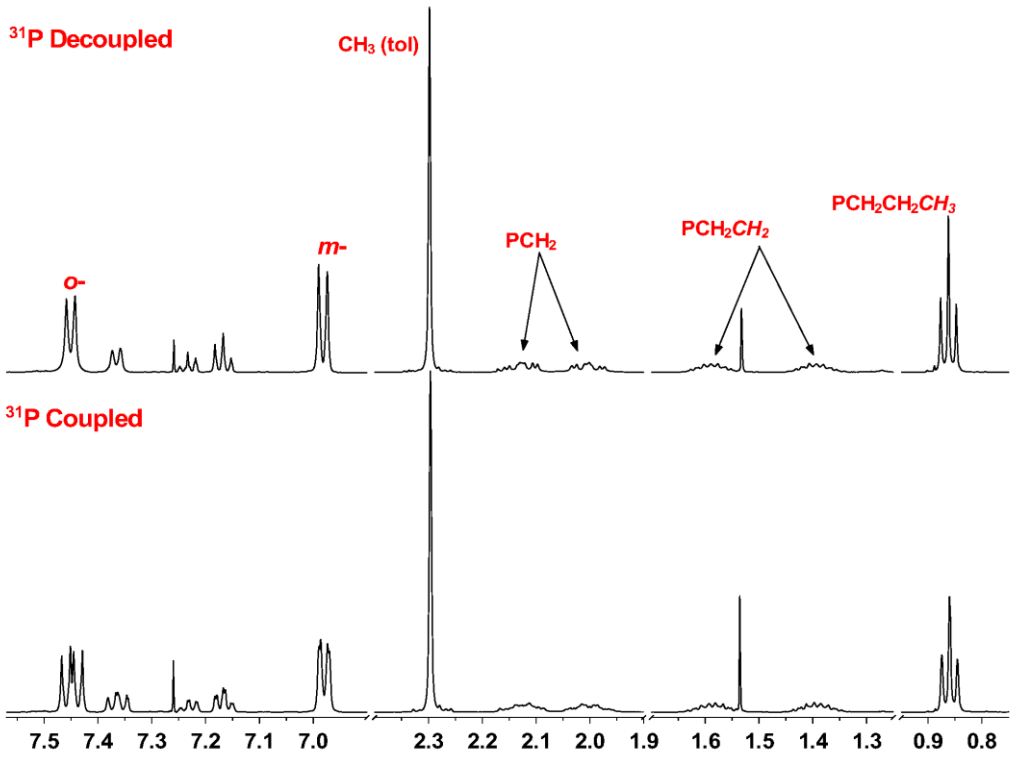


**Figure B-3.** $^{1}H\{^{31}P\}$ NMR (top) and $^{1}H$ NMR (bottom) spectra of **Pt'$C_4$Pt'-d** ($CDCl_3$).

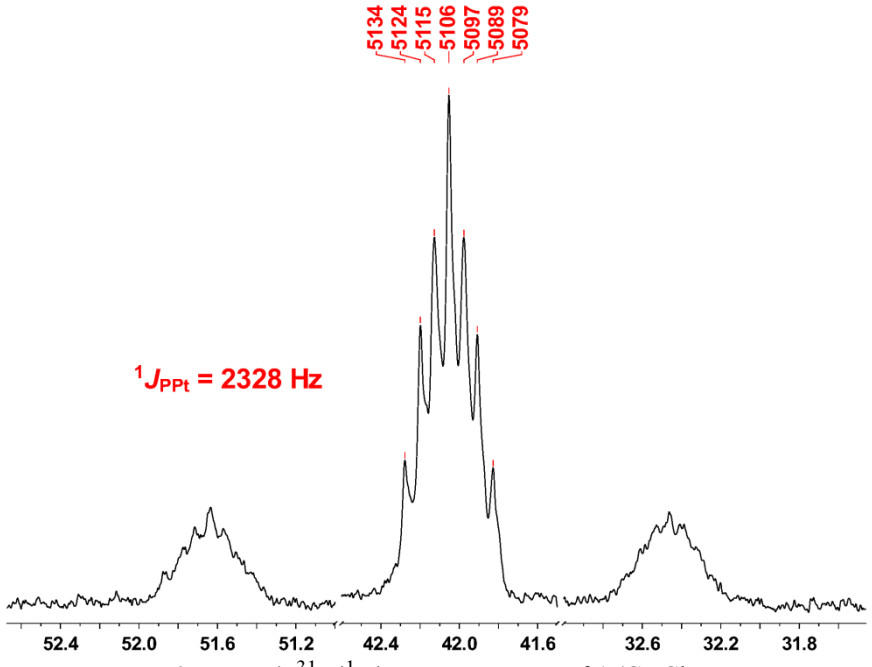


**Figure B-4.** $^{31}P\{^{1}H\}$ NMR spectrum of **1** ($CDCl_3$).

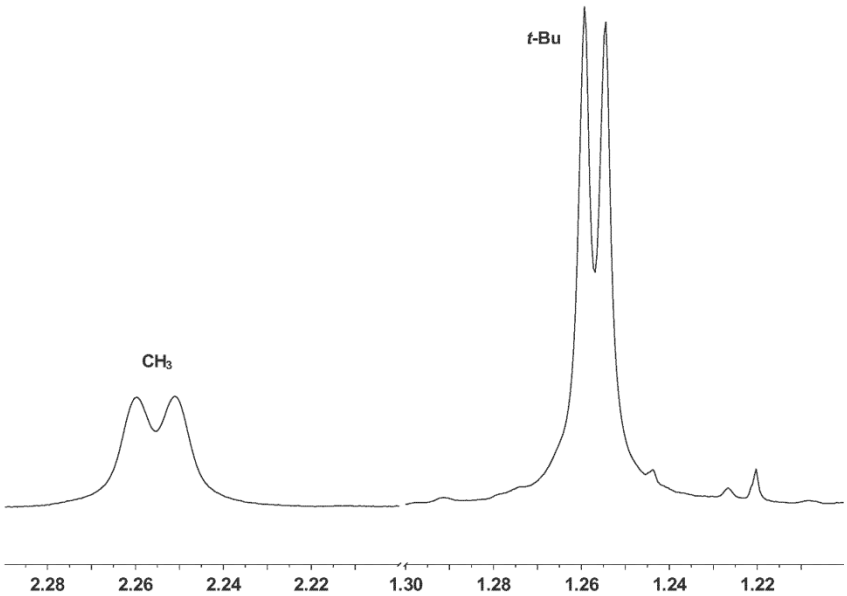


**Figure B-5.** Partial $^{1}$H NMR spectrum of **PtC$_4$Pt"-b** (partial, $CDCl_3$).

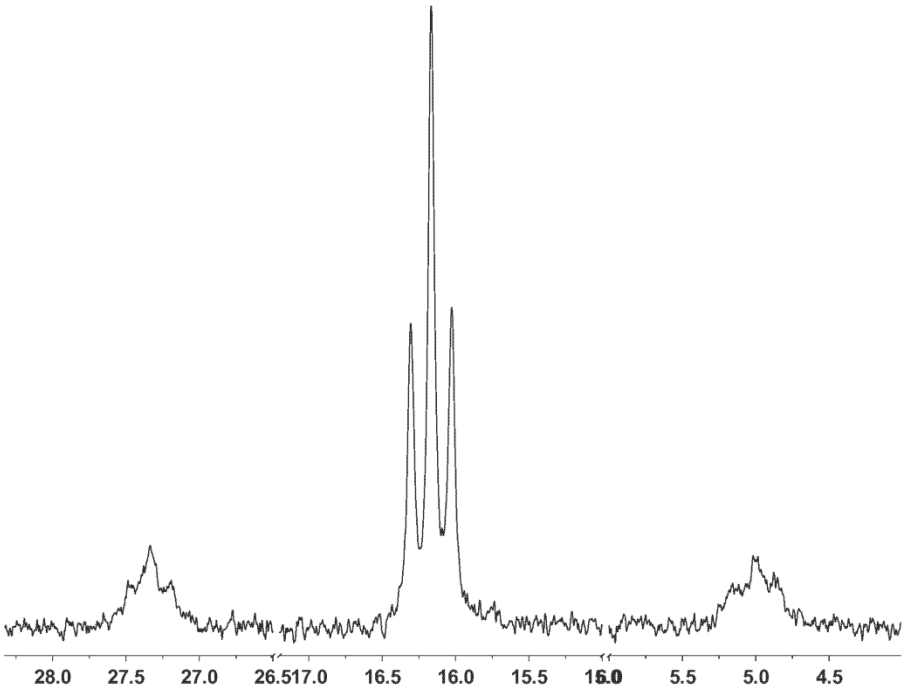


**Figure B-6.** $^{31}$P{$^{1}$H} NMR spectrum of **PtC$_4$Pt"-b** ($CDCl_3$).

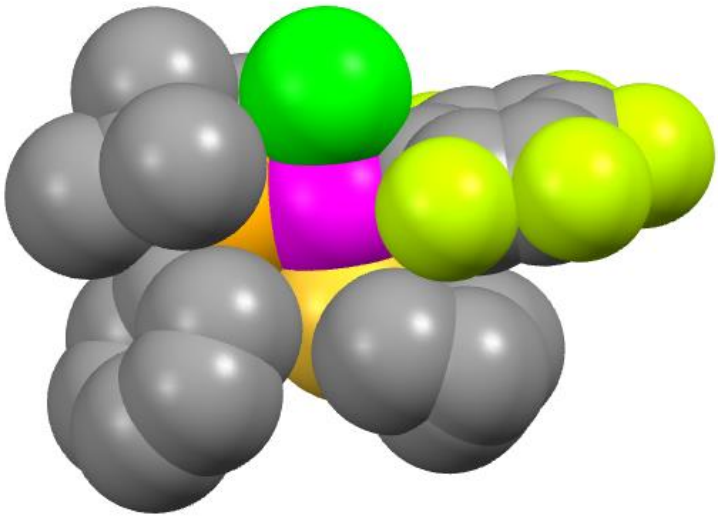

**Figure B-7.** Space-filling representation of **1**.

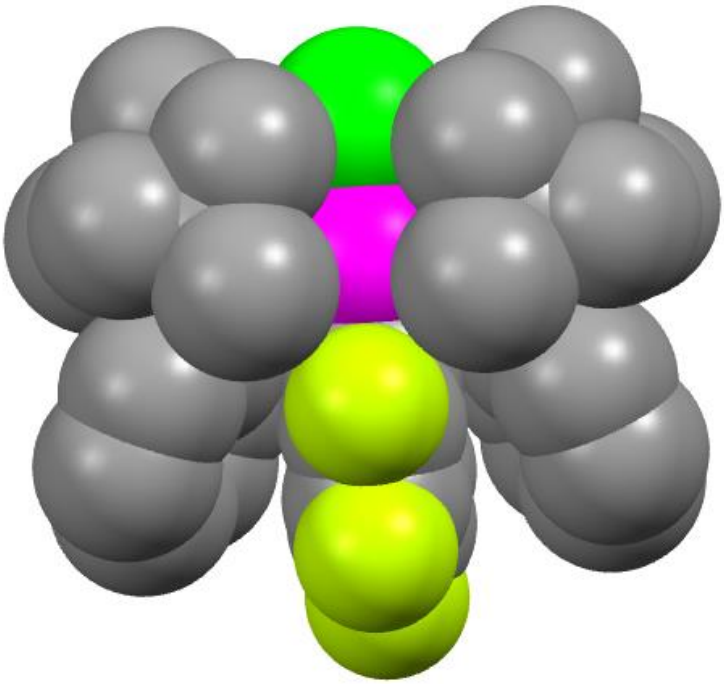

**Figure B-8.** Space-filling representation of **Pt"Cl-e**.

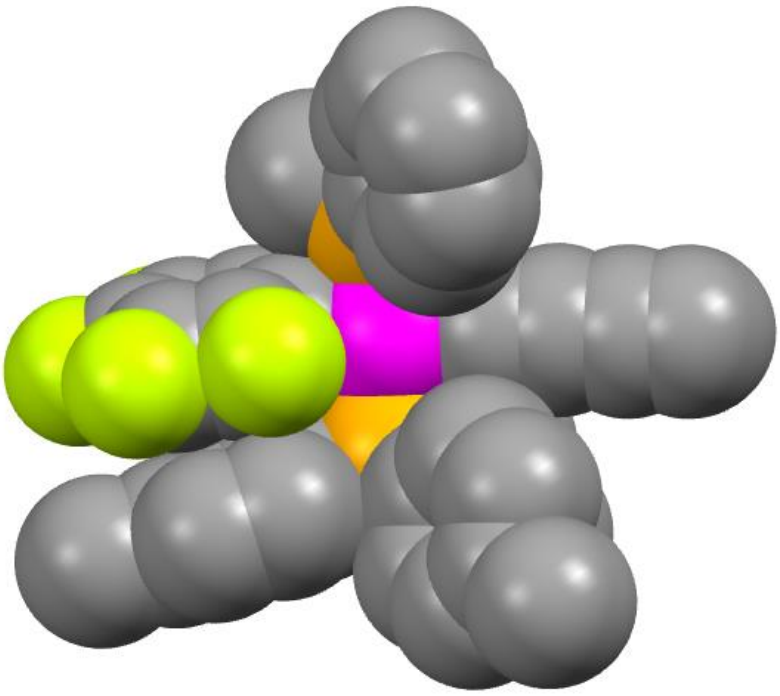

**Figure B-9.** Space-filling representation of **Pt'C$_4$H-a**.

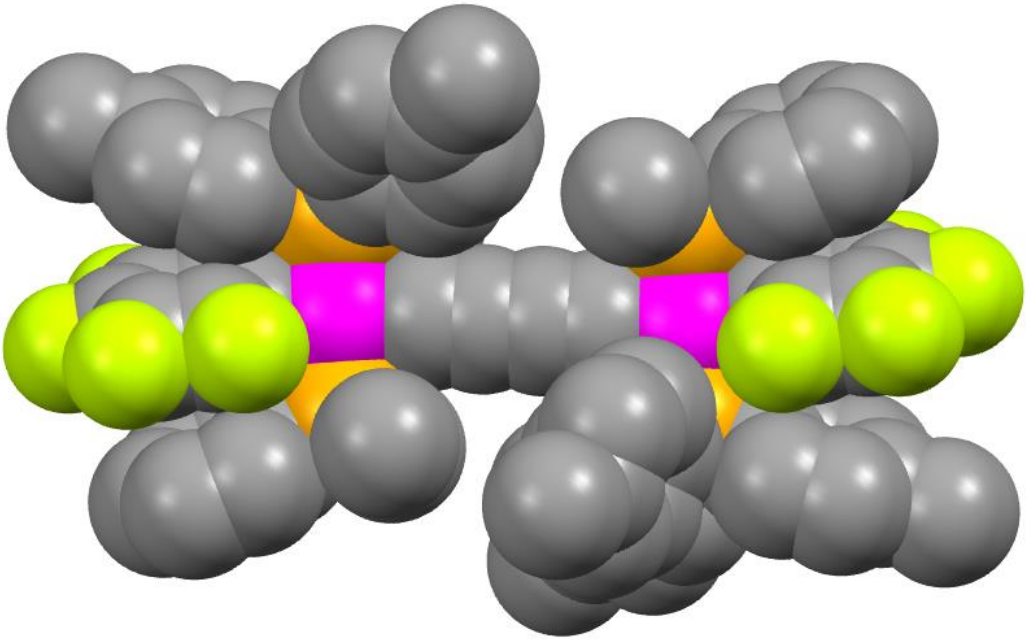

**Figure B-10.** Space-filling representation of **Pt'C$_4$Pt'-a**.

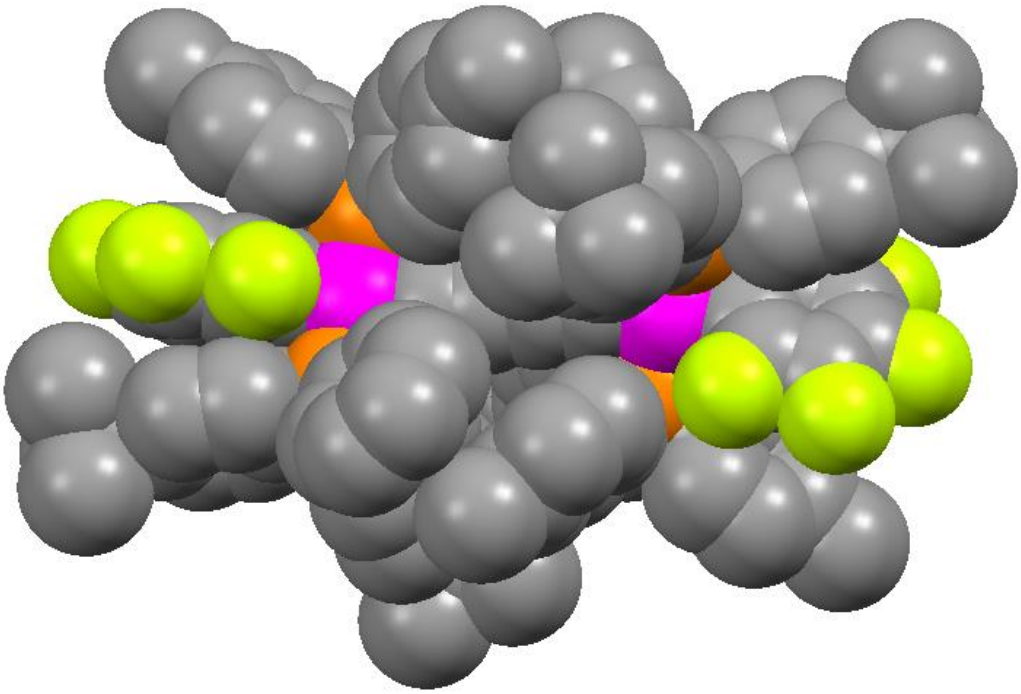

**Figure B-11.** Space-filling representation of **Pt'C$_4$Pt'-b**.

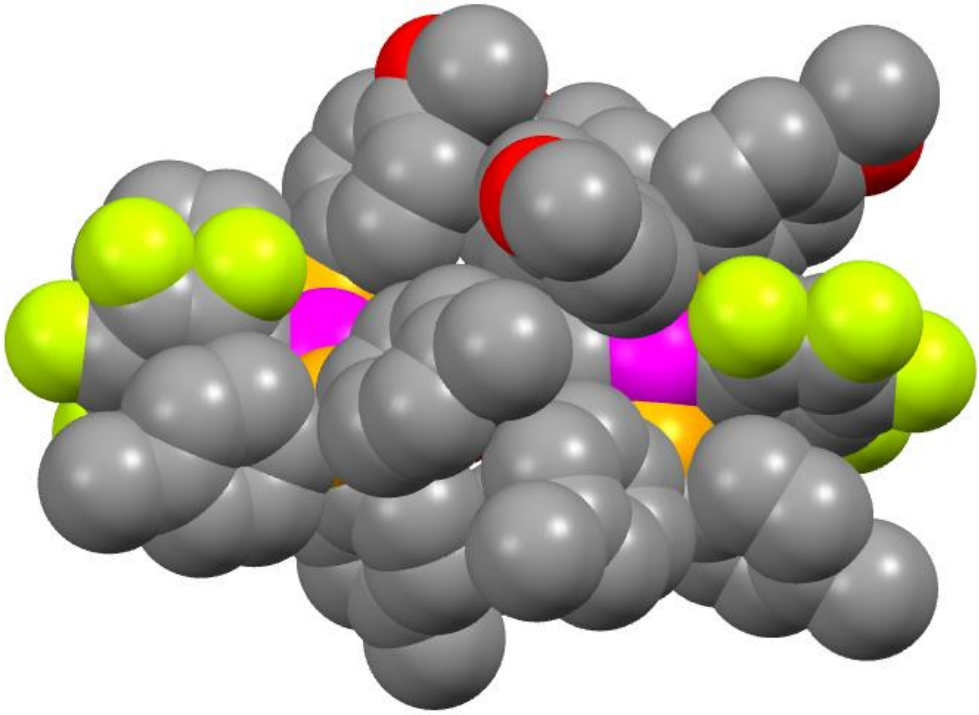

**Figure B-12.** Space-filling representation of **Pt'C$_4$Pt'-c**.

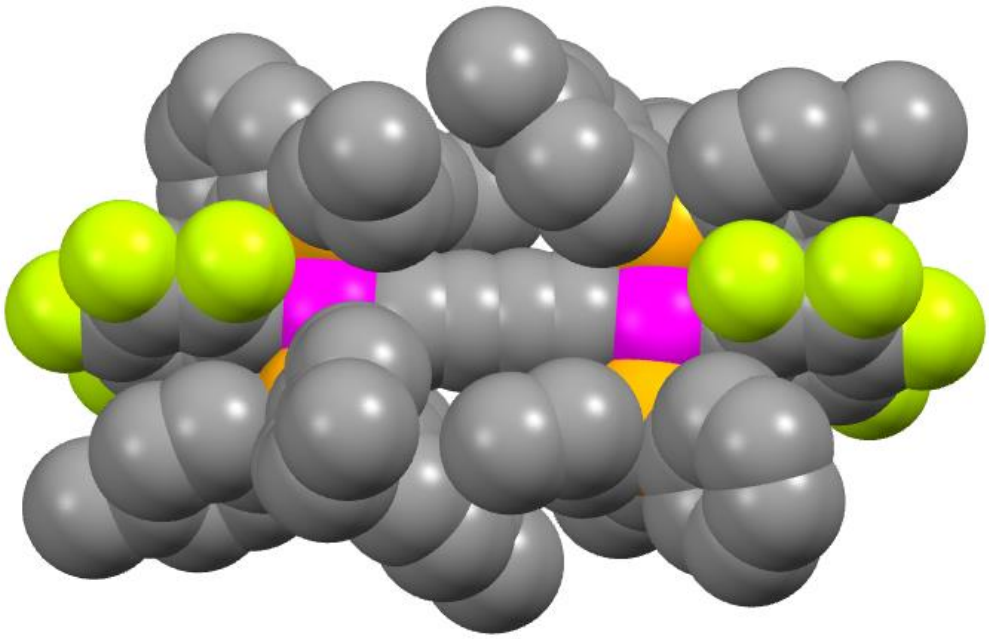

**Figure B-13.** Space-filling representation of **Pt'C$_4$Pt'-d**.

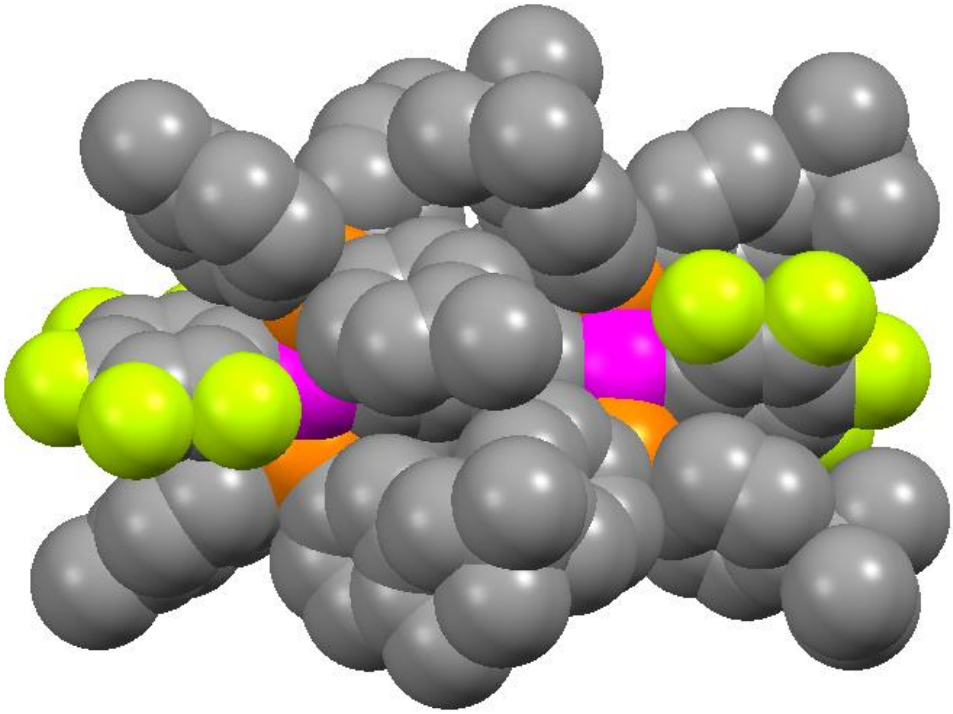

**Figure B-14.** Space-filling representation of **PtC$_4$Pt"-b**.